

University of Southampton Research Repository
ePrints Soton

Copyright © and Moral Rights for this thesis are retained by the author and/or other copyright owners. A copy can be downloaded for personal non-commercial research or study, without prior permission or charge. This thesis cannot be reproduced or quoted extensively from without first obtaining permission in writing from the copyright holder/s. The content must not be changed in any way or sold commercially in any format or medium without the formal permission of the copyright holders.

When referring to this work, full bibliographic details including the author, title, awarding institution and date of the thesis must be given e.g.

AUTHOR (year of submission) "Full thesis title", University of Southampton, name of the University School or Department, PhD Thesis, pagination

UNIVERSITY OF SOUTHAMPTON
FACULTY OF ENGINEERING, SCIENCE AND
MATHEMATICS

National Oceanography Centre
School of Ocean and Earth Sciences

**The Importance of Dissolved Organic Nutrients in
the Biogeochemistry of Oligotrophic Gyres**

By
Angela Landolfi

Thesis for the degree of Doctor of Philosophy

October 2005

**Graduate School of the
National Oceanography Centre**

This PhD dissertation by
Angela Landolfi

Has been produced under the supervision of the following persons:

Supervisors:

Dr. D.A. Purdie
Dr. Richard Sanders

Chair of Advisory Panel:

Prof. Patrick Holligan

UNIVERSITY OF SOUTHAMPTON

ABSTRACT

FACULTY OF ENGINEERING, SCIENCE AND MATHEMATICS
NATIONAL OCEANOGRAPHY CENTRE
SCHOOL OF OCEAN AND EARTH SCIENCES

Doctor of Philosophy

**THE IMPORTANCE OF DISSOLVED ORGANIC NUTRIENTS IN
THE BIOGEOCHEMISTRY OF OLIGOTROPHIC GYRES**

By Angela Landolfi

The aim of this thesis is to contribute to the observational database in order to address fundamental questions as to how dissolved organic nutrients influence N and P budgets, how they affect nutrient cycling and the sustainment of biological production within two major ocean oligotrophic gyres: the Southern Indian Ocean gyre and the subtropical North Atlantic gyre.

A transect across the Indian ocean at 32°S conducted in March/April 2002 was sampled for dissolved oxygen, inorganic and organic nutrients and phytoplankton pigments concentrations. A second cruise was undertaken in April/May 2004 across the oligotrophic North Atlantic Ocean at 24°N. A similar set of samples were collected on the second cruise and in addition the stable nitrogen isotopic signature of particulate organic matter was determined plus surface enzymatic activity and primary production incubation measurements.

The Indian ocean basin is characterized by low N:P ratios both in the inorganic and organic fractions with respect to phytoplankton nutrient requirements driven by an excess of denitrification over N₂ fixation. The strongly non-Redfieldian TON:TOP ratio suggests a decoupling of TON and TOP remineralization processes and indicates a severe TON deficiency brought by the strong nitrate limitation that leads to a community demand for TON. TON and TOP Ekman meridional advection played a small but not trivial role in providing N and P into the gyre to support export production. It is estimated that the contribution of TON advection is of the same order as the new N supplied by N₂ fixation into the gyre. In the Indian Ocean 40% of the net N transported by the overturning circulation across the boundary at 32°S, is attributable to organic nutrients. To close the N budget assuming the upper range estimates of denitrification to be correct, the inclusion of organic nutrient transport by the ITF is required. Hence, the Indian Ocean N budget conforms to a steady state where excess of denitrification over N₂ fixation is compensated for by atmospheric, riverine and a hypothesized flux of DON in through the ITF.

In the permanently stratified North Atlantic subtropical gyre, nutrient supply pathways for the growth of phytoplankton are unclear and appear inadequate for the maintenance of the observed export production. Here the significance of two mechanisms, N₂ fixation and the bioavailability of organic nutrients, has been investigated. The computation of a new geochemical proxy, TNex, for the determination of N to P anomalies suggests that N₂ fixation is more important than previously thought. The spatial distribution of the isotopic composition of particulate organic matter shows a N₂ fixation signal across most of the basin with the exception of the coastal margins and a central region. Thus no latitudinal gradient in diazotrophy, as suggested by other workers, is apparent. TON and TOP represented not only the major component of the upper ocean N and P pools but were also bioavailable to the community through the release of extracellular enzymes. The cycling of TON and TOP was decoupled, with higher turnover rates of the TOP pool as compared to the TON pool. Both

TON and TOP could potentially sustain a significant fraction of primary production and TOP could potentially provide nearly all the P needed by N₂ fixers. In conclusion, in the permanently stratified North Atlantic subtropical gyre, N₂ fixation and the bioavailability of organic N and P appear to be major mechanisms for supplying nutrients and sustaining phytoplankton growth.

Declaration of Authorship

I, **Angela Landolfi**, declare that the thesis entitled "**The importance of dissolved organic nutrients in the biogeochemistry of oligotrophic gyres**" and the work presented in it are my own. I confirm that:

- this work was done wholly or mainly while in candidature for a research degree at this University;
- where any part of this thesis has previously been submitted for a degree or any other qualification at this University or any other institution, this has been clearly stated;
- where I have consulted the published work of others, this is always clearly attributed;
- where I have quoted from the work of others, the source is always given. With the exception of such quotations, this thesis is entirely my own work;
- I have acknowledged all main sources of help;
- Where the thesis is based on work done by myself jointly with others, I have made clear exactly what was done by others and what I have contributed myself;

Signed:

Date:

Acknowledgements

I would like to thank my supervisors Dr. Richard Sanders and Dr. Duncan Purdie for their guidance and support throughout these years. I have benefited greatly from their scientific standards and their enthusiastic approach to science. I would also like to express my gratitude for all their extraordinary commitment to this thesis especially at the very end!

Thank you to Prof. Partick Holligan constant encouragement and advice.

Thank you to Prof. Harry Bryden for his precious comments on this work.

Thanks you to Dr. Elaine McDonaugh, Dr. Stuart Cunningham for sharing their time and data with me.

Thanks to the CD139 and D279 participants for making the cruises a success and helping during the tedious sampling.

Thank you to Dr. Lihini Aluwihare and the Aluwihare Lab for offering fresh prospective and allowing me to spend a very enjoyable time in La Jolla.

Thanks to Prof. Bill Jenkins, for giving me the opportunity to visit and use the facilities of the Noble gas WHOI lab but most of all for the stimulating discussions and thanks to Rachel for taking good care of me during my stay....and thank you for dragging me out jogging in the snow at -10°C...now I now I can do it!

Thanks to my office mates Zöe Bond, Phil, Zöe Roberts and John for making the office such a wild and enjoyable environment!

Many thanks to my friends here in Southampton: Xana, MaaaRc, Chriistos, Taro & Ale, Adriana, Cipo, Zöe Bond, the Saras, Ben, Judith, Sinhue, Matt, Erwon, Maria, Aggie.... and elsewhere: Manfre, siculo, gli aniti, with whom I have shared part of these years, thanks for all their help, the good time spent together and the shared teas and coffees!

Thank you to my extended family here in 94, Milton Rd: Ricca, Hariulis, Anna piragna, Iriiini, and the new entry my little sister Eleo who made my life very enjoyable and thus have greatly contributed to this work (if I survived in these last days I owe it to Haris!).

Thank you to my parents for inspiring me.

None of this could have been possible without the support of Gianluca to whom this thesis is dedicated to. Thank you for your patience, your courage and your constant encouragement, but most of all thanks for Giulia!

Table of Contents

List of Figures	iii
List of Tables	v
List of Equations	vi
1. Introduction.....	1
1.1 The Marine Global N and P Cycles.....	1
1.2 How Do Nutrients Get to the Euphotic Zone?	4
1.3 Dissolved Organic Nutrients	5
1.3.1 Role of Marine DOM.....	6
1.3.2 DOM Composition and Lability.....	7
1.3.3 DOM Production and Removal Processes	8
1.3.4 DOM Global Distribution.....	9
1.3.5 Stoichiometry.....	11
1.4 Thesis goals.	12
2 Methods.....	15
2.1.1 Oxygen and Inorganic Nutrients	16
2.1.2 Pigments	17
2.1.3 Total Nitrogen (TN), Total Phosphorus (TP) and Total Organic Carbon (TOC)	18
2.1.3.1Ultraviolet (UV) Photoxidation	19
2.1.3.2High Temperature Catalytic Oxidation (HTCO)	22
2.1.4 $\delta^{15}\text{N}$ PON	24
2.1.5 Primary Production.....	25
2.1.6 Helium	25
2.1.7 Enzyme Assays.....	26
2.1.7.1 Ecto-enzymes in the marine environment.....	26
2.1.7.2 Sampling and Incubation	27
3 Indian Ocean.....	30
3.1 Introduction	30
3.2 Results	32
3.2.1 Large Scale Inventories of N and P.....	32
3.2.1.1 Discussion.....	39
3.2.1.2 Conclusions	44
3.2.2 DOM Advection into the Subtropical Gyre	45
3.2.2.1 Estimates of Export Production	46
3.2.2.2 Discussion and Conclusion	48
3.2.3 Nitrogen budget	59
3.2.3.1 Nitrogen Sinks.....	50
3.2.3.2 Nitrogen Sources	51
3.2.3.3 Transport Calculations	54
3.2.3.4 N Budget.....	61
3.2.3.5 Conclusions	66
3.3 Final Conclusions	66
4 North Atlantic Subtropical Gyre	68
4.1 Introduction	68
4.1.1 Nutrient Supply in the Euphotic Zone.....	69
4.1.2 N_2 Fixation	70
4.1.2.1 Direct Measurements	70
4.1.2.2 Indirect Geochemical Estimates.....	70

4.1.3 Objectives.....	75
4.2 Derivation of N* DINex and TONex	78
4.3 Stable Nitrogen Isotopes as a Diagnostic Tool Reflecting Nitrogen Processes	80
4.4 Results	82
4.4.1 Deep Waters, N to P ratio anomalies.....	82
4.4.1.1 Discussion.....	85
4.4.1.2 Conclusions	99
4.4.2 Surface Waters – Bulk Distributions.....	101
4.4.2.1 Discussion.....	107
4.4.2.2 Conclusions	108
4.4.3 Enzyme Experiments- Measures of Biological Processes.....	110
4.4.3.1 Discussion.....	119
4.4.3.2 Conclusions	126
4.5 Final Conclusions	127
5 Conclusions	128
6 References	132

List of Figures

Fig. 1.1 Role of the oceans in the global N cycle. Inventory and fluxes are reported in TgNy^{-1} . From Galloway <i>et al.</i> (2004)	2
Fig. 1.2 Scheme of the nitrogen species and the oxidation and reduction processes involved in the marine nitrogen cycle. Please note that the catabolic process is also known as ammonification. From Codispoti <i>et al.</i> (2001)).....	3
Fig. 1.3 Scheme representing the marine P cycle. From Delaney (1998)	4
Fig. 2.1 CD139 Cruise track and bathymetry. CTD stations occupied during the cruise are shown by the red stars. The green dots represent stations where Argo floats were released.	15
Fig. 2.2 D269 Cruise track and bathymetry. CTD stations occupied during the cruise are shown by black dots. Stations where enzyme assay experiments were carried out are shown by the red boxes, red crosses represent stations where Argo floats were released.....	16
Fig. 2.3 Regression line of caffeine standard solutions vs KNO_3 standard solutions. The slope of the regression line represents the oxidation efficiency (b1), the intercept (b0) represents the blank.	23
Fig. 2.4 Linear regression of all the standards weights (μg) and their detection in peak height (nA) used for the calibrations. As all the calibration data are reported here, note the good reproducibility of the calibration curves throughout the analysis of the different batches.	25
Fig. 2.5 Typical calibration curve used for the conversion of fluorescence into concentration units.....	28
Fig. 2.7 Fluorescence increase over time. The enzyme activity was determined from the best fit of the data points before the plateau. The controls are also shown.	29
Fig. 2.6 Flow chart of the methodology followed during enzyme assays experiments.....	29
Fig. 3.1 Section of salinity across the Indian Ocean at 32°S	32
Fig. 3.2 Section of nitrate (top) and (bottom) phosphate (μM) across the Indian Ocean at 32°S	33
Fig. 3.3 Section of total chlorophyll a (ngChlal^{-1}) across 32°S in the Indian Ocean.....	34
Fig. 3.4 Vertical distribution of the contribution of various algal pigments to total pigments (%) in 4 different regions across the Indian Ocean at 32°S	34
Fig. 3.5 Sections of the contribution (%) of zeaxanthin (top) and (bottom) divinyl-chlorophyll a to total pigments across Indian Ocean at 32°S	35
Fig. 3.6 Averaged vertical profiles of DIN, TON HTCO measured, DIP, TOP (μM) and typical Chlorophyll a profile ($\mu\text{g l}^{-1}$). Bars represent range of measurements.....	36
Fig. 3.7 Vertical profiles of TON and TOP contribution (%) to the total N and P pools.....	36
Fig. 3.8 Section of TON (top) (μMN) and TOP (bottom) (μMP) across the Indian Ocean at 32°S . Contours were produced using kriging as interpolation method with anisotropy ratio of 1	37
Fig. 3.9 Scatter plot and regressions line of DIN vs DIP (black) (top left), TN vs TP (cyan)(top right); TON vs TOP red (bottom left); TON vs TOP only surface data (yellow) (bottom right). Full lines represent best fit lines, dotted lines represent $y=16+2.5x$ equation; $b(0)=\text{slope}$, $b(1)=\text{intercept}$	38
Fig. 3.10 Section of $\text{TON}_{\text{HTCO}}/\text{TON}_{\text{UV}}$ ratio across the Indian Ocean at 32°S . Contours were produced using kriging as interpolation method with anisotropy ratio of 1.....	39
Fig. 3.11 Inorganic nitrogen to phosphorus ratio along the water column in the Indian Ocean. Note that the N/P ratio is always <16 even in deep waters.	40

Fig. 3.12 Section of inorganic nitrogen to phosphorus ratio distribution along the Indian Ocean at 32°S.....	40
Fig. 3.13 Vertical profile of Tritium- ³ He ages (y) and AOU ($\mu\text{molO}_2 \text{ kg}^{-1}$) from the WOCE and CD139 datasets.	47
Fig. 3.14 Correlation between AOU ($\mu\text{molO}_2 \text{ kg}^{-1}$) and age (y) from the WOCE and CD139 data set on the $\sigma\tau=25.5 \text{ kg m}^{-3}$. The slope of the regression line has bee used to infer OUR on this isopycnal surface.....	47
Fig. 3.15 Contour of neutral density γ (kg m^{-3}) along the nominal latitude at 32°S in the Indian Ocean. Contours indicate the separation into layers of the water column used for the transport analysis.	56
Fig. 3.16 Cumulative geostrophic transports integrated for layers 1-5 and layer 6-8 (top) and (bottom) cumulative Ekman transport.....	56
Fig. 3.17 Correlation between nitrate ($\mu\text{mol kg}^{-1}$) and total nitrogen ($\mu\text{mol kg}^{-1}$)	57
Fig. 3.18 Cumulative geostrophic and Ekman transport (top) and (bottom) nitrate geostrophic and Ekman transport for all the layers.	58
Fig. 3.19 Mass ($\text{m}^3 \text{s}^{-1}$), TN_1 ($\mu\text{mol s}^{-1}$), NO_3 ($\mu\text{mol s}^{-1}$), and TON ($\mu\text{mol s}^{-1}$) geostrophic (blue) and Ekman (red) transports integrated on each density layer as defined in the text. Northward transport is positive.	59
Fig. 3.20 Longitudinal variation of the Ekman transport of mass (top), NO_3^- (middle) and TN (bottom) across 32°S in the Indian Ocean.....	60
Fig. 4.1 Plot of phosphate versus nitrate. The red solid line represents the mean ocean trend $P=1/16N+0.182$. The inset shows the effect of photosynthesis/respiration, denitrification and N_2 fixation on the N to P ratio. From Gruber and Sarmiento 1997.....	79
Fig. 4.2 Section across the North Atlantic subtropical gyre at 24.5°N of temperature °C (top) and salinity (bottom). Overlying are the contours of sigma-theta $\sigma\tau$ (kg m^{-3}).	82
Fig. 4.3 Section across the North Atlantic subtropical gyre at 24.5°N of AOU ($\mu\text{mol kg}^{-1}$). Overlying are the contours of sigma-theta $\sigma\tau$ (kg m^{-3}).	83
Fig. 4.4 Section across the North Atlantic subtropical gyre at 24.5°N of nitrate $\mu\text{mol kg}^{-1}$ (top) and phosphate $\mu\text{mol kg}^{-1}$ (bottom). Overlying are the contours of sigma-theta (kg m^{-3}).	83
Fig. 4.5 Average vertical profiles of NO_3^- and TON μM (left) and PO_4^{3-} and TOP μM (right). Error bars represent range bars.....	84
Fig. 4.6 Plot of phosphate versus nitrate from samples collected in the North Atlantic at 24.5°N. The black line represents the best fit of all the data points (hollow back circles) collected during D279 cruise. Red line represents the best fit of data points (red dots) selected from 200-600m depth range.	85
Fig. 4.7 Vertical average profiles of DINex and N^* μM (left) and TNex^* μM (right).	86
Fig. 4.8 Plot of sigma theta versus N^* and DINex	87
Fig. 4.9 Plots of NO_3^- (μM , left) and PO_4^{3-} (μM , right) versus dissolved oxygen $\mu\text{mol kg}^{-1}$. Clusters of different $\text{O}_2:\text{NO}_3^-$ and $\text{O}_2:\text{PO}_4^{3-}$ are indicated read text for details	88
Fig. 4.10 Conceptual model of the ratio anomalies between N and Pools and the dynamics between inorganic and organic nutrients.	90
Fig. 4.11 Section of temperature, salinity and sigma-theta of the top 500m across 24.5°N.....	101
Fig. 4.12 Section of nitrate (μM , top) and phosphate (μM , bottom) across 24.5°N. Overlaid (white) are the sigma-theta contours. Please note that the σ_0 contours intervals are different in the two panels.....	102
Fig. 4.13 Section of TON (μM , top) and TOP (μM , bottom) across 24.5°N. Overlaid (black) are the sigma-theta contours. Black dots represent data points. Contours were generated with Kriging interpolation method with an anisotropy ratio of 1.....	103

Fig. 4.14 Section of calibrated fluorescence across 24.5°N. Back dots represent data points.....	103
Fig. 4.15 Section of fraction of divinylchlorophyll <i>a</i> over total chlorophyll <i>a</i> across 24.5°N. Black dots represent data points. Contours were generated with Kriging interpolation method with an anisotropy ratio of 1.....	104
Fig. 4.16 Section of fractions of picoplankton (top), nanoplankton (centre) and microplankton (bottom) community across 24.5°N. Black dots represent data points. Contours were generated with Kriging interpolation method with an anisotropy ratio of 1.....	105
Fig. 4.17 Sections of DINex (top), TONxs (centre) and TNxs (bottom) across 24.5°N. Overlaid (black) are the sigma-theta contours. Black dots represent data points. Contours were generated with Kriging interpolation method with an anisotropy ratio of 1.....	106
Fig. 4.18 Longitudinal variability of net O ₂ production and respiration over a 12h period across the north Atlantic	110
Fig. 4.19 Longitudinal variation of total chlorophyll <i>a</i> and fraction of divinylchlorophyll <i>a</i> (top) and (bottom) fraction of pico-, nano- and microplankton.....	111
Fig. 4.20 Zonal distribution of δPO ¹⁵ N. Black dots represent data points collected from Niskin bottles 10-25m; Red points represent samples collected form the surface by carboys (0m).	112
Fig. 4.21 Zonal distribution of POC/PON ratio. Black dots represent data points collected from 10-25m; Red points represent samples collected form the surface (0m).....	113
Fig. 4.22 Longitudinal distribution of surface AKA, APA and AKA/APA ratio (a), AKSA and APSA (b), AKmax, APmax and AKmax/APmax (c), Specific AKmax and Specific APmax (d).....	114
Fig. 4.23 Scatter plot of AKmax and versus AKA and AKSA and regression line (regression coefficients: b0=intercept, b1=slope).....	115
Fig. 4.24 Scatter plots and regression line (regression coefficients: b0=intercept, b1=slope) of TONexcess versus APA (top left), APA versus TON and TOP (top right), fraction of picoplankton versus APA (bottom).....	116
Fig. 4.25 Scatter plot of picoplankton fraction versus APAmax and regression line (regression coefficients: b0=intercept, b1=slope).....	117
Fig. 4.26 Scatter plot of oxygen production (net and gross μM O ₂ 12h ⁻¹) versus AMmax/APmax ratio and regression line of net oxygen production versus AMmax/APmax ratio (regression coefficients: b0=intercept, b1=slope).....	117
Fig. 4.27 Longitudinal surface distribution of TON and TOP (μM) (top) and TONex (μM) and δ ¹⁵ N PON (%) (bottom)	118
Fig. 4.28 Longitudinal variation of the importance of N ₂ fixation as a source of new nitrogen across the subtropical gyre at 24°N. Calculations were made according to a two end member mixing model. The end members used were -2‰, for the depleted end member and 4.5‰ for the enriched end member.	120

List of Tables

Table 2.1 Chemotaxonomic pigments resolved during the analysis following Barlow <i>et al.</i> (1997). Their occurrence in phytoplankton groups is also reported.	17
Table 2.2 Settings for the Shimadzu 5000A DOC analyser connected in series with the Antek (Model#705E) high temperature combustion analyser.	22
Table 2.3 Common extracellular enzymes, their substrates and products in the marine system.	27
Table 2.4 Substrates (parent molecule) and respective fluorescent molecules. Excitation and emission wavelength for their detection are included.	27

Table 3.1 Average of OUR ($\mu\text{mol kg}^{-1}\text{y}^{-1}$) on 5 isopycnal layers. OUR has been calculated as the slope of the regression line between water mass ages (y) and AOU ($\mu\text{mol kg}^{-1}$). Average depth of each isopycnal layer is reported.	48
Table 3.2 Neutral density layers used for the transport calculation.	55
Table 3.3 Mass, nitrate and total nitrogen transport integrated on each density layer. Nitrate transport is associated with 1.1% error. The total nitrogen transport calculated from derived total nitrogen (TN_1) associated with 5% uncertainty, and the average total nitrogen (TN_2) associated with 30% uncertainty, are reported for comparison, see text for explanation. Estimates of the geostrophic and Ekman velocities are reported in McDonough <i>et al.</i> (2005). The last column represents the contribution (%) of TON to the total N geostrophic transport calculated from TN_1	60
Table 3.4 Sources and sinks of nitrogen into the Indian Ocean north of 32°S. The fluxes are in Tg Ny^{-1}	62
Table 3.5 Revisited N budget of the Indian Ocean north of 32°S. The fluxes are in Tg Ny^{-1}	63
Table 4.1 Average DINxs, TONxs and TNxs calculated for 3 depth ranges.	89
Table 4.2 Fraction of SC (F.SO) and NC (F.NO) along isopycnals at station 50 (West) and 108 (East). Preformed values (P. DINxs, P.AOU, P.TONxs) and the difference between preformed and measured (D. DINxs, D.AOU, D.TONxs) values of DINxs, AOU and TONx are reported. CFC ages are taken from Hansell <i>et al.</i> (2004). TONxs have been calculated with a one end member mixing model. Preformed values of TONxs on the $\sigma_0=27$ layer were not available for analysis.	95
Table 4.3 Production rates of DINxs OUR and TONxs along isopycnal surfaces at station 50 and 108.	95
Table 4.4 Comparison of the N_2 fixation rates estimated from DINex by G&S (1997) and Hansell <i>et al.</i> (2004) and this study on selected 3 isopycnal layers ($\sigma_0= 26, 26.5, 27 \text{ kg m}^{-3}$). Please note that, for better comparison with the N_2 fixation estimates reported in G&S (1997) and Hansell <i>et al.</i> (2004), here are reported the total volume of the 3 isopycnal considered and not the individual volumes of the isopycnal layers used for the calculations. Note the different volumes used in the calculations by G&S (1997) and Hansell <i>et al.</i> (2004). The addition of organic nutrients in this budget (TNex) increases the average fixation rates which become comparable with the rates estimated by G&S (1997) and Hansell <i>et al.</i> (2004) adding the contribution of all isopycnal layers (see table below).	98
Table 4.5 Rates of N_2 fixation estimated from DINex reported by G&S (1997) and Hansell <i>et al.</i> (2004) and TNxs calculated in this study on all the isopycnal layers ($\sigma_0= 25.6-27.6 \text{ kg m}^{-3}$) of the upper 1000m of the water column. Volumes of all isopycnals are not reported in the study by Hansell <i>et al.</i> (2004). In this study average N_2 fixation rates for all isopycnals have been extrapolated from average N_2 fixation rates obtained on 3 specific isopycnals ($\sigma_0= 26, 26.5, 27 \text{ kg m}^{-3}$)	99

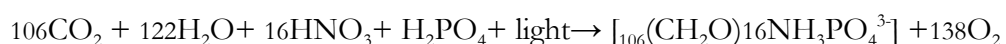
List of Equations

Eq. 2.1	19
Eq. 3.1	46
Eq. 3.2	46
Eq. 3.3	55
Eq. 3.4	58
Eq. 3.5	61

Eq. 4.1.....	78
Eq. 4.2	78
Eq. 4.3	78
Eq. 4.4	78
Eq. 4.5	78
Eq. 4.6	79
Eq. 4.7	79
Eq. 4.8	80
Eq. 4.9	81
Eq. 4.10.....	94
Eq. 4.11.....	94
Eq. 4.12.....	95
Eq. 4.13.....	97

1. Introduction

The oceans contain the largest pool of carbon on the planet and are implicated in the long-term (centuries to millennia) regulation of atmospheric CO₂ through the biological pump which refers to the sinking of organic matter from the surface productive layers to the deep ocean. This mechanism is capable of sequestering atmospheric CO₂ on timescales comparable to ocean overturning (centuries to millennia). The production of marine organic matter from inorganic constituents follows a nominal stoichiometry:



Where the ratios between the dissolved elements and the nutrients necessary for phytoplankton growth (C:N:P= 106:16:1) are termed Redfield ratios (Redfield *et al.* 1963). Thus, the strength of the biological carbon pump and ultimately the impact of ocean biology on atmospheric CO₂ is strongly controlled by the bioavailability of nutrients: mainly nitrate and phosphate. Hence quantifying the processes that control the fluxes of N and P into the oceans and how these nutrients are supplied to surface waters to sustain the growth of phytoplankton, is a fundamental step towards understanding the magnitude at which the ocean takes up carbon dioxide and therefore, is a major issue in current marine biogeochemical research.

1.1 The Marine Global N and P Cycles

The global marine N inventory (6 ·10⁵ TgN of nitrate; Mackenzie 1998) is maintained by inputs of fixed N from a combination of N₂ fixation (87–156TgNyr⁻¹) and other minor sources; riverine inputs (48TgNyr⁻¹) and atmospheric deposition (33TgNyr⁻¹), and losses primarily through denitrification (150 – 450TgNyr⁻¹), sedimentation (14TgNyr⁻¹ shelf and 0.8Tg Nyr⁻¹ deep sediments) (Altabet *et al.* 1995; Codispoti 1995; Altabet *et al.* 2002; Devol 2002) and N₂O emission (4Tg Nyr⁻¹) from the shelves and open ocean (Fig. 1.1). Thus potentially, the lack of bioavailable nitrogen is compensated for by biologically mediated fixation of N₂ gas which draws open a virtually unlimited reservoir. However, N₂ fixation can be limited by the availability of Fe or P (Sanudo-Wilhelmy *et al.* 2001; Mills *et al.* 2004). Although the quantitative contribution of N₂ fixation to the N marine cycle is still poorly constrained, several recent studies indicate that, at present, N₂ fixation and denitrification rates are not in balance (Codispoti *et al.* 2001). This imbalance can cause substantial changes in the

size of the oceanic N pool and therefore determines the degree to which the oceans are either nitrogen or phosphorus limited (Falkowski 1997; Tyrrell 1999; Codispoti *et al.* 2001).

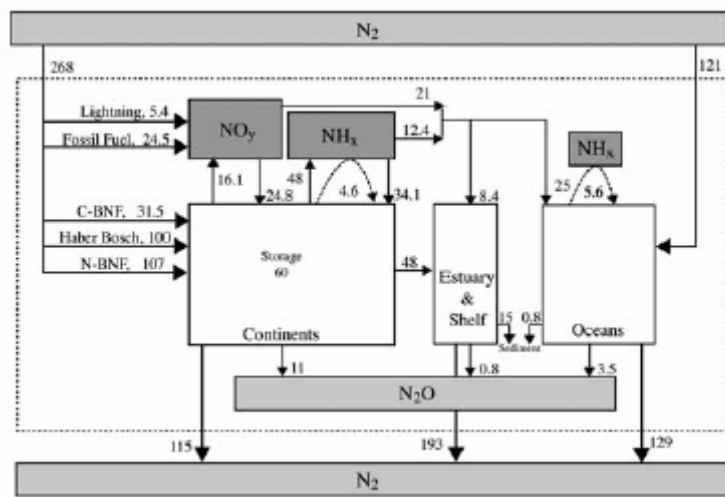


Fig. 1.1 Role of the oceans in the global N cycle. Inventory and fluxes are reported in TgNy⁻¹. From Galloway *et al.* (2004).

Moreover this imbalance has potential impacts on marine productivity and atmospheric CO₂ drawdown (Galloway *et al.* 2004) and can also trigger changes in community structure (Karl *et al.* 2001; Church *et al.* 2002).

N₂ fixation is catalyzed by the enzyme nitrogenase through a metabolic pathway only carried out by a selected group of organisms. The enzyme is inhibited by O₂ but N₂ fixation does occur in oxygenated waters (Falkowski 1997). The distribution of N₂ fixers in the world oceans is also controlled by other factors such as temperature, trace metals and concentrations of NO₃⁻ and PO₄³⁻. These environmental factors explain the success of N₂ fixers in tropical and subtropical waters as opposed to the low N₂ fixation rates found at high latitudes.

Denitrification is a dissimilatory process in which NO₃⁻ replaces oxygen as the terminal electron acceptor during respiration and where the final product is N₂. As the energy yield of this process is substantially lower than that of oxygen based respiration, denitrification usually does not occur in oxygenated waters (Hattori 1983). Thus, water column denitrification occurs only in a few places, the most important being the Arabian Sea (Naqvi 1987) and the Eastern Tropical Pacific (Codispoti and Richards 1976; Codispoti and Packard 1980; Deutsch *et al.* 2001). Benthic denitrification is more widely spread as a consequence of organic rich oxygen poor sediments along the continental margins (Devol 1991; Kristensen *et al.* 1999; Jahnke and Jahnke 2000).

The marine N inventory is distributed among different N species characterized by 5 oxidation states that are transformed into each other by biologically and physically mediated reactions (Fig. 1.2). The most abundant pool, both in the ocean and atmosphere, is N_2 gas, at the zero oxidation state. Due to the ocean's oxidation capacity, the next most abundant element is NO_3^- (+5) followed by the organic forms of N (-3) DON (dissolved organic nitrogen), NH_3 and PON, while NO_2^- (+3) and N_2O are intermediary species during denitrification reactions and can build up in significant concentrations only in suboxic areas. Transformations among the different forms of N, organic-inorganic, are mostly biologically mediated. The reduction of NO_3^- to organic matter is carried out mostly by photosynthesis in the sunlit surface ocean. However, ammonification and nitrification, which oxidize organic matter to NO_3^- , occur not only in the surface euphotic layer but also below the main thermocline.

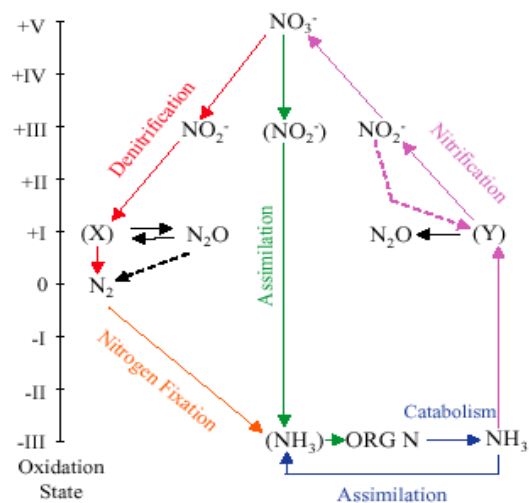


Fig. 1.2 Scheme of the nitrogen species and the oxidation and reduction processes involved in the marine nitrogen cycle. Please note that the catabolic process is also known as ammonification. From Codispoti *et al.* (2001).

Phosphorus does not have analogues of N_2 fixation and denitrification and its inventory is controlled exclusively by the balance between riverine and atmospheric inputs and hydrothermal removal and burial to the sea floor (Fig. 1.3). Hence P represents the ultimate limiting factor for biological production over long time scales (Tyrrell 1999). Phosphorus is mostly present in the ocean in combination with oxygen (i.e. PO_4^{3-}) and is an essential component of DNA, ATP and molecules that constitute cell membranes. Its distribution in the oceans is relatively simple. It is controlled exclusively by the uptake of inorganic nutrients

(PO_4^{3-}) into organic biomass (POP) and dissolved organic matter (DOP) and its remineralization back into the dissolved inorganic fraction (Delaney 1998).

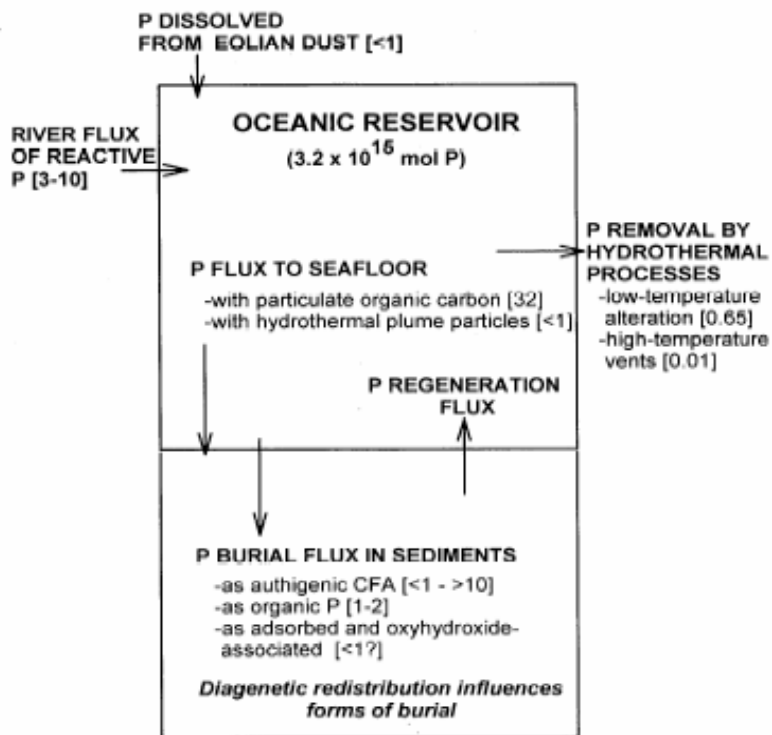


Fig. 1.3 Scheme representing the marine P cycle. From Delaney (1998).

The maintenance of N and P cycling among the different pools is strictly controlled by the return of nutrients back into the sunlit surface ocean, where biochemical reactions take place, and thus also involves physical processes.

1.2 How Do Nutrients Get to the Euphotic Zone?

The maintenance of new production and export production are controlled by the nutrient loop created by fixation, export, sinking, remineralization, and reflux back into the euphotic zone. This cycle involving ventilation, circulation, and mixing, presumably occurs on annual to decadal to century timescales (Jenkins 1988, 1998). Traditionally the supply of nutrients to the surface waters to sustain the growth of phytoplankton has been attributed to diapycnal mixing during wintertime convection. As such, measurement of new production has coincided with the vertical estimate of nitrate supply from the thermocline. This approach, however, is not applicable over the extensive subtropical gyres where convection is minimal. Over these zones, vertical diffusion rates in the thermocline are found to be an order of magnitude lower than is needed (Jenkins 1991; Ledwell *et al.* 1993) to uplift nutrients to the

euphotic zone. Despite this, these zones are estimated to account for half the global export of organic carbon from the surface to the deep ocean (Emerson *et al.* 2001). This prompts the fundamental question as to how nutrients get into the sunlit surface ocean to sustain new production in the subtropical gyres?

A range of mechanisms have been invoked to explain how the additional new N is supplied to subtropical gyres (Williams and Follows 1998). There is evidence that biological fixation of nitrogen gas (Gruber and Sarmiento 1997) and intermittent upwelling of nutrients from the deep ocean, induced by mesoscale eddies (McGillicuddy and Robinson 1997; McGillicuddy *et al.* 1998; Oschlies and Garcon 1998; Oschlies 2002), are important mechanisms in providing nutrients to the surface waters of the subtropics. However, these proposed mechanisms do not fully explain the dynamics and the magnitude of the estimated export production based on independent geochemical methods as the seasonal cycle of surface oxygen production, aphotic zone oxygen utilization and the utilization of excess tritogenic ${}^3\text{He}$ air-sea flux as a nutrient flux gauge. Nitrogen fixation is in fact, limited to areas where there is sufficient iron deposition and requires an independent source of phosphorus. Mesoscale activity has a seasonal component and can become unimportant if nutrient concentrations in the upper thermocline cannot be restored on appropriate time scales. Another proposed potential source of nutrients is marine dissolved organic matter (DOM).

DOM is one of the largest reactive reservoirs of organic carbon, nitrogen and phosphorus on earth (Wada 1991), thus it represents an enormous reservoir of nitrogen and phosphorus in the upper oligotrophic ocean (Jackson and Williams 1985; Rintoul and Wunsch 1991; Williams and Follows 1998). Direct uptake or remineralization of DOM laterally transported from productive areas and/or released by N_2 fixing organisms could significantly impact nutrient cycling and hence the primary productivity of the subtropical gyres.

1.3 Dissolved Organic Nutrients

Dissolved organic nutrients, comprising dissolved organic nitrogen (DON) and dissolved organic phosphorus (DOP) are the dominant fraction of the nutrient pool in the upper oligotrophic ocean (Sharp *et al.* 1995). This pool has only recently been recognised as an important constituent and intermediary of carbon and nutrient cycles.

Dissolved organic nutrients are a part of the broader dissolved organic matter (DOM) pool defined as the fraction of the total organic matter that passes through a $0.2\mu\text{m}$ filter. In the water column, the weight ratios between dissolved organic material, particulate organic material and the living biota (bacteria, phytoplankton, protozoa and zooplankton) are

approximately 100:10:2 (Wada 1991). It is estimated that the oceans together contain about 10^{18} g of DOM (Hansell and Carlson 2002).

Net oceanic primary production produces a quantity of organic matter per year that is only a small percentage of the oceanic dissolved organic pool. Thus, small perturbations in the production and consumption of DOM could strongly affect the balance between oceanic and atmospheric CO₂. The processes controlling the production, consumption and distribution of DOM are therefore biogeochemically significant with regards to C storage and export in the ocean interior (Hansell and Carlson 1998).

1.3.1 Role of Marine DOM

DOM has been shown to play an important role in a variety of ocean processes. A significant fraction of the dissolved pool supports microbial food webs, major element cycles (C, N, P) and energy flows (Cho and Azam 1988). Large amounts (>50%) of phytoplankton fixed carbon are released as DOM (Ducklow 1999, Williams 1990) and are routed through microbial activity to higher trophic levels while a small fraction escapes microbial attack and accumulates in the water. Hansell and Carlson (1998) estimated that 17% of global new production escapes rapid microbial attack and builds up in surface waters as DOM where it is then available for export.

Oceanic primary production is thought to be either limited by nitrogen or phosphorus. Thus mechanisms which may deliver new N and/or P to the oceans may impact on the magnitude of oceanic primary production and CO₂ sequestration. The bulk of DOM constitutes an enormous reservoir of nitrogen and phosphorus in the ocean and can act as a direct or indirect source of nutrients to the oceans (Jackson and Williams 1985).

It has been estimated that DON and DOP can sustain up to 50% of export production (Emerson *et al.* 2001) in oligotrophic gyres. The mechanism hypothesised is that enhanced biological production of DON occurs at the equator by increased phytoplankton production fuelled by upwelled nutrients (Rintoul and Wunsch 1991). DON is then exported from the equator via meridional Ekman transport to low nutrient subtropical waters where it may serve as a significant nitrogenous substrate for phytoplankton production. The dissolved organic nutrient pool could serve as a nutrient buffer by slowly releasing inorganic nutrients as bacterial remineralization takes place. In addition, a DOM pool with intermediate or longer turnover times would make the transport of N and P from coastal zones to the open ocean possible.

There is increasing evidence that DOM can be directly utilised as a substrate by some phytoplankton groups suggesting possible ecological advantages for these species (Palenik and Morel 1990; Palenik and Henson 1997; Karl *et al.* 2001). Picoplankton such as *Synechococcus* and *Prochlorococcus* are the most abundant autotrophic organisms in oligotrophic oceans (Partensky *et al.* 1999). The versatility of these organisms has been related to their ability to grow over a wide range of light conditions and utilise a wide variety of nitrogen sources (Gilbert *et al.* 1986) such as urea (Collier *et al.* 1999) and amino acids (Pearl 1991; Montesinos *et al.* 1997). Several *Synechococcus* strains have been reported to express ectoenzymes, such as aminopeptidase activity, to hydrolyse DOM components (Martinez and Azam 1993). Current knowledge on *Prochlorococcus* *sp.* nutrient assimilation is increasing (Rippka *et al.* 2000), it is now recognised that some strains can utilise both NH_4^+ and urea (Moore *et al.* 2002). Interestingly some strains, adapted to high light conditions, lack the genes required for nitrate utilisation, thus the utilisation of organic forms of nitrogen is very probable. Recently, the entire genome of certain strains of *Synechococcus* (WH8102; Palenik *et al.* 2003) and *Prochlorococcus* *sp.* (Moore *et al.* 2002) have been sequenced and their ability to use amino acids and oligopeptides has been inferred due to the discovery of several transporters. *Synechococcus* *sp.* contains genes for the transport of phosphonates (compounds with C-P bonds) important constituents of the DOP pool (Clark *et al.* 1998). Genome analyses have further demonstrated the presence of alkaline phosphatase, an enzyme required for the break down of organic phosphorus compounds. Although these genes have been found it is not known if they are functional in the marine environment, however their detection has increased our understanding of the possible new links and pathways of DON and DOP in the marine N and P cycle.

1.3.2 DOM Composition and Lability

Dissolved organic nutrients form a diverse pool of material which is highly variable in size and composition. The turnover time of different constituents varies greatly (Bauer *et al.* 1995). A conceptual model describes the DOM pool as composed of 3 fractions of varying lability; labile, semilabile and refractory (Benner *et al.* 1992).

The labile fraction has a turnover time of minutes to days, it is composed of both HMW (high molecular weight) and LMW (low molecular weight) compounds and supports mainly heterotrophic bacterial growth (Amon and Benner 1994, Keil and Kirchman 1999, Skoog *et al.* 1999). The semilabile pool is potentially important for the export of organic material as it resists rapid microbial degradation; has a turnover time of months or years and

is composed mainly of carbohydrates (Benner *et al.* 1992) and heteropolysaccharides (Aluwihare *et al.* 1997).

The turnover time of the biologically refractory pool is on time scales of centuries to millennia (the time scale of ocean mixing and greater than ocean mixing). This pool is dominated by chemically uncharacterised LMW compounds (Benner *et al.* 1992, Amon and Benner 1994, 1996). On average the ^{14}C age of DOM isolated from deep water masses varies from 4000 radiocarbon years in the Atlantic to approximately 6000 radiocarbon years in the Pacific (Druffel *et al.* 1992). The age difference between the two basins is roughly equal to the time of the deep ocean thermohaline circulation (Broecker and Peng 1982). This finding has highlighted that a large fraction of DOM escapes degradation and is transported conservatively within the ocean's conveyor over several ocean mixing cycles (Hansell and Carlson 1998).

1.3.3 DOM Production and Removal Processes

The accumulation of DON and DOP in the oceans is the result of spatial and temporal decoupling of production and removal processes. DON and DOP are principally produced in the ocean's euphotic zone by a variety of biological processes, such as microbial degradation and transformation of particulate organic material, exudation by phytoplankton (Williams 1990) and zooplankton grazing of phytoplankton (Hasegawa *et al.* 2000). Several lines of evidence support the production of DON by diazotrophs, N_2 fixing organisms (Abell *et al.* 2000, Hansell and Waterhouse 1997, Karl *et al.* 1997, Vidal *et al.* 1999). Results from laboratory studies have shown that up to 50% of the fixed N can be released as DON (Capone *et al.* 1994, Glibert and Bronk 1994). However DOM concentrations, in general, are not directly correlated with phytoplankton biomass or primary productivity (Carlson *et al.* 1994) suggesting that DOM pools are the products of complex interactions between physical, chemical and biological processes.

DON and DOP can be removed from the water column by diverse chemical and biological processes such as photoxidation (Mopper *et al.* 1991), phytoplankton assimilation (Antia *et al.* 1991) and microbial respiration which is considered the main sink for recently produced DOM (Azam *et al.* 1983). The factors that contribute to a slow consumption of organic material can be:

1. Limitation of heterotrophic bacterial growth
2. Biological production of recalcitrant organic material
3. Abiotic production of recalcitrant organic material

In a perfect heterotrophic system, with an efficient microbial loop, there would be no accumulation of organic matter. However, in most of the oceanic regimes this is not the case. Thingstad and Sakshaug (1990) have pointed out that the availability of N and P may control mineralization of organic matter. As proteins and polynucleotides are readily remineralized from organic matter to NH_4^+ and PO_4^{3-} the remaining, more refractory, organic material has a low N and P content relative to C. The bacterial mineralization of this refractory pool demands the uptake of N and P. Depending on the C/N/P ratios of the substrate, bacteria compete with primary producers for essential inorganic macro-nutrients (Anderson 1992). Thingstad *et al.* (1997) proposed a hypothesis: “the malfunctioning microbial loop”. According to this hypothesis bacterial carbon consumption is restricted due to food web mechanisms controlling both growth and biomass of bacteria: bacterial growth rate is kept low by bacteria-phytoplankton competition for mineral nutrients, and bacterial biomass is kept low by bacterial predators.

The release of metabolically resistant polysaccharides has been observed in marine diatom cultures (Aluwihare *et al.* 1997) and appears to be an important component of oceanic DOM (Aluwihare *et al.* 1997). Also, extracellular release of cellular wall material may be one source of refractory DOM (Biersmith and Benner 1998). Bacterial derived compounds such as porines and peptidoglycans, are commonly found in oceanic basins (Ogawa *et al.* 2001, Tanoue *et al.* 1996). Several physical mechanisms are also responsible for the production of refractory material. Exposure to UV irradiation may enhance condensation reactions of small molecules into recalcitrant macromolecules (Keil and Kirchman 1994). However in some experiments Benner and Biddanda (1998) found that exposure of DOM samples from different depths produced contrasting results. Hence it was suggested that, the effect of UV on DOM lability and bioavailability appear to be affected by the molecular composition of the organic material (Obernosterer *et al.* 2001).

1.3.4 DOM Global Distribution

Despite many advances in understanding the factors that affect DOM accumulation, our understanding of the interaction of these factors on the control of global DON and DOP distributions are still incomplete. DON concentrations for surface oceans generally range from 0.8 to $13\mu\text{M}$ with a mean of $5.8\pm2\mu\text{M}$ (Table 1.1). The lowest concentrations are found in the open ocean and the highest in estuaries.

Oligotrophic tropical environments do not show seasonal variability in DOM concentrations given the scant overturning of the water column. However seasonal

accumulations are likely to occur in subtropical areas and at high latitudes. Dissolved organic nitrogen and phosphorous concentrations found in different oceanic systems are shown in Table 1.1 and Table 1.2 respectively. Values are often reported as TON and TOP as the filtration step in oligotrophic environments is commonly omitted. In these areas the particulate pool is small (<10%) compared to the risk of contamination and cell breakage during filtration (Abell *et al.* 2000). DOP concentrations in the upper 100m average 0.20-0.22 μ M and represent 70-80% of the TDP pool.

Table 1.1 Literature values of total dissolved nitrogen (TDN, μ M), total organic nitrogen (TON, μ M) and DON/TDN ratio (%). Methods of oxidation of organic matter are also reported: UV=UV oxidation, PO=persulphate oxidation, HTCO=High temperature catalytic oxidation, HTO=High temperature oxidation.

Location	Depth (m)	TDN μ MN	TON μ MN	DON/TDN %	Method	Reference
W. Pacific 10-20S	Upper 50		5.4 \pm 0.3		UV	(Hansell & Feely 2000)
W. Pacific 25-35S	Upper 50		4.84 \pm 0.4		UV	(Hansell and Feely 2000)
E.N Pacific	Upper 85	11 \pm 6.4	4.1 \pm 0.5	48 \pm 29.5	PO	(Loh and Bauer 2000)
Subtrop. Pac.5-21N	Upper 50	5.8 \pm 1.4	5.5 \pm 0.91	97.9 \pm 10.8	UV	(Hansell and Waterhouse 1997)
Equatorial Pac.	Upper 50	16 \pm 6.1	5 \pm 0.71	36.4 \pm 15.6	UV	(Hansell and Waterhouse 1997)
Equatorial Pac.	Upper 40	13.9 \pm 4	8.4 \pm 1	66 \pm 22	PO	(Libby and Wheeler 1997)
Subtropical Pac.	Upper 150	4.8 \pm 0.4	4.5 \pm 0.42	96.6 \pm 8.9	UV	(Hansell and Waterhouse 1997)
Subpolar Pac.	Upper 50	18.3 \pm 6.8	4.3 \pm 0.59	28.5 \pm 14.3	UV	(Hansell and Waterhouse 1997)
Subtrop. Pac. gyre	Upper 50	5.3-6.3	5.2-6.2	98	UV	(Abell <i>et al.</i> 2000)
S. Ocean polar front	Upper 200		6.9-11		HTCO	(Kahler <i>et al.</i> 1997)
Southern Ocean	Upper 150	28.4- 32.8	3.2-6	8-15	HTCO	(Ogawa <i>et al.</i> 2001)
Ross Sea Polynya	Upper 150		2.1-6.3	8-23	UV	Carlson and Ducklow 1995)
Antarctic waters	Upper 100		3.9 \pm 1.3		PO	(Hubberton <i>et al.</i> 1995)
Drake Passage	Upper 50		3.1-7.3	10.25	UV	(Sanders and Jickells 2000)
North Atlantic Sargasso Sea (BATS)	surface		4.4 - 7.4		HTO	(Kahler <i>et al.</i> 1997)
	surface		4-5.5	>95	UV	(Hansell and Carlson 2002)
Equatorial Atla.	Upper 100		5.2-10.9	20-90	PO	(Vidal <i>et al.</i> 1999)
Pac.HMW DON	Upper 100		1.2 \pm 0.2		UV	(Benner <i>et al.</i> 1997)
Atlantic HMW DON	Surface		1		UV	(Benner <i>et al.</i> 1997)
Average		14.2 \pm 9.4	5.8 \pm 2	61.6 \pm 32.9		

Table 1.2 Literature values of TOP concentration and DOP/TDP ratios (%) in oceanic environments. Methods of oxidation of organic matter are also reported: UV=UV oxidation, PO=persulphate oxidation.

Location	Depth (m)	TOP μM	DOP/TDP %	Method	Reference
Southern Ocean	surface	0.16			
	300	0.10		UV	(Sanders and Jickells 2000)
	500	bdl			
North Pacific Subtropical gyre	Surface	0.27			
	100	0.21		UV	(Williams 1990)
	900	0.12			
North Pacific Subtropical gyre	5000	0.22			
	Upper 200	0.18		UV	(Jackson and Williams 1985)
North Pacific Subtropical gyre	0.100	0.15-0.20	57-60	UV	(Smith <i>et al.</i> 1986)
North Pacific Subtropical gyre	Upper 50	0.10-0.35		UV	(Abell <i>et al.</i> 1999)
Gulf Stream	20	0.10		UV-PO	(Ridal and Moore 1990)
NW Mediterranean	surface	0.13	95	PO	(Raimbault <i>et al.</i> 1999)
Sargasso Sea	surface	0.1-0.5	>95	UV	(Cavender-Bares <i>et al.</i> 2001)
Pacific Subtropical gyre	surface	0.074±0.04	99	UV	(Wu <i>et al.</i> 2000)
Average		0.21	75		

Both TON and TOP concentrations decrease with depth in the water column and seem to be inversely correlated to NO_3^- and PO_4^{3-} concentrations. Numerous observations link the depletion of NO_3^- and elevations in N_2 fixation rates to DON accumulation in surface waters (Libby and Wheeler 1997, Karl *et al.* 1997, Bronk *et al.* 1998, Butler *et al.* 1979). A significant correlation between TON concentrations and apparent oxygen utilisation has also been observed (Abell *et al.* 2000). It has been suggested that TON and TOP distribution is primarily the result of the respiration of organic matter (Abell *et al.* 2000) and has been observed that DOP concentrations in general are higher in the North Pacific in comparison to the North Atlantic (Karl *et al.* 2001). This distribution may result from the build up of refractory material along the “conveyor belt” global circulation pattern (Hansell and Carlson 2001).

1.3.5 Stoichiometry

Whether DON and DOP degradation in the ocean follow a Redfield stoichiometry is not known. Sanders and Jickells (2000) compared data from the Drake Passage and the HOTS site in the North Pacific and suggested that a labile surface DON and DOP pool was following a Redfield-type stoichiometry. However generally C: N: P ratios of the organic pool

vary spatially and temporally suggesting shifts in the relative importance of heterotrophic metabolism relative to autotrophic metabolism (Libby and Wheeler 1997). DOP and DON appear to have different turnover rates (Smith *et al.* 1986) and, as a result, are weakly coupled when compared to the inorganic and particulate organic forms of these elements. This weak coupling may result in export rates that diverge from the Redfield stoichiometry (Vidal *et al.* 1999), thereby leading to differential relative losses of nitrogen and phosphorus below the thermocline.

The traditional view of DON and DOP as large refractory pools is rapidly changing. The picture that is emerging is of a pool that is a dynamic component of elemental cycles. However there still exist many unresolved key questions with regards to its size, distribution, and controls over its stoichiometry and bioavailability. Uncertainty in the knowledge of DON and DOP cycling limits our ability to adequately describe the global cycle of N and P (Jackson and Williams 1985).

1.4 Thesis Goals

Despite our increasing knowledge there is still no quantitative appreciation of the role of DON and DOP on nutrient cycling in oligotrophic gyres. Understanding the origin and reactivity of the dissolved organic nutrient pool is critical because this pool is one of the largest reservoirs of nutrients and carbon in the ocean. Furthermore, small changes in the marine organic nutrient pool can potentially effect a large change in other pools (for example CO₂ and inorganic nutrient availability) and have important ecological implications on for example, CO₂ draw-down and changes in community structure (Karl *et al.* 2001, Church *et al.* 2002). Clearly there is much work to be done defining the mechanisms of the processes that contribute to DOM accumulation and, more importantly, quantifying the rates of DOM cycling.

The aim of this thesis is to contribute to the observational database in order to address fundamental questions as to how dissolved organic nutrients influence the N and P budget, how they affect the nutrient cycling and the sustainment of biological production within two major ocean oligotrophic gyres: the Southern Indian Ocean gyre and the subtropical North Atlantic gyre.

The sampling location and collection information for each cruise and the analytical methods used are reported in Chapter 2.

In Chapter 3, the factors controlling the large-scale storage and distribution of dissolved organic nutrients at the southern margin of the subtropical Indian Ocean have been assessed. Nutrient imbalances, with respect to the classical Redfield ratio, of the total N and P pools have been investigated and the role of DOM advection in supporting export production has been assessed. An Indian Ocean nitrogen budget has been estimated. The Indian Ocean is a complex system where important biogeochemical transformations that have significant global implications take place. In this basin, a large contribution to denitrification in the world oceans occurs (Naqvi *et al.* 1987) and the potential for N₂ fixation is high (Gruber and Sarmiento 1997). However, the balance between these processes, responsible for the regional N budget, remains to be elucidated. In this study, the distribution and the inventories of TON and TOP, in conjunction with inorganic nutrient concentrations and the calculation of the physical transport across the hydrographic section (McDonagh *et al.* 2005), allowed the estimation of N transport across the Southern border of the Indian Ocean at 32°S. The balance between N₂ fixation and denitrification in this basin is discussed based on a mass balance approach and the role of DON transport in the nitrogen budget is identified.

In Chapter 4, the large scale studies on the distribution of organic nutrients are complemented by small-scale experiments to define the rates of maximum potential mineralization of DON and DOP in the oligotrophic North Atlantic. The long standing questions on the magnitude of N₂ fixation and the mechanisms that provide nutrients to the euphotic zone in the North Atlantic subtropical gyre are assessed. The primary objectives of this chapter were to 1) quantify large scale N₂ fixation rates 2) determine the spatial distribution and the relative importance of N₂ fixation as a mechanism for supplying N to the surface layer of the subtropical gyre 3) quantify the role of DON and DOP as nutrient sources to the North Atlantic gyre. The first issue has been addressed by using the quasi-conservative tracers DINex and TNex, that integrate over space and time, to provide large-scale constraints on N₂ fixation. To compute actual fixation rates, excess nitrogen was combined with the water ventilation age using two different approaches. The first approach is a novel method that uses total nitrogen excess in the upper 1000m to estimate the net amount of N provided by N₂ fixation. This technique has the major advantage of including the organic nutrient pool in the N inventory, which is a major constituent in the upper ocean and is known to be an important

fraction released by N_2 fixers. Moreover, it unambiguously reflects the balance between N and P inputs into the system. The second approach consists of an isopycnal two end member mixing model as used by Hansell *et al.* (2004), however it evolves from the latter as organic nutrients are included in the analysis. The spatial distribution of N_2 fixers is assessed by measuring the stable isotopic $PO^{15}N$ signal and phytoplankton pigments as markers for diazotrophy. The relative importance of N_2 fixation, as a source of N to phytoplankton biomass, has been identified using a two end member isotopic model. The third objective is addressed by relating the measurement of O_2 production and enzyme activity to estimate the N and P cleaved from organic matter and assess the fraction of primary production potentially supported by organic nutrients. Moreover the potential for DOP in providing a P source for N_2 fixers has been evaluated.

Finally, Chapter 5 contains the conclusions drawn from this study.

2 Methods

Samples were collected along two hydrographic sections that crossed the Subtropical Indian Ocean on cruise CD139 on board RRS Charles Darwin and the North Atlantic subtropical gyre on board RRS Discovery on cruise D279.

Cruise CD139 crossed the Indian Ocean at 32°S in spring 2002. The CD139 cruise track is depicted in Fig. 2.1

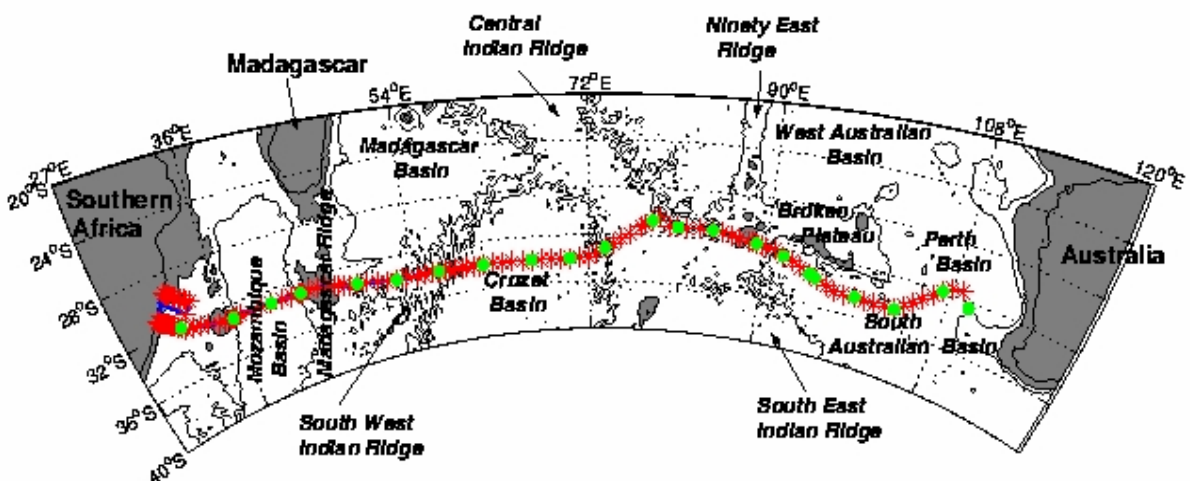


Fig. 2.1 CD139 Cruise track and bathymetry. CTD stations occupied during the cruise are shown by the red stars. The green dots represent stations where Argo floats were released.

Cruise CD139 consisted of 146 full depth CTD casts with discrete samples taken at up to 24 depths using Niskin bottles. Samples for dissolved oxygen, nitrate and nitrite (hereafter nitrate), and soluble reactive phosphorus (hereafter phosphate) were collected and immediately analysed on board. 300 unfiltered seawater samples for Total Organic Nitrogen (TON) and Total Organic Phosphorus (TOP) were collected directly from Niskin bottles into 60ml high-density sterile polystyrene bottles. After collection samples were frozen (-20°C) and stored for a period of 4-6 months prior to analysis. On half of the stations, at 4 depths in the euphotic layer, 5l of water were collected from Niskin bottles and filtered for chlorophyll and photosynthetic pigments analyses. Filters were immediately frozen (-80°C) and were analysed within 4 months.

The North Atlantic subtropical gyre was surveyed along the nominal latitude of 24.5°N in April-May 2004 (Fig. 2.2). During D279 125 full depth CTD stations were occupied

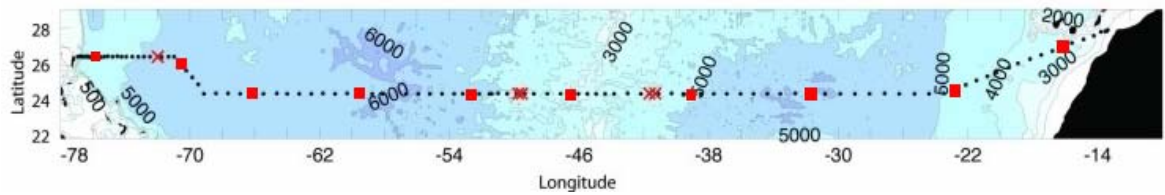


Fig. 2.2 D269 Cruise track and bathymetry. CTD stations occupied during the cruise are shown by black dots. Stations where enzyme assay experiments were carried out are shown by the red boxes, red crosses represent stations where Argo floats were released.

At each station up to 24 water samples were collected in Niskin bottles for the analysis of oxygen, salinity, nitrate, silicate, phosphate and total organic nutrients (TON and TOP). From the top 200m, a total of 300 samples for the determination of phytoplankton pigments were collected directly from Niskin bottles.

From the shallowest (~10m) Niskin bottle, a total of 30 suspended particulate matter (SPM) samples were collected for the determination of the natural isotopic abundance of PO^{15}N . At 9 stations, depicted as red squares on the cruise track (Fig. 2.2), samples were collected directly from the surface (0m) in 25l high density plastic carboys to carry out simultaneous experiments for the determination of DOM hydrolysis through enzyme assays and primary production. During these experiments, samples for the determination of phytoplankton community structure (phytoplankton pigments), DOM concentrations and $\delta\text{PO}^{15}\text{N}$, were also collected.

On both cruises dissolved oxygen, inorganic and organic nutrients and photosynthetic pigments were collected and analysed following the same procedures.

2.1.1 Oxygen and Inorganic Nutrients

Dissolved oxygen was measured on all Niskin bottles samples from all the CTD casts according to the Winkler method using a semi automated whole bottle Winkler titration method with a spectrophotometric endpoint detector manufactured by SIS. The precision of this method was 0.38% for both cruises.

Unfiltered samples for inorganic nutrients ($\text{NO}_3^- + \text{NO}_2^-$ hereafter nitrate, PO_4^{3-} hereafter phosphate, and Si(OH)_4 hereafter silicate) analyses were collected from all bottles on all the CTD casts. Inorganic nutrient concentrations were measured immediately on board using a Skalar San Plus autoanalyser according to standard colorimetric techniques described by Kirkwood *et al.* (1996). The analytical precision, based on the coefficient of variation (CV) of replicate analysis of a single sample, was 1.1% for nitrate and 0.9% for phosphate. The

detection limit of the analyses, calculated as three times the noise of the baseline, was 0.1µM for nitrate and 0.01µM for phosphate.

2.1.2 Pigments

Approximately 5 litres of seawater were collected from 4 different depths for each station and filtered onto GF/F filters for HPLC analysis of photosynthetic pigments. After collection the filters were immediately frozen at -80°C. The stored frozen filters were placed into 15mL centrifuge tubes and 2mL of 90% HPLC grade acetone were added. The samples were then sonicated for 30 sec and centrifuged for 10min at 3000rpm to complete the pigment extraction. The pigment extract was then injected into HPLC vials and loaded onto a constant temperature (2°C) auto-sampler. The pigments were separated and analysed by HPLC according to Barlow *et al.* (1997), to allow the resolution of a large range of key pigments including the separation of mono and divinyl-chlorophylls and the resolution of lutein and zeaxanthin. The HPLC was a ThermoFinigan HPLC system and comprised a Perkin Elmer C18 column, for pigment separation a UV detector (UV6000 diode-array) and a fluorometer (FL3000) supported by Chromquest 4.0 software.

Phytoplankton pigments have strong chemotaxonomic associations with specific phytoplankton groups thus are widely used as biomarkers to characterize the phytoplankton community. Biomarker pigments separated during the analysis are reported in Table 2.1.

Table 2.1 Chemotaxonomic pigments resolved during the HPLC analysis following Barlow *et al.* 1997. Their occurrence in phytoplankton groups is also reported.

Pigment	Abbreviation	Occurrence
Alloxanthin	ALLO	Cryptophytes
19'-Butanoyloxyfucoxanthin	BUT	Chrysophytes, prymnesiophytes
Chlorophyll <i>a</i>	CHL <i>a</i>	Total algal biomass (including cyanobacteria)
Chlorophyll <i>b</i>	CHL <i>b</i>	Chlorophytes, prasinophytes
Chlorophyll <i>c1 c2</i>	CHL <i>c2</i>	Diatoms, prymnesiophytes, chrysophytes, dinoflagellates
Chlorophyll <i>c</i>	CHL <i>c3</i>	Prymnesiophytes, chrysophytes
Diadinoxanthin	DIADINO	Diatoms, dinoflagellates, prymnesiophytes, chrysophytes
Diatoxanthin	DIATO	Diatoms, dinoflagellates, prymnesiophytes, chrysophytes
Divinyl chlorophyll <i>a</i>	DvCHL <i>a</i>	Prochlorophytes
Fucoxanthin	FUC	Diatoms, prymnesiophytes, chrysophytes
19'-Hexanoyloxyfucoxanthin	HEX	Prymnesiophytes
Lutein	LUT	Chlorophytes, prasinophytes
Peridinin	PER	Autotrophic dinoflagellates
Violaxanthin	VIO	Chlorophytes, prasinophytes
Prasinoxanthin	PRAS	Prasinophytes
Zeaxanthin	ZEA	Cyanobacteria, prochlorophytes

Diagnostic pigments, which are the taxonomic pigments specific to phytoplankton groups, were derived to assess the chemotaxonomic composition of the phytoplankton community according to Barlow *et al.* (2004) for samples collected during cruise D279 in the North Atlantic. In particular they were calculated from the sum of 7 biomarker pigments:

$$DP = \text{Allo} + \text{But} + \text{Chlb} + \text{Fuc} + \text{Hex} + \text{Per} + \text{Zea}$$

The proportion of the major phytoplankton size classes, Microplankton, Nanoplankton and Picoplankton, were derived, following Barlow *et al.* (2004), as:

$$\text{Microplankton fraction} = (\text{Fuc} + \text{Per})/DP$$

$$\text{Nanoplankton fraction} = (\text{All} + \text{But} + \text{Hex})/DP$$

$$\text{Picoplankton fraction} = (\text{Chlb} + \text{Zea})/DP$$

2.1.3 Total Nitrogen (TN), Total Phosphorus (TP) and Total Organic Carbon (TOC)

Samples for DON, DOP and DOC analysis were carefully collected directly from Niskin bottles into 60-ml sterile high-density polythene bottles. Sample bottles were rinsed with three times their own volume of sample and immediately frozen. As contamination is the primary concern, these samples were not filtered thus the results represent total organic nitrogen (TON) and total organic phosphorus (TOP). This is a common procedure in oligotrophic waters where the particulate pool is generally considered negligible (<10% of the total N and P pool; Abell *et al.* (2000), whereas the risk of contamination or cell breakage during filtration is very high (Abell *et al.* 2000).

Dissolved organic matter is not analysed by a standard routine nutrient determination procedure. Consequently, for analysis, the organic material in the samples must be subject to a decomposition procedure and subsequent determinations of the inorganic components are required. The result is the total amount (organic and inorganic) of the respective nutrient (TDN and TDP). The organic concentration (TON and TOP) is calculated by subtracting the inorganic concentration (nitrate and nitrite or phosphate) from the total (TDN and TDP):

$$[TON] = [TDN] - [DIN];$$

$$[DIN] = [NO_3^- + NO_2^-];$$

As calculated here, TON includes also dissolved ammonium. However, due to the rapid cycling of ammonium in the surface layer of oligotrophic gyres, the ambient concentration of NH_4^+ was anticipated to be below detection limit ($0.12\mu\text{M}$) of the TDN. Therefore the contribution of this fraction to the TON measurements is considered to be small.

As each of the measurements has an associated analytical error, TON concentration estimates have an error given by the combined uncertainty of 2 analyses TN and DIN. Thus the standard deviation is calculated as:

$$SD_{TON} = \sqrt{(SD_{TDN}^2 + SD_{DIN}^2)} \quad \text{Eq. 2.1}$$

The same basic principle holds for the measurement of DOP. In eutrophic environments or in deep waters, concentrations of inorganic nutrients are many times the concentration of the TON and TOP pool. Under these circumstances DON and DOP concentrations have high standard deviations and negative concentrations can be calculated (Hansell *et al.* 1993).

Two oxidation techniques were used and compared in this study: the High Temperature Catalytic Oxidation (HTCO) method and the UV-photoxidation. The HTCO technique is known to have the highest oxidation efficiency for the most refractory compounds (Bronk *et al.* 2000), whilst some refractory compounds such as urea and EDTA have been reported to be refractory to UV oxidation (D'Elia *et al.* 1977). The HTCO technique allows only the measurement of TON while the UV-oxidation technique permits the measurement of both TON and TOP. As the best recovery of TN was measured during HTCO, and as the HTCO method is less prone to sampling contamination due to less chemical manipulations (Sharp 1997), only the HTCO oxidised TN samples were used for further data analysis.

2.1.3.1 Ultraviolet (UV) Photoxidation

The UV oxidation method oxidises organic N and P to dissolved inorganic nitrogen (hereafter nitrate) and soluble reactive phosphorus (hereafter phosphate) using high intensity ultraviolet light at a wavelength below 250nm in a Metrohom UV705 digester. Nitrate and phosphate generated by the oxidation process are then analysed by automated standard colorimetric techniques.

This method can be carried out in the presence of excess oxygen with the addition of H_2O_2 and other oxidising reagents such as potassium persulphate.

In this study, a number of preliminary analytical tests were carried out to determine the best UV-oxidation analytical procedure to process the field samples.

UV Oxidation Preliminary Tests

Tests were made on standard compounds to evaluate the efficiency of the UV oxidation method with or without additions of oxidising reagents for the measurement of TN and TP. The methods compared were:

- Ultraviolet oxidation (UV)
- UV oxidation with the addition of H_2O_2
- UV oxidation with the addition of Potassium persulphate

Each method has been evaluated on the basis of blanks, oxidation efficiency of standard compounds and analytical recoveries of the inorganic nutrient. Oxidising reagents were added to standard model solutions. The model solutions used for the analyses were MQ water, caffeine (dissolved in MQ and LNSW) and low nutrient seawater (LNSW). Each test was made using 10ml of the model solution and variable aliquots of the different oxidising reagents. Model solution and oxidising reagents were pipetted into acid washed quartz sample tubes. Tubes were capped with graphite stoppers, placed in the UV system and oxidised for 2 hours following Sanders and Jickells (2000). Temperature was kept constant at 90 °C.

The efficiency of the UV oxidation with the addition of H_2O_2 was tested using different aliquots (50,100, 500 μl) of 30% H_2O_2 (Armstrong and Williams 1966).

UV oxidation combined with the addition of persulphate in an alkaline medium was tested following the general protocol of Valderrama (1981), 1.6ml of the oxidising reagent was added to 10ml samples. However the preparation of the oxidising reagent was slightly modified according to Ridal and Moore (1990). The original Valderama (1981) method used high concentrations of persulphate (40mg l^{-1}). However, preliminary colorimetric analyses of the samples treated with this high concentration of persulphate showed that the colour development in the phosphate reaction was very slow resulting in an underestimation of the phosphate content of the sample. In fact, as noted by previous investigations, the colour development is sensitive to the pH/Molybdenum ratio and is impeded when the ratio is greater than 5 (Koroleff 1983, Ridal and Moore 1990). The decrease in pH is attributed to the decomposition of persulphate into sulphuric acid.

The preparation of the modified persulphate *oxidising reagent* required: 0.4g of potassium persulphate (Sigma Aldrich #P9392) and 3g of boric acid dissolved into 35 ml 1M NaOH and brought up to a final volume of 100ml with MQ water.

Blanks were measured for each compound by adding a range of volumes of the different oxidising reagent to ultrapure UV irradiated water. In all the solutions tested,

(LNSW, MQ and caffeine) the N blanks increased by 0.4%, ($r^2=0.85$ n=5) with increasing volumes of H_2O_2 . The addition of increasing volumes of H_2O_2 did not influence the P blanks. The addition of persulphate also, had the disadvantage of increasing the blanks, likely as an effect of N contamination (0.9%, $r^2=0.65$, n=4); persulphate addition did not affect the P blanks. The UV technique had zero blanks.

Low Nutrient Sea Water (LNSW) and standard solutions of caffeine were oxidised with the 3 different techniques and compared to evaluate the **Oxidation efficiency**. The recoveries of N compounds obtained with H_2O_2 , persulphate and UV were $83\pm2.6\%$, $85\pm1.3\%$ and $79\pm0.4\%$ respectively. Similarly P recoveries were $41\pm1.1\%$, $63\pm1.5\%$ and $94\pm1.8\%$ for H_2O_2 , persulphate and UV. Hence the coupled persulphate-UV oxidation method had the highest N recovery, while the highest P recoveries were obtained when no oxidising reagent was added (UV only). As previously suggested the addition of persulphate and H_2O_2 probably inhibited colour development in the autoanalyser reaction for the determination of phosphate.

The **Precision** among repeated measurements has been evaluated on the basis of SD (standard deviation) and the CV (coefficient of variation). The UV method had the lowest (average for N and P) CV (3%) followed by H_2O_2 (4%) and finally persulphate oxidation (5%), n=10.

The UV-oxidation only appears less prone to sample contamination than UV-oxidation coupled with the addition of oxidising reagents since it involves less handling and less chemical manipulation. Thus on the basis of these experiments, the UV photo-oxidation without the addition of oxidising reagents was chosen for the determination of all the field samples.

UV Oxidation of Field Samples

All non volumetric glassware used in these analysis were combusted at 550 °C for 4 h. Volumetric flasks were washed overnight in 10% HCl and rinsed with MQ water.

Samples in duplicate were photoxidised according to the method used by Sanders and Jickells (2000). Samples were directly poured into 15ml quartz tubes to eliminate the pipetting step as a possible source of contamination. Up to 12 tubes were capped with graphite stoppers and oxidised in the UV system. During each oxidation samples were irradiated for 2 h at 90 °C with a Metrohom 705 UV digestion system. The UV lamp oxidation efficiency was checked at every oxidation using a dissolved organic phosphorus standard (adenosin-5monophosphate monohydrate AMP; Kerouel and Aminot 1996). Samples were subsequently

analysed for inorganic N and P according to the standard colorimetric techniques using a Skalar San Plus autoanalyser (Kirkwood *et al.* 1996).

The **oxidation efficiency** of the UV lamp was checked by comparing the oxidation of a standard solution (AMP) to the calculated concentration. The recovery of the AMP compound was 94% of P and only 60% of N.

Precision of TN and TP was checked as each sample was run in duplicates. The mean CV was for nitrate, 2% and for phosphate, 7%.

The **Consistency** of the data set was evaluated. The concentration of a bulk nutrient sample collected on WOCE cruise A23, that has been utilised as a reference standard for over 6 cruises, was determined on each run to provide some measure of the *internal consistency* of the dataset. The results of these determinations were Nitrate $35.69 \pm 0.66 \mu\text{M}$, and Phosphate $2.99 \pm 0.08 \mu\text{M}$; these are equivalent to a variability of 1.84% and 2.67% respectively.

2.1.3.2 High Temperature Catalytic Oxidation (HTCO)

This dry combustion method consists of high temperature combustion of organic material with elemental oxygen in the presence of a Pt catalyst.

In the present study measurement of TOC and TON were performed with a Shimadzu 5000A DOC analyser connected in series with an Antek 705E chemiluminescent nitrogen specific detector (Alvarez-Salgado and Miller 1998). The settings are shown in Table 3. This configuration allows the measurement of TOC and TON on the same injection. Samples (10 ml) were acidified with 100 μl of 10% HCl and decarbonated by purging with high purity N₂. The sample was then directly injected (100 μl) onto the Pt-coated catalyst at high temperature (900 °C) in an atmosphere of high purity oxygen. Four injections for each sample were allowed with a flush time of 180 sec.

Table 2.2 Settings for the Shimadzu 5000A DOC analyser connected in series with the Antek (Model#705E) High temperature combustion analyser.

Variable	Setting
Primary gas line	60 psi
Shimadzu O ₂ carrier gas	150 ml/min
Oxygen rotometer (flow controller)	5 psi
Ozone rotometer (flow controller)	4.5 psi
Furnace temperature	950 °C
Sensitivity	50

Quantitative production of CO₂ and H₂O gases occurs under these conditions. A dehumidifier removes the water and a carrier gas sweeps the CO₂ to an infrared gas analyser detector that measures the carbon concentration. The combustion products are then carried through a furnace into the Antek TN analyser. In a low pressure cell the NO produced is partially transformed into NO₂^{*}, which when reverting to the ground state, emits a photon. The chemiluminescent signal, which is proportional to the TN present in the sample, is then measured by a photomultiplier and converted into an electrical signal.

The instruments system and analytical **blanks** were assessed using the ultrapure UV oxidised water used to make up standard solutions. Generally these were <1 μ MN with a CV of 4% and 6.3 μ MC with a CV of 6%.

The instrument **detection limit**, estimated as three times the SD of the blank (Bronk *et al.* 2000), was typically 0.12 μ MN and 1.3 μ MC.

The **oxidation efficiency** was monitored using caffeine standard solutions of similar N concentration to a range of KNO₃ standard solutions. Fig. 2.3 shows the peak area of caffeine standards compared to the peak area of nitrate solution of similar concentration. The slope of the regression line represents the oxidation efficiency. The oxidation efficiency varied from 96% to 100%. Sample concentrations were not corrected for these recovery estimates.

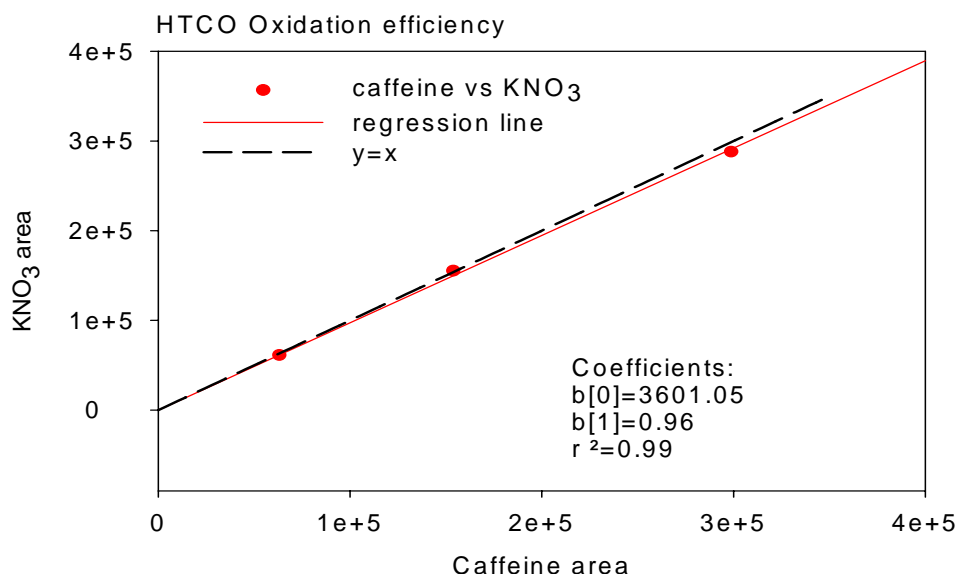


Fig. 2.3 Regression line of caffeine standard solutions vs KNO₃ standard solutions. The slope of the regression line represents the oxidation efficiency (b1), the intercept (b0) represents the blank.

The ***analytical reproducibility*** of the instrument was investigated with 4 replicate injections of the samples. The CV was typically 2% for N and 4% for C. Unfortunately no replication of samples was possible and the added variance due to the subsampling and storage has not been evaluated.

The ***accuracy*** of the HTCO method has been determined by the use of consensus reference (CRM) materials distributed by Dr. Hansell's laboratory, University of Miami. N measurements have an accuracy within 5% of the CRM concentrations. C measurements are less accurate (15%). It must be said that the performance of the HTCO in terms of baselines and calibration curve parameters are highly variable from day to day.

The standard deviation of TON and TOP measurements has been estimated by using the classical error propagation equation (Eq. 2.1). Therefore TON and TOP concentrations incorporate the error of two analyses. The standard deviation of the TON and TOP signal is relatively small when TDN is mainly TON (in the surface waters) and larger when DIN dominates the TDN pool. In surface waters a mean SD for TON and TOP measurements equalled 2.3% and 7% respectively.

2.1.4 $\delta^{15}\text{N}$ PON

During cruise D279 samples were collected for the determination of the natural abundance of ^{15}N in PON from surface niskin bottles (ranging from 10 to 25m) at 30 stations and directly from the surface (0m) during the enzyme experiments that were carried out at 9 locations whilst on board.

Water samples (8 litres) were collected and filtered onto precombusted (550°C for 4 hours) GF/F 47mm filters (Whatman) using a HCl cleaned 1l glass filtration unit. After collection samples were folded in precombusted aluminium foil (550°C, 4 hours) and immediately frozen. Prior to analysis the filters were dried at 60°C for 24h and stored in a desiccator. Stable nitrogen isotopic analysis was performed by a continuous flow isotope ratio mass spectrometer (EA-IRMS) using an Eurovector 3028-Ht elemental analyser connected to a GV Isoprime mass spectrometer at the IRMS facility of the National Oceanography Centre, Southampton. The mass spectrometer was tuned to carry out high sensitivity analyses ($1\text{nA}=5.74\mu\text{gC}$ and $1\text{nA}=1.64\mu\text{gN}$). The filters were cut into 13mm diameter disks, packed into tin capsules and loaded onto the EA autosampler. Samples were run with blank cups and known tyrosine standards in order to correct for the C and N associated with the tin cups and

calibrate for elemental analysis. Blanks were prepared by packing precombusted GF/F (550°C for 4 hours) 13mm filters into tin capsules.

Standards were prepared by weighing (from 1.8 to 90 μ g) of analytical grade tyrosine ($C_9O_3H_{11}N$, mw=181.19, C=59.6685%, N=7.7348%) standards into tin capsules containing 13mm precombusted (550°C for 4 hours) GF/F filters. In Fig. 2.4 a summary of calibration run on different dates are shown.

The results are reported in the standard notation (%), the standard being atmospheric nitrogen N₂ (Mariotti *et al.* 1981):

$$\delta^{15}N\% = \left[\frac{^{15}N/^{14}N_{sample}}{^{15}N/^{14}N_{std}} - 1 \right] \times 1000$$

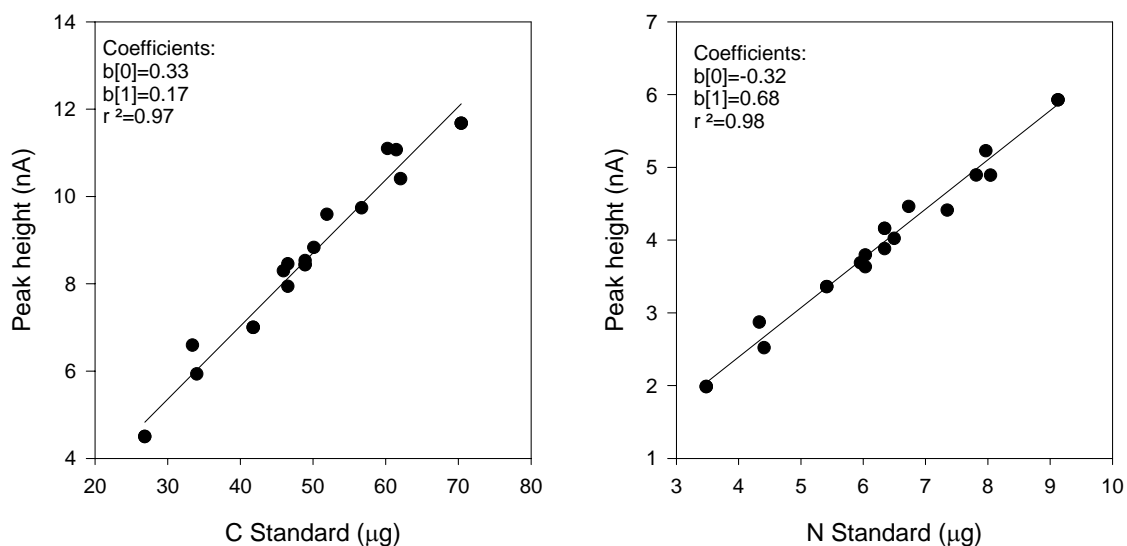


Fig. 2.4 Linear regression of all the standards weights (μ g) and their detection in peak height (nA) used for the calibrations. As all the calibration data are reported here, note the good reproducibility of the calibration curves throughout the analysis of the different batches.

2.1.5 Primary Production

On cruise D279, at 9 stations where enzyme experiments were carried out, gross and net primary production and respiration of sea surface populations were determined by the oxygen evolution and consumption inside borosilicate bottles incubated in light and dark conditions for 12h. Light bottles were incubated in 6 replicates on deck at sea surface temperature and shaded (50% of surface light) from direct light to minimize photoinhibition. Dark bottles, totally shaded from light were incubated under the same conditions.

Respiration was estimated from the difference in oxygen concentration between t_0 and the dark bottles. Net production of oxygen over the course of 12h was estimated as the

difference between the light and the t_0 . Gross production was estimated as the sum of Net production and respiration.

Oxygen was measured by using a semi automated whole bottle Winkler titration unit with spectrophotometric end point detection manufactured by SIS.

2.1.6 Helium

During cruise CD139, approximately 200 water samples were drawn directly from Niskin bottles, through tygon tubing, into copper tubes for helium analysis.

Noble gases (Helium and Neon) were extracted from seawater using a dedicated vacuum system at the Southampton Oceanography Centre Noble gas facility. The objective of the extraction was to transfer all gases dissolved in water (stored in the copper tubes) into glass ampoules so that noble gases can be analyzed on the mass spectrometer system. Prior to extraction all samples were cleaned and weighed.

The samples were then analyzed at the Woods Hole Oceanographic Institution's Helium Isotope Laboratory, during my Woods Hole exchange program sabbatical visit in early 2005, using a mass spectrometer (QMS, Balzers Model QMG-112) for helium isotope analysis. Samples were calibrated against air standards which are prepared by collecting on a weekly basis marine air whilst recording temperature, pressure and relative humidity. Line blanks are run every three hours during sample analysis to determine the magnitude of the blank signal in the machine so it can be corrected for. Manifold blanks are run before the analysis of a sample group to check for leaks in the sample manifold. ^4He concentrations and $\delta^3\text{He}$ (in ‰), have a 0.14% and 0.21‰ uncertainty respectively.

2.1.7 Enzyme Assays

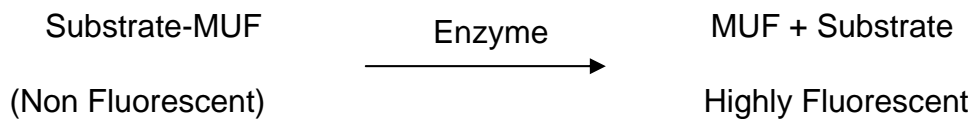
2.1.7.1 Ecto-enzymes in the Marine Environment

The DOM pool in the marine environment is a complex mixture of compounds with variable molecular sizes and lability. The release of either cell surface bound or free extracellular enzymes, by bacteria and phytoplankton (Martinez and Azam, 1993), is the mandatory step towards the hydrolysis of organic matter into monomers that can further support production into the euphotic zone. The marine environment has many important extracellular enzymes specific to various natural substrates (Table 2.3). The introduction of soluble fluorogenic 4-methylumbelliflferone (4-MUF) and 7-amino4-methylcoumarinyl (AMC) derivate as substrates has led to the rapid increase of studies of extracellular enzyme activity in marine environments (Hoppe 2003).

Table 2.3 Common extracellular enzymes, their substrates and products in the marine system.

Enzyme	Substrates	Products
Proteases	Proteins, polypeptides	Polypeptides, amino acids
α/β -glucosidase	Glucose- polysaccharides	Olysaccharides, glucose
Lipase	Lipids	Fatty acids, glycerol
Chitinase	Chitin	N-Acetyl-D-glucosamine
Alkaline phosphatase	Organic phosphates	Inorganic phosphate

In this study, the activities of the enzymes alkaline phosphatase (AK) and aminopeptidase (AP), a specific protease, were determined by measuring the increase in fluorescence over time caused by the release of the fluorescent molecules 4-methylumbelliflferone (4-MUF) and 7-amino4-methylcoumarin (AMC) from the non fluorescent parent molecule:



The substrates used for each enzyme and the wavelength of their detection are reported in Table 2.4

Table 2.4 Substrates (parent molecule) and respective fluorescent molecules. Excitation and emission wavelength for their detection are included.

Enzyme	Substrate	Standard	Excitation nm	Emission nm
Alkaline phosphatase	4-methylumbelliferyl phosphate disodium salt	4-MUF	362	444
Amino-peptidase	l-leucine-7-amido-4-methylcoumarin hydrochloride	AMC	345	438

2.1.7.2 Sampling and Incubation

Water samples for total AKA and APA determination were collected from the sea surface directly into high density plastic bottles at 9 different locations across the N. Atlantic. At each location 3 replicate samples of 3.8 liters were filtered onto precombusted GF/F filters on an acid washed glass 1L filtering system (Millipore). The filters were incubated with 1ml of the filtrate in sterile 10ml culture tubes and the substrates, 4-methylumbelliferyl phosphate disodium salt (4-MUF-P) and l-leucine-7-amido-4-methylcoumarin hydrochloride (L-AMC), were added to a final concentration of 100 μ M. The incubations were carried out in the dark at

room temperature. Sterile ($0.2\mu\text{m}$ -filtered) sea water blank controls were incubated in the same conditions as the samples for each assay. Fluorescence measurements were taken every 5 minutes for 1.5h. At each time step, before the fluorescence reading, to stop the reaction an aliquot ($600\mu\text{l}$) of the incubated sample was mixed with a carbonate stop buffer (1.9ml; final concentration 0.20M). Fluorescence values were converted into μmoles of substrate released $\text{l}^{-1}\text{min}^{-1}$ after calibrating against standard solutions (Fig. 2.5). A flow chart of the analytical steps is shown in Fig. 2.7. The substrate solutions (1mM) were prepared in 50 mM TRIS-HCl buffer solution ($\text{pH}=8.2$). To dissolve the L-leucine-7-amido-4-methylcoumarin hydrochloride salt, it is necessary to add 12mM 2-mercaptoethanol. The substrate stock solutions were stored frozen. The standards stock solutions (1mM) were prepared by dissolving 4-MUF and AMC in 50 mM TRIS-HCl buffer solution $\text{pH}=8.2$ and 12mM 2-mercaptoethanol. The standards were stored at 4°C , away from light.

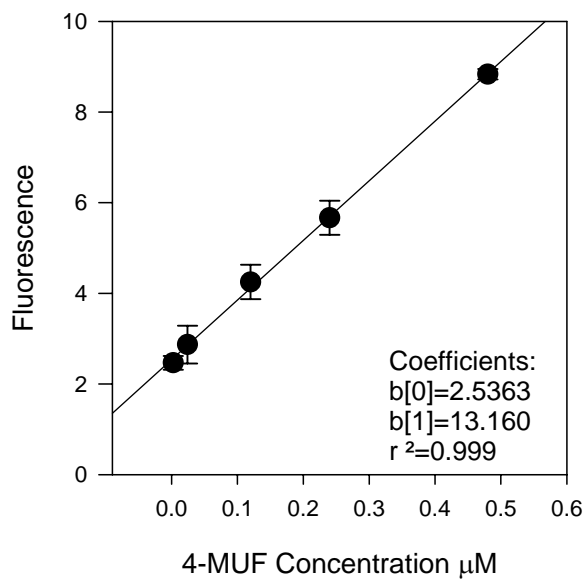


Fig. 2.5 Typical calibration curve used for the conversion of fluorescence into concentration units ($\mu\text{M}_{\text{substrate}}\text{l}^{-1}$).

Fluorescence increased very rapidly in the first half hour until it reached a plateau (Fig. 2.6). Generally, again after a time lag of 80 minutes, a second increase in fluorescence was observed until it plateaued again. This time lag can be interpreted as the time necessary for the community to produce new enzymes required to hydrolyse the remaining substrate. Potentially this time lag may represent the residence time of the most labile fraction of DOM.

The activities of the enzymes were determined from the slope of the best fit of the data points before the fluorescence plateau. The specific activity is the activity normalised to the

biomass expressed as chlorophyll *a*. The curve plateau represents the maximum amount of substrate released by the enzyme present in the sample. This value normalised to the biomass is an index of the amount of enzyme released in the environment per unit biomass.

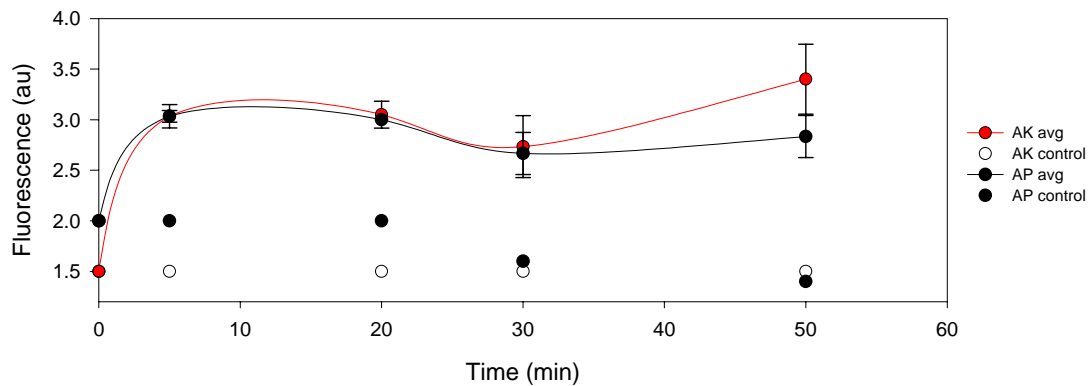


Fig. 2.6 Fluorescence increase over time. The enzyme activity was determined from the best fit of the data points before the plateau. The controls are also shown.

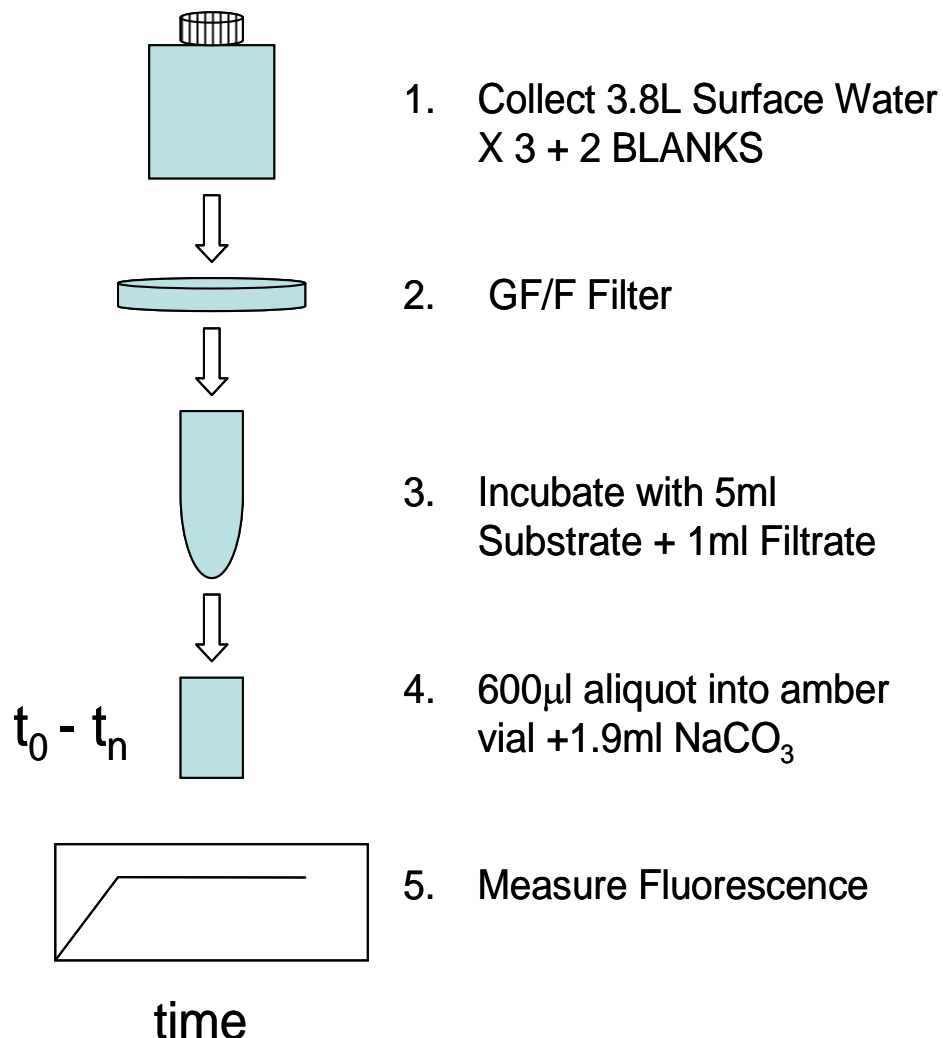


Fig. 2.7 Flow chart of the methodology followed during enzyme assays experiments.

3 Indian Ocean

3.1 Introduction

The marine N inventory is maintained by inputs of fixed N from the combination of N₂ fixation and other minor sources including, riverine input and atmospheric deposition, and losses through denitrification and sedimentation (Codispoti 1995).

Several recent studies however, indicate that at present the oceanic denitrification rate exceeds the oceanic rate of N₂ fixation, implying that the oceans are losing nitrate rapidly. It has been estimated that about 2% of the current stocks of nitrate are being removed each century (Galloway *et al.* 2004). If this imbalance is not occurring, either the oceanic denitrification rates are overestimated or the rates of N₂ fixation must be higher than previously measured (Codispoti *et al.* 2001).

The quantitative contribution of N₂ fixation to the N marine cycle is still poorly constrained. There is growing evidence that the marine N₂ fixation is more important than previously thought (Capone *et al.* 1997; Karl *et al.* 2002). Common accepted rates now range between 100 and 200 Tg Nyr⁻¹ (Capone *et al.* 1997; Falkowski 1997; Gruber and Sarmiento 1997; Karl *et al.* 2002). However there are large discrepancies between direct field studies, limited in time and space and the indirect geochemical estimates of N₂ fixation that integrate over larger time and spatial scales. Indirect geochemical estimates have been based on the quasi conservative tracer N* which quantifies the N to P ratio anomalies inferred to be caused by N₂ fixation and denitrification processes (Michaels *et al.* 1996; Gruber and Sarmiento 1997), stable N isotopic measurements (Altabet 1988; Karl and Yanagi 1997; Altabet *et al.* 2002) and ecosystem models (Hood *et al.* 2004). Direct measurements of N₂ fixation have been mostly performed on the planktonic cyanobacterium *Trichodesmium*. *sp*. However, it has recently been discovered that diazotrophic heterotrophic bacteria, coccoidcyanobacteria and symbiotic associations between phytoplankton and cyanobacteria can all contribute to marine N₂ fixation (Zehr *et al.* 2001).

Recent estimates of global denitrification range from 280 TgNyr⁻¹ (Brandes and Devol 2002) to 300 TgNyr⁻¹ (Codispoti *et al.* 2001) due to benthic denitrification 75TgNyr⁻¹ (Brandes and Devol 2002) and to 150TgNyr⁻¹ (Codispoti *et al.* 2001) due to pelagic denitrification. These estimates have highlighted the possibility of an imbalance of about 100 to 200Tg Nyr⁻¹ in the present marine nitrogen budget. However, uncertainties in these terms are large and it is therefore unclear whether such an imbalance exists (Falkowski 2000.; Codispoti *et al.* 2001), or whether, any of the source/sink terms have been under/overestimated (Brandes and Devol

2002) or whether the N cycle oscillates between excess N₂ fixation and excess denitrification periods (Karl *et al.* 2002). It has been suggested that on geological time scales, due to the strong interaction and feedbacks between the N cycle and the atmospheric CO₂ inventory, the switches between two modes (high fixation-high denitrification) could force the climate system into glacial/interglacial transitions (Altabet *et al.* 1999; Michaels *et al.* 2001.)

Along with the recent estimates of N₂ fixation and denitrification, the average residence time of N in the oceans has been calculated as being as of the order of 1500 to 5000 yr (Galloway *et al.* 2004). As a consequence of this short residence time, any imbalance in sources and sinks of the marine N cycle also has potential implications for marine productivity and atmospheric CO₂ drawdown over short time scales (Devol 2002).

The Indian Ocean is an important site where important biogeochemical transformations take place. In this basin a large fraction of the global denitrification takes place and the potential for N₂ fixation is high.

The Indian Ocean has a unique setting, unlike other oceans it is blocked by landmasses on the northern side and is disconnected from the Arctic environment. In this ocean an annual reversal of the wind regime occurs. Thus the climate is dominated by the northeast monsoon from December through to April and the southwest monsoon from June to October. These geographical and climatological characteristics give to this basin unique physical qualities inducing a shallow overturning circulation (Schott *et al.* 2002). The subduction of water masses in the Indian Ocean occurs mostly in the southern hemisphere; upwelling does not occur along the equator but rather in the northern hemisphere during the summer months off the coasts of Somalia, the Arabian Peninsula and India, leading to high biological productivity and production of organic matter in these regions (Schott *et al.* 2002).

These characteristics contribute to the formation of special ecological niches where biogeochemical transformations take place and make this region globally significant for the cycling of marine elements. A strong minima in oxygen concentration occurs from 150 to 1000m in the Arabian Sea, with high rates of water column denitrification (Naqvi 1987; Mantoura *et al.* 1993). Low concentrations of oxygen are also found in the Bay of Bengal. Although few studies of denitrification have been carried out, the Bay of Bengal may also contribute significantly to oceanic denitrification (Hattori 1983), although no active denitrification has yet been found in this region (Naqvi 1994; Howell *et al.* 1997).

The surface waters of the Indian Ocean display biogeochemical signatures of water column N₂ fixation (Gruber and Sarmiento 1997). Observations of *Trichodesmium* abundance (Carpenter 1983) and a few direct rate measurements (Capone *et al.* 1997) appear consistent

with such a conclusion. To date, despite its importance for the global oceanic N cycle, little is known about the balance of N fluxes and the sizes of the different N pools in the Indian Ocean.

This chapter consists of two sections. The first section describes the large scale distribution of N and P in relation to the physical and biological environment along a section at 32°S in the Indian Ocean. The aim of this section is to assess the factors controlling the large scale storage and distribution of dissolved organic nutrients at the Southern margin of the subtropical Indian Ocean and the nutrient imbalances, with respect to the classical Redfield ratio, of the total N and P pools. In this section, the potential impact of organic nutrient advection into the basin on export production occurring within the basin has also been quantified. In the second section, in order to understand the role of the Indian Ocean in the global N cycle, a nitrogen budget is constructed from ancillary data and the mass transport calculated across the hydrographic section at 32°S by McDonagh *et al.* (2005).

3.2 Results

3.2.1 Large Scale Inventories of N and P

The surface mixed layer depth was constant across the section at around 60m. Surface temperature decreased from west to east (data not shown) while salinity values were homogeneous along the section (Fig.3.1).

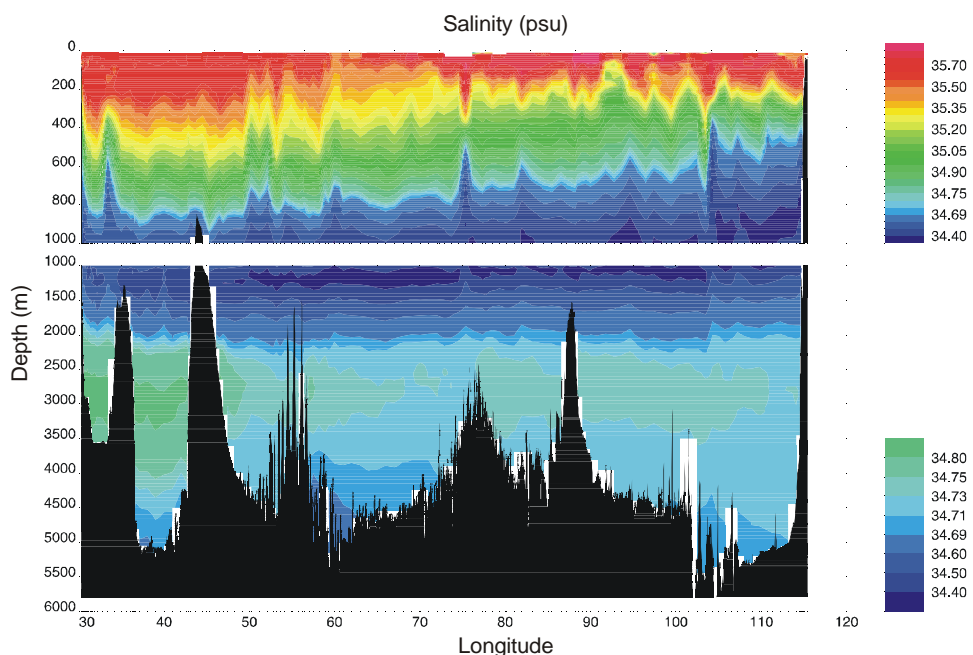


Fig. 3.1 Section of salinity across the Indian Ocean at 32°S.

Throughout the water column different water masses were present. At about 1000m depth the Antarctic Intermediate Water (AAIW) was indicated by a salinity minimum. Below 2000m the inflow of the Circumpolar Deep Water (CDW) was characterised by high salinity and also high oxygen and low nutrient concentrations.

Nitrate and phosphate concentrations in the upper 300 meters of the water column are shown in Fig. 3.2. DIN concentrations were $<0.1\mu\text{M}$ in the euphotic layer across the whole sampled area. The depth of the nitracline was on average 75m on the western side of the basin and increased towards the east where it reached 140m. At the edge of the gyre DIP surface layer concentrations were very low ($<0.01\mu\text{M}$) while in the centre of the gyre, from 65°E to 105°E, DIP concentrations reached $0.2\mu\text{M}$.

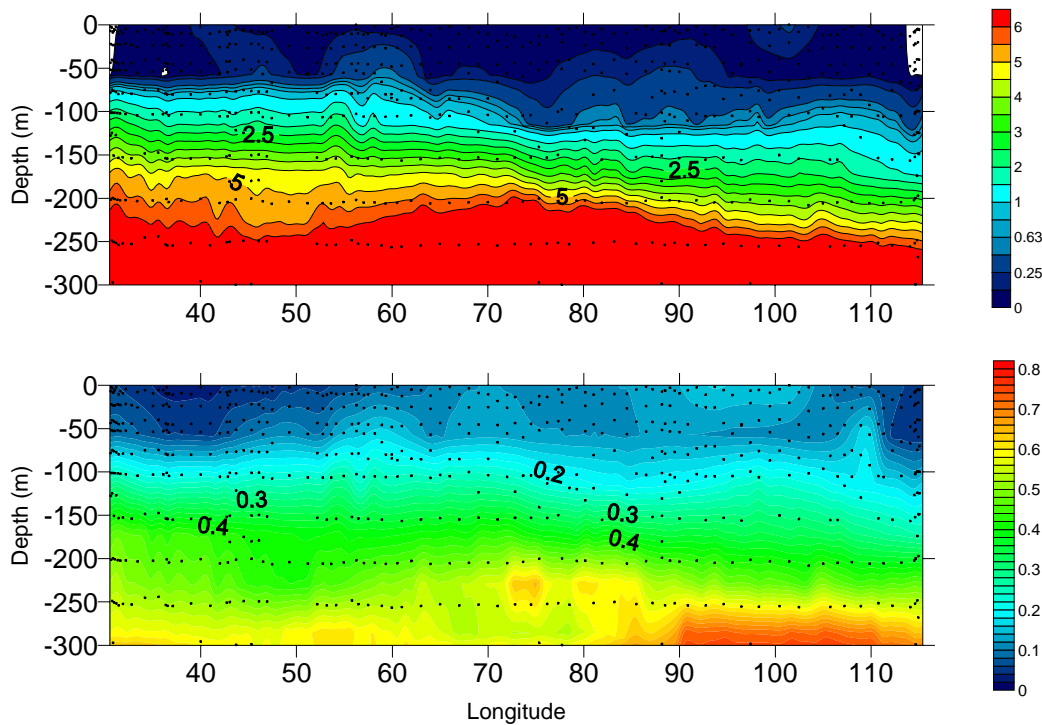


Fig. 3.2 Section of nitrate (top) and (bottom) phosphate (μM) across the Indian Ocean at 32°S.

Both DIN and DIP increased with depth with the highest values reached around 2000m coincident with the oxygen minimum (data not shown).

Photosynthetic biomass, measured by HPLC as total chlorophyll *a* (Welshmeyer 1994), ranged from 1.32ngChlal^{-1} to 100ngChlal^{-1} with an average value of 26ngChla l^{-1} . The

distribution of chlorophyll *a* in the upper 200m (Fig. 3.3) exhibited a deep chlorophyll maximum (DCM) typical of oligotrophic areas.

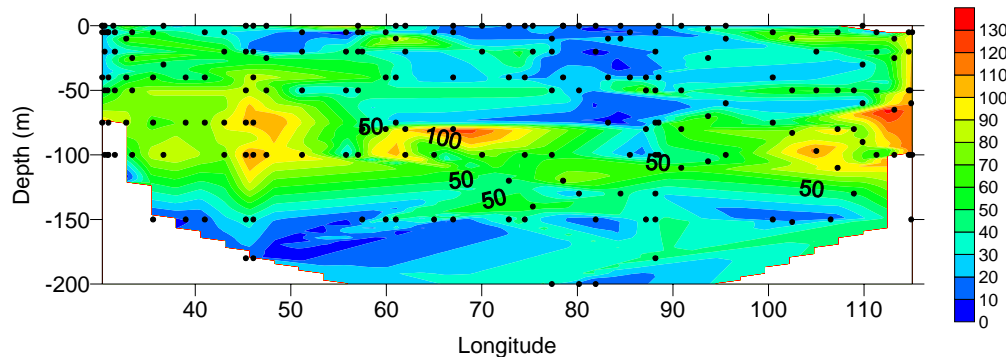


Fig. 3.3 Section of total chlorophyll a (ngChlal⁻¹) across 32°S in the Indian Ocean.

The depth of the DCM varied along the transect; from 30°E to 60°E the DCM covered a wide depth range from 50 to 80 m. From 60°E to 75°E it occurred around 80m. Moving towards the east (75°E to 95°E) it reached 120m and as the Australian coast approached, it shallowed to 65m.

The percentage contribution of individual pigments to total pigment levels in the euphotic zone has been calculated for 4 different areas characterised by the same DCM depth (Area A=from 30°E to 60°E; Area B= from 60°E to 75°E; Area C= from 75°E to 90°E; Area D= from 90°E to 115°E) (Fig. 3.4).

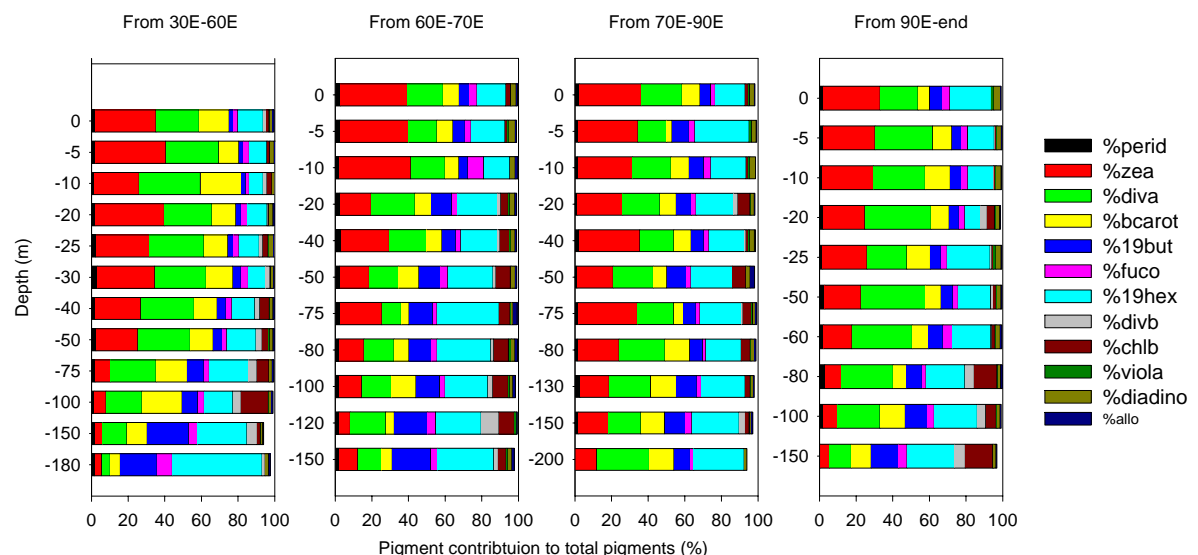


Fig. 3.4 Vertical distribution of the contribution of various algal pigments to total pigments (%) in 4 different regions across the Indian Ocean at 32°S.

As expected, the major taxonomic groups were cyanobacteria (identified by the characteristic pigment zeaxanthin) and prochlorophytes (containing the taxonomic pigment divinyl-chlorophyll *a*) which constitute together the picoplankton group. In addition prymnesiophytes (identified by the pigment 19-hexanoylfucoxanthin) were important contributors to plankton biomass. Together these pigments represented on average 20%, 22% and 20% respectively of total pigments. Down the water column the importance of cyanobacteria decreased while prymnesiophytes, indicated by 19-Hex, and chrysophytes, indicated by 19-But, increased (Fig. 3.4). At the gyre flanks, in the DCM, prochlorophytes were dominant (30%), while prymnesiophytes (27%) contributed mostly to the DCM in the centre of gyre (Fig. 3.4).

In the surface layer, the pigments that exhibited the major spatial variability were zeaxanthin and divinylchlorophyll *a*. In this layer zeaxanthin, representing picoplankton constituted 40% of all the pigments in a wide area from 40-85°E (Fig. 3.5) while divinylchlorophyll *a*, indicating the presence of prochlorophytes, was mostly important on the gyre flanks (Fig. 3.5).

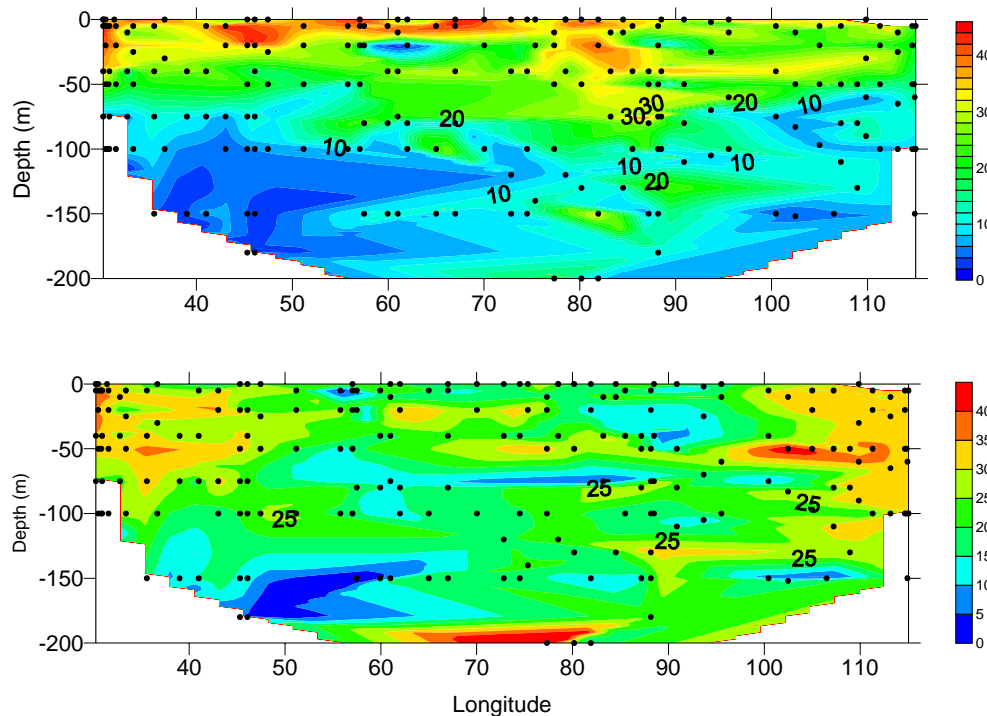


Fig. 3.5 Sections of the contribution (%) of zeaxanthin (top) and (bottom) divinyl-chlorophyll *a* to total pigments across Indian Ocean at 32°S.

Averaged DIN, DIP, TON_{HTCO}, TOP and a typical Chla *a* vertical profile are shown in Fig.3.6. High TON and TOP concentrations were found in the upper 100m of the water column (average: $4.3 \pm 0.7 \mu\text{M}$, $0.35 \pm 0.08 \mu\text{M}$ respectively) in agreement with the general concept that organic matter is produced in the surface layer by biological production.

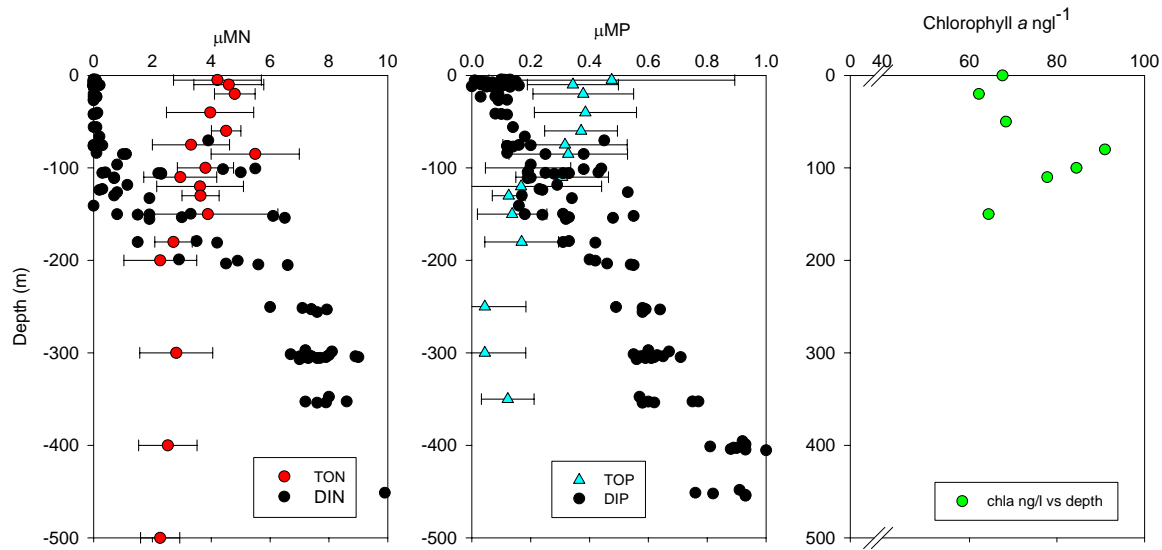


Fig. 3.6 Averaged vertical profiles of DIN, TON HTCO measured, DIP, TOP (μM) and typical Chlorophyll *a* profile (ng l^{-1}). Bars represent range of measurements.

TON and TOP concentrations abruptly decreased in the nitracline (the depth where the maximum variation in nitrate concentrations occurs). Below 200m TON decreased to $2.5 \pm 0.7 \mu\text{MN}$ and TOP became a small, however detectable, pool $0.08 \pm 0.05 \mu\text{MP}$. Both TON and TOP contributed significantly to the total dissolved N and P pool in the Indian Ocean (Fig. 3.7).

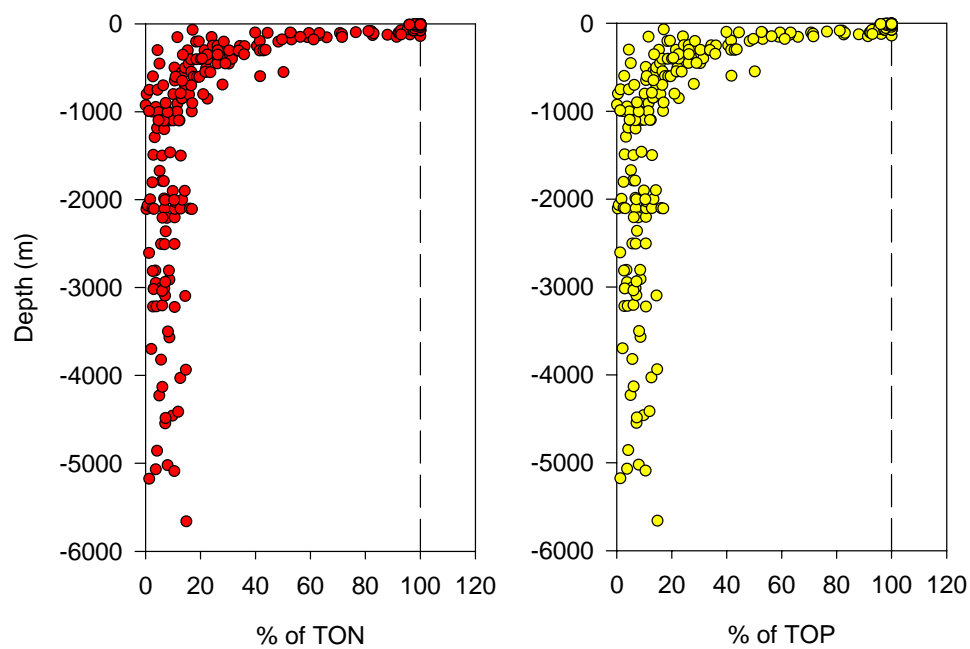


Fig. 3.7 Vertical profiles of TON and TOP contribution (%) to the total N and P pools.

TON and TOP constituted the majority (100%) of the total dissolved nutrient pool in surface waters. TON and TOP were not negligible in the deeper layers where they represented on average 10% of the nutrient pool (Fig. 3.7).

TON distribution across the subtropical Indian Ocean showed a significant zonal trend (Fig. 3.8). The highest values, ranging from $3.5\mu\text{M}$ to $5\mu\text{M}$, were found in the top layer stretching from the western end to 80°E . The depth of the isoline of $3.5\mu\text{M}$ TON decreased (West to East) remarkably from 150m to the surface in this eastern region. TOP (Fig. 3.8) did not exhibit the same strong spatial gradient but had in general higher values on the western flank.

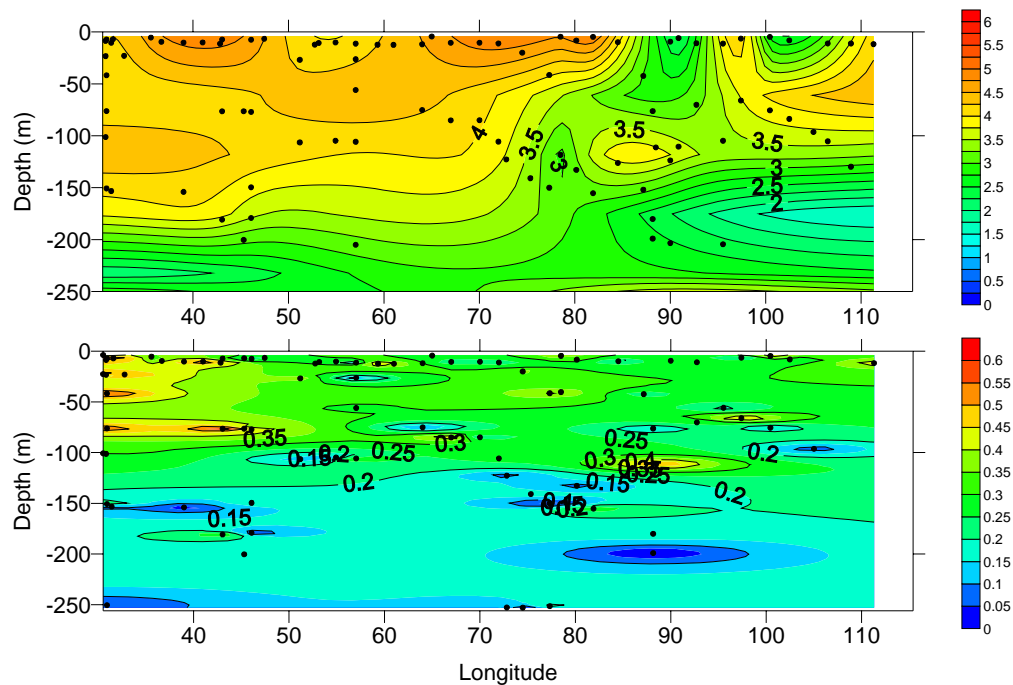


Fig. 3.8 Section of TON (top) (μ MN) and TOP (bottom) (μ MP) across the Indian Ocean at 32°S. Contours were produced using kriging as interpolation method with anisotropy ratio of 1.

The relationship between the N and P pools is shown in Fig. 3.9. The slope of the inorganic nitrogen to phosphorus regression is in good agreement with the classical Redfield ratio (15.2N:1P as opposed to 16N:1P) and the intercept is negative, i.e P is >0 when N=0, indicating that nitrate is likely to run out before phosphate (Fig. 3.9, black). If the total N and P pool (organic plus inorganic) are considered, the ratio between N and P becomes lower than the Redfield value (14.4) (Fig. 3.9, cyan) and the intercept becomes positive. A different picture emerges if only the organic fraction of the nutrient pool (Fig. 3.9, red) is taken into account. The data appears more scattered and the regression line is not statistically significant; however the majority of the data clusters below the $N=16P+2.5$ line (where the average TON $2.5\mu\text{M}$ concentration represents the average refractory TON pool; Sanders and

Jickells 2000; Jackson and Williams 1985) and TON values were largely positive when the TOP pool was zero. This trend was particularly evident when only surface data points were considered (Fig. 3.9, yellow).

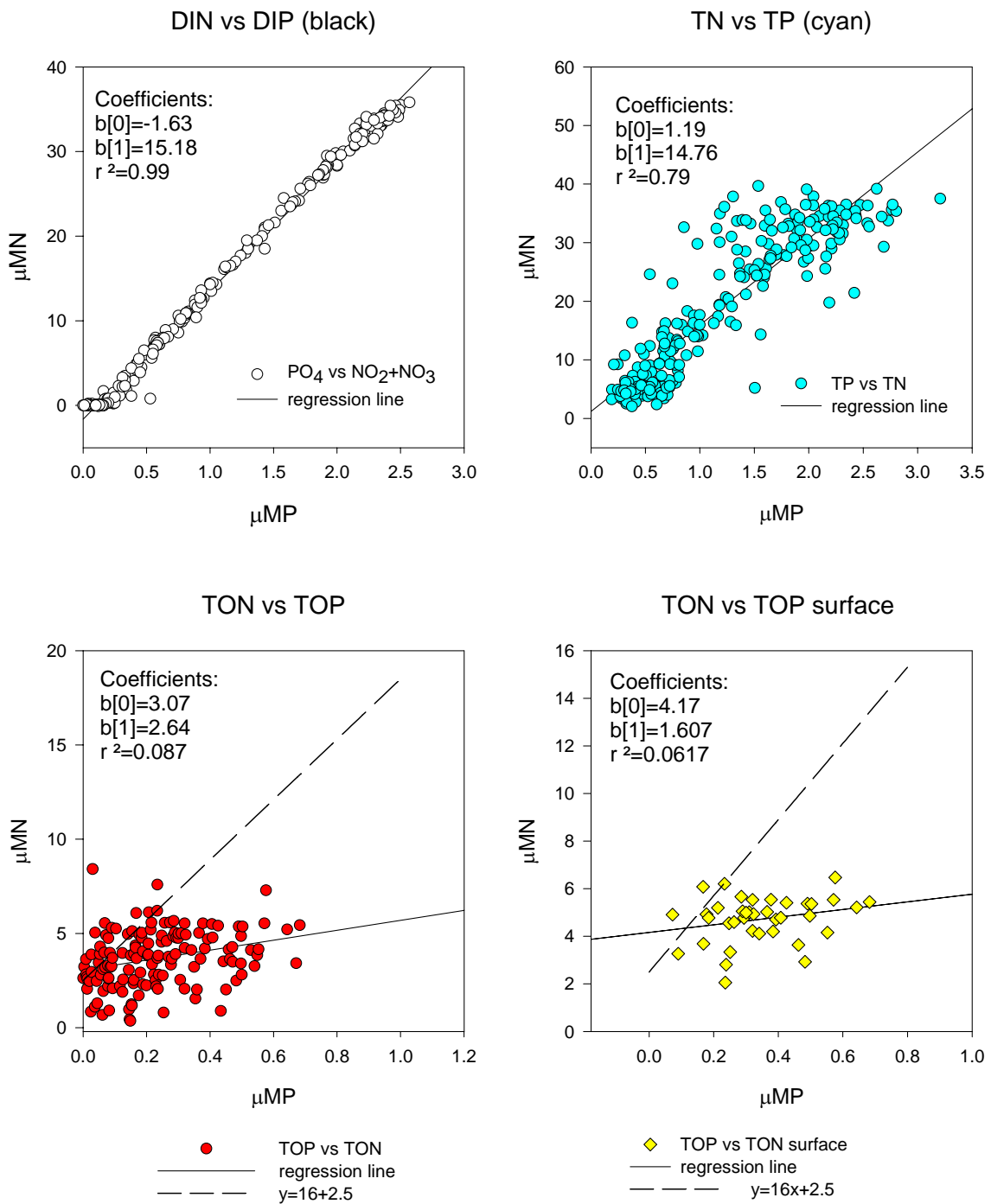


Fig. 3.9 Scatter plot and regressions line of DIN vs DIP (black) (top left), TN vs TP (cyan)(top right); TON vs TOP red (bottom left); TON vs TOP only surface data (yellow) (bottom right). Full lines represent best fit lines, dotted lines represent $y=16+2.5x$ equation; $b(0)$ =slope, $b(1)$ =intercept.

The marine organic nutrient pool is composed of a complex matrix of compounds with different residence times and labilities. Most (>90%) of the DOM in deep waters remains

uncharacterized at the molecular level (Benner *et al.* 1997) however surface DOM is composed of relatively fresh and bioreactive organic matter. In this study the ratio of TON measured with HTCO to TON measured with UV has been used as a qualitative index indicative of the refractory/labile ratio of organic matter (Fig. 3.10). Very few data points are available below 150m along the section and this will introduce some errors of interpretation at depth.

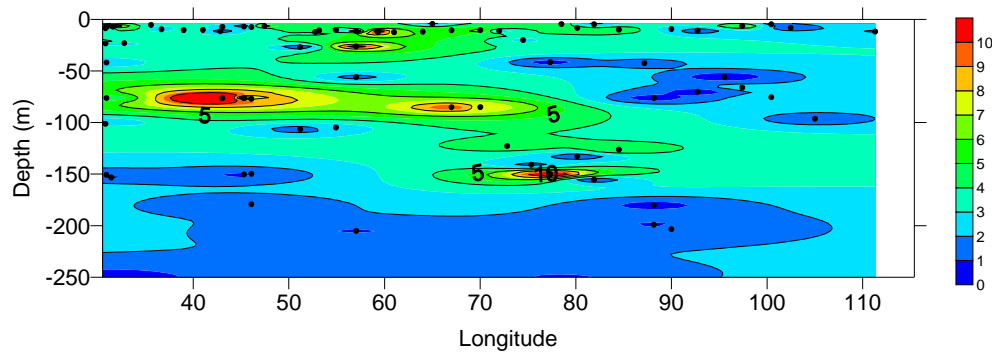


Fig. 3.10 Section of TON_{HTCO}/TON_{UV} ratio across the Indian Ocean at 32°S. Contours were produced using kriging as interpolation method with anisotropy ratio of 1.

The HTCO method is known to have the highest oxidation efficiency for the most refractory compounds (Bronk *et al.* 2000) while the UV method yields high recoveries only for labile material. The TON_{HTCO}/TON_{UV} ratio can serve as an index of lability, with high values indicating a refractory TON pool. Interestingly, the areas where the highest TON concentrations (surface layer from 50-80°E) were found were also characterized by lower lability.

3.2.1.1 Discussion

N:P Stoichiometry

As inferred from the regression analysis (Fig. 3.9), the area sampled was characterised by inorganic nitrogen limitation. This observation is confirmed also by the characteristic left sided T- shape N/P ratio profile (Fig. 3.11) observed by Karl *et al.* (2001) in the North Pacific. A negative offset from the Redfield ratio value is also observed in deep waters (i.e deep N/P values <16). The extent of this inorganic N limitation increased towards the east as shown by the DIN to DIP ratio in the upper 500m (Fig. 3.12). This gradient is likely the consequence of the deeper nitracline depth towards the Australian continent (~120m compared to ~80m on the Western side) which precludes the availability of nitrate to surface layers exacerbating the already present nitrogen deficit and also by the possible presence of N_2

fixers in the western end of the transect that, as will be discussed later, may alleviate regional N limitation (Fig. 3.11).

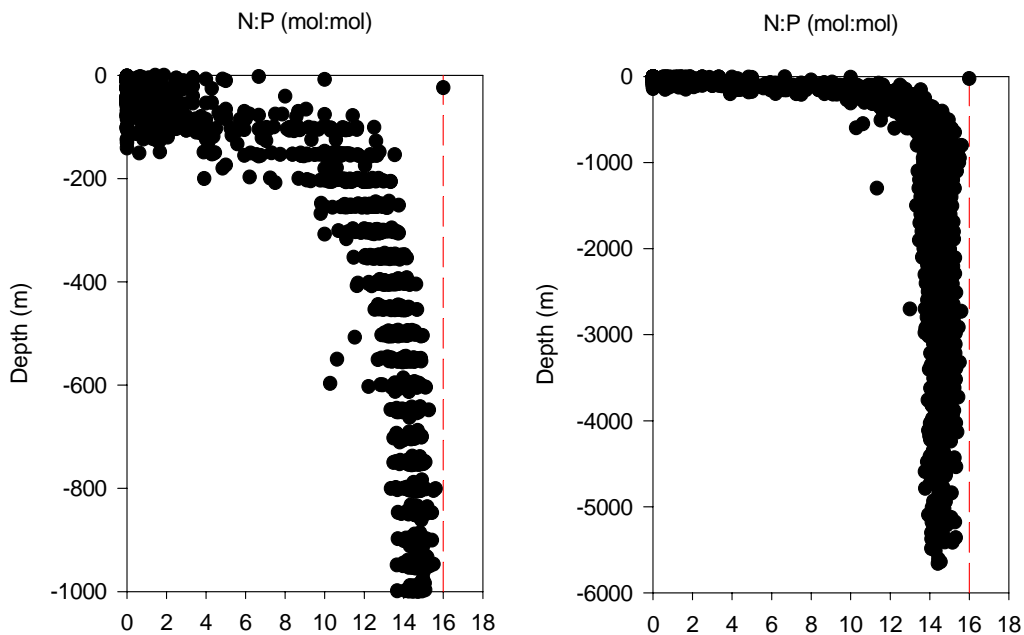


Fig. 3.11 Inorganic nitrogen to phosphorus ratio along the water column in the Indian Ocean. Note that the N/P ratio is always < 16 even in deep waters.

From the N to P ratio regression analyses (Fig. 3.9) it is possible to infer the existence of a residual pool of PO_4^{3-} when NO_3^- is depleted. This scenario is similar to the one found in the North Pacific where $\text{NO}_3^-:\text{PO}_4^{3-}$ ratios are lower than 16 resulting in N limiting conditions caused by limited N_2 fixation due to scarce iron supply (Wu *et al.* 2000).

Low $\text{NO}_3^-:\text{PO}_4^{3-}$ ratios in the Indian Ocean are not surprising considering that this site is where a substantial fraction of the ocean's denitrification takes place (Gruber and Sarmiento 1997).

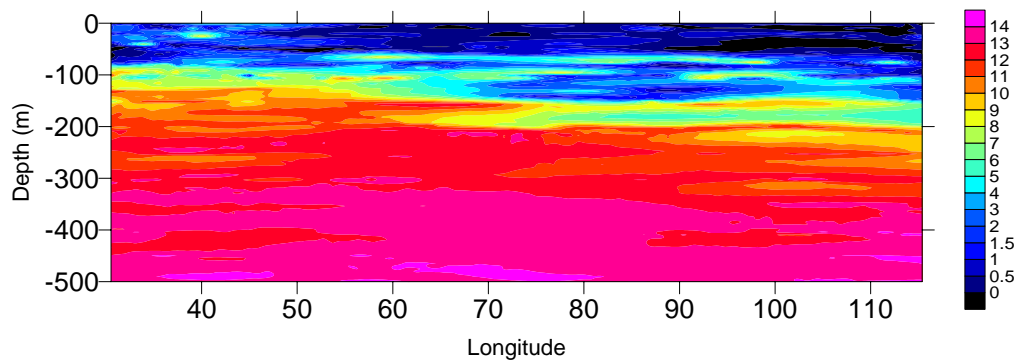


Fig. 3.12 Section of inorganic nitrogen to phosphorus ratio distribution along the Indian Ocean at 32°S .

To infer imbalances in N to P ratios however, it is necessary to consider the total dissolved nutrient pool. A shift to a positive residual of N, when P is numerically close to zero, occurs when the organic nutrients are included in this analysis (Fig. 3.9). This indicates that a large amount of N is accumulated in the organic fraction and implies that, when TOP levels are potentially limiting, there is a TON pool in surface waters, of unknown lability, which plankton might be able to access. Thus, despite the low inorganic nitrate to phosphate ratios, the Subtropical Indian Ocean N pool does not appear depleted with respect to P due to the large “storage” of N in organic matter as also observed in other oligotrophic regions (Sanders and Jickells 2000). This could have several important ecological advantages depending on the ability of organisms to access the organic pool. One of the puzzles of DOM production by phytoplankton is that it is an energy consuming process and it is unlikely that phytoplankton cells produce it, by active exudation, under N limiting conditions (Williams 1990). However the build up of a semirefractory DON pool could be an important mechanism to buffer the loss of fixed N through the denitrification process. The organic fraction could then re-supply N under strictly limiting conditions.

Interestingly, from the regression analysis above mentioned (Fig. 3.9), although TOP appears to be drawndown before TON, the observation of TON/TOP ratios well below the Redfield ratio indicates a severe TON deficiency with respect to TOP. This suggests either a tendency to a preferential usage of TON from the DOM pool or preferential production of TOP with respect to TON. Processes preferentially producing low TON/TOP organic material are unknown, whilst preferential TON consumption may be due to the strong inorganic N deficiency observed. Therefore, a consumption of TON and not TOP from the dissolved pool is a likely explanation for the low TON/TOP ratio observed.

Large scale utilisation of TON and TOP in Redfieldian stoichiometry has not been directly observed. However, data from the Antarctic and Subtropical Pacific (Sanders and Jickells 2000) suggest that TON and TOP surface pools are tightly coupled, being produced and consumed in a ratio close to the Redfield ratio.

The data here presented do not support this hypothesis; instead a consistent preferential consumption of TON relative to TOP is hypothesised. This might follow large-scale differences in ecosystem structure and functioning at the various sites. Both areas studied by Sanders and Jickells (2000) are regions where there is little interannual variability in the surface nutrient concentrations, being permanently high in the Antarctic and permanently low at the HOTS site, a study area also impacted by N₂ fixation (a process linked to higher DON concentrations levels; Karl *et al.* 1997). Consequently there is no reason to preferentially utilise

the TON pool compared to the TOP pool at either site. In contrast our data were collected in a region where denitrification is an important process (Gruber and Sarmineto 1997) leading to a community demand for TON, in addition this system becomes seasonally N limited when P appears to be still present.

Plankton community distribution, east to west gradients in TON and TOP concentrations, lability of organic matter

The magnitude of the TON and TOP inventory and its distribution is the result of the complex interactions between physical and biological processes. Here I investigate which processes were mainly involved in controlling the observed DOM distribution.

The TOP pool was rather constant across the transect in contrast to the strong variability in TON concentrations (Fig. 3.8). As the northward Ekman transport of DOM was quantitatively more significant on the east (Fig. 3.20), the flux of TON from more productive areas into the gyre, cannot explain the observed gradients of TON which showed instead enhanced concentrations in the west.

A general concept is that organic matter is mainly produced by phytoplankton and consumed by heterotrophic bacteria and to some extent by phytoplankton (Bronk and Glibert 1993) depending on the availability of inorganic forms of N and P (Jackson and Williams 1985; Anderson 1992). Given that Ekman transport is ineffective at influencing DOM zonal distribution (Fig. 3.20) the spatial and temporal coupling of production and consumption processes appear the main mechanisms of control of TON and TOP inventories.

In our study area, the West to East variability of zeaxanthin was well coupled with the west to east gradient in the concentrations of TON. This observation suggests that organisms containing this pigment may be involved in the production of TON. Zeaxanthin is a taxonomic pigment specific to cyanobacteria. Among common zeaxanthin containing cyanobacteria are N₂ fixers such as *Trichodesmium*, a filamentous cyanobacteria, and also the recently isolated unicellular cyanobacteria phylogenetically close to *Synechococcus* (Zehr *et al.* 2001). Field studies, have documented the release of large amount of recently fixed N₂ as DON (Glibert and Bronk 1994; Mulholland *et al.* 2004). Measured accumulations of DON in parts of the Subtropical Pacific and Atlantic oceans have been attributed to the release of DON associated with N₂ fixation (Hansell and Waterhouse 1997; Karl *et al.* 1997; Vidal *et al.* 1999; Abell *et al.* 2000). Although the presence of TON and Zeaxanthin strongly suggest the occurrence of diazotrophy, due to their different residence time (Zeaxanthin representing an instantaneous standing stock while TON inventory presumably integrates over longer timescales) this observation cannot be used directly as evidence for N₂ fixation.

The area studied appears to be an environment where diazotrophs may potentially be very important for several reasons, these include low inorganic N/P ratios and surface stratification. Hence the observed TON concentration gradient may be partly associated with the release of DOM from diazotrophs. This hypothesis is supported by the observation of enhanced *Trichodesmium* blooms in western boundary currents (LaRoche and Breitbarth 2005). Also, on the Eastern African coast, *Trichodesmium thiebautii* appears to be a permanent component of phytoplankton (LaRoche and Breitbarth 2005). The occurrence of *Trichodesmium* blooms during the northeastern (November-April) monsoon in the western Indian Ocean has also been documented by Bergman (2001).

If N₂ fixation is driving the observed TON distribution, which factors are in turn controlling N₂ fixation, limiting its importance to the western side of the transect and below the level at which it would elevate N/P ratios above the low values caused by the excess of denitrification over nitrogen fixation?

The environmental factors controlling the patterns and rates of N₂ fixation are concentrations of nutrients, temperature, and ambient and trace metals. Could any of these factors have driven differential N₂ fixation across the Indian Ocean?

It is known that nitrogen fixers grow and fix nitrogen successfully under nitrate deplete conditions as the enzyme nitrogenase, that catalyses the reaction, is inhibited by the presence of nitrate (Zehr *et al.* 2001). Low nitrate levels always applied to the surface waters studied.

Recently it has been suggested that N₂ fixing organism are limited by the scarce availability of P (Sanudo-Wilhelmy *et al.* 2001). However, the excess of DIP and TOP detected in study area suggests that P was not a limiting factor for the growth of N₂ fixers.

Diazotrophs are most successful in sunlit warm stratified waters due to the high energy requirements associated with N₂ fixation (LaRoche and Breitbarth 2005). The temperature gradient observed across the Indian Ocean, moving from west (25°C) to the east (22°C), could have created better conditions for N₂ fixer's growth in the west.

Dust deposition during the CD139 cruise was collected by the University of East Anglia Aquatic and Atmospheric Biogeochemistry group. Witt (2003) observed a variation of the composition of the aerosol due to different source regions. Higher ratios of iron to aluminium were measured in aerosols close to South Africa and have been attributed to the anthropogenic release of iron to the atmosphere (Witt, personal communication). Thus the difference in aerosol sources moving from Africa to Australia may have contributed to a different availability of iron across the transect, favouring higher rates of N₂ fixation on the western side of the gyre.

Together these factors may explain the gradient observed in TON concentrations as a result of TON production driven by N_2 fixation; however they do not clarify the different lability of TON across the gyre, thus other factors must be acting across the transect.

On the western side, the higher concentrations and lower availability of DOM as inferred from the TON_{HTCO}/TON_{UV} ratio, suggests that fresh DOM has been produced and that the labile DOM has been rapidly used up leaving the refractory material to accumulate in accordance with the enhanced N_2 fixation on this side of the transect.

In the eastern side of the basin, the low DOM concentrations, instead suggest a tight coupling between production and consumption processes. This is also confirmed by the low refractory/labile index (TON_{HTCO}/TON_{UV}) which implies the utilisation of both labile and refractory TON. As observed above (Fig. 3.9), the area sampled was characterised by a nitrate deficiency with respect to the Redfield ratio which increased in magnitude towards the eastern flank of the gyre. Hence, the presence of both inorganic and organic phosphorus and the strong N limitation may have triggered the utilization of the entire TON pool by the community consistent with the deficiency of TON with respect to TOP.

3.2.1.2 Conclusions

Inorganic nutrient distributions in the Indian Ocean indicate a strong depletion of NO_3^- relative to PO_4^{3-} in relation to the elemental requirements of phytoplankton biomass. The strong NO_3^- limitation found in the area sampled may result from the enhanced levels of denitrification that occur in the low oxygen waters of the Indian Ocean (Gruber and Sarmiento 1997). However, the ultimate limiting nutrient becomes P when dissolved organic nutrients are also included in estimates of the elemental ratio (positive intercept in the TDP vs TDP regression analysis) suggesting that a significant fraction of N is stored and cycles through the organic fraction.

TON and TOP are the dominant fractions of the N and P pools of the upper surface layers; TON is strongly deficient with respect to TOP according to the classical Redfield ratio indicating a decoupling of TON and TOP remineralization processes likely driven by the community demand for TON as a consequence of the strong N limitation brought on by an overall excess of denitrification over N_2 fixation.

Low TON to TOP ratios and the contrasting TON and TOP distributions, with strong spatial variability in TON levels as opposed to the relatively constant TOP levels, suggests that differential DOM production and consumption processes act across the gyre. The strong N deficiency and favourable environmental conditions may trigger local N_2 fixation and thus the localised production of TON on the western side of the transect. These conditions do

not apply of the eastern side where, instead, N limitation is not mitigated by N_2 fixation thus promoting larger TON consumption and a smaller TON pool.

The coexistence of N_2 fixation and low inorganic N/P ratios it is not as contradictory as it could seem at first sight. Firstly, N_2 fixation is triggered by low inorganic N/P ratios, only under these conditions diazotrophs out compete other phytoplankton. Secondly, N_2 fixation and the build up of N and P inventories are processes that have very different spatial and temporal scales. N_2 fixation is a localised temporary process subject to seasonal variability (LaRoche and Breitbarth 2005) while nitrate:phosphate ratios average, over long times scales, the balance between N_2 fixation and denitrification. Hence the low N/P ratios observed do not rule out the presence of localised N_2 fixation in the study area but indicate that denitrification rates are higher than N_2 fixation consistent with the computation of N^* by Gruber and Sarmiento (1997) and the N_2 and denitrification rates presented in the N budget analysis in 3.2.3.4

3.2.2 DOM Advection Into the Subtropical Gyre

Much attention has focused on the potential role of DOM in providing new nutrients to the subtropical gyres when advected from nutrient rich areas (Williams and Follows 1998). In the surface waters, advection is a result of both the wind-induced Ekman transport and the geostrophic component of the gyre circulation. In the Indian Ocean the northward geostrophic gyre transport (from nutrient rich polar areas) occurs mainly in deep layers (Robbins and Toole 1997) thus the surface layer Ekman transport is therefore the only mode for transporting surface waters from the high nutrient regimes northwards into the subtropical gyre. The northward Ekman nutrient flux was calculated as the product of the meridional component of the Ekman transport and the nutrient concentration in the Ekman layer (section 3.2.3.3). The Ekman northward flux supply of inorganic nutrients is negligible compared to the transport of the organic fraction (Table 3.3). The calculated fluxes lead to an average supply of $10.3 \pm 2.7 \text{ kmol TN m}^{-2} \text{ yr}^{-1}$ and $0.87 \pm 0.31 \text{ kmol TP m}^{-2} \text{ yr}^{-1}$ across the section, which correspond to $32.5 \pm 8.5 \text{ mmol TN m}^{-2} \text{ yr}^{-1}$ and $2.8 \pm 1.0 \text{ mmol TP m}^{-2} \text{ yr}^{-1}$ given a gyre area of approximately 10^{10} m^2 (20°S - 35°S , 50°E - 110°E).

To asses the quantitative importance of TON and TOP advection into the gyre as sources of nutrients in supply of export production, these estimates have been compared to export production estimates based on oxygen utilization rates on isopycnal layers.

3.2.2.1 Estimates of Export Production

The oxidation of exported carbon from the euphotic zone results in oxygen consumption in the aphotic zone leading to an undersaturation of oxygen termed apparent oxygen utilization (AOU). Previous studies (Jenkins and Wallace 1992) have used AOu and ventilation ages to compute the rate of oxygen consumption and make estimates of export production.

In this study, for this purpose, oxygen, Helium (${}^3\text{He}$) and Tritium (${}^3\text{H}$), has been gathered from the WOCE data set from 20°S-35°S available on http://www-pord.ucsd.edu/whp_atlas//indian_index.htm, and data collected during cruise CD139 (Sanders *et al.* 2005)

Calculation of water mass age: Tritium- ${}^3\text{He}$ dating

Tritium, the heaviest isotope of hydrogen, is unstable and decays to Helium with a half life of 12.45 years following the radioactive decay equation:

$${}^3\text{H}_{(t)} = {}^3\text{H}_{(0)} e^{-\lambda t} \quad \text{Eq. 3.1}$$

Where ${}^3\text{H}_{(0)}$ is the tritium concentration at the sea surface and λ is the radioactive decay constant ($1.76 \cdot 10^9 \text{ s}^{-1}$). This equation can be exploited to compute the Tritium- ${}^3\text{He}$ age indicating the elapsed time since the particle of sea water has left the surface (Jenkins 1998).

$$t = \lambda^{-1} \ln \left[1 + \frac{{}^3\text{He}_{(t)}}{{}^3\text{H}_{(0)}} \right] \quad \text{Eq. 3.2}$$

Calculation of oxygen utilization rates

The calculation of OUR involves the measurements of AOu and age along isopycnal gradients (Jenkins 1992, 1997). The concept of this technique is that, moving along isopycnals a water particle's age and AOu will increase and their correlation will give OUR.

In the Indian Ocean the AOu increased with depth as the age of the water parcel increases (Fig. 3.13).

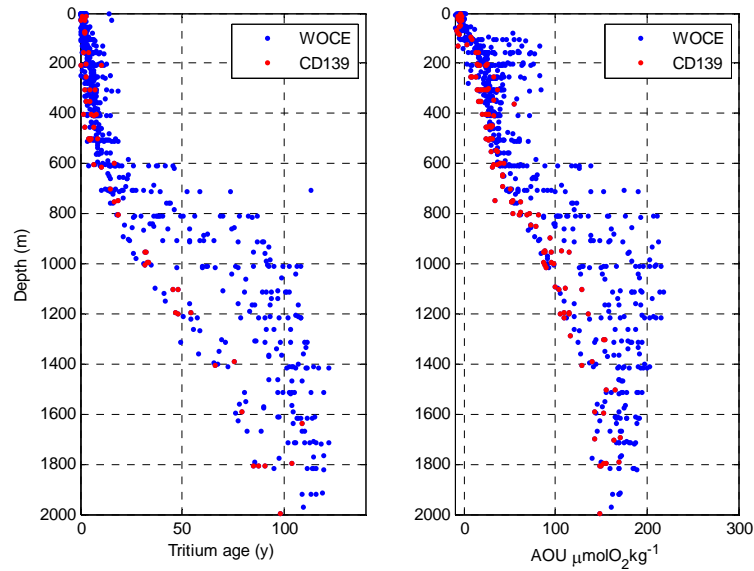


Fig. 3.13 Vertical profile of Tritium- 3 He ages (y) and AOU ($\mu\text{molO}_2 \text{ kg}^{-1}$) from the WOCE and CD139 datasets.

The correlation between age and AOU (Fig. 3.14), along 5 isopyncals ($\sigma_0=25.5, 26, 26.5, 27, 27.5 \text{ kgm}^{-3}$), has been used in this study to infer OUR (Table 3.1).

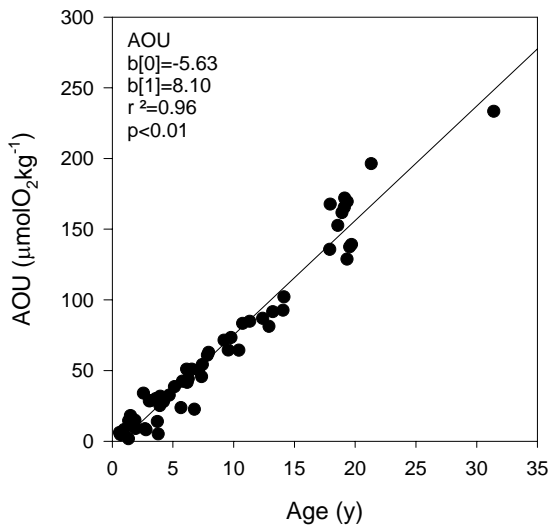


Fig. 3.14 Correlation between AOU ($\mu\text{molO}_2 \text{ kg}^{-1}$) and age (y) from the WOCE and CD139 data set on the $\sigma_0=25.5 \text{ kgm}^{-3}$. The slope of the regression line has been used to infer OUR on this isopycnal surface.

The average OUR decreased with depth (Table 3.1) as less organic material for oxidation is available and as the age of the water parcel increases. At the top of the aphotic zone (150m) OUR was around $8.1 \pm 1.9 \text{ mmolm}^{-3} \text{ y}^{-1}$, lower than observed at the top of the aphotic zone of the North Atlantic ($20 \text{ mmolm}^{-3} \text{ y}^{-1}$; Jenkins and Wallace 1992),

Table 3.1 Average of OUR ($\mu\text{molkg}^{-1}\text{y}^{-1}$) on 5 isopycnal layers. OUR has been calculated as the slope of the regression line between water mass ages (y) and AOU (μmolkg^{-1}). Average depth of each isopycnal layer is reported.

Isopycnal Layer $\sigma_0(\text{kgm}^{-3})$	Average Depth (m)	Average age	Average OUR $\mu\text{molkg}^{-1}\text{y}^{-1}$
25.5	185	9±7	8.1±1.9
26	211	12±10	7.0±2.4
26.5	300	11±8	5.5±2.9
27	700	40±14	2.8±0.5
27.5	1200	85±20	2.1±0.4

The integration of OUR over the 5 isopycnal layers, where the majority of the oxygen is consumed (150m-1200m), yields a water column oxygen demand of the order of $3.1\pm1.4\text{ molesO}_2\text{m}^{-2}\text{y}^{-1}$. Knowing the stoichiometric ratio of oxygen consumed to carbon oxidized (1.62; Takahashi *et al.* 1985) it is possible to compute the export production of carbon as $1.91\pm0.86\text{ molesC m}^{-2}\text{y}^{-1}$ corresponding to $0.3\pm0.13\text{ molesN m}^{-2}\text{y}^{-1}$ and $0.02\pm0.01\text{ molesP m}^{-2}\text{y}^{-1}$ using the Redfield ratio (106C:16N:1P). These values of export production are reasonable relative to other findings in other oligotrophic regions using similar indirect methods (ALOHA: 2molesC $\text{m}^{-2}\text{y}^{-1}$ Emerson *et al.* (1997); BATS: 3.3molesC $\text{m}^{-2}\text{y}^{-1}$, Jenkins and Wallace (1992)).

3.2.2.2 Discussion and Conclusion

A comparison of the Ekman meridional nutrient fluxes and the export production estimated above imply that the meridional Ekman transport of organic nutrients into the gyre can potentially supply about 10% and 15% of fraction of N and P respectively needed to support export production.

These estimates represent an upper limit as the entire DON and DOP pools have been considered fully available for biological production. The limited role of organic nutrients in supporting export production in the Indian Ocean subtropical gyre is comparable with the limited role found by Mahaffey *et al.* (2004) in the North Atlantic gyre. In a comparable study in the Pacific however, DON and DOP Ekman fluxes, from the equator to the North Pacific gyre, were estimated to supply approximately $20\pm10\%$ and over 40% of the N and P required for new production (Abell *et al.* 2000).

Interestingly, the contribution to new production of the horizontal supply of DOP is higher than that of DON. This finding has already been observed by other authors (Mahaffey *et al.* 2004; Abell *et al.* 2000). Given the difficulty of supplying P from the atmosphere (Baker

et al. 2003) and, due to the lack of an equivalent mechanism of N_2 fixation for injecting new P into the ocean, it seems reasonable that the lateral supply of DOP is quantitatively more important than the supply of DON for the maintenance of export production.

Moreover, although the contribution of DON advection to new production in this region is small, it is in the same order of magnitude of the N supplemented by N_2 fixation ($0.048\text{molNm}^{-2}\text{y}^{-1}$, Bange *et al.* 2000) (Table 3.4).

Overall the advection of organic nutrients can provide a small but not trivial contribution to the supply of N and P into the gyre for the sustainment of export production.

3.2.3 Nitrogen Budget

Nitrogen is a limiting nutrient for the growth of phytoplankton in large areas of the oceans. Changes in the inventory of N could enhance the strength of the biological pump and thus the role of the oceans in sequestering atmospheric CO_2 . For these reasons the processes involved in controlling nitrogen inventories have become the matter of some interest.

Despite the importance of the Indian Ocean for the global marine N cycle, at present it is unknown whether the N budget of this basin is in balance. Although Ganashaud and Wunsch 2002, suggest it is close to being balanced based on the analysis of multiple hydrographic sections based on inverse techniques. Budgeting basins individually is a necessary contribution to achieving a global understanding of the N cycle.

Here the N budget is calculated using a box model, delimited to the north by land masses and to the south by the 32°S hydrographic transect. Ancillary data regarding N sources and sinks within and to the Indian Ocean were collected from the literature; calculations of geostrophic and Ekman nitrogen transport across 32°S were carried out using transport estimates from the hydrographic data.

The main components of the box model are:

Nitrogen Sinks

1. Denitrification
2. Sedimentation

Nitrogen Sources

1. River run off
2. Atmospheric dry/wet deposition
3. N_2 fixation
4. Indonesian Throughflow
5. Advection (Net geostrophic transport, Ekman transport)

3.2.3.1 Nitrogen Sinks

Denitrification

Extensive observations made in the Arabian Sea establish that it is one of the major oceanic NO_3^- reducing sites, accounting for 20% of global water column denitrification (Bange *et al.* 2000). The contribution of the Indian Ocean to global oceanic denitrification occurs mostly in the Arabian Sea (Galloway *et al.* 2004). The Arabian Sea is characterized by strong mid water oxygen minimum zones (OMZ), generally extending from 150m to 1000m. Typically, these zones underlie regions of high biological productivity and thus high production of organic matter. The transition from oxic to anoxic conditions involves important biogeochemical shifts. In the absence of oxygen, nitrate is used to oxidize organic material. Nitrate is reduced to molecular nitrogen through the production of several intermediates. Denitrification removes nitrate and nitrite ions from the water column transforming them into N_2 that can be then released to the atmosphere and thus represents a major sink for oceanic fixed N. In the Arabian Sea, rates of denitrification have been estimated following various techniques. Howell *et al.* (1997) used 'NO', a geochemical tracer, to estimate an integrated denitrification rate of about 21TgN yr^{-1} . The NO tracer quantifies the amount of denitrification from the nitrate deficit, ΔN , which is a measure of the N transformed by the reduction of NO_3^- and NO_2^- to N_2 and N_2O . This compares favorably with an extrapolation of direct rate measurements (Naqvi and Shailaja 1993) and box models (Naqvi 1987) which range from $12\text{-}34\text{TgN yr}^{-1}$. More recently, Bange *et al.* (2000) have allocated a larger area to the OMZ affected by denitrification and estimated the total loss of N through denitrification in the Arabian Sea to amount to on average 33TgN yr^{-1} ; these estimates are in good agreement with the previous estimates of 30TgN yr^{-1} by Naqvi (1994) in the same region. Codispoti *et al.* (2001) included among the processes that could contribute to denitrification in the Arabian Sea the annamox reaction, where NO_2^- oxidizes NH_3 and both species are converted to N_2 (Arrigo 2005), suggesting a revisited estimate of water column denitrification in the permanently suboxic areas of the Arabian sea of 60Tg N yr^{-1} . On the basis of the evidence provided here, I decided to use the most common accepted pelagic denitrification estimate of Bange *et al.* (2000). Shelf and deep sediments are also globally important sites of denitrification (Christensen *et al.* 1987). Bange *et al.* (2000) used the model of Seitzinger and Giblin (1996) to derive an Arabian Sea shelf sediment denitrification rate of 6.8Tg N yr^{-1} . The contribution of deep sediment denitrification has been estimated to be 1.8Tg N yr^{-1} by Galloway *et al.* (2004). Thus, total denitrification (pelagic and sediment) in the Indian Ocean is here estimated to amount to $\sim 40 \pm 1.5\text{Tg N yr}^{-1}$ where the error reflects only the

variability of the range of the estimates of Arabian Sea water column denitrification from the literature. This error does not take into account the interannual and seasonal variability and the uncertainty associated with the reported measurements/estimates; hence the error is suspected to be higher than that reported here.

These estimates are also confirmed by nitrous oxide measurements. In the past, denitrification rates have been estimated from N_2O fluxes to the atmosphere using a 1:50 ratio based on the assumption that the $\text{N}_2\text{O}/\text{N}_2$ production ratio in the region of 1:50 (Nevison *et al.* 1995). Nitrous oxides are intermediaries of the redox chemistry of the denitrification process. As a result, the greatest fluxes of N_2O to the atmosphere occur in the major zones of anoxic waters such as the Indian Ocean. In the Arabian Sea the N_2O flux across the air-sea interface has been estimated to amount to 0.4TgNyr^{-1} (Bange *et al.* 2000) suggesting a denitrification rate of 20TgNyr^{-1} , this estimate however is thought to be conservative as the seasonal emissions of N_2O from the Indian continental shelf appear to be very high and have been not accounted for (Bange *et al.* 2000, 2005). For the entire Indian Ocean, Galloway and co workers (2004) using the N_2O gas flux model of Nevison *et al.* (1995), more recently reported a loss of N_2O 0.9TgNyr^{-1} to the atmosphere which corresponds approximately to a denitrification rate of 45TgNyr^{-1} using a 50:1 ratio.

Sedimentation

Sediments underlying highly productive low-oxygen waters are characteristically rich in organic matter. The burial of N in the deep sea sediments in the central and northern portions of the Arabian Sea was estimated to be 0.26 Tg Nyr^{-1} (Bange *et al.* 2000). This estimate however excludes the high accumulation rates found in the Oman Sea (Sirocko *et al.* 1991) and thus is not representative of all the major areas of the Indian Ocean influenced by the high productivity of the continental margins. From the suggested annual C burial rate (Hedges and Keil 1995), Galloway *et al.* (2004) estimated, using a C:N=10:1, a shelf sedimentation rate of **1.6TgNyr^{-1}** for the entire Indian Ocean. Only a smaller proportion of burial occurs in the abyssal sediments (Hedges and Keil 1995); the estimated deep sea burial of N amounts to **0.17TgNyr^{-1}** (Galloway *et al.* 2004). Thus the total N burial in sediments for all the Indian Ocean amounts to **1.8 Tg Nyr^{-1}** , no error is estimated for this small term.

3.2.3.2 Nitrogen Sources

River run off

Indian rivers contribute about 4% of the global annual riverine discharge and carry a large amount of nutrients to the ocean. Asia emits the largest amount of total nitrogen

through rivers to the oceans of any of the continents reflecting the high river flows, the intensive agriculture and large population (19Tgy^{-1} ; Galloway *et al.* 2004, Green *et al.* 2004). In addition to the Ganges, Brahmaputra, and Indus, which are among the major rivers of the world, another 46 smaller rivers flow into the Indian Ocean from the Indian subcontinent.

The freshwater discharge varies seasonally. The maximum runoff occurs during the monsoon season. On annual average, the total river discharge into the Indian basin is estimated to be $160 \times 10^{10} \text{m}^3\text{y}^{-1}$ (Subramaniam 1979). The major discharge is located in the Bay of Bengal ($126 \times 10^{10} \text{m}^3\text{y}^{-1}$) which is approximately four times the discharge that occurs into the Arabian Sea (Kumar *et al.* 1992).

Estimates of dissolved organic carbon discharge are $4 \times 10^{12} \text{gy}^{-1}$, whereas the rate of particulate organic carbon discharge is $1.4 \times 10^{12} \text{gy}^{-1}$ (Ittekkot and Arain 1986). In a review by Kumar *et al.* (1992) it was estimated that $61 \times 10^9 \text{gy}^{-1}$ of nitrate and $53 \times 10^9 \text{gy}^{-1}$ of phosphate were released from the Indian rivers to the Indian Ocean; in this analysis however important rivers, such as the Godavari, Brahmaputra and the Indus, were not considered. There are few systematic direct studies of river nitrogen discharge of the Indian rivers. A model by Seitzinger and Kroeze (1998) predicted the export of dissolved inorganic nitrogen by the Indian rivers to marine environments to be 4.6Tgy^{-1} . This estimate nearly doubles when considering the organic loads as well. The flux of total nitrogen (organic plus inorganic) discharge to the Indian Ocean costal areas was estimated to amount to 46.35TgNyr^{-1} (Green *et al.* 2004). These authors, considering a 84% burial in estuaries and ocean shelves estimated that the open Indian Ocean receives 7.44TgNyr^{-1} of nitrogen. Estimates of the uncertainties are not reported however, the inerannual variability of river discharge due to climatic variability may lead to high errors.

Atmospheric deposition

The atmospheric dry and wet deposition of both the oxidised (NO , NO_2^- , NO_x^-) and reduced form of N (NH_3 and NH_4^+) are very high in the northern Indian Ocean (Galloway *et al.* 2004). This pattern is consistent with the high rates of emission and creation of these species from the Asian continent due to the large agricultural and industrial activities of the countries surrounding the Indian Ocean in the Northern hemisphere. As expected, the concentrations of these species over the Indian Ocean vary seasonally following the movements of the inter-tropical convergence zone which is most pronounced during the south-western monsoon in the summer months.

The most comprehensive report of atmospheric deposition, comprising both the north and the southern hemisphere in the Indian Ocean, is in Galloway *et al.* (2004). These authors

computed annual mean deposition rates based on NO_x and NH_x emissions. They estimated a total deposition in the Indian Ocean of **3.2 Tgy⁻¹** and **4.1 Tgy⁻¹** due to NO_x and NH_x respectively; no errors are reported.

N₂ fixation

Very few direct estimates of N_2 fixation exist in the surface waters of the Indian Ocean (Carpenter 1983). However, there is biogeochemical evidence of localized water column N_2 fixation (Gruber and Sarmiento 1997) consistent with the results presented earlier in section 3.2.1. Bange *et al.* (2000) estimated an annual fixation rate of 3.3 Tg N yr⁻¹ for the Arabian Sea, calculated from a ¹⁵N isotope mass balance by Brandes *et al.* (1998). A global recent estimate of N_2 fixation in the Indian Ocean was carried out by Galloway *et al.* (2004). These authors provide a minimum estimate for oceanic N_2 fixation by extrapolating the rates of N_2 fixation by *Trichodesmium sp.* to oligotrophic surface waters warmer than 25°C. They chose a daily rate of 1.82 mg N m⁻² day⁻¹ corresponding to 130 $\mu\text{mol N m}^{-2}\text{day}^{-1}$. This approach yielded an estimate of **20 Tg N yr⁻¹** fixed in pelagic environments over the Indian Ocean. This estimate provides a lower limit of N_2 fixation as it does not take into account the large contribution of other marine diazotrophs and the limitation of the temperature control which might not apply to other N_2 fixing organisms. A second approach has been utilized by extrapolating the rates of N_2 fixation provided by Bange *et al.* (2000) and scaling them to the average area of warm surface waters of the Indian Ocean ($30 \cdot 10^6 \text{ km}^2$), this method gained an estimate of 19 Tg N yr⁻¹ which is proximate to the previous estimate. Also high rates of benthic N_2 fixation have been suggested (Capone and Carpenter 1982). Benthic N_2 rates have been subject to revaluation by Howarth *et al.* (1988) and in the Indian Ocean are thought to amount to **0.19 Tg N yr⁻¹**. Overall N_2 fixation estimates for the Indian Ocean amount to **$19.7 \pm 0.5 \text{ Tg N yr}^{-1}$** where the error reflects only the range of the reported estimates. However in view of the considerable extrapolations associated with the listed N_2 fixation estimates it is very likely that further investigations of N_2 fixation in the Indian Ocean may lead to an upward revision of the current error estimate.

Indonesian Throughflow

The Indonesian throughflow (ITF) is an important site where the link between the Pacific and the Indian Oceans occurs. Warm and fresh waters are carried from the Pacific to the Indian Ocean across this section (Fieux *et al.* 2005). Extensive research has focused on the water exchange through this archipelago due to its involvement in the global thermohaline circulation (Gordon 1986). Because of the high interannual and seasonal variability of this

region, transports estimate of the Indonesian through flow encompass a large range of values (Fieux *et al.* 2005). In this study, the contribution of the Indonesian throughflow is taken from the results of an inverse box model of the global circulation by Ganachaud and Wunsch (2002). These authors derive a westward flow of 15Sv (1Sv=10⁶m³s⁻¹) through the Indonesian passages which is in good agreement with estimates of the net geostrophic transport calculated during a recent occupation of the section, which encompasses the throughflow between the Pacific and the Indian Oceans (Fieux *et al.* 2005). Ganachaud and Wunsch (2002) diagnose a flow into the Indian ocean of $-155 \pm 80 \text{ kmol s}^{-1}$ (for convention negative indicates a southward or westward transport) of nitrate which corresponds to an average of $68 \pm 35 \text{ Tg Ny}^{-1}$ where the uncertainty reported represents the range of the estimates which take into account the temporal (seasonal and interannual) variability of the mass transport.

3.2.3.3 Transport Calculations

On the basis of the measurements of inorganic and organic nutrients during the CD139 cruise and the recent estimates of water transport across 32°S by McDonagh *et al.* (2005) estimates of NO_3^- and TON advection, across the southern border of the Indian Ocean at 32°S, have been computed. The Indian Ocean is closed to the north and the 32°S section is considered the southern boundary of the Indian Ocean in this analysis.

The geostrophic circulation, referenced to the lowered-Acoustic Doppler Current Profiler (LADCP), was calculated based on the hydrographic data collected during CD139; the determination of the velocity fields is thoroughly described in McDonagh *et al.* (2005). Here a brief overview of the methods used is given; the same methodology was adopted to calculate the transport of inorganic and organic nutrients across the section.

The CD139 section across the Indian Ocean consisted of 133 full depth stations. This section covered the major Indian Ocean basins: the Mozambique basin, Madagascar basin, Southeast Indian Ridge and Perth Basin. On average, the spacing between stations was 46km, however in some cases station spacing was reduced to limit the depth of the bottom triangles (the triangular area remaining below the deepest common level for each pair of stations) which allowed to represent the bathymetry more accurately. Hence, 13 simulated stations were generated to lie at the crest of each ridge on the Southwest Indian ridge system and a total of 146 stations were used in the transport calculations. The geostrophic velocity was calculated with the thermal wind equation using the shear velocity between two adjacent stations. Thus densities were linearly interpolated onto full depth profiles from the two contiguous stations to generate 145 velocity profiles from the 146 station section. The velocities were referenced to the LADCP data and the velocity in the bottom triangle had to be simulated so that an

estimate of the transport through the bottom triangle was possible. Below the deepest common level, the velocity was reproduced by LADCP data for 43 stations and for the remaining ones the value of geostrophic velocity at the deepest common level was assumed to be constant throughout the bottom triangle.

From the Hellerman and Rosenstein (1983) wind climatology the wind driven surface Ekman transport was calculated as:

$$T_{Ekm}^{Prop} = \int \frac{\tau}{f} \cdot Prop_{Ek} \cdot dx \quad \text{Eq. 3.3}$$

Where the Ekman transport of any property is given by the integral in the Ekman layer of the product of the cross-section wind stress component τ and the mean value of the property in the Ekman layer $Prop_{Ek}$ divided by the Coriolis parameter f . In this analysis the depth of the Ekman layer is considered to be 60m.

In their analysis, McDonagh *et al.* (2005) calculated the circulation field on 8 layers defined by neutral density surfaces corresponding to different water masses similar to the analysis carried out by Robbins and Toole (1997) (Table 3.2, Fig 3.15).

Table 3.2 Neutral density layers used for the transport calculation.

Layer Number	Water Mass	Sigma (kgm^{-3})
1	Surface water	26.5
2	Sub Antarctic mode water	26.9
3	Upper Antarctic intermediate water	27.36
4	Lower Antarctic intermediate water	27.7
5	Upper deep water	27.96
6	Lower deep water (NADW influence)	28.11
7	Upper bottom water	29.23
8	Lower bottom water	Sea floor

Their circulation resulted in a net southward geostrophic transport of 23.6Sv, which was partially balanced by the northward wind Ekman transport of 2Sv and an implied net input from the Indonesian throughflow of 22Sv. This is larger than the 15Sv calculated by Ganashaud and Wunsch (2002) but is within the range that they calculate. Since in the nitrogen budget which is derived in this chapter it is necessary to use transport estimates which balance the mass flux I have used the upper limit of nitrogen transport through the Indonesian Throughflow calculated by Ganashaud and Wunsch (2002) which is associated with the 22Sv upper limit of mass flux.

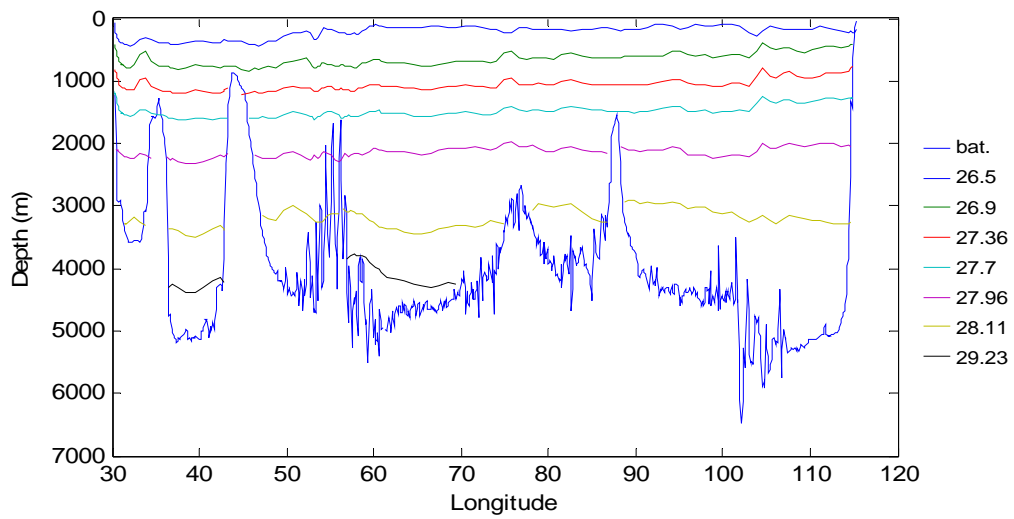


Fig. 3.15 Contour of neutral density γ , (kg m^{-3}) along the nominal latitude at 32°S in the Indian Ocean. Contours indicate the separation into layers of the water column used for the transport analysis.

The cumulative transport integrated for layers 1-5 and layers 6-8 (Fig. 3.16) indicated that the upper layer was dominated by a southward transport while deep layers were dominated by a net northward transport (Fig. 3.16). This transport was only in minor part balanced by the equatorward Ekman transport (Fig. 3.16).

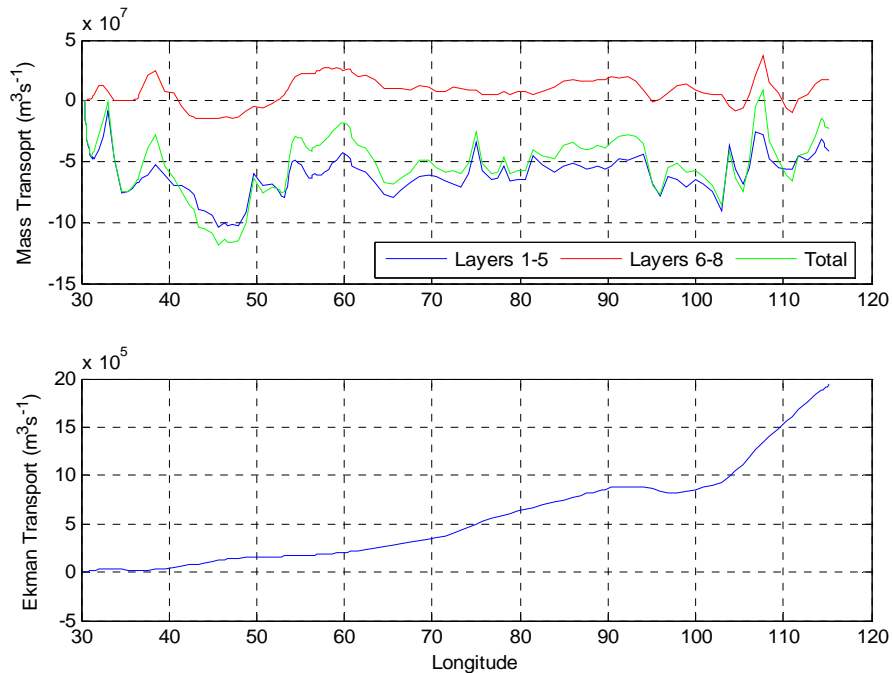


Fig. 3.16 Cumulative geostrophic transports integrated for layers 1-5 and layer 6-8 (top) and (bottom) cumulative Ekman transport.

The dominant northward transport occurs below 2000db in the 7th layer and is associated with the bottom water layer (Fig. 3.18). Also, significant is the inflow of North Atlantic Deep Water (NADW) in the 6th layer (Robbins and Toole 1997). The upper and lower Antarctic intermediate waters (layers 3-4) are both associated with a poleward transport (Fig. 3.18).

To calculate the flux of nitrate and TN carried by the geostrophic transport, the discrete Niskin bottle measurements were vertically interpolated on a 20dbar grid for each station to fit the calculated geostrophic velocities.

Nitrate was analyzed over the full depth of the water column for each of the 133 stations sampled during CD139; hence this bottle property data was interpolated on to the 146 stations described earlier and from a 2dbar onto a 20dbar grid using a linear regression. The data was then interpolated for each pair of stations, for a total of 145 profiles to match the velocity fields. The data was then averaged for each station on each density surface.

Samples for TN analysis were collected approximately every 3rd station. The strong correlation which exists between TN and NO_3^- (Fig. 3.17) has been used to extrapolate the missing data, from the total 50 profiles, to match the grid of 145 station profiles at given depths as described above.

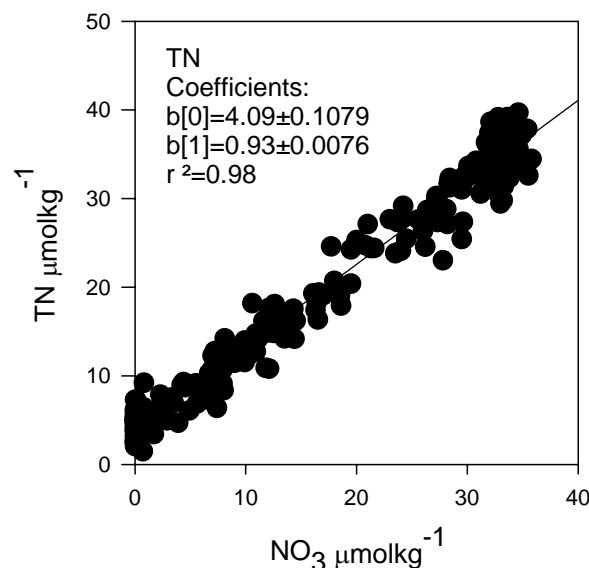


Fig. 3.17 Correlation between nitrate (μmolkg^{-1}) and total nitrogen (μmolkg^{-1}).

The values of TN derived using this method (hereafter TN_1), had a 5% uncertainty assuming that the mass transport had no error, were then averaged onto density surfaces. The resulting fields were then multiplied by *in situ* density and geostrophic velocities, and integrated over the entire section area to obtain the net advective NO_3^- and TON transport:

$$T_N = \int_{E-h}^W \int_o N \cdot v \cdot \rho_{\text{stp}} \cdot dx \cdot dz \quad \text{Eq. 3.4}$$

where T_N is the transport of the nitrogen pool in question, N is the concentration of the N pool, v is the geostrophic velocity and ρ_{stp} is the in situ density calculated over the entire water column (0-h) from the eastern coast of South Africa (W) to the western coast of Australia (E).

A second method to calculate the TN flux exploits the relative constant vertical distribution of TN. This method consists of multiplying the average TN concentration on each layer by the mass transport in each layer and yielded similar results as the TN derived method (see TN_2 results in Table 3.3) however these TN transport estimates were characterized by bigger uncertainties (30%) due to a range of different TN concentrations on the density layers. The additional component of the surface net flux due to the Ekman transport was calculated for both NO_3^- and TN_1 following Eq. 3.3.

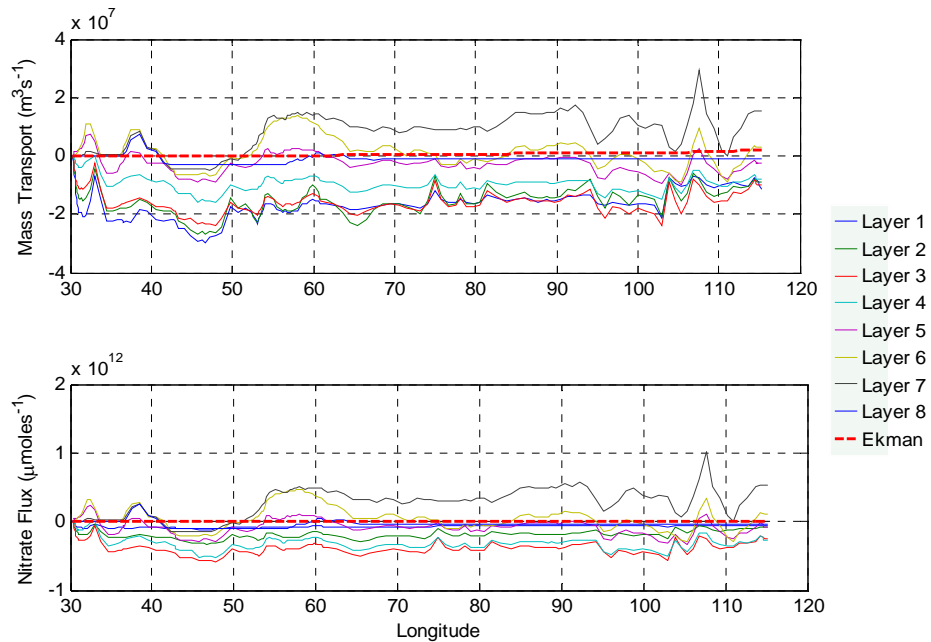


Fig. 3.18 Cumulative geostrophic and Ekman transport (top) and (bottom) nitrate geostrophic and Ekman transport for all the layers.

The geostrophic and Ekman transports of mass, nitrate and total nitrogen integrated on each density layer are shown in Fig. 3.19, where positive values correspond to a northward transport. Nitrate and TN fluxes generally agree with mass transports. The upper 2000m (layer 1-5) are dominated by a southward transport. The lower layers (6 to 8), associated with the upper bottom waters and the NADW, have a net northward transport. The transport of nitrate above the thermocline (the first two layers; <1000m) is very small, due to low NO_3^- concentrations. In these layers the majority of the N transport is carried out by the organic

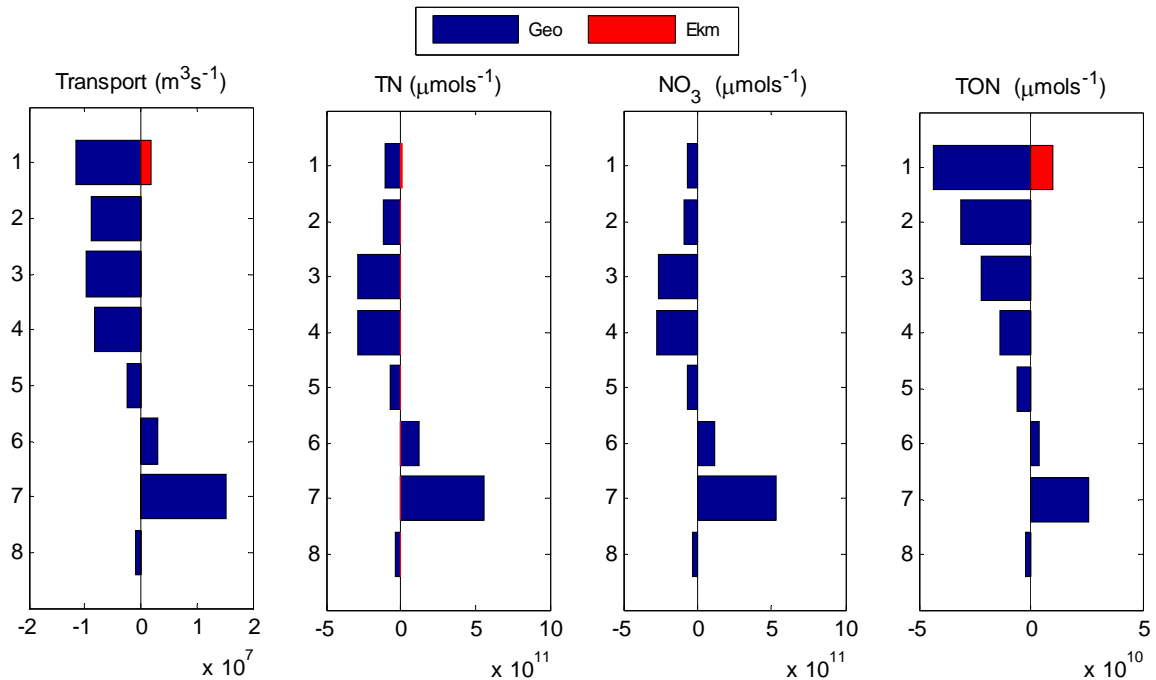


Fig. 3.19 Mass (m^3s^{-1}), TN_1 (μmols^{-1}), NO_3^- (μmols^{-1}), and TON (μmols^{-1}) geostrophic (blue) and Ekman (red) transports integrated on each density layer as defined in the text. Note different scales. Northward transport is positive.

component TON. With depth, as the concentrations of organic nutrients decrease, their contribution to the net transport on each layer diminishes (Table 3.3). The net geostrophic transport, integrated for all layers, sums to a southward flow of -134 kmols^{-1} for nitrate. This southward flow increases up to 222 kmols^{-1} when adding in the organic component of the N pool, which thus give a 40% contribution to the net southward transport of the organic N pool. As observed before, the contribution of TON to the total TN flux is highest on the surface density layer (40%) and decreases with depth ($\sim 5\%$) however, the contribution of TON to the net N transport across 32°S stays 40% (Table 3.3) this is due to the fact that the northern and southern nitrate fluxes counterbalance themselves along the density layers leaving the organic fraction to play a major role in the net N flux. The northward nitrate flux due to Ekman transport is minor due to the low concentrations of dissolved nitrate in the surface waters ($4.81 \cdot 10^{-3} \text{ kmols}^{-1}$) (Fig. 3.20). More significant is the northward wind forced Ekman transport of TN (10.3 kmols^{-1}), which increases towards the east (Fig. 3.20). The TN Ekman transport partially balances the southward geostrophic flow, reducing the net southward transport of TN to 212 kmols^{-1} .

Table 3.3 Mass, nitrate and total nitrogen transport integrated on each density layer. Nitrate transport is associated with 1.1% error. The total nitrogen transport calculated from derived total nitrogen (TN_1) was associated with 5% uncertainty, and the average total nitrogen (TN_2) associated with 30% uncertainty, are reported for comparison, see text for explanation. Estimates of the geostrophic and Ekman velocities are reported in McDonagh *et al.* (2005). The last column represents the contribution (%) of TON to the total N geostrophic transport calculated from TN_1 .

Layer	Mass Tr. $10^6 \text{ m}^3 \text{s}^{-1}$	EK Mass $10^6 \text{ m}^3 \text{s}^{-1}$	NO_3 Tr. kmol s^{-1}	EK NO_3 kmol s^{-1}	TN_1 Tr. kmol s^{-1}	TN_1 EK. kmol s^{-1}	TN_2 Tr. kmol s^{-1}	TN_2 EK. kmol s^{-1}	Contribution of TON (%)
1	-11.51	1.942	-62.9	4.81E-3	-106	10.3	-76	11.3	41
2	-8.96		-88.9		-120		-130		26
3	-9.79		-261		-283		-230		8
4	-8.1		-276		-290		-282		5
5	-2.59		-69.3		-75		-97		8
6	3.03		121		125		105		3
7	15.3		535		561		549		5
8	-1.065		-32.2		-34		-37		6
Total	-23.6	1.942	-134	4.81E-3	-222	10.3	-200	11.3	40

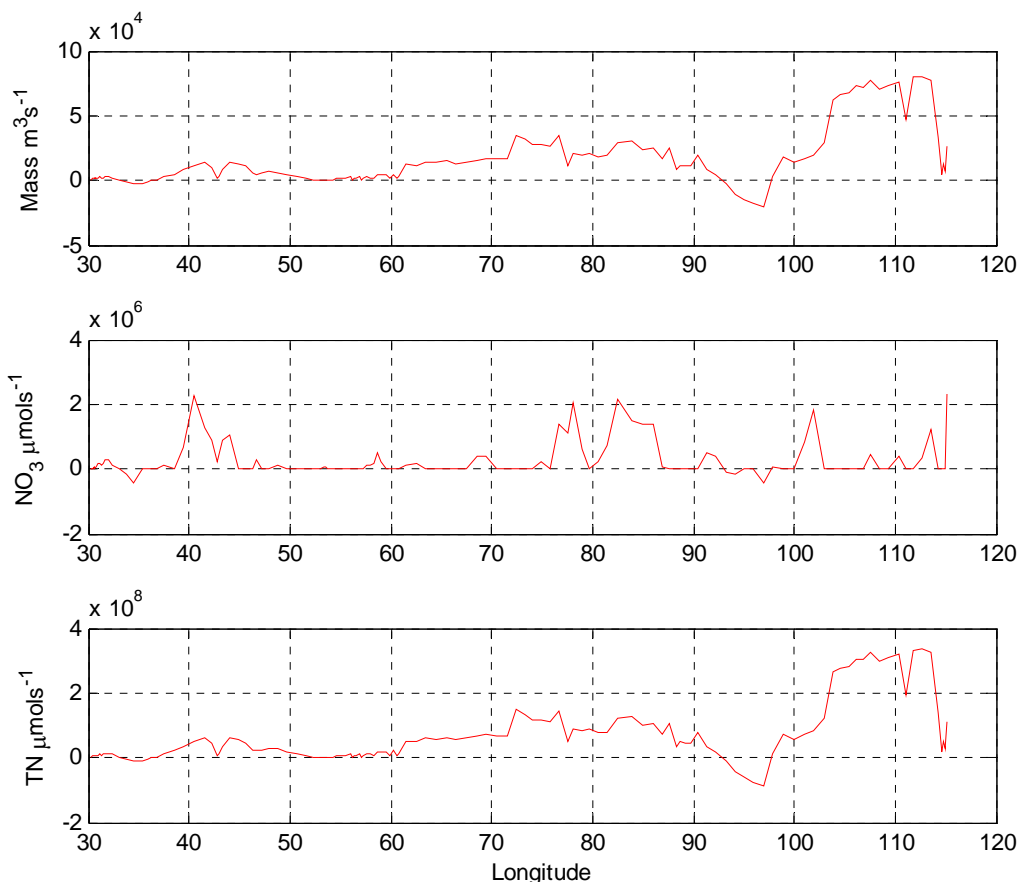


Fig. 3.20 Longitudinal variation of the Ekman transport of mass (top), NO_3^- (middle) and TN (bottom) across 32°S in the Indian Ocean.

3.2.3.4 N Budget

It is now possible to compile a budget of nitrogen for the Indian Ocean North of 32°S using the TN divergence values from ocean transport, atmospheric deposition, river inputs, N₂ fixation estimates and losses due to denitrification and sedimentation. If the N inventory, north of 32°S, is in a steady state over the regional overturning time scales the inputs minus the outputs terms would be balanced following Eq. 3.5:

$$\frac{dT\bar{N}}{dt} = 0 \quad \text{Eq. 3.5}$$

A summary of the fluxes in and out of the Indian Ocean at 32°S based on literature data, the hydrographic work of McDonagh *et al.* (2005), and the total N measurements made on CD139 are presented in Table 3.4. Please note that, to balance the mass, the transport of ITF has been estimated to be 22Sv which corresponds to the upper range of the ITF transport reported by Ganachaud and Wunsch (2002). Hence the associated nitrate flux has been scaled to this transport and will correspond to the upper limit of the range reported by Ganachaud and Wunsch (2002) (100 Tgy⁻¹) and thus has no error associated with it. In Tables 3.4 and 3.5 terms in bold are used for the final calculations. It must be stated that the uncertainties calculated for the nitrate, TN and TON transports are given by only the error associated with the analytical procedure and do not account for the error (given by temporal variability) in the mass transport, hence they are not fully accounted for and represent only a lower limit.

The biggest term in the budget is the overturning circulation followed by the ITF. The contribution of internal processes such as N₂ fixation and denitrification is small compared to physical processes. Rivers and atmospheric N deposition play a minor role.

The nitrogen budget of the Indian Ocean is, according to Table 3.4, balanced within 2 TgNy⁻¹ or about 0.5% of the summed source or sinks terms. However, the computed balance can be compromised by the observed seasonal and inter-annual variability of the Indonesian throughflow (Fieuex *et al.* 2005) and the associated large (~50%) uncertainty of the ITF transport (Ganachaud and Wunsch 2002). Moreover the above analysis assumes that there is no organic nitrogen load carried by the Indonesian Throughflow. Whilst no data exists to confirm or refute this suggestion it seems likely that such low latitude waters will have significant organic nitrogen concentrations and hence that this may be an important process. At 32°S in the Indian Ocean about 40% of the total N transport is carried in the organic phase (Table 3.3), extrapolating this to the ITF would result in an extra 40TgNyr⁻¹ being carried into the Indian Ocean which the hydrographically balanced circulation would be unable to remove.

Table 3.4 Sources and sinks of nitrogen into the Indian Ocean north of 32°S. The fluxes are in TgN yr^{-1}

Sources	TN Tg yr^{-1}	Reference
Atmospheric Dry & Wet deposition	7.3	Galloway <i>et al.</i> 2004
N_2 fixation		
Pelagic	19.5 ± 0.5	Galloway <i>et al.</i> 2004
Benthic	0.19	Howarth <i>et al.</i> 1988
Rivers	7.5	Greene <i>et al.</i> 2004
ITF Nitrate (15Sv)	(68 ± 35)	Ganachaud and Wunsch 2002
Nitrate (22Sv)	100	
North ward transport at 32°S		
NO_3	290 ± 3.2	
TON	13 ± 0.65	This study
TON (Ekman)	5 \pm 0.25	
$\sum \text{Sources}$	443 ± 5	
Sinks		
Denitrification		
Pelagic	- 31 ± 1.5	Bange <i>et al.</i> 2000;
Benthic	-6.4	Christensen <i>et al.</i> 1987;
Deep Sediments	-1.8	Codispoti <i>et al.</i> 2001.
N Sedimentation	-1.8	Hedges and Keil 1995
South ward transport at 32°S		
NO_3	-349 ± 3.8	
TON	-52 ± 2.6	This study
$\sum \text{Sinks}$	-445 ± 8	
$\sum \text{Sources} - \sum \text{Sinks}$	-2 \pm 13	

To keep the budget in balance either N is accumulating in the Indian Ocean, or the hydrographic flows are incorrect, or sink terms have been underestimated. On balance it seems more likely that, assuming the hydrographic flows are correct, any extra organic N carried by the ITF is being removed rather than accumulating as such an accumulation would likely be detectable in the long time series of nitrate measurements at 32°S and such an increase is not observed. If this is not accumulating in the Indian Ocean it must be being removed, i.e. one of the sink terms in Table 3.4 must be seriously underestimated. The most likely candidate is denitrification which would have to increase from 40 to 80 TgN yr^{-1} to balance the budget. Is an additional sink for N feasible? Recently Codispoti *et al.* (2001) proposed a denitrification rate of 60TgN yr^{-1} for the Indian Ocean, approximately twice the ‘traditional’ value consistent with recent suggestion that the annamox process may be more widely occurring in the oceans than previously thought (Arrigo 2005), suggesting that a balanced N budget with a substantial organic nitrogen flux through the ITF may not be unreasonable. In addition no estimate of denitrification from the Bay of Bengal is included in Table 3.4. Taken together it seems feasible then that the Indian Ocean N budget may be close

to being balanced. Further it is likely that it may have been unbalanced in the recent past when riverine and atmospheric N transport were lower stimulating lower denitrification rates (Codispoti *et al.* 2001). Hence assuming that the circulation has not changed substantially over the last 150 years, the Indian Ocean may have been a net sink of N in the preindustrial age.

Therefore I propose a revisited N budget which includes the contribution of organic nitrogen from the ITF and the higher denitrification rates proposed by Codispoti *et al.* (2001) (Table 3.5). It must be further stated that the limits of this analysis are the small errors associated with the major internal processes such as denitrification and N₂ fixation which are however likely to be underestimated due to the lack of adequate coverage of direct measurements on a regional basis. Moreover, oceanic variability remains the main source of uncertainty, which needs to be accounted for, for an improvement of the error analysis associated with the N budget.

Table 3.5 Revisited Nitrogen budget into the Indian Ocean north of 32°S. The fluxes are in TgNy⁻¹

Sources	TN Tgy ⁻¹	Reference
Atmospheric Dry & Wet deposition	7.3	Galloway <i>et al.</i> 2004
N ₂ fixation		
Pelagic	19.5±0.5	Galloway <i>et al.</i> 2004
Benthic	0.19	Howarth <i>et al.</i> 1988
Rivers	7.5	Greene <i>et al.</i> 2004
ITF Nitrate (15Sv)	(68±35)	Ganachaud and Wunsch 2002
Nitrate (22Sv)	100	Ganachaud and Wunsch 2002
TON (22Sv)	40	Estimated this study
North ward transport at 32°S		
NO ₃	290±3.2	
TON	13±0.65	This study
TON (Ekman)	5±0.25	
\sum Sources	483±5	
Sinks		
Denitrification		
Pelagic	(-31±1.5)	Bange <i>et al.</i> 2000
Pelagic	60	Codispoti <i>et al.</i> 2001
Benthic	-6.4	Christensen <i>et al.</i> 1987
Deep Sediments	-1.8	Codispoti <i>et al.</i> 2001
N Sedimentation	-1.8	Hedges and Keil 1995
South ward transport at 32°S		
NO ₃	-349±3.8	
TON	-52±2.6	This study
\sum Sinks	-445±8	
\sum Sources – Sinks	-8±13	

Table 3.5 suggests that the removal of fixed nitrogen by denitrification is not compensated for by the combined nitrogen inputs due to fixation, rivers and the atmosphere. Thus hydrographically the Indian Ocean is not balanced with respect to the N flows, the flow at 32°S and via the ITF to the basin is larger than the outflow at 32°S and hence we can therefore view the basin as being unbalanced in terms of its communications to the remainder of the oceans. Therefore the excessive denitrification over fixation is occurring and that this is substantially compensated for by the physical transport of organic nitrogen through the ITF.

The revised budget is consistent with a reduced N/P ratio in the intermediate outflowing layers. This is because of the extensive N removal in the basin by denitrification. Additional factors in this may be the P delivered by atmospheric and riverine inputs. Both of these mechanisms deliver high N/P ratio nutrient pools to the ocean. For example Baker *et al.* (2003) suggest that the mean N/P ratio of inputs to the Atlantic along the Atlantic Meridional Transect (AMT) transect is $>> 16:1$ and particle sorption processes in the turbid plumes of the large rivers are likely to selectively remove P relative to N as a consequence of its greater particle reactivity (Benitez-Nelson 2000). This apparent problem (high N/P ratio inputs leading to low N/P outflows) can be rationalized by considering that the role of the N delivered by the rivers and the atmosphere to the basin is for it to balance some of the excess of denitrification over nitrogen fixation within the basin. Thus any extra input of P from the atmosphere or rivers will serve to reduce the outflowing N/P ratio. A consequence of the analysis presented here is thus that it implies that the basin may be a source of P to the remainder of the oceans as suggested by Ganashaud and Wunsch (2002); unfortunately a comprehensive evaluation of the P budget was not carried out due to the lack of available ancillary data.

High denitrification rates in the basin are may be supported in part by the high anthropogenic inputs which can lead to the increased anoxia and in turn enhance denitrification (Codispoti *et al.* 2001). Atmospheric and river N loads have incremented over the last ~ 150 years as a consequence of industrial activities. Galloway *et. al.* (2004) estimated that N created by anthropogenic activities has incremented by a factor of 10 from 1860 to the early 1990s. Much of this N created was dispersed into the environment, 30% of which was released from the continents to the marine environment through atmospheric and riverine export. Atmospheric deposition and riverine inputs of nitrogen are the two major interfaces that allow the connection between continents and oceans, and their importance has increased as the load of nitrogen sources from the continents to the ocean has increased with time. Thus, as anthropogenic N fixation on land increases, the supply of nitrogen from the

continents to ocean basins may become increasingly more important relative to marine N_2 fixation.

Although Indian Ocean denitrification currently likely exceeds local N_2 fixation by 2-3 fold the regional N budget is balanced. In particular, as observed above one compensating source of N is organic nitrogen carried by the ITF. This means that ultimately imbalances in the sinks and source terms are coupled through circulation i.e. the nitrogen that is being removed in the Indian Ocean is being replaced by an external flux of N coming from elsewhere. As, on a global scale N_2 fixation is the most important source of N to the oceans, it is likely that this source of fixed N is N_2 fixation. Therefore the coexistence of high denitrification rates and a balanced N budget in this basin can be explained by invoking the existence on a global scale of N_2 fixation rates that can compensate for the loss of N in the Indian Ocean. Whether the N inputs from this source are large enough to make the global N budget balanced is addressed in chapter 5 when the estimates of nitrogen fixation in the North Atlantic made using a novel tracer are extrapolated to the global ocean.

This hypothesis agrees with the recent present day global marine N budget by Gruber (2004). According to this author the present day marine N budget is in approximate balance. To stabilize the N cycle, he suggests a tight coupling between N_2 fixation and denitrification processes, on the timescales of the N turnover (approximately 3000yr). The coupling occurs through a series of feedback mechanisms that act as a “N cycle Homeostat”. This concept describes an internally stabilized system that mutually interacts with other systems such as the carbon cycle. Two of the main negative feedback loops are prompted by N to P ratios in the surface waters. High N/P ratios stimulate denitrification which in turn leads to a decrease in export production and lower oxygen demand in the thermocline and in marine sediments closing the loop with a decrease in denitrification (Codispoti 1989). In low N/P conditions, N_2 fixing organisms have an ecological advantage outcompeting other phytoplankton (Capone *et al.* 1997). N_2 fixation refurbishes N to the ocean until the high N/P ratios are reached switching the system back to denitrification. These feedback loops secure the ocean against running out of nitrogen and also provide a balance between the N and the P inventory.

The budgets derived here stress that the omission of dissolved organic nutrients from current regional budgets can lead to erroneous conclusion (i.e. omitting the role of DON transported by the ITF would imply the Indian Ocean being a net sink of N due to the excess of denitrification, assuming that Codispoti *et al.* (2001) is correct) regarding nutrient imbalances. Alternatively the hypothesised organic nutrient supply via the ITF can be regarded as in some senses validating the Codispoti *et al.* (2001) high denitrification rate estimate. Given

the relatively short residence time of the N pool, if such nutrient imbalances are real (i.e. excessive denitrification over nitrogen fixation) then they affect the marine N inventory with potential impacts on marine productivity and atmospheric CO₂ drawdown. Hence the role of organic nutrients seems to be fundamental in reconciling apparent discrepancies in nutrient budgets.

3.2.3.5 Conclusions

Given the profound impact of the marine nitrogen cycle on the marine carbon cycle, it is not surprising that extensive research has been focusing on whether the marine N cycle is in balance or not. The re-evaluation of the magnitude of denitrification by Codispoti *et al.* (2001) and Brandes and Devol (2002) has highlighted the possibility that the present marine ocean is losing nitrogen (Codispoti 1995, 2001), prompting a re-thinking of global N₂ fixation estimates to bring the present day N cycle back into a steady state.

As the Indian Ocean is one of the most important sites for global marine denitrification, the measurement of the N budget in this basin is of particular importance.

According to the data presented here, the present day marine N cycle in the Indian Ocean conforms to a steady state scenario using the upper range denitrification rate reported in literature (Codispoti *et al.* 2001). The overturning circulation is the major player in the budget and the inferred organic flux by the ITF is fundamental in compensating for the loss of fixed N in denitrification.

3.3 Final Conclusions

The Indian Ocean, despite its hypothesized importance for the global oceanic N cycle, lacked basin scale measurements of organic nutrients. The data provided in this chapter addresses this issue.

Dissolved organic nutrients are an important fraction of the nutrient pool and need to be taken into account to clarify nutrient imbalances and quantify nutrient inventories. The Indian ocean basin is characterized by low N:P ratios both in the inorganic and organic fractions with respect to phytoplankton nutrient requirements due to the denitrification rates being greater than N₂ fixation. The strongly non-Redfieldian TON:TOP ratio suggest a decoupling of TON and TOP remineralization processes and indicate a severe TON deficiency brought by the strong N limitation which leads to a community demand for TON. Despite the measured low N:P ratios and an occurrence of nitrate exhaustion before

phosphate, a consistent fraction of TON is potentially available when TOP levels are limiting implying that this basin would run out of P before N.

In this basin, the surface distribution of dissolved organic nutrients is mainly controlled by the interplay between production and consumption processes whilst the role of physical processes is minor. In particular, N_2 fixation occurring locally is likely to be an important process in controlling the regional distribution of TON although, on a basin scale, its impact is minor compared to denitrification.

TON and TOP Ekman meridional advection play a small but not trivial role in providing N and P into the gyre to support export production. The contribution of TON advection is of the same order of the new N supplemented by N_2 fixation into the gyre. The advection of TOP is quantitatively more important than that of TON. This finding agrees with the difficulty of supplying P into the gyre due to the limited atmospheric deposition and the lack of an equivalent mechanism of N_2 fixation for phosphorus.

In the Indian Ocean 40% of the net N transported by the overturning circulation across the boundary at 32°S, is attributable to organic nutrients. To close the N budget assuming the upper range estimates of denitrification to be correct, the inclusion of organic nutrient transport by the ITF is required. The Indian Ocean N budget conforms to a steady state where excess of denitrification over N_2 fixation is compensated for by atmospheric, riverine and a hypothesized flux of DON in through the ITF.

4 North Atlantic Subtropical Gyre

4.1 Introduction

The North Atlantic subtropical gyre has been traditionally viewed as a marine desert due to the anticyclonic gyre scale circulation which results in low inorganic nutrient concentrations and low phytoplankton biomass. Although much of the production derives from regenerated nutrients (Eppley and Peterson 1979), geochemical tracers and oxygen mass balances have indicated that a consistent fraction of production (Jenkins 1988) is associated with export production (Jenkins and Goldman 1985, Jenkins 1988). These findings have highlighted the possibility of subtropical gyres accounting for up to 50% of the marine export production (Emerson *et al.* 1997) and raised the problem of identifying the pathways by which nutrients are supplied to phytoplankton in these oligotrophic waters.

In the North Atlantic subtropical gyre, the estimated flux of inorganic nutrients of $0.21\text{molNm}^{-2}\text{y}^{-1}$ into the euphotic zone by diapycnal mixing, atmospheric deposition and convection (McGillicuddy *et al.* 1998), is not sufficient to maintain the estimates of export production ($0.48\pm0.14\text{molNm}^{-2}\text{y}^{-1}$ Williams and Follows 1998; 0.67 ± 0.14 to $0.78\pm0.15\text{molNm}^{-2}\text{y}^{-1}$; Jenkins and Doney 2003). Thus, much research has focused on finding alternative transport mechanisms to satisfy the additional nutrients required to explain the observed export production.

In the last decade, the picture of a non uniform regime involving different mechanisms supporting new production within the subtropical gyre, has emerged (Lipschultz *et al.* 2002). Hence the subtropical gyre has been divided into a northern sector and a southern sector separated by the boundary of convective mixing at $\sim 30^\circ\text{N}$.

The northern sector experiences winter convective mixing that brings nutrients into the surface layers leading to the well observed winter bloom and the production and export of significant amounts of DOC (Menzel and Ryther 1960; Carlson *et al.* 1994; Hansell and Carlson 1998, 2001). Wintertime new production accounts for 25-60% of annual new production (Jenkins and Wallace 1992). The northern sector undergoes an oligotrophic period when the onset of summer stratification leads to a complete consumption of nutrients (Wu 2000; Lipschultz 2001). During this period, although the input of nutrients by diapycnal mixing is negligible (Ledwell *et al.* 1993), a large draw down of DIC is observed at the southern boundary of the northern sector where the Bermuda Atlantic Timeseries (BATS) is located (Bates *et al.* 1996; Michaels *et al.* 1996). This major enigma has laid the base for

extensive research on possible mechanisms involving N_2 fixation, significant deviations from Redfield stoichiometry (Anderson and Pondaven 2003) and atmospheric N inputs.

The southern sector of the subtropical gyre remains permanently stratified preventing winter convection; hence this sector is permanently oligotrophic and the maintenance of new production is an open question.

4.1.1 Nutrient Supply in the Euphotic Zone

If the nutrient supply were to be satisfied by diapycnal mixing (Jenkins 1988), then a much larger turbulent mixing coefficient would be needed than the ones observed; ($10^{-3}\text{m}^2\text{s}^{-1}$) would be necessary but the observed thermocline mixing rates appear to be two orders of magnitude lower, Ledwell *et al.* 1993). This has led to the suggestion that nutrients could be supplied by alternative transport mechanism such as isopycnal transport or mesoscale eddies (Jenkins and Wallace, 1992).

Further investigations highlighted that the estimated isopycnal mixing rates in the Sargasso Sea (Jenkins 1991) were much too low to explain the observed ^3He flux into the thermocline (Jenkins and Doney 2003) implying that isopycnal transport is not an efficient mechanisms for nutrient supply in the upper layers.

Intermittent eddy-induced upwelling events are estimated to potentially support $\sim 0.25\text{molNm}^{-2}\text{y}^{-1}$ (McGillicuddy and Robinson 1997, McGillicuddy *et al.* 1998, Oschlies and Garcon 1998). This transport mechanism, however, is unlikely to fully explain the observed CO_2 drawdown occurring at BATS as the uplift of nutrient rich waters into the euphotic zone would carry a consistent amount of CO_2 (Bates 2001). Moreover, estimates of the significance of these “eddy pumping” events rely on unrealistic fast nutrient remineralization rates below the thermocline, thus their efficiency is probably lower than previously suggested (Martin and Pondaven 2003, Oschlies 2002).

Other processes have therefore been studied. Convergence of inorganic nutrients in the Ekman layer has been shown to play a significant role at the gyre boundaries but not in the interior where the lifetime of inorganic nutrients is limited (Williams and Follows 1998). However, this process might be important in transporting dissolved organic nutrients, which are relatively refractory and can be advected over longer distances, into the gyre (Rintoul and Wunsch 1991; Oschlies and Garcon 1999, Abell *et al.* 2000) but its importance will strongly depend on DOM bioavailability.

At present, there is evidence that nitrogen fixation could be a further source of N for this region, especially in the southern Sargasso sea (Carpenter *et al.* 2004) although an

independent source of P into the system would be required (Michaels *et al.* 1996, Gruber and Sarmiento 1997) to sustain biological production.

4.1.2 N_2 Fixation

4.1.2.1 Direct Measurements

Very recently, direct measurements of N_2 fixation rates in the south-western North Atlantic have been reassessed (Capone *et al.* 2005) and found to support very high fixation rates. These rates, ranging from 60 to $898\mu\text{mol Nm}^{-2}\text{d}^{-1}$ (average= $239\mu\text{mol Nm}^{-2}\text{d}^{-1}$), are consistent ($500\text{--}2500\mu\text{mol Nm}^{-2}\text{d}^{-1}$; Michaels *et al.* 1996) or higher (197 or $300\mu\text{mol Nm}^{-2}\text{d}^{-1}$ depending on whether the N:P ratio of N_2 fixers is of 125 or 45 respectively; Gruber and Sarmiento 1997; $70\text{--}208\mu\text{mol Nm}^{-2}\text{d}^{-1}$; Hansell *et al.* 2004) than those derived from indirect geochemical estimates and are much larger than direct measurements from older studies (Capone and Carpenter 1982, Carpenter 1983, Orcutt *et al.* 2001).

The large variability among the measured N_2 fixation rates has been attributed to the large spatial variability of *Trichodesmium* abundance (ranging from 0 at 34°N to 250 at 26°N colonies m^{-3}) with lower abundances in the northern sector of the Sargasso Sea (Orcutt *et al.* 2001, Carpenter *et al.* 2004). There is also evidence of seasonal variability in N_2 fixation with the lowest rates in January followed by an increase in spring and maximal rates being measured during the summer period when water column stability is at its maximum. Recently, Bates and Hansell (2004) have suggested an increase in the strength of N_2 fixation during a positive phase of the North Atlantic Oscillation (NAO) induced by higher dust deposition into the surface ocean.

4.1.2.2 Indirect Geochemical Estimates

Anomalous N:P ratio: the N^ concept*

Geochemical estimates of the large scale distribution and rate of N_2 fixation have been based upon NO_3^- to PO_4^{3-} ratio anomalies (Michaels *et al.* 1996, Gruber and Sarmiento, 1997). The global-scale oceanic distribution of NO_3^- versus PO_4^{3-} reveals a global trend that is well described by a regression with a slope of about 16:1. The existence of a relatively constant N:P ratio is known as the Redfield ratio (Redfield *et al.* 1963) and reflects the N and P demand and composition of marine phytoplankton. Michaels *et al.* (1996) first introduced the concept of the geochemical tracer N^* based on deviations from the classical 16:1 ratio between nitrate and phosphate, which describes the production or consumption of nitrate, with a N:P stoichiometry different from 16:1. In determining N^* it is assumed that N_2 fixing organisms

have a N:P stoichiometry that is different from the Redfield ratio (N:P=125). This assumption has been based on the observation of a N:P ratio of 125 during a *Trichodesmium* bloom (Karl *et al.* 1992); however it is now a matter of debate as field and culture studies of *Trichodesmium* have reported much wider ranges of N:P ratios (La Roche *et al.* 2005). Using this tracer, Michaels *et al.* (1996) deduced rates of N_2 fixation for the North Atlantic of 50-90TgNyr⁻¹. Based on the global distribution of N^* , Gruber and Sarmiento (1997) suggested that the tropical and subtropical North Atlantic ocean and the Mediterranean Sea are the major contributors to N_2 fixation in the global ocean. A more recent examination of N^* (Deutsch *et al.* 2001) indicates that the Subtropical North Pacific ocean may also contribute up to 50% of global N_2 fixation rate. The high rates of N_2 fixation estimated at the BATS site, based on geochemical evidence, could reconcile the large summer time draw-down of CO_2 but are not supported either by the direct measurements of N_2 fixation rates (Orcutt *et al.* 2001) nor by the dissolved (Hansell and Carlson 2001) or particulate fluxes of organic matter out of the euphotic zone (Hood *et al.* 2001). Thus the large N^* signal, at BATS is probably transported, following the gyre circulation, from the south west region where N_2 fixation estimates are 12 fold higher.

To date the fate of recently fixed nitrogen is still poorly known. Recent field studies have documented the release of up to 50% of the recently fixed N_2 as DON (Glibert and Bronk 1994; Mulholland *et al.* 2004), mostly as amino acids (Capone *et al.* 1994). Thus, the transport of this recently fixed N may provide a source of excess nitrogen to support production and may explain the observed deviations from the Redfield stoichiometry in areas where extensive N_2 fixation has not been observed. Measured accumulations of DON in parts of the Subtropical Pacific and Atlantic oceans have been attributed to the release of DON associated with N_2 fixation (Hansell and Waterhouse 1997; Karl *et al.* 1997; Vidal *et al.* 1999; Abell *et al.* 2000). On a transect from the Canary Islands to Argentina, Vidal *et al.* (1999) found that for many areas of the Atlantic Ocean the upward flux of nitrate was closely balanced by the downward flux of DON. However, at around 10°N, the downward flux of DON could not be fully accounted for by the upward N flux and at this location the large abundance of *Trichodesmium* suggested that N_2 fixation supplied the additional N needed to balance the DON flux out of the euphotic zone.

An alternative explanation of the discrepancy between measured and estimated N_2 fixation rates questions the interpretation of elemental ratio anomalies revealed by the geochemical tracer N^* . The N^* concept has some limitations as it relies on the assumption that the only significant, non-conservative processes that perturb the canonical Redfield

elemental stoichiometry are denitrification and N_2 fixation. However, preferential uptake of inorganic P with respect to inorganic N in the surface layers, and the atmospheric deposition of N would also contribute to a nitrogen excess with respect to phosphorus and thus a positive N^* signal (Baker *et al.* 2003). Another scenario that would induce a similar N^* signal is the preferential remineralization of TOP from DOM. This faster cycling of TOP in the upper layers would lead to the production of nitrogen rich DOM which could be advected laterally by Ekman transport, or exported into the thermocline thus providing a source of excess nitrate in areas distant from the original source of DOM. If this process were important, then N to P ratios would reflect a near Redfield stoichiometry in the surface ocean and increase gradually with depth as the remineralization of P takes place. The potential for this scenario would depend on the bioavailability, remineralization rates and residence times of DON and DOP in the surface ocean as compared to their export timescales.

Stable Nitrogen isotopes

The ratio of the stable isotopes $^{15}\text{N} : ^{14}\text{N}$ in the ocean has proved to be powerful tracer of the transformations that occur within the nitrogen cycle (Mariotti *et al.* 1981) and can provide evidence of N_2 fixation in the ocean (Liu *et al.* 1996; Carpenter *et al.* 1997; Karl *et al.* 1997). Dissolved N_2 , the substrate for marine N_2 fixers, has a $\delta^{15}\text{N}$ of 0.6‰, close to the value expected for equilibrium with atmospheric N_2 . N_2 fixation has little isotopic fractionation so that the produced organic compounds will be slightly depleted in ^{15}N relative to their substrate ($\delta^{15}\text{N}$ of 0 to -1 ‰, Carpenter *et al.* 1997; Wada 1991). The large oceanic nitrate reservoir has a mean $\delta^{15}\text{N}$ of ~5‰ (Sigman *et al.* 1999) thus the relative importance of N_2 fixation compared to upwelled nitrate in supporting primary production should be discernable based on the $\delta^{15}\text{N}$ of the fixed nitrogen. However, several processes act to fractionate N isotopes in the marine environment (Altabet 1988). Low $\delta^{15}\text{N}$ in particulate organic matter might reflect both N_2 fixation and recycled production. Secondary producers excrete ammonia depleted in ^{15}N and produce ^{15}N enriched faecal pellets, which sink out of the euphotic zone leaving a ^{15}N depleted N reservoir in the upper ocean. Thus a depleted ^{15}N signal in PON could be misinterpreted.

In the subtropical North Atlantic, the upper water column N budget (Montoya *et al.* 2002) and stable isotopic signatures of PON (0-2‰; Mino *et al.* 2002; Montoya *et al.* 2002; Mahaffey *et al.* 2003) suggest high N_2 fixation rates. The relative importance of N_2 fixation and upwelled nitrate as sources involved in supporting primary production have been estimated using a two end member isotope mixing model by several authors. N_2 fixation was estimated

to supply 13 to 68% of the N to the oligotrophic North Atlantic Ocean (Mahaffey *et al.* 2003, Montoya *et al.* 2002, Mino *et al.* 2002, Capone *et al.* 2005) with a south and westward increase in the intensification of the contribution of N₂ fixation (Montoya *et al.* 2002, Capone *et al.* 2005).

N₂ fixation: leading to P limitation?

Although a lot of progress has been made in the recent years, the magnitude of N₂ fixation in the North Atlantic is still debated. The discrepancy between direct measurements and indirect geochemical estimates may be in part due to the fact that direct measures of N₂ fixation rates have concentrated mostly on *Trichodesmium* and have not taken into account the contribution of recently discovered widespread unicellular N₂ fixers (Zehr *et al.* 2001), and may also be the result of the different spatial and temporal scales of direct (small/short scale) and indirect geochemical methods that integrate over long spatial and temporal scales.

Also, the controls over oceanic N₂ fixation remain to be determined. It is known that *Trichodesmium* colonies are only successful in areas where sea water temperature is above 20°C; whether this requirement is also applicable to the recently discovered N₂ fixing coccoid cyanobacteria and bacterioplankton (Zehr *et al.* 2001) is not known.

It has been suggested that Fe supply may control N versus P limitation through modulation of N₂ fixation. The bioavailability of iron is an important factor affecting the productivity of diazotrophs. Iron is an essential requirement for the enzyme nitrogenase that regulates N₂ fixation, and N₂ fixers such as *Trichodesmium* have a high Fe quota (Berman-Frank *et al.* 2001). The observed global patterns of N* and N₂ fixation appear to be consistent with the iron enrichment resulting from dust deposition which results in high N₂ fixation rates in the North Atlantic, which receives consistent dust deliveries from the African continent. However, N₂ fixation can be limited by the scarce bioavailability of iron, even in regions subject to high dust deposition such as the South China Sea, probably due to the lack of Fe-binding organic ligands in the surface water (Wu 2003).

Most of the Fe in seawater exists in the particulate form due to the scarce solubility of Fe(III) under oxidising conditions above pH4 (Jickells *et al.* 2005); this form is unavailable for biological uptake. Most of the soluble portion of Fe in sea water is bound to organic complexes that, depending on their chemical nature, may increase the bioavailability of iron to phytoplankton. Siderophores, high affinity Fe(III) chelating ligands, have been found to be synthesised by cyanobacteria and heterotrophic bacteria (Wilhelm and Trick 1994; Venter *et al.* 2004) and some *Synechococcus* strains (Trick and Wilhelm 1995) and to scavenge Fe during periods of Fe limitation.

There is evidence that *Trichodesmium* *sp.* in the western North Atlantic have an increased affinity for siderophore-bound Fe(III) (Achilles *et al.* 2003); it is not known however, if these organic complexes are created directly by the diazotrophs or are produced by colony associated heterotrophic bacteria (Barbeau *et al.* 2001).

In the subtropical and tropical North Atlantic, contrasting evidence suggests N₂ fixation is either phosphorus limited (Sanudo-Wilhelmy *et al.* 2001; Dyhrman *et al.* 2002) or co-limited by P and Fe (Mills *et al.* 2004) despite the high dust inputs. In the North Atlantic, phosphate concentrations are extremely low in comparison with the subtropical Pacific (Wu 2000). These authors suggested that a higher availability of Fe in the North Atlantic, compared to the North Pacific, induces high rates of N₂ fixation, which in turn lead to the complete drawdown of P and phosphate limitation.

Although inorganic P is depleted in the subtropical north Atlantic, the bioavailability of DOP to the phytoplankton community represents a potential source of P that is currently not well characterised. The extracellular hydrolysis of DOP by the cell surface enzyme alkaline phosphatase (AK) associated with *Trichodesmium* has been observed both *in situ* and in culture experiments (Dyhrman *et al.* 2002; Mulholland *et al.* 2002).

The ecto-enzyme AK catalyses the hydrolysis of a wide range of phospho-monoesters (Karl and Yanagi 1997). AK is mainly produced during periods of P deficiency, hence its presence indicates areas of strong inorganic P deficiency where the enzymatic release of inorganic P from DOP hydrolysis may provide a P source into the environment (Vidal *et al.* 2003). AK can be repressed by high concentrations of inorganic P (Mulholland *et al.* 2002). Per colony rates of AK activity (AKA) range from 0.03 to 0.24 $\mu\text{mol } \mu\text{gChla}^{-1}\text{h}^{-1}$ in natural *Trichodesmium* populations of the western subtropical N. Atlantic (Mulholland *et al.* 2002). Significant AKA was detected also at the eastern margin of the N. Atlantic subtropical gyre at 24°N ($\sim 20 \text{ nmol l}^{-1}\text{h}^{-1}$) mostly associated with the picoplanktonic community (Vidal *et al.* 2003). The findings support the hypothesis of a high level of P stress in the subtropical N. Atlantic.

N deficiency may induce cells to synthesise aminopeptidases (AP) ectoenzymes that hydrolyze peptides and proteins. In the same way that AK serves as an index of phosphate limitation, AP may serve as an indicator of nitrate deficiency (Hoppe *et al.* 1988).

However, the activities of ectoenzymes alone may not be indicative of the trophic status of the system as their activity may be function of the biomass of producers (Sala *et al.* 2001). The enzyme activity therefore needs to be related to the biomass of the potential producers. In the literature this has been frequently done by calculating specific activities by dividing by the amount of phytoplankton biomass represented by chlorophyll *a* (Mulholland *et al.* 2002,

Vidal *et al.* 2003). Clearly this procedure has the bias of underestimating the ability of many non phytoplanktonic marine organisms, such as heterotrophic bacteria, to synthesise ectoenzymes, leading to incomparable and unrealistic results. Sala *et al.* (2001) have emphasised the use of the ratio of ectoenzymes activities, instead of their activity alone, to bypass the problem of calculating specific activities.

The ratio AKA/APA has been used as a proxy of P versus N deficiency (Sala *et al.* 2001). These authors found an AKA/APA ratio of about 2 in phosphorus deficient Mediterranean waters; they showed a clear decrease in the AKA/APA ratio when phosphate was added due to the repression of AK activity; they concluded that the ratios of these two enzymes reflect the nutrient imbalances that were experimentally induced. Thus, oligotrophic environments may largely rely on the production of ectoenzymes to hydrolyse dissolved organic compounds to enhance nutrient availability.

Although efforts are currently underway, there is not a quantitative and deterministic view of the cycling of nutrients into the North Atlantic gyre. A one dimensional view is clearly no longer adequate for describing the return pathways of the nutrients in the upper thermocline as the importance of horizontal processes has been recognised. Recently Jenkins and Doney (2003) have proposed a 3-D, gyre-scale nutrient spiral that combines diapycnal mixing, isopycnal mixing, wintertime convection and eddy processes to uplift thermocline remineralised nutrients into the euphotic zone. This hypothetical nutrient pathway could control new production, on decadal timescale, in those areas where winter time convection and eddy heaving processes are significant; however it can not explain the summer draw-down of nutrients at BATS. Also, this mechanism would be inefficient in supplying nutrients in the permanently stratified oligotrophic areas.

The picture that is emerging is a very complex one, where the overlap of the meridional overturning circulation (Alvarez *et al.* 2002; Lavin *et al.* 2003) and the horizontal gyre circulation or eddies (Rintoul and Wunsch 1991) cannot explain alone the N and P budgets and the sustainment of new production over the North Atlantic subtropical gyre (Rintoul and Wunsch 1991; Ganachaud and Wunsch 2002). Processes such as N_2 fixation and the lateral advection or *in situ* production of DOM and its consequent subduction and remineralization along isopycnals could significantly impact nutrient cycling and primary production.

4.1.3 Objectives

The primary objectives of this Chapter are to identify the major source of nutrients into the permanently stratified oligotrophic North Atlantic Subtropical gyre. This has been

addressed by 1) investigating the large scale contribution of N_2 fixation to the water column N budget 2) examining the spatial distribution and the relative importance of N_2 fixation versus upwelled deep nitrate in providing a N source for the plankton community in the upper ocean 3) quantifying the bioavailability, the turnover rates and the role of DON and DOP as nutrient sources for plankton production in the North Atlantic gyre 4) investigating the nutrient limitation of the biological community in the surface layer 5) examining the extent of DOP in providing a P source for N_2 fixing organisms

The first objective is addressed using the quasi-conservative tracers N^* and TNex, which integrate over space and time, to provide large-scale constraints on N_2 fixation. To compute actual fixation rates the excess nitrogen pool was combined with water ventilation ages following two different approaches. The first one is a novel method that uses total nitrogen excess in the upper 1000m to estimate the net amount of N provided by N_2 fixation. This method has the major advantage of including in the N and P inventories the organic nutrient pools, which are a major constituent of the N and P pools in the upper ocean; a large part of which (TON) is known to be an important fraction released by N_2 fixers. Moreover, it unambiguously reflects the balance between N and P inputs into the system allowing the investigation of the long overdue question of whether the N^* signal is actually due to N_2 fixation or is instead attributable to differential remineralization of N versus P. The second approach, used to validate the first method, consists of an isopycnal two end member mixing model as used by Hansell *et al.* (2004), however it evolves from the latter as it includes organic nutrients in the analysis.

The spatial contribution of N_2 fixation in the upper water column is investigated by determining the stable isotopic composition of PON and biomarkers (phytoplankton pigments). The relative importance of N_2 fixation and upwelled nitrate in sustaining the observed biomass is identified using an isotopic two end mixing model (Montoya *et al.* 2002).

The third, fourth and fifth objectives are addressed by producing the first data set across the basin of the activity of the 2 ecto-enzymes, AK and AP, which are synthesised by bacteria and phytoplankton (Martinez and Azam 1993) to hydrolyse DOM. The activities of these enzymes are related to measurements of O_2 production and the organic nutrient pool size to allow the calculation of the turnover rates of organic matter and the fraction of primary production potentially supported by organic nutrients. The relative importance of the activity of the two enzymes are used to provide information on the nutrient deficiencies of the *in situ* biological communities. Additionally, the potential for TOP to meet N_2 fixer's phosphorus

demand is evaluated by calculating a hypothetical *Trichosdesmium* P demand based on literature values and relating it to the observed AK activity.

4.2 Derivation of N* DINex and TONex

The large scale distribution and estimates of N₂ fixation rates have been based on NO₃⁻ to PO₄³⁻ ratio anomalies (Michaels *et al.* 1996, Gruber and Sarmiento 1997). The global oceanic distribution of NO₃⁻ versus PO₄³⁻ reveals a global trend that is well described by a line with a slope of about 16:1. The existence of a relatively constant NO₃⁻:PO₄³⁻ ratio is known as the Redfield ratio (Redfield *et al.* 1963) and reflects the nutrient demand and composition of marine phytoplankton. Deviations from the classical 16:1 ratio between nitrate and phosphate have been used to define a quasi-conservative tracer, N*, which describes the production or consumption of nitrate with a N:P stoichiometry different from 16:1.

N* was initially defined by Michaels *et al.* (1996) using a dataset from the North Atlantic as:

$$N^* = [NO_3^-] - 16[PO_4^{3-}] + 2.7 \mu\text{mol kg}^{-1} \quad \text{Eq. 4.1}$$

This linear combination of nitrate and phosphate with an intercept of 2.7 was achieved to eliminate the main processes occurring with a N/P ratio of 16:1.

N* was revisited by Gruber and Sarmiento (1997) who derived N* from the linear combination of the tracer continuity equation of nitrate and phosphate as:

$$N^* = (N - r_{nit}P + const) \cdot \left(\frac{r_{denit}}{r_{denit} - r_{nit}} \right) \quad \text{Eq. 4.2}$$

Where r_{nit} (-104) and r_{denit} (16) represent the stoichiometric ratios of nitrification and denitrification respectively. Gruber and Sarmiento (1997) determined the constant of 2.9 $\mu\text{mol kg}^{-1}$ by forcing the GEOSECS nutrient dataset N* global mean to zero. Using the given N:P ratios the definition of N* simplifies to:

$$N^* = ([NO_3^-] - 16[PO_4^{3-}] + 2.9 \mu\text{mol kg}^{-1}) 0.87 \quad \text{Eq. 4.3}$$

More recently, Deutsch *et al.* (2001) modified the N* equation eliminating the multiplying factor which gives N* a global mean of zero; this latter equation has been used to calculate the N* parameter in this study:

$$N^* = [NO_3^-] - 16[PO_4^{3-}] + 2.9 \mu\text{mol kg}^{-1} \quad \text{Eq. 4.4}$$

N* evolved into the excess nitrate (DINxs) concept described by Hansell *et al.* (2004) as:

$$DINxs = [NO_3^-] - 16[PO_4^{3-}] \quad \text{Eq. 4.5}$$

Despite the various parametrizations, N* and DINxs represent the deviation from the intercept of the 16:1 line. A positive N* anomaly implies an excess of NO₃⁻ relative to PO₄³⁻, a

negative N^* anomaly implies a deficit of NO_3^- with respect to PO_4^{3-} (Fig. 4.1). DINxs and N^* reflect only the NET impact of processes that add or remove NO_3^- with a N:P stoichiometry different from 16:1. Generally processes other than N_2 fixation and denitrification are considered to be small, thus the non-conservative behavior of N^* and DINxs is mainly interpreted as the net balance between N_2 fixation and denitrification.

Building on the concepts of N^* and DINxs and on the fact that organic nutrients are the major fraction of the nutrient pool in the surface ocean, two new variables, TONxs and TN xs, were computed:

$$\text{TONxs} = [\text{TON}] - 16[\text{TOP}] \quad \text{Eq. 4.6}$$

$$\text{TNxs} = [\text{TN}] - 16[\text{TP}] \quad \text{Eq. 4.7}$$

The interpretation of TONxs and TNxs is similar to N^* and DINxs, with the advantage of including the organic nutrient pool for a more comprehensive analysis of the total nutrient inventory.

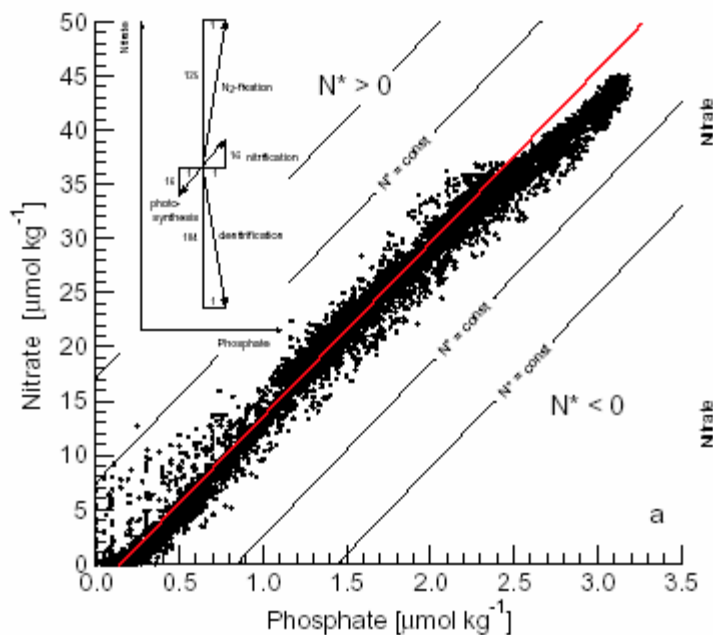


Fig. 4.1 Plot of phosphate versus nitrate. The red solid line represents the mean ocean trend $P=1/16N+0.182$. The inset shows the effect of photosynthesis/respiration, denitrification and N_2 fixation on the N to P ratio. From Gruber and Sarmiento (1997).

TONxs and TNxs represent the vertical distance of a TON and TOP or a TN and TP pair from the mean oceanic trend line of 16:1. Positive TONxs values can reflect both additional inputs of TON and/or preferential remineralization of TOP with respect to TON.

A positive TN_{xs} anomaly, however, would only reflect a net excess of N over P, which can only be the result of preferential N inputs due to N₂ fixation or atmospheric deposition. This is because preferential TOP consumption would result in an increase in DIP with no resulting variation in TP. Hence, TN_{xs} unambiguously represents the balance present between the N and the P inventories in the area studied.

4.3 Stable Nitrogen Isotopes as a Diagnostic Tool Reflecting Nitrogen Processes

The ratio of the naturally occurring stable isotopes ¹⁵N:¹⁴N in the ocean is a powerful tracer of the transformations that occur within the nitrogen cycle (Mariotti *et al.* 1981) and can provide evidence of N₂ fixation in the ocean (Liu *et al.* 1996; Carpenter *et al.* 1997, Karl *et al.* 1997). The conventional measure of ¹⁵N abundance is given as

$$\delta^{15}\text{N}\text{\%} = \left[\frac{{}^{15}\text{N}/{}^{14}\text{N}_{\text{sample}}}{{}^{15}\text{N}/{}^{14}\text{N}_{\text{std}}} - 1 \right] \times 1000 \quad \text{Eq. 4.8}$$

where N_{std} is the atmospheric N₂ standard (Mariotti *et al.* 1981).

Variations in ¹⁵N abundance reflect discrimination between ¹⁵N and ¹⁴N isotopes caused by the different reactivities and velocities of N during reactions within the N cycle. Generally, the lighter isotope reacts faster than the heavier isotope.

The $\delta^{15}\text{N}$ of the nutrient source and isotopic fractionation during assimilation are the two major factors that affect the nitrogen isotope composition of marine plankton and suspended particulate material (Wu *et al.* 1997).

The $\delta^{15}\text{N}$ of dissolved N₂ is 0.6‰. As some isotopic fractionation occurs during N₂ fixation ($-2.6 \pm 1.3\text{\%}$; Brandes and Devol 2002), the resulting $\delta^{15}\text{N}$ of POM will reflect the low isotopic composition (-2.1 to $+2.9\text{\%}$) of the N₂ source (Wada and Hattori 1976; Saino and Hattori 1987; Carpenter *et al.* 1997).

In contrast, if the N source was upwelled deep nitrate, two scenarios could occur. In the first case, in an oligotrophic environment, all the nitrate present is converted into biomass, thus the PON pool will reflect the isotopic composition of the deep NO₃⁻ pool (4.7-6 ‰) (Sigman *et al.* 1999; Montoya *et al.* 2002). In the second scenario, under nutrient replete conditions, phytoplankton preferentially incorporates the lighter isotope, ¹⁴N, causing an increase in the $\delta^{15}\text{N}$ of the residual nitrate pool and ¹⁵N depleted phytoplankton biomass. Isotopic enrichment also occurs along the food web as excretory processes tend to retain ¹⁵N within animal tissues. These processes act to excrete ¹⁴N rich NH₄⁺, which is recycled and

retained within the upper layers, and export to deep layers POM enriched in ^{15}N , which causes the observed $\delta^{15}\text{NO}_3^-$.

During this study measurements of $\delta\text{PO}^{15}\text{N}$ have been used to complement N* interpretations and trace regions of N_2 fixation. In addition, following previous studies (Mahaffey *et al.* 2004, Montoya *et al.* 2002, Mino *et al.* 2002), the contrast between the isotopic signature of deep nitrate (4.5‰) and the biomass N_2 fixers (-2‰) has been exploited to compute a two end member source model to assess the relative importance of these two nutrient sources in supporting phytoplankton biomass in the study region.

The relative importance of N_2 fixation relative to the upwelling of deep nitrate, in supporting the biomass production of the region, has been calculated by an isotopic mixing model:

$$N_{fix} (\%) = 100 \left(\frac{\delta^{15}\text{PON} - \delta^{15}\text{NO}_3\text{deep}}{\delta^{15}\text{N}_2 - \delta^{15}\text{NO}_3\text{deep}} \right) \quad \text{Eq. 4.9}$$

Where N_{fix} is the PON nitrogen fraction supplied by N_2 fixation and the two end member values are $\delta^{15}\text{NO}_3^-$ deep (4.5‰) and $\delta^{15}\text{N}_2$ (-2‰), characteristic of the North Atlantic Subtropical gyre (Montoya *et al.* 2002).

4.4 Results

4.4.1 Deep Waters, N to P ratio anomalies

Physical properties and Apparent Oxygen Utilization (AOU)

The D279 transect intersected the North Atlantic subtropical gyre at an approximately constant latitude of 24.5°N. The waters in the surface 150m were the high salinity surface waters created by strong evaporation over the subtropical gyre (Bryden *et al.* 1996) (Fig. 4.2).

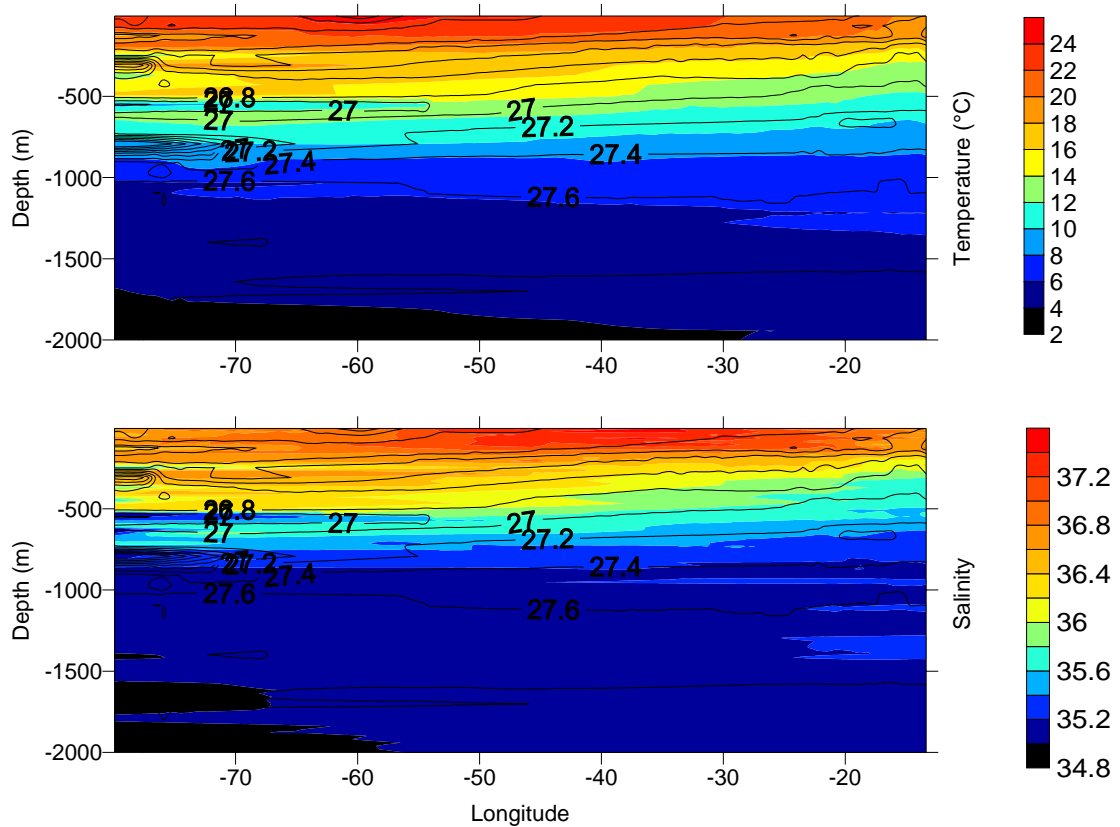


Fig. 4.2 Section across the North Atlantic subtropical gyre at 24.5°N of temperature °C (top) and salinity (bottom). Overlying are contours of sigma-theta σ_θ (kgm^{-3}).

AOU increased with depth following isopycnals (Fig. 4.3). Positive AOU started to develop below the $\sigma_\theta=26$ kgm^{-3} isoline. The core of the highest signal in AOU (up to $140\mu\text{molkg}^{-1}$) was found at 900 metres on the eastern side of the gyre and protruded along the σ_θ 27.2 kgm^{-3} isopycnal surface towards the west. The high AOU signal is also characterized by high nutrient content (Fig. 4.4).

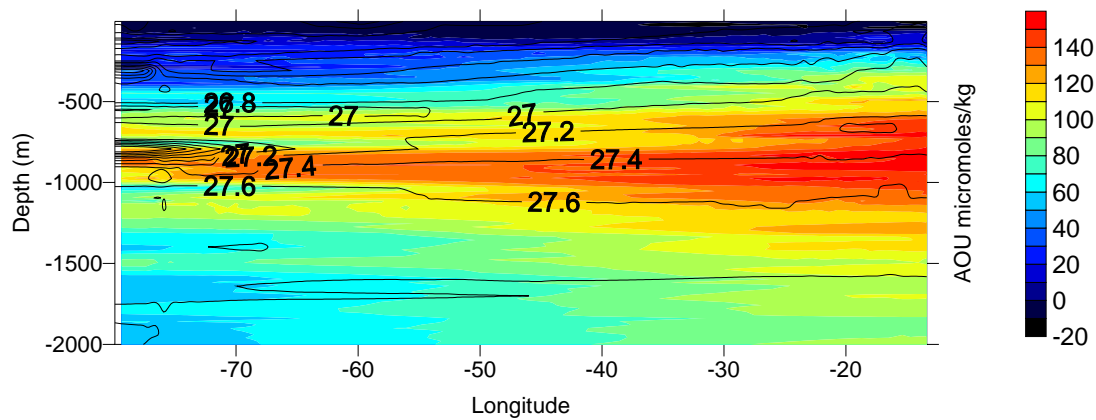


Fig. 4.3 Section across the North Atlantic subtropical gyre at 24.5°N of AOU (μmolkg^{-1}). Overlying are contours of sigma-theta σ_θ (kgm^{-3}).

Deep Water Dissolved N and P Pools

As expected, nitrate and phosphate concentrations increased with depth as the remineralization of organic matter occurs during particle settling (Fig. 4.4).

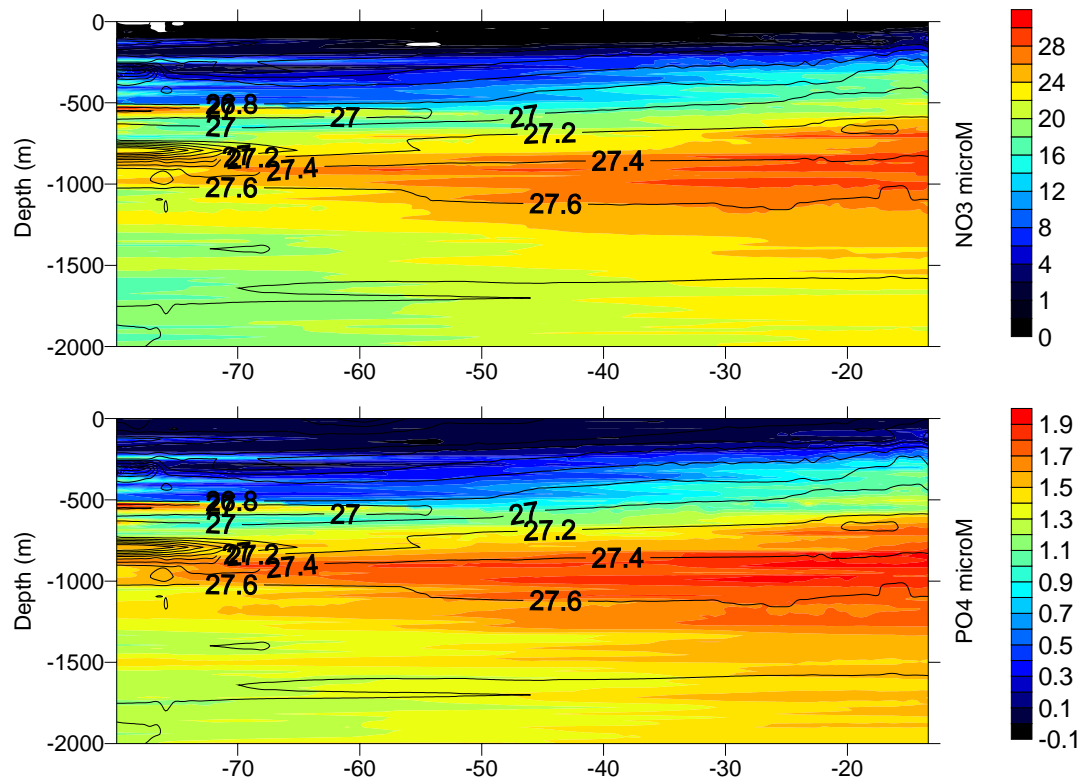


Fig. 4.4 Section across the North Atlantic subtropical gyre at 24.5°N of nitrate μmolkg^{-1} (top) and phosphate μmolkg^{-1} (bottom). Overlying are contours of sigma-theta σ_θ (kgm^{-3}).

Nitrate and phosphate concentrations followed isopycnal contours in a similar manner to AOU. Nutrient rich waters were closer to the surface at the eastern side of the subtropical

gyre due to the effect of outcropping isopycnals ($<26 \text{ kgm}^{-3}$). The highest concentrations of both NO_3^- and PO_4^{3-} were associated with low oxygen waters from the Mediterranean at around 1000m.

Average vertical profiles of dissolved inorganic and organic N and P are shown in Fig. 4.5. Nitrate and phosphate concentrations increased dramatically from the surface to 1000m where the maximum concentrations reached $25.6 \pm 5.8 \mu\text{MNO}_3^-$ and $1.60 \pm 0.52 \mu\text{M PO}_4^{3-}$ respectively. Below 1000m concentrations became rather constant, both for nitrate ($21.0 \pm 0.4 \mu\text{MNO}_3^-$) and phosphate ($1.43 \pm 0.08 \mu\text{M PO}_4^{3-}$).

Unlike NO_3^- and PO_4^{3-} , concentrations of TON and TOP were higher at the surface and decreased with depth (Fig. 4.5). Average TON concentrations decreased from $4.6 \pm 1.8 \mu\text{M}$ in the surface to $1.7 \pm 0.1 \mu\text{M}$ at 1000m and did not vary much below this depth. TOP decreased similarly from $0.11 \pm 0.11 \mu\text{M}$ to almost undetectable concentrations ($0.03 \pm 0.01 \mu\text{M}$) below 1000m.

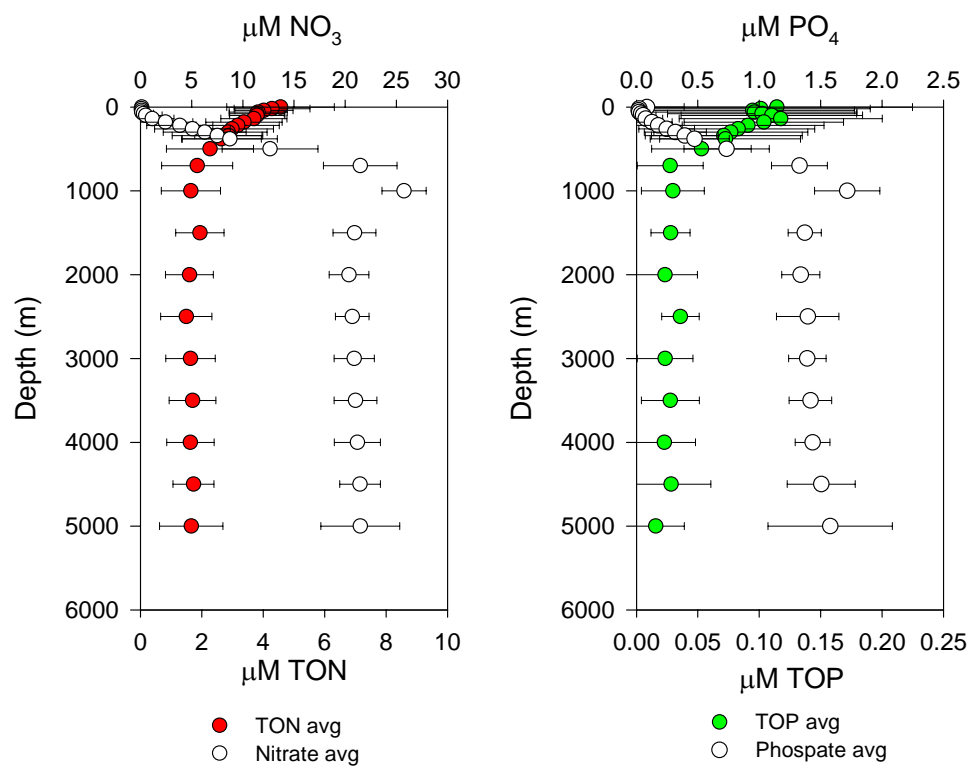


Fig. 4.5 Average vertical profiles of NO_3^- and TON μM (left) and PO_4^{3-} and TOP μM (right). Error bars represent range bars.

In general, the nitrate to phosphate ratio slightly deviated from the expected 16:1 Redfield ratio ($\text{N}/\text{P}=14.7$). The NO_3^- to PO_4^{3-} ratio reached a near Redfield stoichiometry and a positive intercept only in the depth range 200-600m (Fig. 4.6).

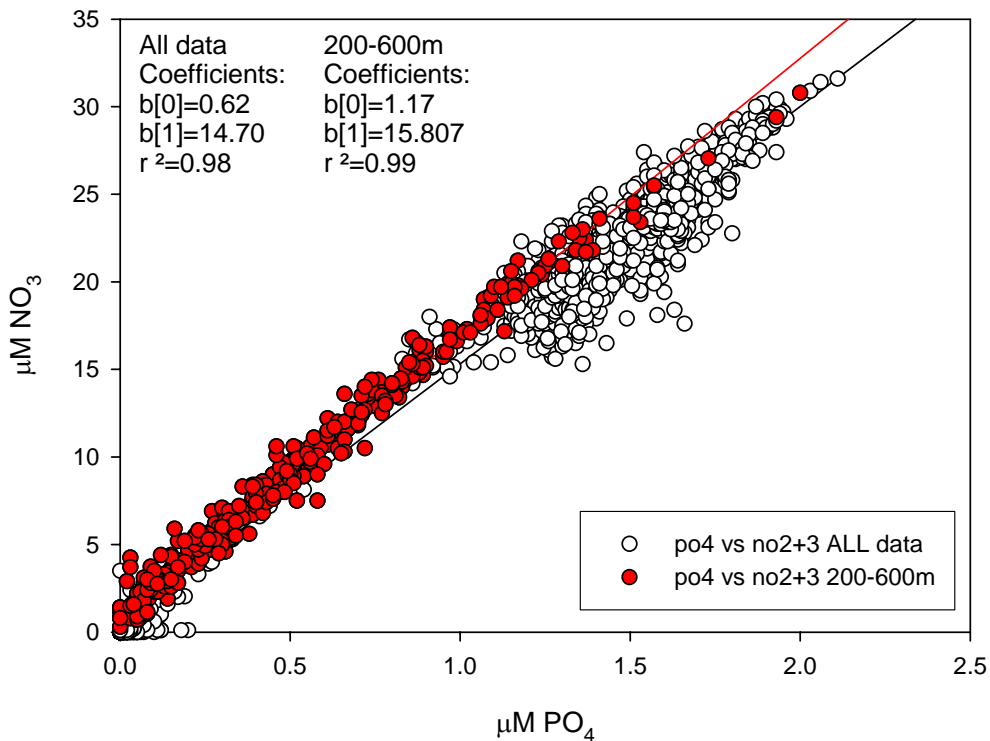


Fig. 4.6 Plot of phosphate versus nitrate from samples collected in the North Atlantic at 24.5°N. The black line represents the best fit of all the data points (hollow back circles) collected during D279 cruise. Red line represents the best fit of data points (red dots) selected from 200-600m depth range.

4.4.1.1 Discussion

To infer large scale rates and constraints on N_2 fixation and NO_3^- versus PO_4^{3-} limitation, values of DINxs and N^* were computed, following the parameterization by Hansell *et al.* (2004) and Deutsch *et al.* (2001) respectively, as biogeochemical signatures of water column nutrient imbalances across the North Atlantic.

DINxs and N^* reflect only the NET impact of N_2 fixation and denitrification and any other process that adds or removes NO_3^- with a N:P stoichiometry different from 16:1. Thus high values of DINxs and N^* represent the excess of NO_3^- over PO_4^{3-} with the assumption of a fixed N:P ratio of 16:1 and can result from several causes:

1. N_2 fixation
2. Mineralization of N rich material
3. Selective uptake of PO_4^{3-}
4. Advection of N rich DOM and subsequent remineralization
5. N input via atmospheric dust

In the literature, however, the interpretation of N^* has relied on the assumption that the only significant, non-conservative processes that perturb the canonical Redfield elemental stoichiometry, are denitrification and N_2 fixation; other processes such as the preferential uptake of inorganic P with respect to inorganic N in the surface layers, atmospheric deposition of N and preferential remineralization of TOP from DOM leading to the production of nitrogen rich DOM, have been considered negligible (Gruber and Sarmiento 1997, Gruber 2004).

Vertical profiles of N^* and DINex are shown in Fig. 4.7 DINex is negative in the top 120m ($-0.2 \pm 0.1 \mu\text{M N}$) indicating that nitrate is less abundant than one would expect from Redfield stoichiometry and ambient P levels. DINex becomes positive immediately below the seasonal thermocline at 150m develops a large positive anomaly between 260 and 400 meters ($1.2 \pm 0.01 \mu\text{M N}$) on the $\sigma_t=26.27.5$ isopycnal surface (Fig. 4.8).

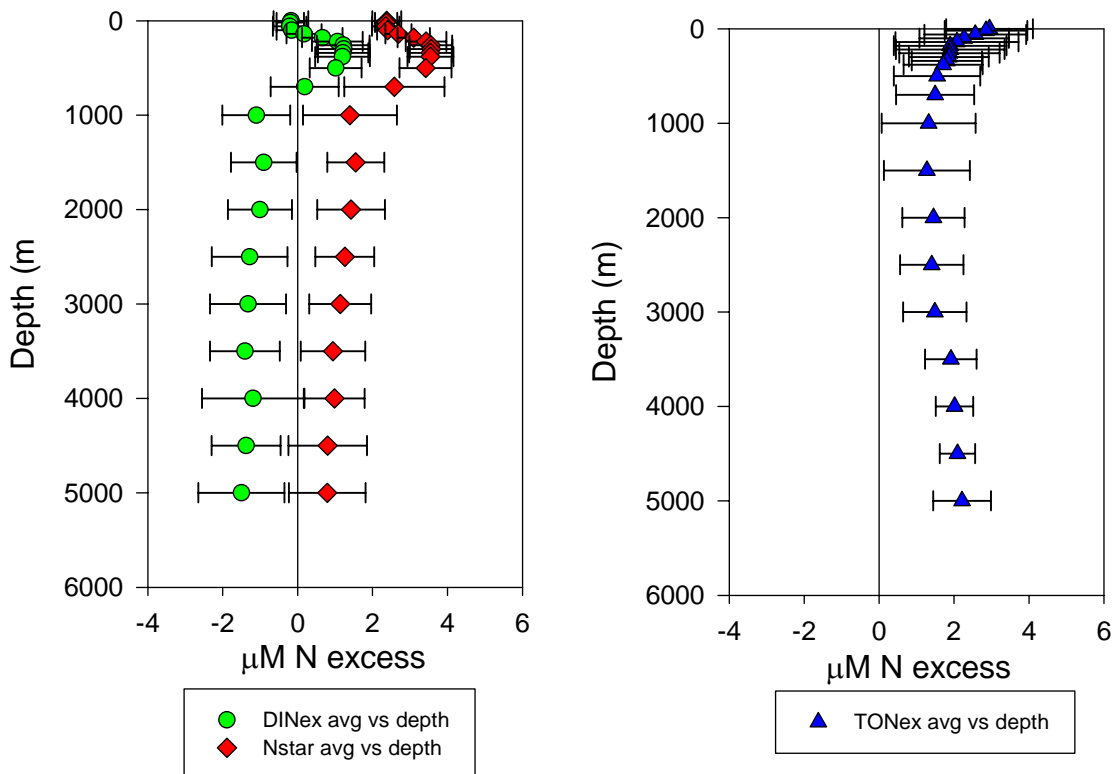


Fig. 4.7 Vertical average profiles of DINex and N^* μM (left) and TONex* μM (right).

The N^* maximum reached $3.6 \pm 0.01 \mu\text{M N}$ in the region between 260-700m, while deep waters were at a constant value of $1.2 \pm 0.3 \mu\text{M N}$. These values are in good agreement with those reported in the thermocline of the subtropical North Atlantic by Gruber and Sarmiento

(1997). Below 800m DINxs became negative again and was fixed to a constant value of $-1.5 \pm 0.3 \mu\text{M N}$ deeper in the water column. A similar pattern was observed for the distribution of N^* obviously with an offset of $2.9 \mu\text{M N}$, which results from the different parameterization.

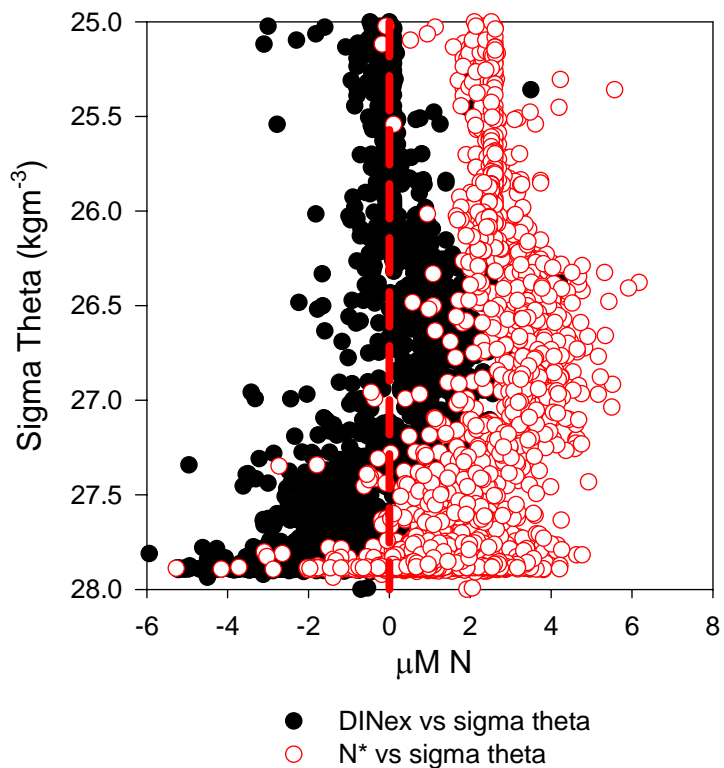


Fig. 4.8 Plot of sigma theta versus N^* and DINex.

To investigate if the observed DINxs excess was the result of the preferential uptake of PO_4^{3-} , an analysis of dissolved inorganic nutrients versus oxygen was performed (Fig. 4.9). Two clusters with different O_2 to NO_3^- and O_2 to PO_4^{3-} ratio could be seen, possibly reflecting the oxidation of different DOM pools or also different water masses with preformed nutrient and oxygen concentration. From the $\text{O}_2:\text{NO}_3^-$ (cluster (a)=4.75, (b)=11.86) and $\text{O}_2:\text{PO}_4^{3-}$ (cluster (a)=71.41, (b)=174.41) ratios, it is possible to infer that the remineralization affected both nitrate and phosphate following a quasi Redfieldian ratio (N/P cluster (a)=15, (b)=14.7) indicating that no preferential remineralization of either NO_3^- or PO_4^{3-} was occurring. This suggests that the observed excess of DINxs and the N^* signals are mostly due to an excess of nitrate with respect to phosphate and are not to the preferential remineralization of PO_4^{3-} . Also, the vertical patterns of DINex and N^* suggest that the preferential remineralization of PO_4^{3-} plays a minor part in the formation of the nitrogen excess signal. The preferential remineralization of PO_4^{3-} would result in an increase in DINex and N^* with depth, as the phosphorus is gradually stripped off from organic matter; while this data suggest that NO_3^-

was in excess with respect to PO_4^{3-} only in a small portion of the water column, confined between 150m and 1000m. This indicates a nitrate deficiency relative to phosphate throughout the majority of the deep waters, as can also be inferred from the scatter plot of phosphate versus nitrate, for phosphate and nitrate values greater than $\sim 1 \mu\text{M} \text{PO}_4^{3-}$ and $\sim 15 \mu\text{M} \text{NO}_3^-$ respectively (Fig. 4.6). This observation was already made by Hansell *et al.* (2004).

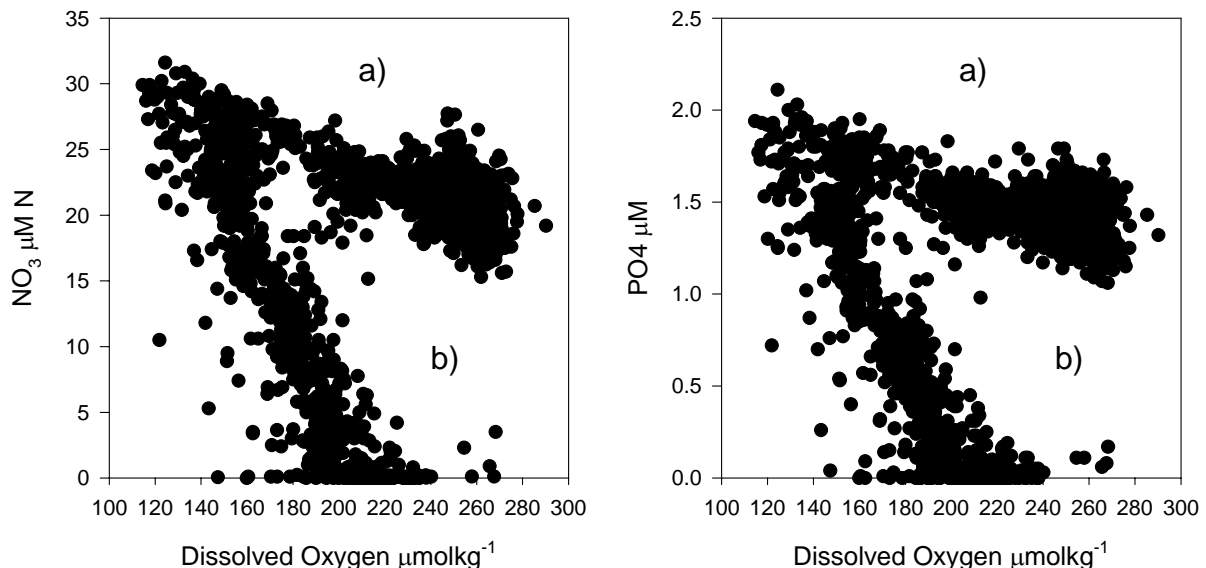


Fig. 4.9 Plots of NO_3^- (μM , left) and PO_4^{3-} (μM , right) versus dissolved oxygen $\mu\text{mol kg}^{-1}$. Clusters of different $\text{O}_2:\text{NO}_3^-$ and $\text{O}_2:\text{PO}_4^{3-}$ are indicated read text for details.

Although there is some indication that the excess nitrate does not result from preferential uptake of PO_4^{3-} , the controversial issue of the correct interpretation of the origin of positive N^* and excess nitrogen in the DINex signal can be resolved unambiguously by considering the entire N and P pools and not only their inorganic constituents. A major fraction of the nutrient pool of the oceans consists of TON and TOP, and a major fraction of fixed nitrogen is released as TON (Gilbert and Bronk, 1994). Thus their absence in the N and P mass balances limit our knowledge of oceanic processes that involve N and P cycling. To have a complete picture of the N:P stoichiometry, the organic pool was measured and TNex and TONxs were computed following Eq. 4.6 and Eq. 4.7.

In the North Atlantic, the average values across 24.5°N of TONxs never became negative throughout the water column (Fig. 4.7). In the top 150 metres TON was on average $2.7 \pm 0.3 \mu\text{M}$ in excess with respect to TOP. TNex decreased to $1.9 \pm 0.3 \mu\text{M}$, from 150m to 700m, probably contributing between 70-80% to the concomitant build up of DINex. Below 1000m, mean TNex was $1.4 \pm 0.2 \mu\text{M}$, which very closely balanced the DIN deficit

($-1.4 \pm 0.3 \mu\text{M}$). This strongly suggests that below 1000m, TONxs mainly results from the residual TON pool left by TOP preferential remineralization.

Schematically, the water column can be crudely divided into the top 1000m where TN is in excess (positive anomaly) by $2.5 \pm 0.6 \mu\text{M}$ over TP and below 1000m where TN and TP are approximately in balance ($0.0 \pm 0.4 \mu\text{M}$) with respect to the Redfield ratio (Table 4.1).

Table 4.1 Average DINxs, TONxs and TNxs values and standard error calculated for 3 depth ranges.

Depth (m)	DINxs (μM)	TONxs (μM)	TNxs (μM)
0-150	-0.1 ± 0.1	2.7 ± 0.2	2.5 ± 0.3
150-700	1.1 ± 0.3	1.9 ± 0.3	2.7 ± 0.3
1000-5000	-1.4 ± 0.3	1.4 ± 0.2	0 ± 0.4

A conceptual model of the dynamics between the organic and the inorganic pools in the North Atlantic subtropical gyre is presented in Fig. 4.10. The N and P inventories are distributed among the organic and the inorganic fractions; the size of these pools will depend on which of the two processes, inorganic uptake or organic remineralization, is more effective. It is necessary to bear in mind though, that the resultant of these processes will not vary the concentrations of the total inventories (TN and TP) and thus TNxs. With this in mind it is possible to describe the observed nutrient anomalies following the concepts schematised in Fig. 4.10 as follows:

A) The left panel shows that negative DINex values can be the effect of either TOP remineralization or NO_3^- preferential uptake. DINex positive values can result from several processes, which are preferential TON remineralization/remineralization of N rich organic matter (and subsequent production of NO_3^-), PO_4^{3-} uptake and N atmospheric deposition

B) The central panel shows that a TONex positive anomaly can be the result of TOP remineralization or the input of TON by atmospheric deposition or preferential TON production

C) The right panel shows that positive TNex reflects the net excess of N over P, regardless of the form in which N and P exist (inorganic-organic). This net excess is produced either by N_2 fixation or atmospheric N deposition. When TNex is equal to zero, there is a balance between N and P with respect to the Redfield Ratio of 16:1.

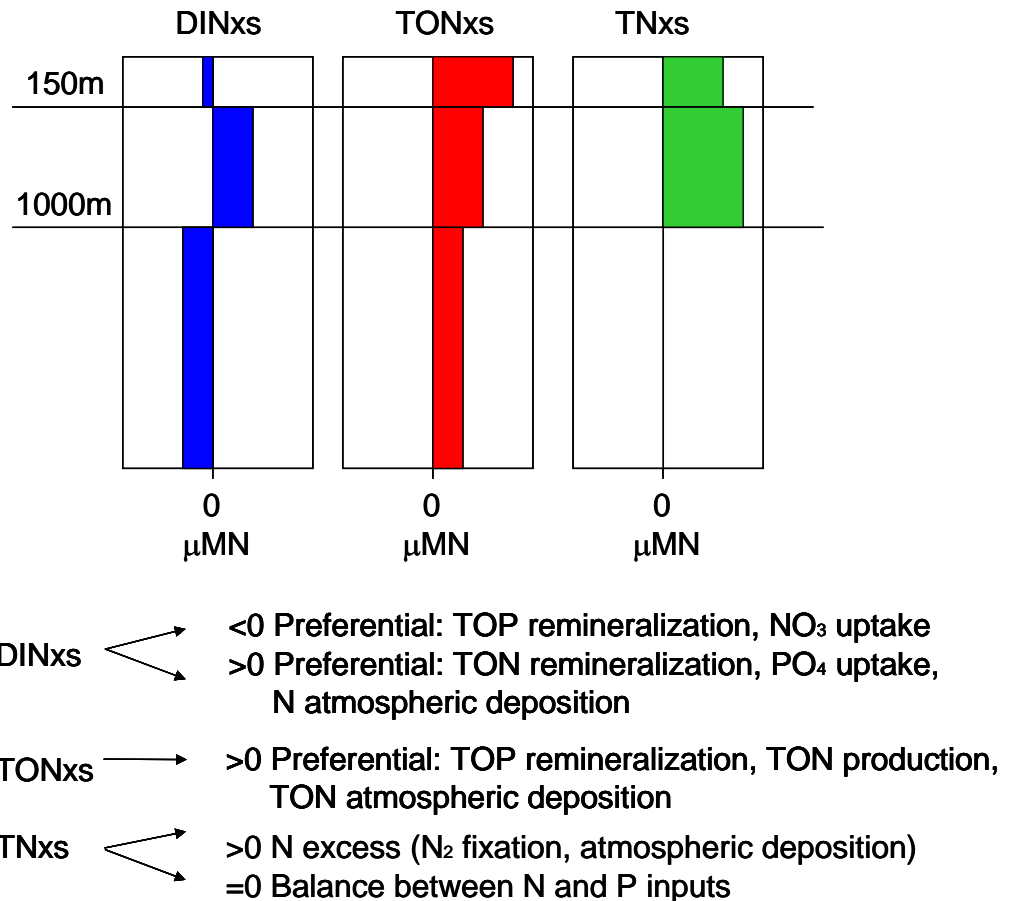


Fig. 4.10 Conceptual model of the ratio anomalies between N and P pools and the dynamics between inorganic and organic nutrients.

In the top 150m of the North Atlantic it is likely that the labile fraction of DOM is readily remineralized and a stronger P demand induces TOP to cycle faster than TON. This in turn will cause a negative DINxs anomaly and part of the observed positive TONxs anomaly. Thus, part of the positive TONex is caused by the preferential remineralization of TOP and can be accounted for as it is numerically equal to the DINxs negative anomaly. The remainder of the TONxs positive anomaly is given by selective input of TON either by N_2 fixation or atmospheric deposition. Hence, by adding DINxs (DINxs is negative) from TONxs, the remaining TONex will be equal to TNex which represents the net N excess due only to either by N_2 fixation or atmospheric deposition

In the depth range between 150m and 1000m, TONex decreases following two possible pathways 1) preferential TON remineralization resulting in NO_3^- production and subsequent DINex increase 2) an increase in the TOP pool as a result of preferential PO_4^{3-} uptake. Although both pathways are likely to occur, the resultant TNex still reflects only the excess of N with respect to P in these layers. This excess is likely the product of N rich DOM (resulting

both from TOP preferential remineralization and N rich DOM production) exported into the main thermocline, where it builds up and where the semi labile component gets remineralized.

Below 1000m, only the refractory N rich DOM pool is left as all the TOP is remineralized leaving behind the refractory TON and producing the negative DINex. Below this depth, it appears that the P pool lies in the inorganic fraction, while a consistent proportion of the N pool lies in the organic fraction, so that the nitrate deficit is compensated by the TON excess. This results in the balance, with respect to Redfield ratio, of the N and P total inventories.

In conclusion, the surface subtropical North Atlantic is a net source of nitrogen for the system while P is limiting, thus TOP is readily remineralized enhancing the N:P ratio of organic material. The N rich organic material produced via this mechanism gets exported into deeper layers where P gets stripped off and the relatively labile TON is remineralized leaving behind a refractory TON pool. N and P inventories are decoupled as they cycle on different time scales and are partitioned differently within the organic and inorganic pools. The N pool, except for a thin layer (150-1000m), is mostly “stored” in the organic fraction while the organic P rapidly gets remineralized and thus the P inventory primarily consists of the inorganic fraction.

If the build up of net TN excess above 1000m is all attributed to N_2 fixation then considering the average age of the water masses from CFC data (Hansell *et al.* 2004) in the top 150m (5 years) and in the depth range from 150 to 1000m (22 years), the integration of excess total nitrogen in the top 1000m yields an N_2 fixation rate estimate of $0.19 \pm 0.03 \text{ mol N m}^{-2} \text{ y}^{-1}$ where the error represents only the variability of measured TNex in the upper 1000m.

This input of new N would account for 24 to 28% of the N required to sustain the observed export production (0.67 ± 0.14 to $0.78 \pm 0.15 \text{ mol N m}^{-2} \text{ y}^{-1}$; Jenkins and Doney (2004); $0.48 \pm 0.14 \text{ mol N m}^{-2} \text{ y}^{-1}$; Williams and Follows 1998).

Atmospheric deposition can be excluded as a major factor in producing the observed excess nitrogen in the top 1000m of the water column, as estimates of its size (17 to $21 \text{ mmol N m}^{-2} \text{ y}^{-1}$; Prospero *et al.* 1996) are within the error of the N_2 fixation estimate through TNxs. Hence, subtracting the contribution of atmospheric N deposition would not change significantly the above estimate of N_2 fixation rate.

To a first approximation, these estimated N_2 fixation rates are largely sufficient to explain the seasonal TCO_2 drawdown observed at BATS during the oligotrophic period ($0.08 \text{ mol N m}^{-2} \text{ y}^{-1}$; Ono *et al.* 2001) if the excess N were transported to that site.

This estimate is higher than the ones reported by Gruber and Sarmiento (1997) ($0.072\text{molNNm}^{-2}\text{y}^{-1}$) and Hansell *et al.* (2004) ($0.045\text{molNNm}^{-2}\text{y}^{-1}$) for the North Atlantic, but is in agreement with previous geochemical estimates of N_2 fixation which range from $0.18\text{-}0.9\text{molNm}^{-2}\text{y}^{-1}$ (Michaels *et al.* 1996) and the recent direct N_2 fixation rates measured in the tropical and subtropical North Atlantic which range from $0.022\text{-}0.33\text{molNm}^{-2}\text{y}^{-1}$ with an average of $0.087\text{molNm}^{-2}\text{y}^{-1}$ (Capone *et al.* 2005).

It is important to bear in mind that Gruber and Sarmiento (1997) and Hansell *et al.* (2004) calculated N_2 fixation rates from the N^* and DIN_{xs} anomalies created within isopycnal layers of the North Atlantic gyre and thus are dependant on the areas and the number of the isopycnal layers chosen for the calculations. The differences in the N_2 fixation rates reported by the above mentioned authors are hence attributable to the different areal and vertical distributions of N^* and DIN_{xs} development considered. Moreover, these studies average the values of nitrate anomalies over large areas of the North Atlantic.

The N_2 fixation estimates presented here differ from the above mentioned studies. The first point to make is that, in this study N_2 fixation rates are estimated from the vertical integration of excess N over the entire top 1000m where the TN excess is observed. Hence a higher fixation rate estimate, using this method, is expected firstly due to the fact that, the N excess due to organic nitrogen is not accounted for in the N^* and DIN_{xs} concepts and secondly, because the TN excess has been calculated including the upper $\sim 200\text{m}$ which are instead, omitted from the N^* and DIN_{ex} calculations as no significant N^* develops in these surface layers. Finally the vertical integration represents an average of the water column at 24°N where relatively high fixation rates have been found (Orcutt *et al.* 2001) compared to higher latitudes, that is, this average does not encompass areas where N_2 fixation rates are low ($\sim 30^\circ\text{N}$).

It must be said that this mass balance approach is limited to a one dimensional view. However, the observed N excess is not only supported by “local” N_2 fixation but also by other processes, such as the lateral advection of N rich material, which might contribute to enhanced N_2 fixation estimates. Similarly, N rich material produced due to local N_2 fixation can be exported away to areas where N_2 fixation is low providing a source of excess N. Moreover, to estimate rates of N_2 fixation the water mass ventilation age has been used, thus this estimate integrates the build-up of TN_{xs} over the entire lifetime of a water parcel and hence represents an average of a regional scale process. The other limit is that it relies on the basic assumption that remineralized material releases N and a P with a fixed stoichiometric

ratio of 16:1, which is the central concept of the N* tracer and its derivations but might not be the always the case (Anderson and Sarmiento 1994).

As a validation of this N₂ fixation estimate, a second approach has been used to estimate N₂ fixation rates from the observed development of DINex and DONex on specific isopycnal layers. Observing that the depths of maximum DINex and N* development coincide with the $\sigma_0=26.2-27.2\text{kgm}^{-3}$ isopycnal surfaces (Fig. 4.8) an isopycnal two end member mixing model, following Hansell *et al.* (2004), was used. This model assumes that the transport occurs along isopycnals surfaces and that the mixing on any isopycnal surface can be described by a two or one end member mixing model. An end member is a water mass which has characteristic properties of any conservative tracer (salinity, potential temperature) and non conservative (DINxs, age) tracers at the end member location. As the water parcel is transported away from its original location it loses its original characteristics properties (one end member mixing model) and can get mixed with other water masses (two end member mixing model) following a conservative mixing of conservative tracers. A two end member mixing model allows us to infer non conservative change, in any non conservative property, by calculating the theoretical expected value (preformed value) of that property if only linear mixing among two water masses occurred. The difference between the preformed value and the measured value quantifies the non conservative behaviour (development/ consumption) of the property.

In Gruber and Sarmiento (1997) and Hansell *et al.* (2004) this technique was used to calculate the non conservative development of N* and DINxs on specific isopycnal surfaces and, allowing for the effect of elevated N/P ratios (125) of organic matter released by N₂ fixers, infer rates of nitrogen fixation.

In the North Atlantic the potential density surfaces: $\sigma_0=26.2$ and 27.2kgm^{-3} represent the subtropical and subpolar mode waters respectively. Waters entering these isopycnal surfaces from the north and from the south have low preformed values of N* and DINxs. On these isopycnals a non conservative N*/DINxs behaviour within the North Atlantic gyre is observed due to the remineralization of N rich organic matter (Gruber and Sarmiento 1997; Hansell *et al.* 2004). On other density layers, DINxs and N* show a nearly conservative behaviour meaning that N* and DINxs values on these layers are the ones that one would expect from the linear mixing of two water masses (Gruber and Sarmiento 1997).

The $\sigma_0=26.2-27.2\text{kgm}^{-3}$ isopycnals lie in the upper 1000m where they outcrop in the top 200 meters in the eastern North Atlantic (Fig. 4.2). In accordance with the conceptual model of Hansell *et al.* (2004), as DINxs starts developing below $\sim 150\text{m}$, because these isopycnals

are shallower in the east, the development of DINxs in the east will be weak on the $\sigma_0=26$ (shallowest) surface. In the west, the $\sigma_0=26$ surface deepens and intersects the depth of DINxs production (>150m). The $\sigma_0=27$ layer is deeper than the depth of DINxs production in the West and here it is strongly impacted by the “dilution” of the low DINxs content waters.

The distribution of potential temperature, CFC ages, DINxs, AOU and TONxs on three isopycnal surfaces has been used to infer the rates of DINxs, AOU and TONxs production. The two end member water masses used for the calculation were the Northern Component (NC) and the Southern Component (SC) described in Hansell *et al.* (2004). Reference values of DINxs, CFC ages and AOU for each water mass are therein provided. TONxs characteristic values of the NC and SC were not reported in the Hansell *et al.* (2004) study and have been computed as follows: TONxs values representative of the NC have been taken from stations (103 and 114) characterised by high percentage (~100%) of NC waters on the $\sigma_0=26$ and 26.5 isopycnals respectively. As no station was fully representative of the SC, a one end member mixing model has been used to calculate TONxs development.

The preformed values (the preformed concentrations expected from only the mixing of the two water masses/end members or the evolution from its original water mass in the case of a one end member mixing) of DINxs, AOU and TONxs were calculated using potential temperature as a conservative tracer on the $\sigma_0=26$, 26.5 and 27 (kgm^{-3}) isopycnal layers:

$$fa = \frac{(\theta b - \theta m)}{(\theta b - \theta a)} \quad \text{Eq. 4.10}$$

$$fa + fb = 1$$

where fa and fb are the fractions of the two end members, a and b , in the mixed water region, θa and θb are the potential temperatures of the two end members and θm is the measured potential temperature.

The preformed concentrations of DINxs were obtained for a two end member mixing model as follows:

$$\text{DINexcess}_{\text{preformed}} = fa \bullet \text{DINexcess}_a + fb \bullet \text{DINexcess}_b \quad \text{Eq. 4.11}$$

where DINexcess_a and DINexcess_b are the values of the DINexcess in the a and b components respectively. Similarly for a one end member mixing model (end member a):

$$DINexcess_{preformed} = fa \bullet DINexcess_a \quad \text{Eq. 4.12}$$

Similar parameterizations have been made to obtain preformed AOU and TONxs concentrations. The difference between DINxs preformed and the measured value of DINxs accounts for the non conservative development of DINxs due to processes such as N₂ fixation/denitrification.

Rates for DINxs and TONxs development and OUR, were computed for two stations. ST 50 on the western side of the transect and ST 108 on the eastern side of the transect were chosen to match the analyses made by Hansell *et al.* (2004). The ages have been computed considering a linear mixing between the ages of the NC and the SC as in Hansell *et al.* 2004. For TONxs calculations one end member mixing has been computed. That is, the expected property change is calculated by considering its evolution from the original water mass.

The results of the preformed values of DINxs, AOU and TONex and the difference between the preformed values and the measured ones are presented in the Table 4.2.

Table 4.2 Fraction of SC (F.SO) and NC (F.NO) along isopycnals at station 50 (West) and 108 (East). Preformed values (P. DINxs, P.AOU, P.TONxs) and the difference between preformed and measured (D. DINxs, D.AOU, D.TONxs) values of DINxs, AOU and TONx are reported. CFC ages are taken from Hansell *et al.* (2004). TONxs have been calculated with a one end member mixing model. Preformed values of TONxs on the $\sigma_0=27$ layer were not available for analysis.

ST	σ_0 kgm ⁻³	F.SO	F.NO	P.DINxs μmolkg ⁻¹	P.AOU μmolkg ⁻¹	P.TONxs μmolkg ⁻¹	CFC age	D.DINxs μmolkg ⁻¹	D.AOU μmolkg ⁻¹	D.TONxs μmolkg ⁻¹
50	26.0	0.30	0.70	-0.1	24.63	2.3	4.5	0.8	0.83	-0.6
50	26.5	0.06	0.94	0.5	21.44	1.0	3.4	1.2	18.88	2.1
50	27.0	0.42	0.58	-0.5	76.21	na	25.4	0.5	42.19	-
108	26.0	0.04	0.96	-0.1	10.41	3.8	1.8	-0.7	-16.54	-0.6
108	26.5	0.23	0.77	0.1	36.95	0.8	5.2	0.7	5.09	0.7
108	27.0	0.17	0.83	0.0	42.18	na	23.5	1.1	64.97	-

The production rates of DINxs, AOU and TONxs, have been calculated by dividing the difference between the preformed and measured value by the CFC age (Table 4.3)

Table 4.3 Production rates of DINxs OUR and TONxs along isopycnal surfaces at station 50 (West) and 108 (East).

ST	σ_0 kgm ⁻³	Depth (m)	F.SO	F.NO	CFC age (y)	Prod.R DINxs μmolkg ⁻¹ y ⁻¹	OUR μmolkg ⁻¹ y ⁻¹	Prod.R TONxs μmolkg ⁻¹ y ⁻²
50	26.0	163	0.30	0.70	4.53	0.2	-0.40	-0.1
50	26.5	360	0.06	0.94	3.36	0.3	7.44	0.6
50	27.0	700	0.42	0.58	25.44	0.0	3.84	
108	26.0	20	0.04	0.96	1.75	-0.4	-7.70	-0.3
108	26.5	200	0.23	0.77	5.24	0.1	-1.95	0.2
108	27.0	500	0.17	0.83	23.47	0.1	4.68	

The $\sigma_0=26$ surface, in the eastern station (ST 108), was too shallow to experience DINex or TONex accumulation (the depth of $\sigma_0=26$ surface is 163m in the west and only 20m in the east); while both nitrate and TON appeared to be consumed on this surface. On the western side this surface was deep enough to experience DINex development (ST 50).

The $\sigma_0=26.5$ surface experienced the strongest DINxs development, starting at 200m on the eastern side ($0.1\mu\text{molkg}^{-1}\text{year}^{-1}$) and reached $0.3\mu\text{molkg}^{-1}\text{year}^{-1}$ on the western side at 360m. Deeper, on the $\sigma_0=27$ surface, the production of DINex decreased both on the western and eastern side due to the dilution with the Southern component waters. TONxs decreased at a rate of $0.1\mu\text{molkg}^{-1}\text{year}^{-1}$ on the shallowest ($\sigma_0=26$) isopycnal. Deeper, at 360m on the $\sigma_0=26.5$ surface, TONxs production increased to $0.6\mu\text{molkg}^{-1}\text{year}^{-1}$ together with OUR. No data was available to evaluate TONxs development on the deepest isopycnal surface. OUR was highest between 360-500 meters and low on those isopycnal surfaces that lie above 200m, indicating oxygen enrichment due to biological production or supersaturation. The maximum development of DONxs, TONxs and OUR appeared on the $\sigma_0=26.5$ surface on the western side, where strong limitation of P with respect to N or an input of N rich DOM must have occurred.

What arises from these results is a zonal gradient in the development of both DINxs and TONxs. At station 50 (65°W) the accumulation of total N with respect to P amounts to $1.34\text{molNkg}^{-1}\text{y}^{-1}$ (between 360-163m); At station 108 (24.7°W) either preferential uptake or export of N seems to be occurring with a consequential loss of $-0.4\text{ molNkg}^{-1}\text{y}^{-1}$. Higher fixation rates in the west North Atlantic have been previously reported by Gruber and Sarmiento (1997) and other authors (Capone *et al.* 2005), but this suggestion has been recently contradicted by the finding of Hansell *et al.* (2004), who suggested that N_2 fixation might also occur at high rates in the eastern basin where the inputs of dust are high.

To compare these results with those reported by Hansell *et al.* (2004) and Gruber and Sarmiento (1997), an areal estimate (using the areas/volumes reported in the above mentioned studies) of the total N excess developed from the north east gyre to the south western Sargasso Sea on the three isopycnal layers ($\sigma_0=26, 26.5, 27$) was performed (Table 4.4).

It must be said that the divergence in the estimates of excess nitrogen production in the results of Hansell *et al.* (2004) and Gruber and Sarmiento (1997) are due to the difference in the domain area considered for the calculations. Gruber and Sarmiento (1997) reported N* anomalies between 10° to 50°N and 10° to 90°W on the $\sigma_0=26, 26.5, 27$ isopycnals; thus a very large area of the North Atlantic of $\sim 27.8 \times 10^6\text{km}^2$ was used to derive a basin wide rate

of N_2 fixation. In contrast, Hansell *et al.* (2004) reported nitrogen excess in a much smaller area of $6.8 \times 10^6 \text{ km}^2$, which extends approximately from 15° to 25°N and 25 to 75°W , so that their estimates are regional and not gyre wide.

To obtain the estimates of N_2 fixation comparable with the ones reported by Gruber and Sarmiento (1997) and Hansell *et al.* (2004), the production of DINxs and TNxs on each isopycnal has been divided by a factor 0.76 (Hansell *et al.* 2004, Gruber and Sarmiento 1997). This factor of 0.76 originates from the N^* tracer continuity equation computed by Gruber and Sarmiento (1997) that results from a liner combination of the continuity equation of nitrate and phosphate which has been simplified, to reflect only the sources minus sink terms of denitrification and N_2 fixation, to:

$$\frac{d(N^*)}{dt} = J_{\text{denit}}(N) + \left(\frac{r_{\text{denit}}}{r_{\text{denit}} - r_{\text{nit}}} \right) \cdot \left(\frac{r_{\text{N}_2\text{fix}} - r_{\text{nit}}}{r_{\text{N}_2\text{fix}}} \right) \cdot J_{\text{N}_2\text{fix}}(N) \quad \text{Eq. 4.13}$$

where $J_{\text{denit}}(N)$ and $J_{\text{N}_2\text{fix}}(N)$ represent the source minus the sink terms due to denitrification and N_2 fixation respectively and the r_{nit} , r_{denit} and $r_{\text{N}_2\text{fix}}$ represent the stoichiometric ratios of remineralization (16) denitrification (-104) and N_2 fixation (125) processes, hence the multiplying factor in the last term equals to 0.76. As denitrification is considered to be negligible in the oxygenated waters of the North Atlantic ($J_{\text{denit}}(N) = 0$) then $J_{\text{N}_2\text{fix}}(N)$ can be estimated from the rate of change of N^* divided by 0.76.

The so derived estimates of N_2 fixation have then been multiplied individually by the volume of each isopycnal layer to obtain an areal fixation rate (moly^{-1}) for each isopycnal and then summed to provide an areal fixation rate (moly^{-1}) for the whole of the three isopycnals where the majority of the DINxs and TNxs production occurs. The regional and gyre scale average fixation rate for the North Atlantic have then been calculated by dividing the areal fixation rate (moly^{-1}) by the areas reported Hansell *et al.* (2004) and Gruber and Sarmiento (1997) respectively.

Using the volumes reported by Hansell *et al.* (2004) of the 3 isopycnal layers the areal estimate of DINex amounts to $1.51 \cdot 10^{11} \text{ mol}\text{Ny}^{-1}$, which is close to the $1.18 \cdot 10^{11} \text{ mol}\text{Ny}^{-1}$ estimated by Hansell *et al.* (2004). Similarly, using the much larger areas of the 3 isopycnal layers reported by Gruber and Sarmiento (1997) (hereafter G&S 1997), N_2 fixation estimates amount to $8.89 \cdot 10^{11} \text{ mol}\text{Ny}^{-1}$ higher, but not significantly different from, the $8.69 \cdot 10^{11} \text{ mol}\text{y}^{-1}$ reported by the same authors validating these calculations. Thus, the estimates of DINxs production and the inferred N_2 fixation rates in this study are consistent with those in the literature. The novelty of this study however, is to also consider the overlooked organic

nutrient production on these isopycnal surfaces and therefore to “correct” N_2 fixation estimates for N source. The addition of the organic fraction (Table 4.4), to the mean N_2 fixation rate, calculated from the development of TN on three isopycnals ($\sigma_0 = 26, 26.5, 27\text{kgm}^{-3}$) amounts to $0.05\text{mol m}^{-2}\text{y}^{-1}$, using the volumes reported in Hansell *et al.* (2004) (Table 4.4).

Table 4.4 Comparison of the N_2 fixation rates estimated from DINex by G&S (1997) and Hansell *et al.* (2004) and this study on selected 3 isopycnal layers ($\sigma_0 = 26, 26.5, 27\text{kgm}^{-3}$). Please note that, for better comparison with the N_2 fixation estimates reported in G&S (1997) and Hansell *et al.* (2004), here are reported the total volume of the 3 isopycnal considered and not the individual volumes of the isopycnal layers used for the calculations. Note the different volumes used in the calculations by G&S (1997) and Hansell *et al.* (2004). The addition of organic nutrients in this budget (TNex) increases the average fixation rates which become comparable with the rates estimated by G&S (1997) and Hansell *et al.* (2004) adding the contribution of all isopycnal layers (see table below).

DINxs					
	Volume of 3 isopycnals (m^3)	Area (m^2)	DINex Prod. ($\text{mmol m}^{-3} \text{y}^{-1}$)	Areal fix. Rate (mol y^{-1})	Avg. fix rate ($\text{mol N m}^{-2} \text{y}^{-1}$)
G&S (1997)	4.8×10^{15}	27.8×10^{12}	0.61	8.69×10^{11}	0.031
This study	4.8×10^{15}	27.8×10^{12}	0.69	8.89×10^{11}	0.032
Hansell <i>et al.</i> (2004)	8.7×10^{14}	6.83×10^{12}	0.56	1.18×10^{11}	0.017
This study	8.7×10^{14}	6.83×10^{12}	0.69	1.51×10^{11}	0.022
TNxs					
This study	4.8×10^{15}	27.8×10^{12}	1.34	20.09×10^{11}	0.097
This study	8.7×10^{14}	6.83×10^{12}	1.34	3.47×10^{11}	0.05

If the DINxs development was calculated on all isopycnal layers and not only on the $\sigma_0 = 26, 26.5$ and 27kgm^{-3} isopycnals then, the average fixation rate, using the DINxs production and the areas reported by Hansell *et al.* (2004), would amount to $0.045\text{mol m}^{-2}\text{y}^{-1}$. This estimate is very close ($0.05\text{mol m}^{-2}\text{y}^{-1}$) to the average fixation rate estimated from the development of TNxs reported in this study.

Similarly, using the areas reported by Gruber and Sarmiento (1997) N_2 fixation estimates, calculated from TNxs development, amount to $0.097\text{mol m}^{-2}\text{y}^{-1}$, which is in good agreement with that one reported by Gruber and Sarmiento (1997) $0.072\text{mol m}^{-2}\text{y}^{-1}$ when the contribution of N^* development in the upper water column is summed (Table 4.5). Assuming that the 3 isopycnal layers ($\sigma_0 = 26, 26.5, 27\text{kgm}^{-3}$) contribute about 40% to the total DIN excess over the entire upper 1000m, a rough calculation would suggest that the N_2 fixation rate, calculated with TNex over the entire depth range, would amount to $0.24\text{mol m}^{-2}\text{y}^{-1}$. This

rate is 3 to 5 times higher than previously reported by Hansell *et al.* 2004 and Gruber and Sarmiento 1997, and compares well with the estimates of N_2 fixation rates obtained by the integration, along the water column, of TNex ($0.19 \text{ mol m}^{-2} \text{ y}^{-1}$) indicating that this model can well describe the processes which are altering the N and P balance over a portion of the North Atlantic subtropical gyre. Therefore the contribution of organic nutrients for the evaluation of N to P anomalies to infer rates of N_2 fixation cannot be ignored.

Table 4.5 Rates of N_2 fixation estimated from DINex reported by G&S (1997) and Hansell *et al.* (2004) and TNxs calculated in this study on all the isopycnal layers ($\sigma_0 = 25.6-27.6 \text{ kg m}^{-3}$) of the upper 1000m of the water column. Volumes of all isopycnals are not reported in the study by Hansell *et al.* (2004). In this study average N_2 fixation rates for all isopycnals have been extrapolated from average N_2 fixation rates obtained on 3 specific isopycnals ($\sigma_0 = 26, 26.5, 27 \text{ kg m}^{-3}$).

DINxs	Volume of all isopycnals (m^3)	Area (m^2)	DINex Prod. $\text{mmol m}^{-3} \text{ y}^{-1}$	Areal fix. Rate mol y^{-1}	Avg. fix rate $\text{mol N m}^{-2} \text{ y}^{-1}$
G&S (1997)	26.76×10^{15}	27.8×10^{12}	2.62	23×10^{11}	0.072
Hansell <i>et al.</i> (2004)	na	6.83×10^{12}	na	3.1×10^{11}	0.045
TNxs					
This study	na	27.8×10^{12}	na	50×10^{11}	0.24
This study	na	6.83×10^{12}	na	8.8×10^{11}	0.125

4.4.1.2 Conclusions

What can be discerned from this data analysis is that both organic and inorganic nutrients must be taken into account when considering the balance between N and P pools. A new geochemical tracer, TNxs, which combines both the organic and inorganic N to P anomalies is therefore, more appropriate for calculating the impact of N_2 fixation in the gyre.

By considering both inorganic and organic pools in the gyre, it is clear that the cycling of N and P are decoupled. The storage of N in the TON pool provides a mechanism by which nitrogen can be transported into the gyre independently of phosphorus. Such a mechanism is required for elemental mass balance in the gyre because nitrogen fixation introduces excess nitrogen to the euphotic zone without any stoichiometrically equivalent phosphorus. To maintain the elevated N:P ratio in areas where N_2 fixation is not a significant process, nitrogen must somehow be selectively transported to the gyre; this is possible for example through gyre scale circulation which transports water masses with high TONxs singal.

In conclusion, the inclusion of organic nutrients in the N and P inventory of the upper layers of the North Atlantic subtropical gyre have allowed the computation of a new geochemical tracer, TNxs, which indicate that N_2 fixation, in the North Atlantic, is more

important than previously thought and that the N excess, introduced by this process, can be carried around the gyre in a relatively refractory TON pool.

4.4.2 Surface Waters – Bulk Distributions

Physical properties

In the top 500m, water temperature decreased gradually moving eastwards. Saline waters were found to be located between 50°W and 35°W (Fig. 4.11).

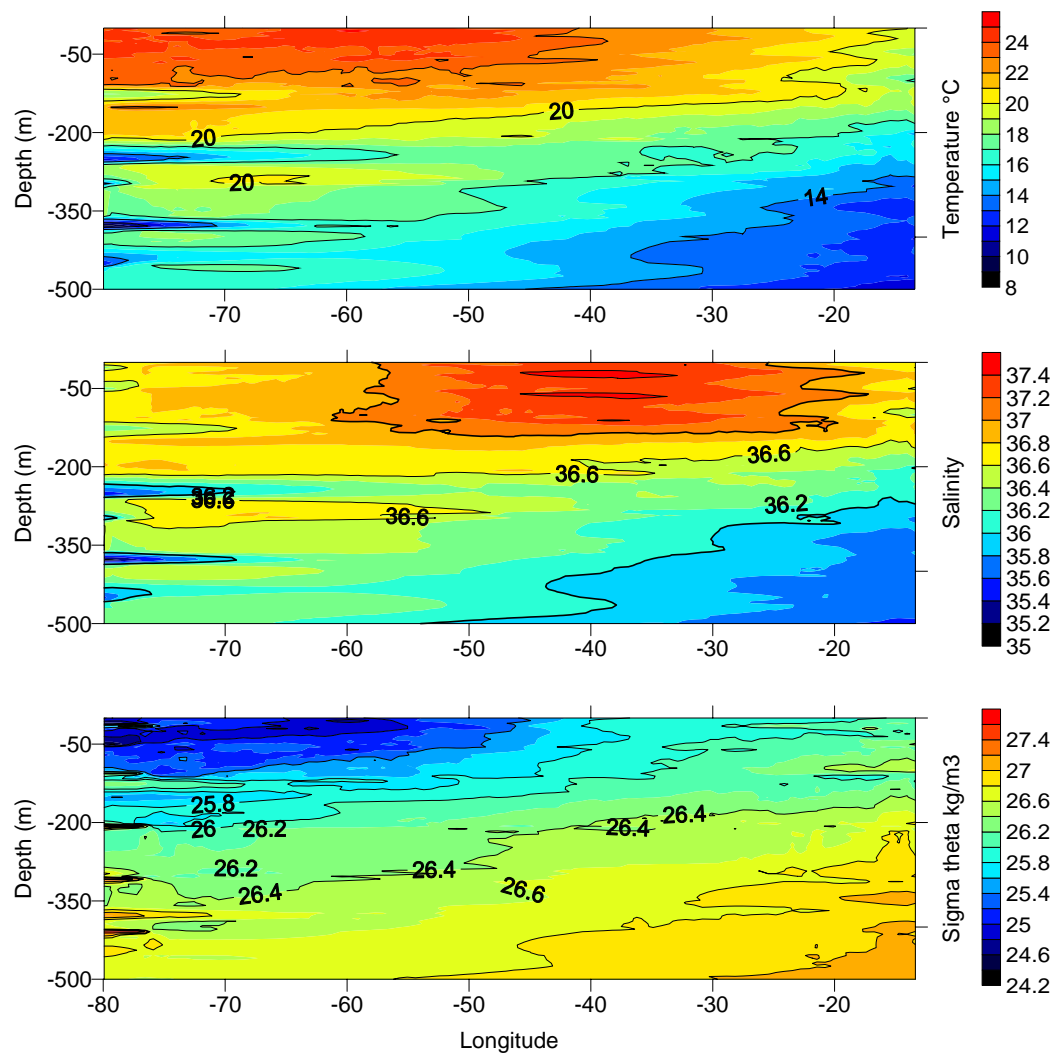


Fig. 4.11 Section of temperature (°C, top), salinity (centre) and sigma-theta (kgm^{-3} , bottom) of the top 500m across 24.5°N.

On the western side of the basin, from 70 to 80°W, intrusions of cooler and less saline water were observed at 125m, 250m and 350m. The density field seemed to be controlled more strongly by temperature and showed a similar zonal gradient (Fig. 4.11). Isopycnal surfaces heavier than $\sigma_0=26\text{kgm}^{-3}$ outcropped on the eastern side of the transect and were as deep as 200m in the far west.

Inorganic N and P distribution

In the centre of the gyre, inorganic nutrients were close to the detection limit ($0.1\mu\text{M}$ NO_3^- , $0.01\mu\text{M}$ PO_4^{3-}) in the top 100m (Fig. 4.12). Both nitrate and phosphate concentrations increased between $\sigma_0=26\text{kgm}^{-3}$ and $\sigma_0=26.5\text{kgm}^{-3}$ following the slope of these isopycnal surfaces meaning that concentrations of $>0.1\mu\text{M}$ NO_3^- and $>0.01\mu\text{M}$ PO_4^{3-} were measurable at 50m in the east (20°W) and only deeper, at 150m, in the centre of the gyre. At the western end, from 75°W to 70°W , nitrate and phosphate were measurable at the surface (0.5 and $0.05\mu\text{M}$, respectively); these measurable concentrations of nutrients were likely to be associated with coastal influences. Nitrate levels greater than $0.1\mu\text{M}$ were measurable at 25m from 46°W to 50°W while no significant phosphate values were detected at the same stations. At 125m, from 65°W to 80°W , the signal of cooler, less saline, upwelled water carrying high nutrients could be detected.

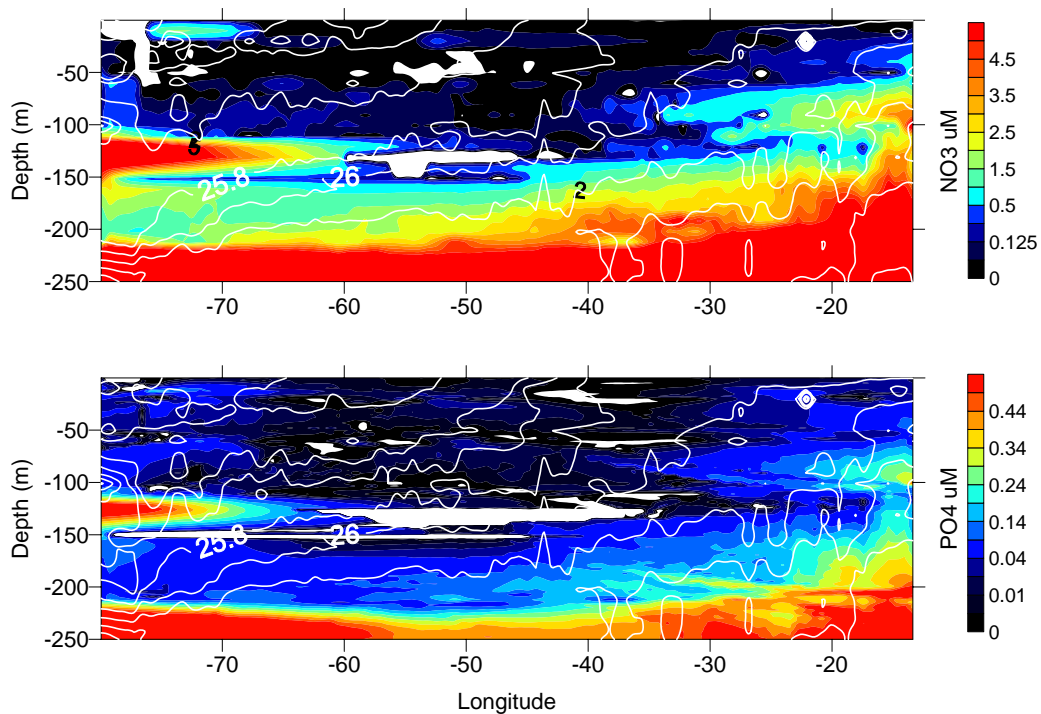


Fig. 4.12 Section of nitrate (μM , top) and phosphate (μM , bottom) across 24.5°N . Overlaid (white) are the sigma-theta contours. Please note that the σ_0 contours intervals are different in the two panels.

Organic Nutrient Distribution

The spatial distribution of dissolved organic nutrients varied across the subtropical gyre (Fig. 4.13). TON concentrations were highest at the surface, reaching up to $9\mu\text{M}$ at station 58 (60°W). The area from 60°W to 40°W was generally characterised by high TON concentrations whereas, in contrast, in this same area, TOP concentrations were low. As no

particular physical structure was found here, local production of TON is hypothesised. High concentrations of TON and TOP were found at around 225 meters in the zone extending from 45°W to 30°W; probably caused by the accumulation of organic matter and hence bacterial remineralization.

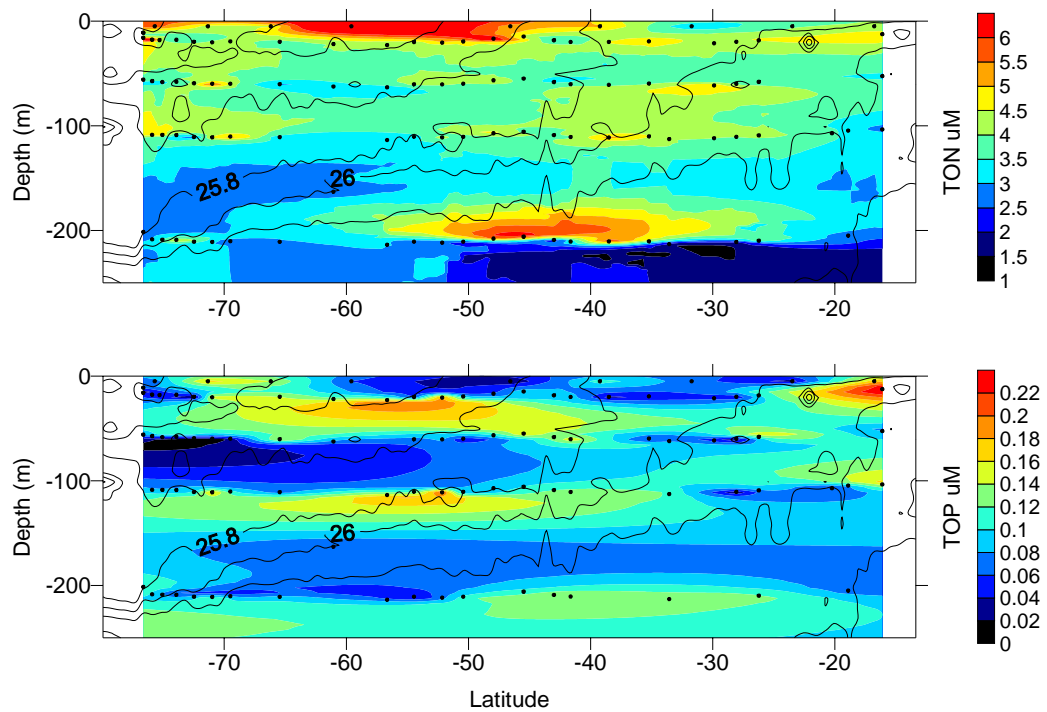


Fig. 4.13 Section of TON (μM , top) and TOP (μM , bottom) across 24.5°N. Overlaid (black) are the sigma-theta contours. Black dots represent data points. Contours were generated with Kriging interpolation method with an anisotropy ratio of 1.

Phytoplankton Pigments

CTD calibrated chlorophyll α was very low in the surface layers and in the centre of the gyre (Fig. 4.14). The highest values were found at the western and eastern flanks of the gyre; the depths of the deep chlorophyll maximum increased towards the centre where it generally coincided with the depth of the mixed layer ($\sim 100\text{m}$).

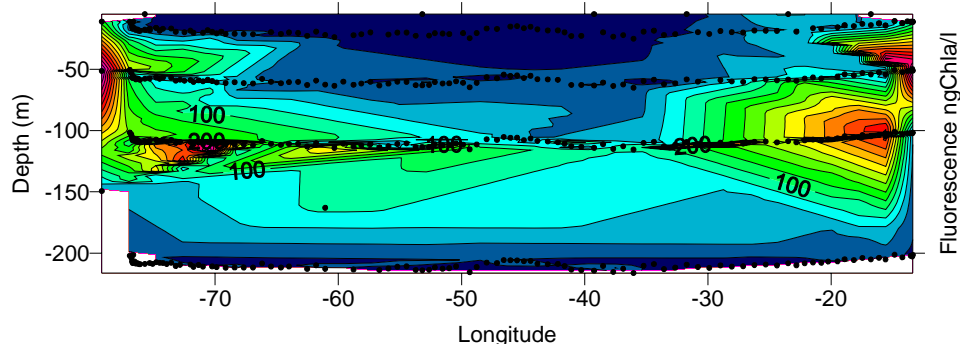


Fig. 4.14 Section of calibrated fluorescence (ngChla l^{-1}) across 24.5°N. Black dots represent data points.

Picoplankton, nanoplankton and microplankton fractions constituted the phytoplankton community. The picoplankton community is mostly composed of the divinylchlorophyll α containing prochlorophytes and cyanobacterias, such as *Synechococcus*, which contain zeaxanthin as their main pigment. This fraction was a major component (65 to 89%) of the phytoplankton surface populations (Fig. 4.16). Divinylchlorophyll α distributions generally opposed the temperature gradient (Fig. 4.15). The 22°C isotherm tracks the limit where the contribution of Divinylchlorophyll α to total chlorophyll α was low (5-15%). With depth and cooler temperatures, prochlorophytes became a major fraction of chlorophyll α (35-55%). As prochlorophytes were not a major fraction of total chlorophyll α in the surface, the strong picoplankton signal is attributable to the presence of cyanobacteria. Picoplankton were important also at 50m from 50°W to 35°W. Here, however, the major component of picoplankton community was prochlorophytes.

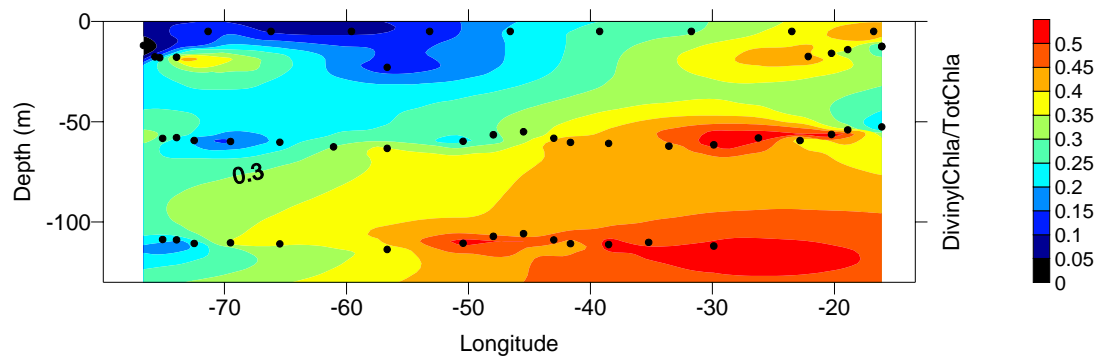


Fig. 4.15 Section of fraction of divinylchlorophyll α over total chlorophyll α across 24.5°N. Black dots represent data points. Contours were generated with Kriging interpolation method with an anisotropy ratio of 1.

Nanoplankton constituted on average 20% of the surface phytoplankton community and nearly 40% at stations 47 and 67. Nanoplankton importance increased with depth complementing picoplankton (Fig. 4.16).

Microplankton was only a minor component (less than 10%) of the autotrophic community, its major contribution was found in the western end of the transect (Fig. 4.16).

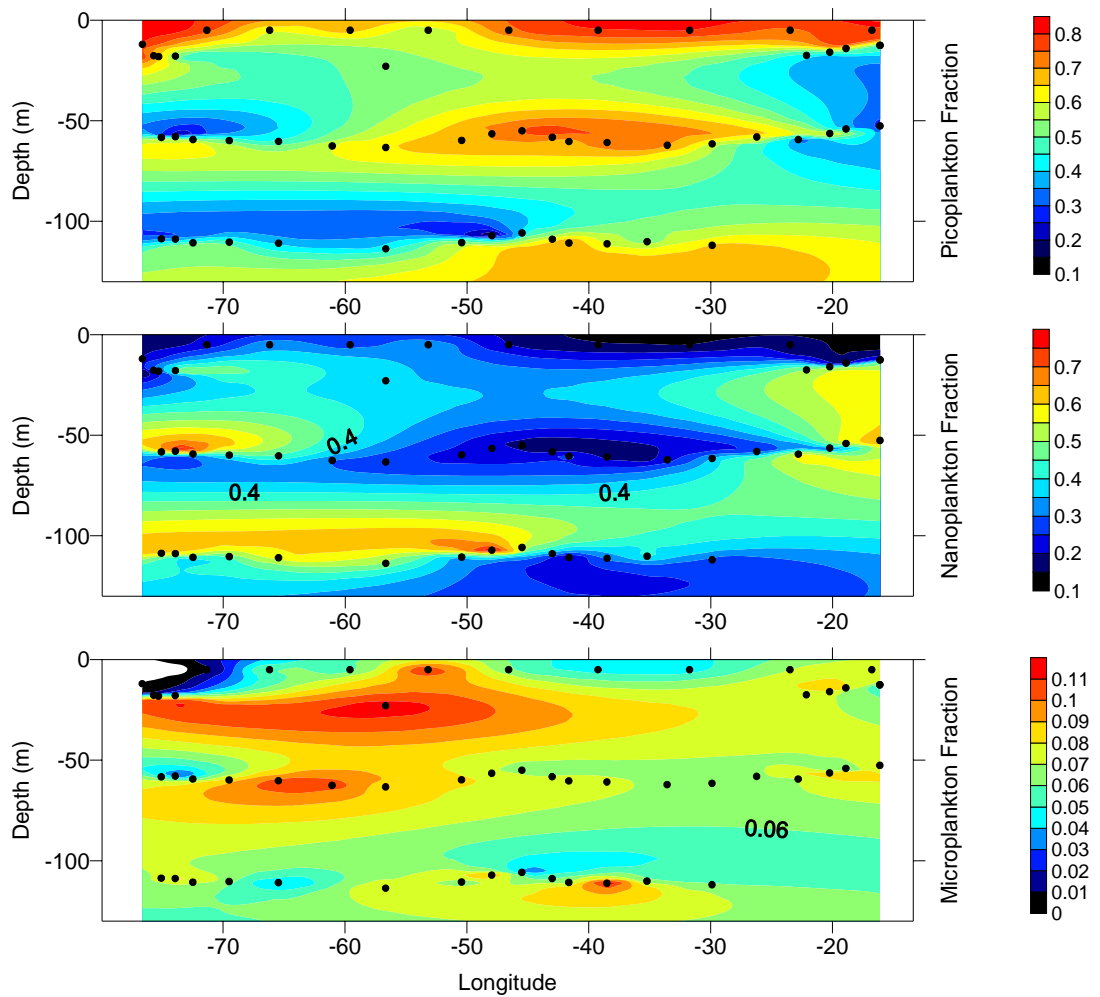


Fig. 4.16 Section of fractions of picoplankton (top), nanoplankton (centre) and microplankton (bottom) community across 24.5°N. Black dots represent data points. Contours were generated with Kriging interpolation method with an anisotropy ratio of 1.

DINxs Distribution

The distribution of N to P imbalances, assuming a Redfield type stoichiometry, in both the organic and the inorganic pools (Fig. 4.17) were determined. The zero nitrogen excess isoline represents the limit between excess nitrate ($>0 \mu\text{M}$) relative to phosphate and vice versa ($<0 \mu\text{M}$). In the upper 100m across the subtropical gyre DINxs values were nearly always negative ($-0.5 \mu\text{M}$) except in localised areas in the surface around 62°W, and from 42°W to 30°W. High DINxs values ($> 0 \mu\text{M}$) started showing at 100m in the centre of the gyre and were expressed only deeper at the borders of the gyre. Positive DINxs values indicated that organic matter remineralization and hence the consumption of oxygen started occurring at these depths. At this depth however, the euphotic layer is still affected by oxygen production by phytoplankton therefore the AOU signal is still very low.

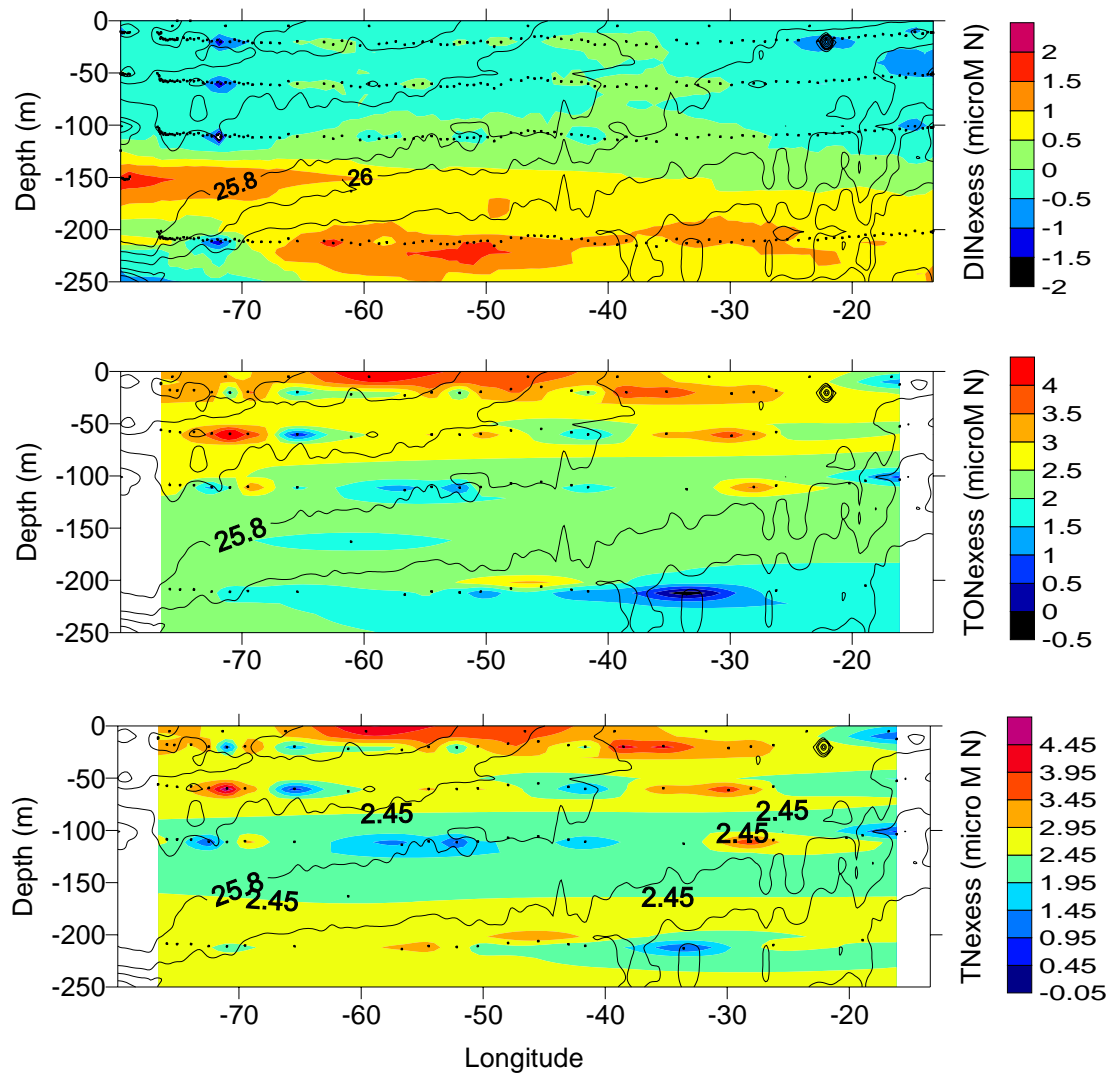


Fig. 4.17 Sections of DINex (top), TONxs (centre) and TNxs (bottom) across 24.5°N. Overlaid (black) are the sigma-theta contours. Black dots represent data points. Contours were generated with Kriging interpolation method with an anisotropy ratio of 1.

This area was also characterised by a strong presence of prochlorophytes and a low TONxs. It is likely that, the dominant *Prochlorococcus* sp., which are known to be able to utilise organic forms of N (Gilbert and Bronk 1994) and survive at low irradiances, are utilising TON in the region lowering TONxs and producing oxygen. DINxs increased ($>0.5 \mu\text{M}$) at depths greater than 100m. A peak in DINxs was observed at 150m on the western flank of the gyre. This signal is produced by deep upwelled waters that carry excess nitrate with respect to phosphate and is confirmed by the cooler and saltier water spike observed at the same depth (Fig. 4.11). TONxs was always positive throughout the water column. The highest values were confined to the top 70 meters ($2.9 \pm 1.3 \mu\text{M N}$). The spatial variability of TONxs in surface layer ranged from $4 \mu\text{M N}$, in 62°W to 40°W , to $1.5 \mu\text{M N}$ on the eastern flank of the gyre. The TONxs maximum

coincided broadly with an area characterised by low $\delta^{15}\text{N}$ in PON (data presented later in this chapter) and the observation of *Trichodesmium* colonies during the cruise. These findings fit well with the studies that documented the release of DON by N_2 fixing cyanobacteria (Gilbert and Bronk 1994, Mulholland *et al.* 2004). The high excess of TON over TOP may be an effect of both the release of N rich DOM and a preferential uptake of TOP. The relative importance of these two processes is unclear. Analysing the DINxs alone, one would conclude that, in the top 250m, nitrate is seldom in excess with respect to phosphate suggesting N as a limiting factor in the area studied. In contrast, when considering the total dissolved nutrients in the surface layer P is depleted with respect to N, as suggested by the total nitrogen pool excess (TNex) (Fig. 4.17).

4.4.2.1 Discussion

The west to east trends observed give some indication of the different physical or biological controls acting on nutrient dynamics across the transect.

In the region spanning from 80-70°W, the surface zonal gradient in the distribution of organic and inorganic nutrients indicates the advection of DOM from nutrient rich areas where it is produced towards the centre of the gyre where it is consumed (Fig. 4.13). In this region, there is no covariance between surface dissolved organic and inorganic nutrients as might be expected if a consistent fraction of inorganic nutrients were being converted to the dissolved organic form. This is in contrast to the findings in coastal upwelling zones where upwelling initially increases the standing stock of inorganic nutrients and promotes primary productivity, which in turn transforms a fraction of assimilated nutrients to DON and DOP. Thus these findings suggest that at the western end of the transect DOM and inorganic nutrients were transported from areas where both inorganic and organic nutrients were available, and were not locally produced or upwelled by eddy heaving or similar processes. This is confirmed also by the DOC distribution (data not shown), which is well correlated with temperature. Strong correlations between DOC and temperature have been observed in other high nutrient regimes such as the Ross Sea and the equatorial Pacific (Hansell and Waterhouse 1997, Hansell and Carlson 1998; Carlsson *et al.* 2000) and have been attributed to a DOC distribution primarily controlled by physical processes. The gyre circulation pattern and nutrient streams created by the western boundary current (Williams and Follows 2005) allow tropical waters to act as possible sources of organic matter and nutrients for this region. Recent biogeochemistry models (Cunha *et al.* 2005) have highlighted the possibility of South American rivers (Amazon and Orinoco) to impact the nutrient budget and primary production

of the Tropical and Subtropical Atlantic. According to this model, river discharges are advected northwards by the North Brazil Current and entrained into the gyre circulation spreading their biogeochemical signatures, with high inputs of DOM and micronutrients such as Fe, towards the Caribbean. To test for the possibility of a terrigenous influence on organic matter, the isotopic composition of $\delta\text{PO}^{13}\text{C}$ was analyzed. Although no significant west to east trend was found, a light $\delta\text{PO}^{13}\text{C}$ signal (-21‰) coincided with enriched $\delta\text{PO}^{15}\text{N}$ (6‰) (data shown later in this chapter) which could suggest sources of N and C coming from terrestrial origin (Wada 1991).

Moving eastwards, from 65°W to 45°W, the abrupt decrease in inorganic nutrients and TOP suggest biological consumption of all the nutrients. Interestingly, TON concentrations increase in this region implying local production. A source of TON, without any significant addition of nitrate or phosphate can be caused by N_2 fixers, which can release a substantial part of their fixed nitrogen into DON (Gilbert and Bronk 1994, Mulholland *et al.* 2004). The source of P, to sustain N_2 fixation, can potentially be TOP as suggested by the decrease in TOP concentrations, this hypothesis is addressed shortly. In support of N_2 fixation in this area is the taxonomic signature of phytoplankton pigments which indicate a cyanobacteria dominated community and, as will be shown in section 4.4.3, the light isotopic signature of $\delta\text{PO}^{15}\text{N}$ (<2‰) in the region.

From 45°W towards the eastern flank of the gyre, DOM concentrations decrease. Here, the phytoplankton community structure shifts from a picoplankton community dominated by cyanobacteria to a picoplankton community dominated by *prochlorococcus* *sp.* These organisms are characteristic of oligotrophic regions and have the potential to utilise organic forms of N (Moore *et al.* 2002). Interestingly, some strains, adapted to high light conditions, MED 4 and MIT9313, lack the genes required for nitrate utilisation (NO_3^- permease and NO_3^- reductase) so that the utilisation of organic forms of nitrogen is very probable (Zubkov *et al.* 2003).

4.4.2.2 Conclusions

In conclusion, several lines of evidence (DOM and inorganic nutrient distributions and phytoplankton community structure) support a transition from west to east of the mechanisms for providing nutrients to the euphotic zone and thus supporting phytoplankton growth.

In the western most stations concentrations of inorganic nutrients and DOM are supported by lateral advection from nutrient rich areas. Towards the centre of the gyre,

inorganic nutrients are depleted and TOP and TON represent the sole sources of nutrients. Here N_2 fixation is likely to be a major source of new N, a significant fraction of which is released as TON.

4.4.3 Enzyme Experiments - Measures of Biological Processes

Primary Production

Oxygen production over a 12h period was characterised by a high variability among the 6 replicates (Fig. 4.18). Nevertheless the average oxygen net production was $0.89 \pm 0.40 \mu\text{M O}_2 \text{12h}^{-1}$. The maximum O_2 produced was reached at station 49 (66°W) ($1.67 \pm 1.53 \mu\text{mol O}_2 \text{kg}^{-1} \text{12h}^{-1}$), and the minimum at station 67 (53°W) ($0.36 \pm 2.18 \mu\text{mol O}_2 \text{kg}^{-1} \text{12h}^{-1}$). Gross production averaged at $1.69 \pm 0.38 \mu\text{mol O}_2 \text{kg}^{-1} \text{12h}^{-1}$ and respiration at $0.82 \pm 0.65 \mu\text{mol O}_2 \text{kg}^{-1} \text{12h}^{-1}$. Respiration was not detectable at station 76 (46°W). These values of oxygen production are consistent with data reported by Maranon *et al.* (2000)

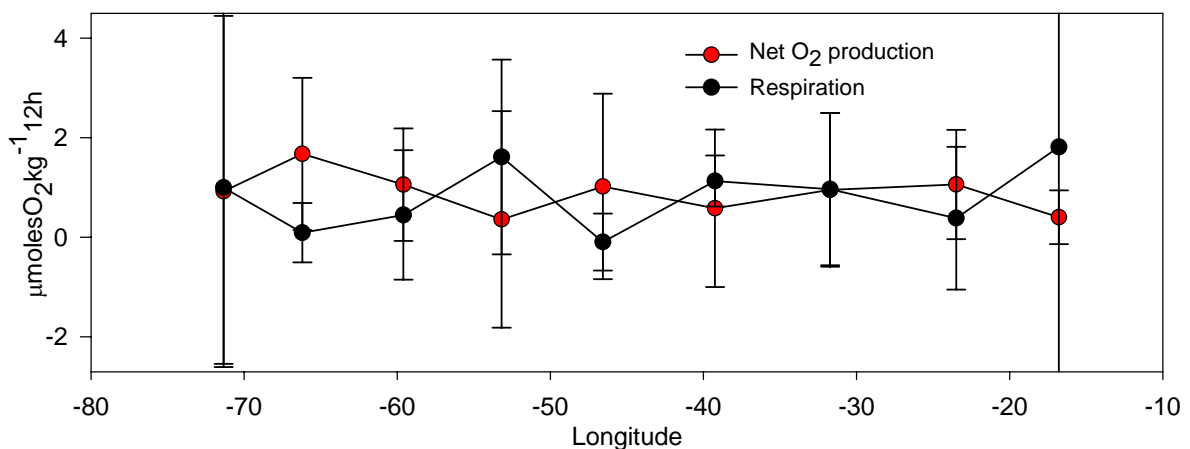


Fig. 4.18 Longitudinal variability of net O_2 production and respiration over a 12h period across the north Atlantic.

Phytoplankton Pigments

Total chlorophyll *a* was variable across the gyre. Increased phytoplankton biomass was found in the area from $65\text{--}60^\circ\text{W}$ and close to the Canary coast (Fig. 4.19). The separation of pigments using HPLC allowed the quantification of the contribution of different taxonomic groups to the total phytoplanktonic biomass calculated according to Barlow *et al.* (2004).

The Picoplankton community was the largest ($\sim 80\%$), followed by nanoplankton ($\sim 15\%$) with microplankton being the smallest component ($\sim 5\%$) (Fig. 4.19). Divinylchlorophyll *a*, a marker for the presence of prochlorophytes, which are part of the broader picoplankton fraction, increased zonally towards the east while the picoplankton

fraction remained constant (Fig. 4.19). This suggests that the picoplankton community shifts from a cyanobacteria to *Prochlorococcus* dominated group moving from west to east.

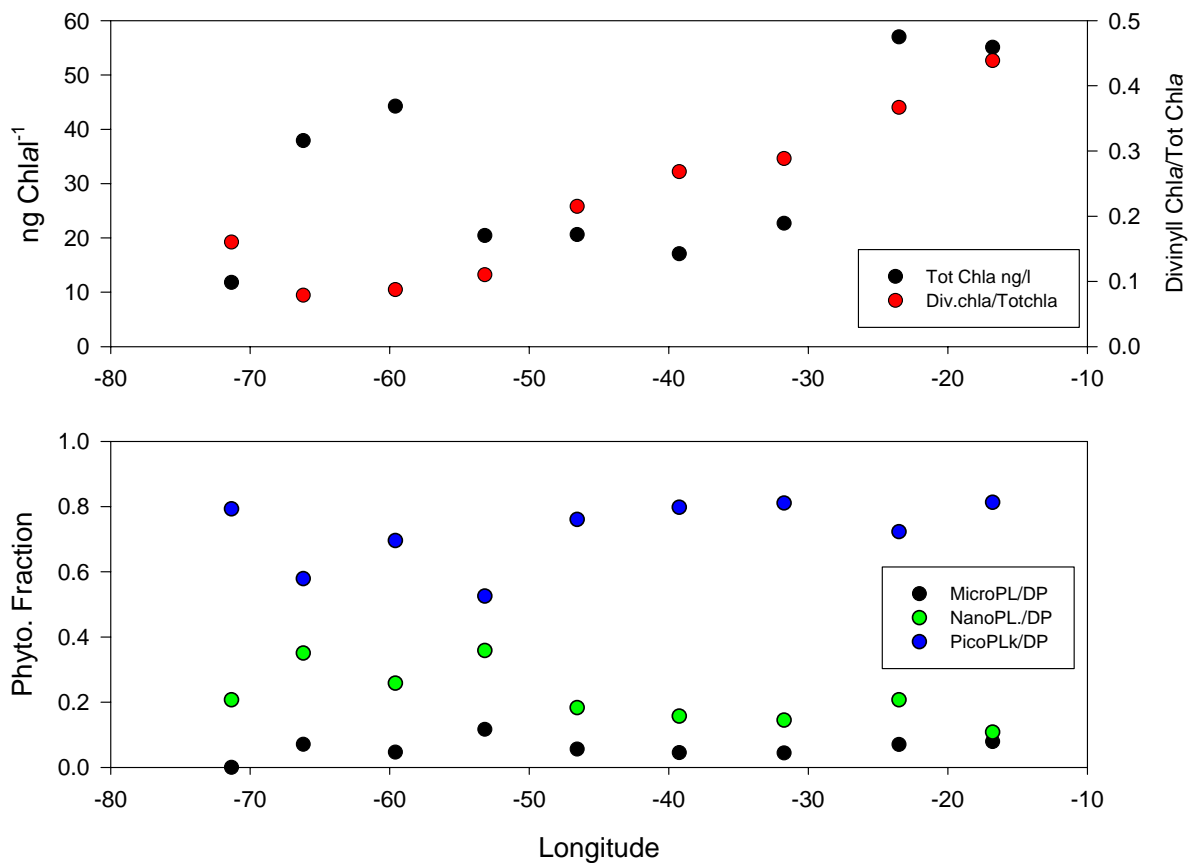


Fig. 4.19 Longitudinal variation of surface total chlorophyll a and fraction of divinylchlorophylla (top) and (bottom) fraction of pico-, nano- and microplankton.

Natural Abundance of $\delta^{15}\text{N}$ PON and POC/PON ratios

The PON samples collected during the enzyme experiments appear to be enriched in ^{15}N with respect to the ones collected from the surface Niskin bottles (Fig. 4.20). These differences may reflect the different methodologies used for the collection of the suspended material. During the enzyme experiments PON was collected directly from the surface into large neck 25L carboys (see methods), thus the inclusion of large sinking particles: zooplankton detritus and faecal pellets is plausible; while for all the other samples, sea water was collected directly from Niskin bottles where the inclusion of sinking particles is less likely. To evaluate if the effect of this trophic bias was real, the relationship between $\delta^{15}\text{N}$ of PON and PON/Chlorophyll a was examined (Waser *et al.* 2000). The $\delta\text{PO}^{15}\text{N}$ of samples collected

from the surface, using the 25L carboys, were positively related to the PON/Chlorophyll α ratio ($r^2=0.4$, $n=8$) indicating that the enriched signals were likely due to the inclusion of higher trophic levels, which are typically enriched in ^{15}N (Wada and Hattori 1980). No relationship was observed for the samples collected with the Niskin bottle ($r^2=0.03$, $n=24$). Thus, the isotopic composition of these latter samples reflect the original phytoplankton isotopic natural abundance while samples collected with carboys not only represent the isotopic composition of phytoplankton but also of higher trophic levels. The inclusion of heterotrophs or faecal pellets in bulk measurement of $\delta^{15}\text{N}$ PON can bias the isotopic signal towards an enriched $\delta^{15}\text{N}$ signal and has to be taken into account in the interpretation of the isotopic data.

In the biased samples however, localised isotopic depleted signals were observed from 65°W to 40°W (Fig. 4.20, red dots). This evidence exacerbates the need of a light source of N to balance the isotopic budget of the surface layer and explain the low $\delta^{15}\text{N}$. The two enriched ($>6\text{\textperthousand}$) ^{15}N PON peaks, on the very western edge and at 30°W , (Fig. 4.20, red dots) are likely to have been created by fractionation during secondary production.

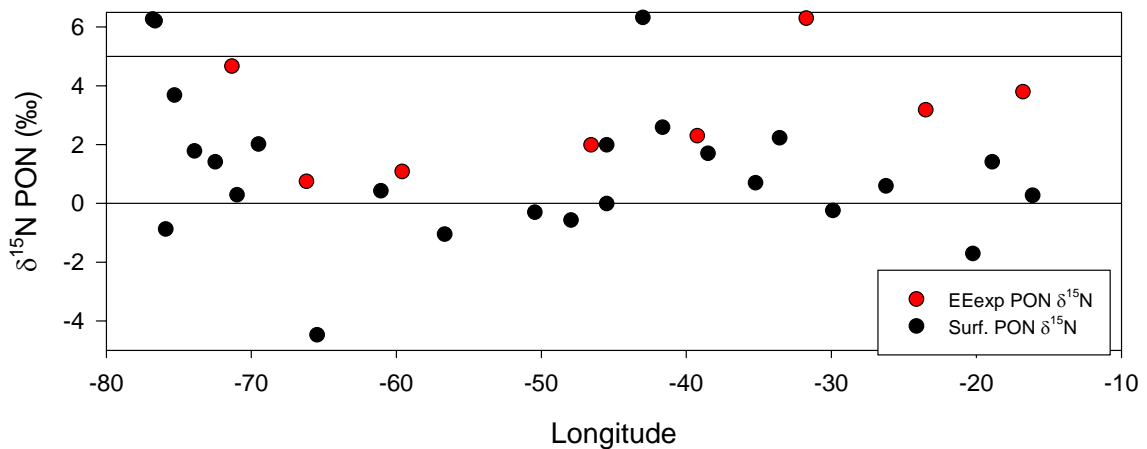


Fig. 4.20 Zonal distribution of $\delta\text{PO}^{15}\text{N}$. Black dots represent data points collected from Niskin bottles 10-25m; Red points represent samples collected from the surface by carboys (0m).

According to the isotopic signatures measured from PON samples collected by Niskin bottles, five different domains have been distinguished (Fig. 4.20, black dots). In the westernmost stations PON was highly enriched in ^{15}N ($\sim 6\text{\textperthousand}$). In the region between 75° and 70°W , $\delta^{15}\text{N}$ PON was quite variable with an average of $1.38 \pm 1.55\text{\textperthousand}$. In this region NO_3^- and PO_4^{3-} were very close to detection limits but were measurable (from 0.1 to $0.2\mu\text{M}$) thus, the low PON isotopic signal might reflect isotopic fractionation during NO_3^- uptake by phytoplankton (Mariotti *et al.* 1981). PON was isotopically depleted from 65°W to 45°W with an average

value of $-1\% \pm 1.77\%$ when excluding the lowest $\delta^{15}\text{N}$ of the data set (-4.47%). Here, NO_3^- was depleted, so I exclude isotopic fractionation and hypothesize that phytoplankton were utilising a light source of N. In the region from 43°W to 38°W the isotopic composition of PON was enriched ($3.54 \pm 2.44\%$). From about 35°W to the eastern flank of the gyre PON was again depleted in ^{15}N ($0.44\% \pm 0.70\%$).

PON C/N ratios were highest from 65°W to 40°W (7.63 ± 2.51), which coincides broadly with the area affected by low isotopic ^{15}N enrichment (Fig. 4.21).

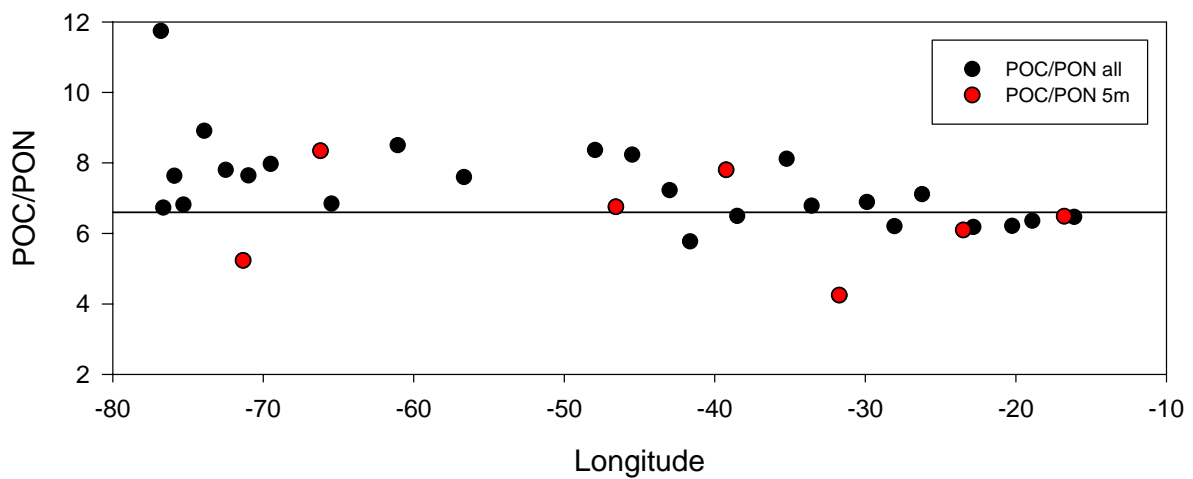


Fig. 4.21 Zonal distribution of POC/PON ratio. Black dots represent data points collected from 10-25m; Red points represent samples collected from the surface (0m).

Enzymes

Alkaline phosphatase activity (AKA), measured as the hydrolysis rates of MUF-P, ranged from $6.48 \pm 0.21\text{nmol l}^{-1}\text{h}^{-1}$ in the centre of the gyre to $62.82 \pm 0.38\text{nmol l}^{-1}\text{h}^{-1}$ at station 98 (30°W) (Fig. 4.22a). These rates are comparable to the rates ($17\text{--}81\text{nmol l}^{-1}\text{h}^{-1}$) measured by Mulholland *et al.* (2002) in the Western tropical and subtropical Atlantic and by Vidal *et al.* (2003) in the Eastern North Atlantic ($\sim 20\text{nmol l}^{-1}\text{h}^{-1}$) from 20 to 30°N . AKA was not correlated with TOP, TON, total Chlorophyll a , or any of the phytoplanktonic fractions (picoplankton, nanoplankton and microplankton). Generally, AKA increased with increasing net and gross production although this trend was not statistically significant.

AK specific activities (AKSA) were computed by normalising AKA to total chlorophyll a (Fig. 4.22b). Specific activities can give an indication of the physiological status of the cells; high specific activities indicate that few enzymes are released but are very efficient. AKSA was homogeneous across the basin (Fig. 4.22b), except for the western most station and at 30°W .

AKSA peaks suggest either a large production of AK per unit phytoplankton or that non autotrophic cells have contributed to the release of AK.

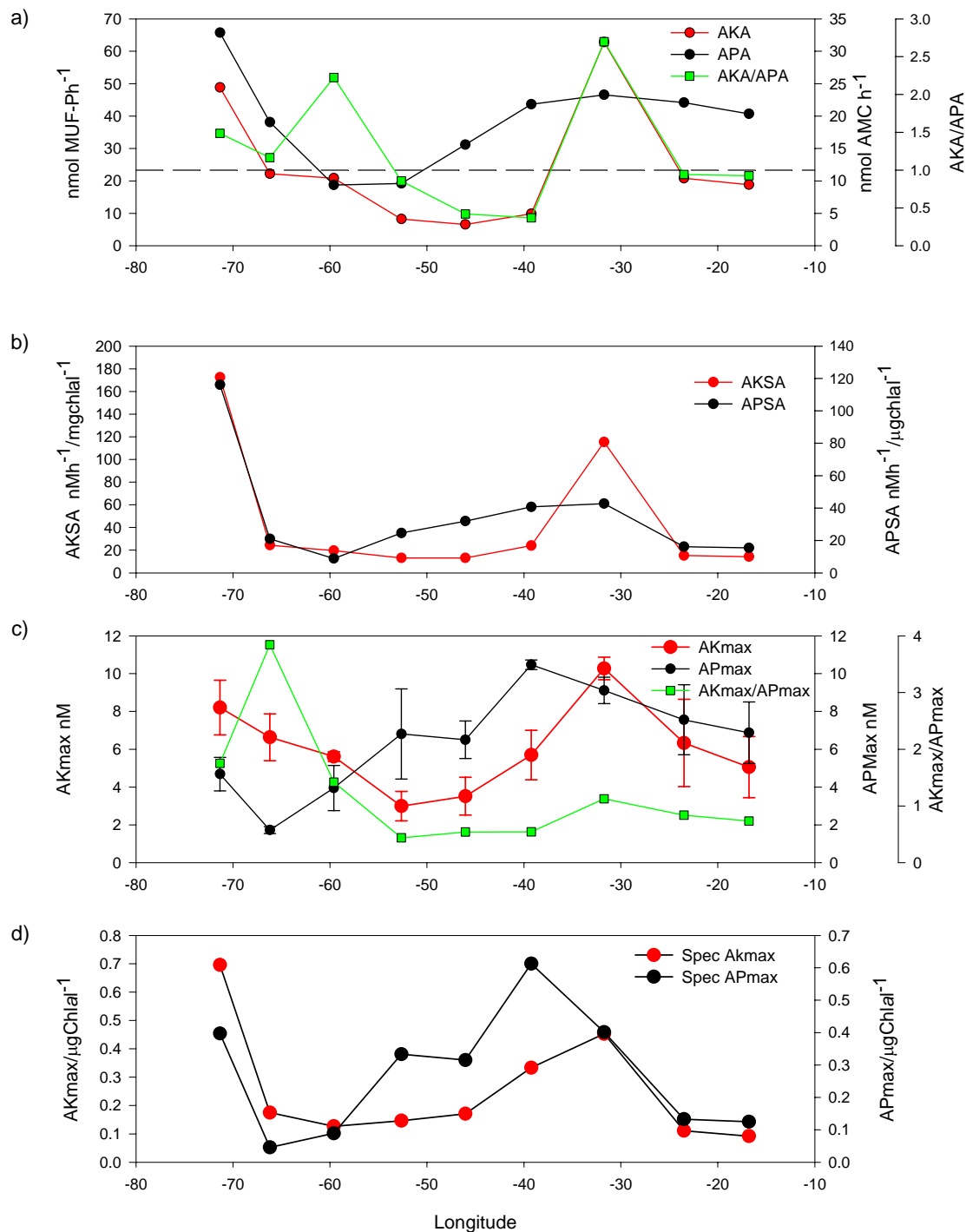


Fig. 4.22 Longitudinal distribution of surface AKA, APA and AKA/APA ratio (a), AKSA and APSA (b), AKmax, APmax and AKmax/APmax (c), Specific AKmax and Specific APmax (d).

The maximum amount of substrate released by alkaline phosphatase, indicated by the height of the plateau (the height at which fluorescence increase over time plateaus, Fig. 2.6), has been indicated here as AKmax (Fig. 4.22c). AKmax I interpret as being a function of the

amount of enzyme present in the environment and thus is related to both the bacterial and autotrophic biomass and the availability of the substrate. As expected AKmax increased with AK activity (Fig. 4.23, black dots) however, when AK activity was normalised to biomass this relationship did not hold true (Fig. 4.23, red dots) confirming that both Akmax and AKA were mostly controlled by autotrophic biomass.

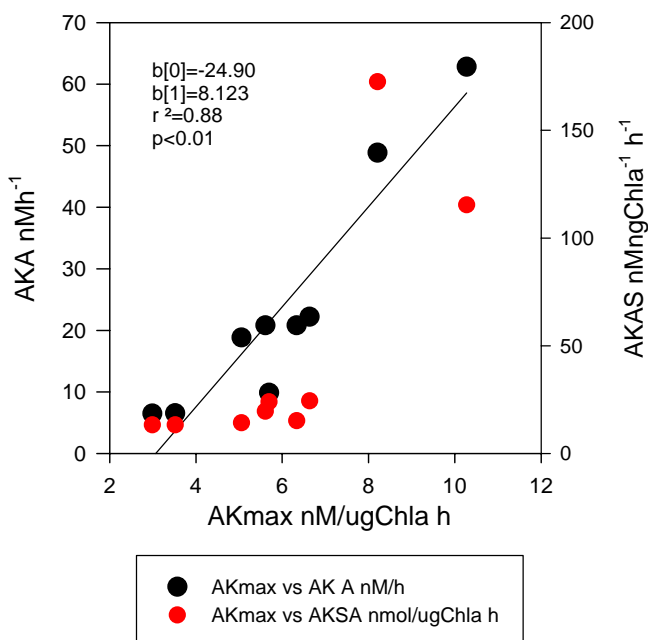


Fig. 4.23 Scatter plot of AKmax and versus AKA and AKSA and regression line (regression coefficients: b_0 =intercept, b_1 =slope).

Spatial variations in AKmax are shown in Fig. 4.22c. The AKmax peak coincided with AKA max at station 98 (30°W); AKmax appeared to be increasing with increasing net and gross production and had an opposing pattern to TON concentrations however, no significant statistical correlation was found. No clear relation occurred between AKmax, TOP and phytoplanktonic classes except for a slight negative relation with the microplankton fraction.

AKmax normalised to chlorophyll *a* has been qualitatively considered a representation of the amount of enzyme released per unit cell. Interestingly, the highest specific AKmax (Fig. 4.22d) occurred at the western end of the gyre and at 30°W. This indicates that many enzymes are released in these areas, however it cannot be ruled out that also heterotrophic organisms contribute to the release of AK.

Aminopeptidase activity (APA) was highest at the western end of the transect ($32.9\text{nmoll}^{-1}\text{h}^{-1}$), decreased rapidly until $\sim 50^\circ\text{W}$ ($9.4\pm 0.2\text{ nmoll}^{-1}\text{h}^{-1}$) and started to increase again towards the eastern side of the gyre where it reached a constant value of about

$20.61 \pm 2.9 \text{ nmol l}^{-1} \text{ h}^{-1}$ (Fig. 4.22a). APA was negatively correlated with TON concentrations and TONexcess (Fig. 4.24) and increased with increasing importance of Divinylchlorophyll *a*. Aminopeptidase Specific activity (APSA) (Fig. 4.22b) had a smoother but similar trend to APA.

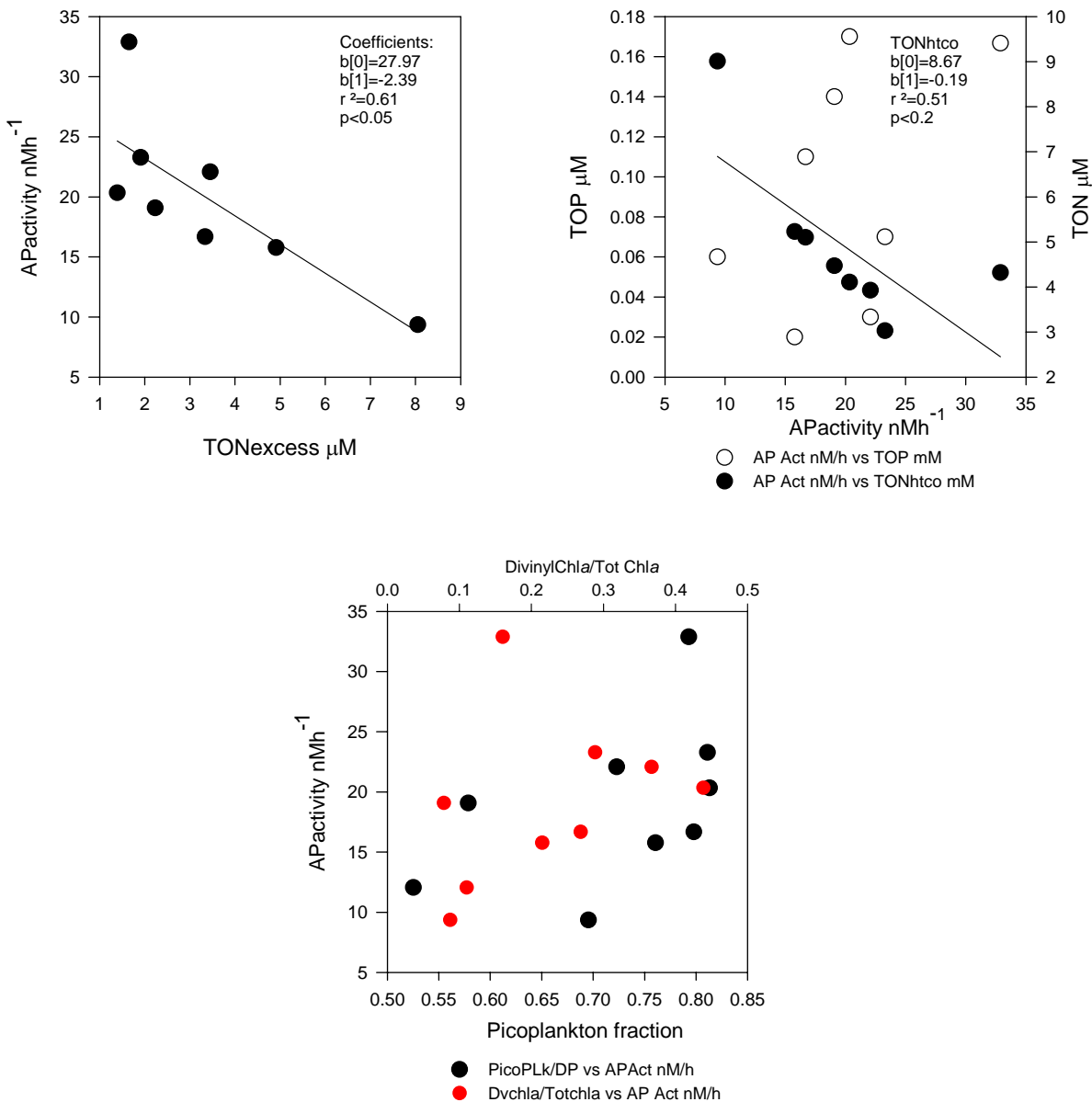


Fig. 4.24 Scatter plots and regression line (regression coefficients: b_0 =intercept, b_1 =slope) of TONexcess versus APA (top left), APA versus TON and TOP (top right), fraction of picoplankton versus APA (bottom).

No correlation occurred between AP maximum substrate release (APmax) and either TON or TOP concentration. This suggests that the enzyme released was not directly related to the amount of DOM substrate available but probably depended in a more complex manner on the lability of the substrate itself. AP was probably released by the phyto-picoplanktonic

community in particular by the divinylchlorophyll α containing *Prochlorococcus* as the positive trend (Fig. 4.25) suggests.

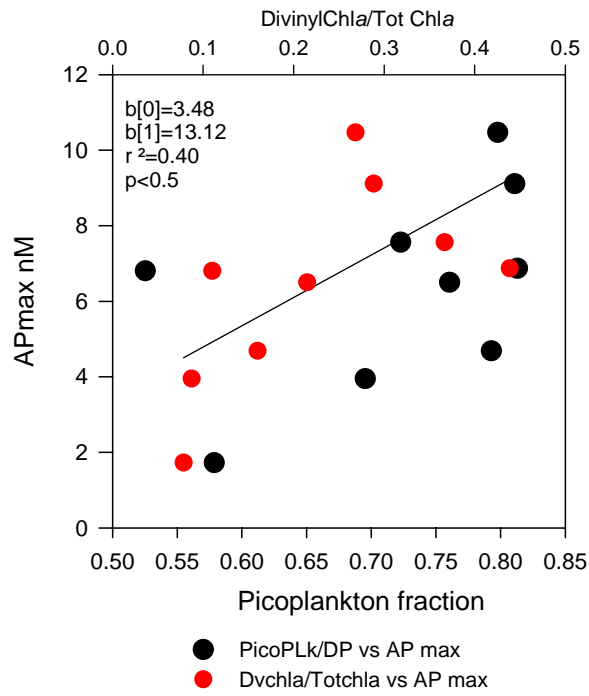


Fig. 4.25 Scatter plot of picoplankton fraction versus APmax. Regression line is reported although not statistically significant (regression coefficients: b_0 =intercept, b_1 =slope).

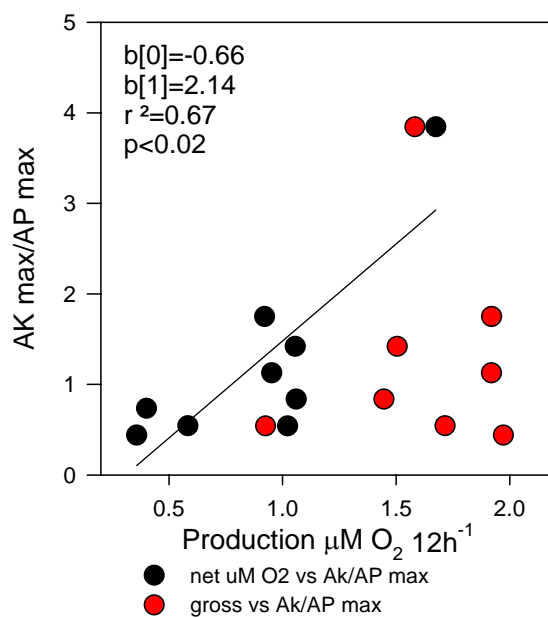


Fig. 4.26 Scatter plot of oxygen production (net and gross $\mu\text{M O}_2 12\text{h}^{-1}$) versus AMmax/APmax ratio and regression line of net oxygen production versus AMmax/APmax ratio (regression coefficients: b_0 =intercept, b_1 =slope).

To quantify TON versus TOP cycling and evaluate the nutrient limitation of the planktonic communities an analysis of ratios between AK and AP has been carried out. The use of AKA/APA ratio gives us an indication of AK and AP activity independently of the biomass present and allows me to omit the normalization of the enzyme activity to the biomass, which is a major problem due the complex nature of these exoenzymes which are released by both the bacterial and phytoplanktonic biomass.

The spatial distribution of AKA/APA ratio can be seen in Fig. 4.22a. The most interesting feature was the 2 peaks reached at 60°W and 30°W. These peaks correspond to stations where a strong depletion in ^{15}N of suspended material was found (Fig. 4.20). Similarly, the central area of the gyre where AKA/APA ratio overlapped with enriched $\delta^{15}\text{PON}$ signals (Fig. 4.20).

The spatial variation of the ratio AKmax/APmax is shown in Fig. 4.22c. The ratio AKmax/APmax shows a positive relationship with net primary production (Fig. 4.26) indicating that more AK enzymes are released with respect to AP when net primary production is high.

Total organic nutrients

The longitudinal surface TON and TOP distribution is shown in Fig. 4.27. The TON maximum ($\sim 9.5\mu\text{M}$, $\sim 60^\circ\text{W}$) corresponds to a peak in AKA/APA ratio as does the TON minimum ($\sim 32^\circ\text{W}$) indicating that at these two sites TON concentrations were controlled by different dynamics.

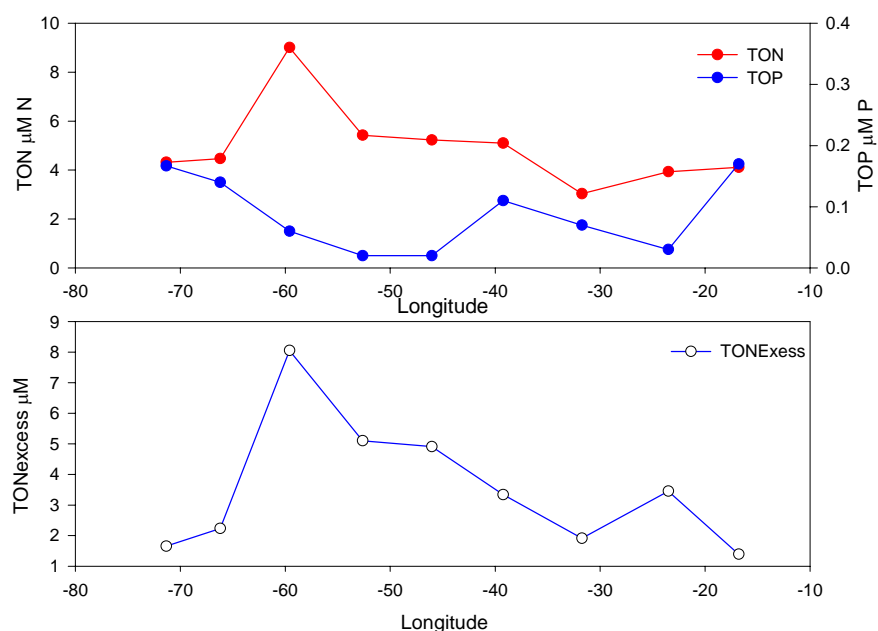


Fig. 4.27 Longitudinal surface distribution of TON and TOP (μM) (top) and TONex (μM) (bottom). Errors in these analyses are described in section 2.1.32.

TOP was higher at both ends of the transect and was generally low in the centre. TON and TOP concentrations were decoupled in the West suggesting a common factor which produces TON and selectively consumes TOP, as confirmed by high TONexcess in this area (Fig. 4.27).

4.4.3.1 Discussion

Spatial distribution of N_2 fixation

Interpretation of the isotopic signal

The nitrogen isotopic composition of marine plankton and suspended particulate material reflects both the original nutrient source and the isotopic fractionation that has occurred during its assimilation (Wu *et al.* 1997). This study aims to quantify the importance of the different sources of combined N that support biological production, thus it is necessary to assess the importance of fractionation, which occurs during biological processes, to correctly interpret the isotopic data.

The area sampled was a typical oligotrophic environment, where surface inorganic nutrients were completely exhausted; hence, fractionation due to preferential light nitrate uptake, can be excluded as a potential process responsible for the depleted PON isotopic signal observed (Wu *et al.* 1997). Other important biological processes leading to fractionation occur during secondary production along each step of the food chain. Secondary producers become enriched in ^{15}N ($\sim 3\text{\textperthousand}$) relative to their diet, excrete ^{15}N depleted ammonia and produce enriched ^{15}N faecal pellets, which sink out of the euphotic zone, leaving a ^{15}N depleted N reservoir in the upper ocean (Checkley and Miller 1989). Thus the inclusion of heterotrophs or faecal pellets in bulk measurement of $\delta^{15}\text{N}$ PON can bias the isotopic signal towards an enriched $\delta^{15}\text{N}$ signal of organic matter in the upper water column. As mentioned above, the variation of the isotopic signal of PON collected from Niskin bottles reflects predominantly algal biomass; while, the slightly positive trend ($r^2=0.4$, $n=8$), between $\delta^{15}\text{N}$ PON and PON/chlorophyll a ratio in the samples collected by carboys suggests the possible inclusion of higher trophic levels which can bias the isotopic signal.

To explain the depleted $\delta^{15}\text{N}$ observed in large portions of the subtropical gyre a light source of N is needed. This requirement is even more pronounced to explain the depletion of

PON of the biased samples. If this light source of N was recycled ammonia it would not be light enough to balance the enrichment of the higher trophic levels in the biased samples.

N_2 fixation seems to be the only possible mechanism for introducing significant quantities of depleted ^{15}N into the system. Also, geochemical evidence of N:P imbalances (Fig. 4.17) coupled with the presence of cyanobacteria biomarkers (Fig. 4.19) are independent evidence pointing towards a major role of N_2 fixation in providing ^{15}N depleted nitrogen thus ruling out recycled production as a dominant cause of low $\delta^{15}\text{N}$ of surface particles. Similar conclusions have been made by other authors (Mino *et al.* 2002, Montoya *et al.* 2002, Mahaffey *et al.* 2004, Capone *et al.* 2005).

Quantification of the relative importance of N_2 fixation

By analysing PON samples collected from Niskin bottles, in very low nutrient concentration systems, the assumption that isotope fractionation was a negligible process and that $\delta^{15}\text{N}$ PON reflects only the different sources of combined nitrogen, is reasonable. The contrast between the isotopic signal of deep water nitrate (4.5/5‰) and N_2 fixers biomass (-2/0‰) can be used to provide quantitative information on the relative contribution of these two different processes in sustaining phytoplankton biomass in the near surface waters. Here this contribution is estimated using a two end member isotope mixing model (Montoya *et al.* 2002). The end members chosen for the analysis were -2‰ to match the ^{15}N depleted diazotrophs and 4.5‰ for nitrate, the enriched isotope source (Fig. 4.28).

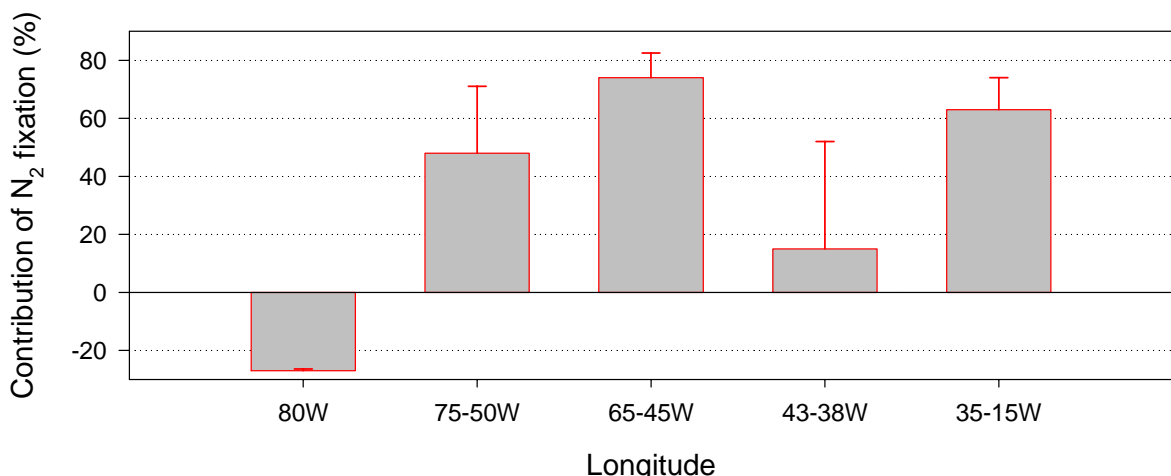


Fig. 4.28 Longitudinal variation of the importance of N_2 fixation as a source of new nitrogen across the subtropical gyre at 24°N. Calculations were made according to a two end member mixing model. The end members used were -2‰ for the depleted end member and 4.5‰ for the enriched end member.

At 80°W, close to the Bahamas shoreline, there is a very high enrichment of ^{15}N in PON; the unrealistic negative percentage of N_2 fixation contribution is due to the higher PON isotopic signal than the enriched isotopic end member (4.5%). If 6‰ is used as the isotopic enrichment of the end member than the contribution of N_2 fixation becomes $0.3\pm0.5\%$, indicating that upwelled nitrate is the major source of N in this area.

Away from the western coast, the contribution of N_2 fixation becomes significant where it can supply on average $74\pm8\%$ and up to 85% of the new N used in plankton production.

In the centre of the gyre N_2 fixation is possibly less important ($15\pm37\%$). One limitation of this two end member mixing model is that it is strongly dependent on the values of the 2 end members chosen. Although, it is generally assumed that the only significant source of enriched N is deep nitrate, there is recent evidence that also DON carries an enriched $\delta^{15}\text{N}$ (~4.1‰; Benner *et al.* 1997; Knapp *et al.* 2005), signal, which needs to be considered when interpreting isotopic data. In this area, nitrate concentrations were very low thus, it is possible that other sources of potentially enriched N, such as DON, were sustaining phytoplankton biomass.

On the eastern side of the mid-Atlantic ridge N_2 fixation contributed less to the signal than on the west side but still represented a substantial source of N for this area ($62\pm11\%$).

These estimates are higher than, but consistent with, similar analyses carried out by several authors who estimate that N_2 fixation could supply 13 to 68% of N to the oligotrophic North Atlantic Ocean (Mino *et al.* 2002, Montoya *et al.* 2002, Mahaffey *et al.* 2003, Capone *et al.* 2005). The high contribution of N_2 fixation estimated in this study, may have been favoured by the stratification of the water column and dust input which is at its highest at this time of the year (Goudie 1983). It must be stated that, the observations made by Mahaffey *et al.* (2003) and Mino *et al.* (2002) were made along a latitudinal transect across the Eastern Atlantic, hence only few data points match the analysis presented here. Similarly the studies carried out by Capone *et al.* (2005) and Montoya *et al.* (2002) are mostly concentrated on the western tropical North Atlantic.

This data, collected during spring, shows for the first time in the subtropical gyre (North of 15°N) at 24.5°N, only a light west to east trend in the magnitude of N_2 fixation but instead a gap of N_2 fixation in an area coinciding with the mid-Atlantic ridge.

A gap in the contribution of N_2 fixation matches the observations made in autumn further south (10°N) by Mills *et al.* (2004). The lack of N_2 fixation centred broadly on the mid-Atlantic ridge might be the cause of the observed discrepancies in West to East trends of N_2 fixation. Some authors report higher N_2 fixation rates in the West (Montoya *et al.* 2002;

Capone *et al.* 2005) likely due to the fact that the easternmost station during their surveys were centred in this area where no N_2 fixation is observed. Similarly, other authors (Mills *et al.* 2004) report higher N_2 fixation rates in the eastern North Atlantic as their westernmost station lay in this region. Thus the hypothesis of seasonal variability being responsible for a zonal N_2 fixation pattern can be excluded although it is likely that the central region where N_2 fixation rates are found to be low can become larger or smaller following a seasonal pattern.

The observation of a low contribution of N_2 fixation in the central region of the North Atlantic stimulates the question why is N_2 fixation limited in this region and not elsewhere?

Mills *et al.* (2004) measured N_2 fixation rates and carried out nutrient limitation assays to determine which nutrient was limiting production and diazotroph activity at 3 stations, (35°W, 24°W, 18°W) the westernmost of which coincides with the “ N_2 fixation gap” observed in this study. They concluded that N was the proximate limiting nutrient in all the stations and that N_2 fixation was co-limited by P and Fe especially at the western most station at 35°W.

As discussed shortly, the limitation of phosphate was probably mitigated by diazotrophs through the utilization of TOP. Thus a more likely process to limit N_2 fixation is iron availability.

Although this region is subject to high mineral dust deposition (Gao *et al.* 2001), it has been shown that the Saharan dust has a very low solubility (Baker and Linge 2005; Mline *et al.* 2005). Thus, the bioavailable Fe fraction (iron hydroxy species) cannot always meet the Fe demand of N fixers (Voss *et al.* 2004). Most of the Fe in sea water exists in the particulate form because of the low solubility of Fe(III) under oxidising conditions above pH4 (Jickells *et al.* 2005), this form is unavailable for biological uptake and has short residence times due to particle scavenging processes (Croot *et al.* 2004). The soluble bioavailable fraction of iron (Jickells *et al.* 2005) is mainly bound to organic complexes which, depending on their chemical nature, may increase the bioavailability of iron to phytoplankton.

In the western North Atlantic, it has been reported that *Trichodesmium* *sp.* have an increased affinity for siderophore-bound Fe(III) (Achilles *et al.* 2003). Siderophores, high affinity Fe(III) chelating ligands, which have been found to be synthesised by cyanobacteria and heterotrophic bacteria (Wilhelm and Trick 1994; Venter *et al.* 2004) and some *Synechococcus* strains (Trick and Wilhelm 1995), to scavenge Fe during periods of Fe limitation. It is possible that, the presence of a picoplankton community, dominated by cyanobacteria, in the western side of the North Atlantic may have contributed in alleviating the iron stress present in the surface waters by the release of the siderophores.

In the Eastern North Atlantic the high N₂ fixation can possibly be maintained by the supply of high levels of dust which might relieve Fe limitation of diazotrophy (Mills *et al.* 2004).

Therefore it is likely that, the gradient observed in the pattern of N₂ fixation is controlled by the scarce bioavailability of iron, which is mitigated in the West, by the release of Fe-binding organic ligands in the surface water (Wu 2003) by cyanobacteria and in the East, by the very high dust deposition rates. In the centre however, neither of these two processes are likely to occur resulting in the limited importance of N₂ fixation.

Moreover, it cannot be ruled out that the sources of iron from west to east change and thus might their bioavailability. A general concept is that Saharan dust provides the majority of the iron in the North Atlantic and that iron in this material has a very low solubility (Baker and Linge 2005; Mline *et al.* 2005). However, there is increasing evidence that Fe can be provided by Amazon river plume transported northwards by the North Brazil Current and that this can spread its biogeochemical signatures towards the Caribbean (Voss *et al.* 2004; Cunha *et al.* 2005) and the western subtropical gyre.

TON and TOP bioavailability and turnover rates

The detection of AK and AP activity across the gyre implies that surface DON and DOP are dynamic pools. The variability of TON and TOP distributions, the enzymes released in the environment and their activities suggest that these two pools cycle in a decoupled manner. The importance of the ectoenzymes is determined by two factors, 1) the amount of enzymes released in the environment and 2) their activity.

AK and AP have a complex origin as they are released by both autotrophic and heterotrophic organisms and their activity will depend on the trophic state of the system. In this study, their release is mainly controlled by autotrophic biomass (Fig. 4.23; Fig. 4.25) although the contribution of heterotrophs cannot be excluded. AK is not correlated with any specific phytoplankton group whilst AP is strongly linked to the presence of the divinylchlorophyll *a* biomarker of *Prochlorococcus* *sp.* suggesting that this species is mostly responsible for the release of AP. The fact that AK is not correlated with any specific group is not surprising as this enzyme is known to be released by many groups of phytoplankton (Hoppe 2003) thus, it is likely that the intense phosphate limitation has stimulated AK production by many organisms. Similarly, the shortage of nitrate in the surface waters stimulated the utilization of the DON pool, which is an important N reservoir exploitable only by specialised species thus it is plausible that the AP signal was controlled mainly by *Prochlorococcus* *sp.*

The above observations provide evidence that AK and AP have been released in large part also by autotrophic organisms indicating that the utilization of DON and DOP may have partly fuelled primary production.

The fraction of primary production potentially supported by organic nutrients is assessed by relating the oxygen production, scaled by N and P using the Redfield ratio, to the N and P cleaved by AK and AP. These calculations suggest that AP and AK could supply, on average, 1.2 ± 0.43 times the N requirement and 23 ± 16 times the P demand of the observed gross oxygen production. This estimates represent upper limits as it is assumed that AK and AP are only released by algal biomass and that no bacterial production is sustained. The large discrepancy between the potential supply of N and P can also be explained by the fact that N can be preferentially supplied in the North Atlantic by N_2 fixation and atmospheric deposition. Thus, the importance of DON as a N source is limited compared to the role of DOP given the difficulty in providing P from mechanisms analogous to N_2 fixation.

An upper limit of the turnover rate of TON and TOP can be calculated by assuming that AK and AP activities were constant over a day and that all the TON and TOP pools were available for hydrolysis. On average TON turned over in 13 ± 11 days while the TOP pool was turned over at a much faster rate of 5 ± 4 hours consistent with the P deficiency described in the next section. Although these rates represent maximum rates, they give indication that the DON and DOP pools are very active and contribute significantly to the turnover and transport of N and P through the food web.

N versus P limitation

In the North Atlantic there is a longstanding uncertainty as to whether N or P limit phytoplankton productivity. Although recent evidence suggests that primary productivity in the Tropical North Atlantic is N-limited due to limited diazotrophy (Mills *et al.* 2004), it is argued that N_2 fixation has the potential to mitigate N deficiency introducing new N into the system but that this process is in turn limited by P bioavailability.

In the past, AK and/or AP assays has been used in many environments as an indicator of phosphate or nitrate deficiency as AK and AP are inhibited by the presence of phosphate and nitrate respectively (Martinez and Azam 1993; Sala *et al.* 2001; Hoppe 2003). Here, the contemporaneous determination of these two ectoenzymes and their ratio, has allowed to asses the nutrient imbalance of the system. It has been previously reported that the ratio AKA/APA reflects nitrate versus phosphate deficiency in experimentally induced nutrient limitation conditions (Sala *et al.* 2001).

If the AKA/APA=1 is taken as the reference value of equal N to P deficiency (AK/AP close to 2 has been observed in the extremely P poor Mediterranean Sea; Sala *et al.* 2001) then, the North Atlantic subtropical gyre appears nearly everywhere phosphate deficient except at the very centre of the gyre, from about 53 to 40°W, where AP appears to be more active suggesting a stronger nitrate limitation (Fig. 4.22). This region, where nitrate deficiency seems to be occurring, coincides with the area where a N₂ fixation gap was observed indicated by the isotopic enrichment of PON (Fig. 4.20). Similarly, where the phosphate deficiency seems to be at its maximum (AKA/APA peaks, Fig. 4.22a) isotopic data indicate that, N₂ fixation appears to be a major source of new nitrogen.

These data imply that, where the contribution of N₂ fixation is low surface waters seem to be nitrate limited. When N₂ fixation is a major process occurring in the surface waters, the system is pushed towards phosphorus deficiency indicated by the large AKA compared to APA.

The potential of phosphorus to be a limiting nutrient in the Atlantic Ocean is consistent with previous studies (Wu *et al.* 2000; Cavender-Bares *et al.* 2001) and fits well with the anomalies of N:P ratios in the inorganic and the organic N and P pools observed in this study. However, from this data for the first time in the North Atlantic there is direct evidence that N₂ fixation is pushing the system into P limitation; similar conclusions were suggested by Karl *et al.* (2001) in the North Pacific. These authors hypothesised that climate conditions of the last decades have favoured a phytoplankton community shift towards N₂ fixing organisms in the North Pacific leading to phosphorus deficiency in this environment.

The pattern in the AK/AP ratio (Fig. 4.23), interpreted here as an indication of N versus P limitation, fits well with the trend in N₂ fixation as inferred from PON ¹⁵N depletion (Fig. 4.20) and also explains the surface distribution of TON, TOP and TNxs (Fig. 4.27).

In the west (60°W), the relative maximum of the AKA/APA coincides not only with isotopic depleted PON but also with a TON peak. This implies that N₂ fixers were utilising TOP by releasing AK and were releasing TON which resulted in the high TONxs values. This conclusion is also supported by high phytoplankton biomass and pigment data which suggest the presence of cyanobacteria

Interestingly at 30°W, where a second AK/AP peak was observed, although a light ¹⁵N PON was measured, no TON accumulation occurred. A key difference from the observations at 60°W is the picoplankton community structure. At 30°W it is likely that the phytoplankton community dominated by *Prochlorococcus* *sp.* was preventing the build up of TON through its utilization, a suggestion supported by the increase of AP activities towards east.

The consistency between AK/AP and the isotopically depleted PON signals are a clear indication of the DOP utilization by diazotrophs. Results from culture studies (Mulholland *et al.* 2002) and natural populations have already demonstrated that the most important N₂ fixer known in the oceans, *Trichodesmium*, is capable of hydrolysing DOP by the release of alkaline phosphatases and growing on DOP as its sole source of P.

Based on literature values of *Trichodesmium* cellular P content (1.1nM P colony⁻¹, Sanudo-Wilhelmy *et al.* 2001), and number of colonies per litre (Mulholland *et al.* 2002) I estimated whether DOP turnover could meet the *Trichodesmium* P demand. Considering *Trichodesmium* doubling time to be in the range of 2 to 5 days (Mulholland *et al.* 2002) the lower limit of the AK activities measured could supply from 57% to 95% of the P required for its growth.

The results presented here have important implications for our understanding of the controls on biological production and N₂ fixation in the North Atlantic. The nutrient imbalances as inferred from enzyme assays indicate that the biological community of the surface subtropical North Atlantic at 24.5°N was mostly phosphate limited. In addition, contrary to recent suggestions (Mills *et al.* 2004; Sanudo-Wilhelmy *et al.* 2001), these data imply that although phosphate was deficient in surface waters N₂ fixation was not P limited as diazotrophs mitigated the P deficiency through the utilization of TOP. Instead I speculate that, N₂ fixation was limited in a limited region of the central North Atlantic Subtropical gyre by the bioavailability of Fe.

4.4.3.2 Conclusions

The data presented here do not support a zonal trend in the magnitude of N₂ fixation instead they suggest a gap in N₂ fixation in the centre of the gyre. This gap has already been observed by others (Voss *et al.* 2004) and can explain the contrasting West to East trends observed by other authors. N₂ fixers seem to compensate for the P deficiency by the utilization of TOP, thus it is speculated that a limited bioavailability of iron in the central region is driving the observed spatial distribution of N₂ fixation.

The input of new N by N₂ fixation leads the system towards phosphate deficiency in some areas of the North Atlantic subtropical gyre. In the centre of the gyre, where N₂ fixation is a minor source of N, the system appears to be nitrate limited.

TON and TOP represent not only the major components of the N and P pools in the surface waters but were also bioavailable to the community through the release of extracellular enzymes. TON and TOP bioavailability compensated for the deficiency of inorganic nutrients. This finding has important implications for the understanding of nutrient deficiencies and

sheds new light on concepts of nutrient limitation of biological productivity in ultra-oligotrophic gyres.

4.5 Final Conclusions

In the permanently stratified North Atlantic subtropical gyre, nutrient supply for the growth of phytoplankton and the maintenance of the observed export production has been a major problem. Here the significance of two mechanisms, N_2 fixation and the uptake of organic nutrients, have been investigated by analyzing data collected along a zonal transect which crossed the subtropical North Atlantic gyre at 24.5°N.

Large scale N to P anomalies suggests that the surface subtropical North Atlantic is a net source of nitrogen to the system and that P may be the limiting nutrient. The computation of a new geochemical tracer, TNxs, allowed an estimate of N_2 fixation rates which are higher than previously thought.

Contrary to recent suggestions (Capone *et al.* 2005; Mills *et al.* 2004) the spatial distribution of N_2 fixation at 24.5°N does not show a zonal gradient but instead reveals a gap in N_2 fixation in the centre of the basin as reported by Voss *et al.* (2004). From the isotopic data it is estimated that up to 68% of phytoplankton N requirements can be provided by N_2 fixation in certain regions.

Dissolved organic nutrients are active components of the nutrient pool and are bioavailable to the biological community through the release of exoenzymes. TON and TOP cycling are decoupled with higher TOP relative to TON turnover rates. TON and TOP can potentially contribute significantly to primary production and TOP appears to be of major importance in mitigating phosphate limitation of diazotrophs.

Finally, in the permanently stratified North Atlantic subtropical gyre N_2 fixation and the bioavailability of organic N and P appear to be major mechanisms for supplying nutrients and sustaining phytoplankton growth.

5 Conclusions

The oceans constitute the largest pool of carbon on the planet and are implicated in the long-term regulation of atmospheric CO₂ through the biological pump. The strength of the biological carbon pump and ultimately the impact of ocean biology on atmospheric CO₂ are strongly controlled by the bioavailability of nutrients. Hence quantifying the processes that control the fluxes of N and P into the oceans and how these nutrients are supplied to surface waters to sustain the growth of phytoplankton is a fundamental step towards understanding the rate at which the ocean takes up CO₂. Although subtropical gyres constitute a major fraction of the global ocean, a quantitative understanding of the mechanisms that control nutrient fluxes into these areas remains elusive. In these areas dissolved organic nutrients constitute the largest fraction of the nutrient pool in the sunlit ocean. It has long been suggested that this pool might significantly contribute to the sustainment of biological production into these ocean deserts. However, the role of organic nutrients in nutrient cycling has not been fully assessed due to the limited basin scale datasets available, as well as the large uncertainties regarding the bioavailability of these pools.

This thesis contributed to the observational database in order to address fundamental questions as to how dissolved organic nutrients influence N and P budgets, how they affect nutrient cycling and the maintenance of biological production within two major ocean oligotrophic gyres: the Southern Indian Ocean gyre and the subtropical North Atlantic gyre.

These two gyres differ greatly from each other. The Indian Ocean is a site where denitrification is suspected to overwhelm N₂ fixation, leading the system into N deficiency and possibly driving the N budget out of balance with a net N loss. Conversely, the North Atlantic subtropical gyre is thought to be a major contributor to global oceanic N₂ fixation, enhanced by elevated iron deposition.

In the Indian Ocean, nitrate is limiting with respect to phytoplankton nutrient requirements and TON may represent an important source of N, indicating that this pool is actively responding to environmental nutrient imbalances.

Contrary to recent suggestions, despite denitrification exceeding N₂ fixation, the Indian Ocean does not appear to be losing N (Codispoti *et al.* 2001) instead, the N budget is balanced by a combination of riverine and atmospheric inputs and an excess of N flowing into the basin. The role of organic N delivered by the ITF appears to be crucial in the regional N balance. Overall the basin is a sink for N but its budget is balanced leading to reduced N/P ratios of the total N and P pools.

In the North Atlantic subtropical gyre, the computation of a new geochemical tracer, TN_{xs}, suggests that N₂ fixation is more important than previously thought.

This study does not support to the hypothesis of a latitudinal gradient in diazotrophy in the North Atlantic subtropical gyre, but instead suggests that the N₂ fixation signal is important across most of the basin with the exception of the coastal margins and a central region. Moreover, contrary to recent findings (Mills et al. 2004, Dyhrman et al. 2002, Sanudo-Wilhelmy et al. 2001) these data suggest that N₂ fixation is not phosphate limited as diazotrophs may alleviate their P deficiency through the utilization of TOP which appears to be an extremely dynamic pool. The utilization of DOP as a source of P by diazotrophs has already been observed in the Western North Atlantic (Mulholland et al. 2002). Instead, other limiting factors, such as the bioavailability of iron are suspected to be involved in controlling the spatial distribution of diazotrophs.

Furthermore, despite recent findings suggesting that biological communities are N limited in the Tropical Atlantic (Mills et al. 2004), the data presented here suggests that the system was pushed towards phosphate deficiency by N₂ fixation.

In this basin organic nutrients appear to be active components of the N and P pools and have a large potential role in sustaining primary production by providing nitrogen and phosphorus for phytoplankton growth. The relative bioavailability of dissolved organic nutrients to phytoplankton communities sheds new light on our understanding of marine primary production and thus argues for a revision of the concept of inorganic nutrient regulation of phytoplankton productivity. Hence, for a comprehensive understanding of nutrient cycling and its effect biological productivity the inclusion of this component in future studies is required.

Given the results obtained from the Indian Ocean where the loss of nitrogen was compensated for by the influx of TON from the ITF, it is possible to speculate regarding the potential for TON to close the N budget of the North Atlantic subtropical gyre. Several authors have diagnosed an overall loss of nitrate over the subtropical North Atlantic (Rintoul and Wunsch 1991; Ganachaud and Wunsch 2002) which would require, for a steady state to be maintained, an additional nitrogen source. Rintoul and Wunsch (1991) proposed that the additional N comes from the additional influx of TON at 36°N but had no data to support this hypothesis. But might there be a northwards TON flow at 24°N which could contribute to the closure of the N budget over the North Atlantic subtropical gyre?

TON concentrations are highest in surface waters and increase towards the tropics while nitrate concentrations follow the opposite trend with high concentrations in deep waters

and at high latitudes. Thus, the importance of the TON flux, due to both the overturning and the gyre scale circulations will decrease moving away from the tropics and with depth. Hence, if in the Indian Ocean at 32°S the net contribution of TON was 40% of the total N transport, in the North Atlantic, at a nominal latitude of 24.5°N, the contribution of the TON flux to the TN flux is expected to be higher. It is thus possible that the zero nitrate flux at 24.5° diagnosed by Rintoul and Wunsch (1991) may be accompanied by a northward flux of DON which is larger than the northward flux of TON at 36°N. Hence these extrapolations, although not quantitative, give some indication that a northward TON flux at 24.5°N might be important to compensate for the nitrate loss over the North Atlantic gyre.

The observed biogeochemical differences (enhanced levels of N_2 fixation in the North Atlantic and excess of denitrification in the Indian Ocean) of the two gyres analysed are reflected not only in the N:P ratios of the nutrient pools but also in the organic nutrient vertical profiles. Phosphorus deficiency in the Subtropical North Atlantic is suggested also by low TOP concentrations through out the water column ($\sim 0.01\text{--}0.4\mu\text{M}$) as compared to the ones found in the Indian Ocean gyre ($\sim 0.4\text{--}0.1\mu\text{M}$). The vertical distribution of TON in the two different gyres appears to be controlled by more complex processes. In the North Atlantic gyre surface TON concentrations are higher ($\sim 5\mu\text{M}$) than the ones observed in the Indian Ocean ($\sim 4\mu\text{M}$). This picture is reversed at depth where the refractory TON pool of the Indian Ocean appears to larger ($>2\mu\text{M}$) than the one observed in the North Atlantic ($<2\mu\text{M}$). This peculiar vertical distribution of TON can be explained by the different “ecological” requirements of these regions. In the surface North Atlantic the “storage” of N in the organic pool can be a mechanism to continue promoting N_2 fixing (otherwise nitrate concentrations would inhibit nitrogenase activity) and explain the apparent paradox of high N_2 fixation rates in a non N limiting environment. At depth, the “storage” of N in the organic pool in the Indian Ocean can be of importance in mitigating the loss of fixed N through denitrification.

Despite the biogeochemical differences of the two oceanic gyres analysed, dissolved organic nutrients appeared to be dynamic pools that cycle in a decoupled manner driven by the different nutrient requirements of the two basins, meaning that they are active in supporting biological communities.

I now combine the results from chapters 3 and 4 to address the current controversy of whether the ocean is losing nitrogen due to an excess of denitrification over nitrogen fixation

(Codispoti *et al.* 2001). The question I address is whether my re-evaluation of the Indian ocean N budget (which argues that TON fluxing from the Pacific to the Indian Ocean partially compensates for the current excess of denitrification over nitrogen fixation) and my revaluation of the magnitude of N_2 fixation in the North Atlantic can be combined to balance the global oceanic N budget derived by Codispoti *et al.* (2001) which has a deficit of about 150 Tg N yr^{-1} . Current estimates of global pelagic N_2 fixation oscillate from 100 to 200 Tg Ny $^{-1}$ (Karl *et al.* 2002) and denitrification oscillates from 350-450 Tg Ny $^{-1}$ (Gruber 2004).

To balance the observed global excess of denitrification (Codispoti *et al.* 2001) N_2 fixation estimates have to be increased (Codispoti *et al.* 2001). In the North Atlantic Chapter 4 suggests that N_2 fixation is twice as important as previously thought based on a new geochemical tracer, TNxs, which takes into account the contribution of the excess organic pool in the surface of the ocean primarily caused by N_2 fixation. If extrapolated globally this would lead to a new global N_2 fixation estimate of 440 Tg Ny $^{-1}$ which would decrease the imbalance hypothesized in the present-day marine N budget to 50 Tg Ny $^{-1}$ (considering the upper range of the present day N_2 fixation and denitrification rates). This latter term could in turn be balanced by the unaccounted large source of anthropogenic atmospheric DON ranging from 28-84 Tg Ny $^{-1}$ as suggested by Cornell *et al.* (1995). Hence the hypothesized enhancement of denitrification as a consequence of the massive alteration of the global N cycle by humans (Codispoti *et al.* 2001) may be balanced by marine N_2 fixation and the global oceanic N cycle may be in balance although more accurate estimates of all terms need to be made.

6. References

Abell, J., A. Devol and S. Emerson (1999). "Isotopic composition of dissolved organic nitrogen in the subtropical North Pacific." *Abstracts of Papers of the American Chemical Society* 218: 22-GEOC.

Abell, J., S. Emerson and P. Renaud (2000). "Distributions of TOP, TON and TOC in the North Pacific subtropical gyre: Implications for nutrient supply in the surface ocean and remineralization in the upper thermocline." *Journal of Marine Research* 58(2): 203-222.

Achilles, K. M., T. M. Church, S. W. Wilhelm, G. W. Luther and D. A. Hutchins (2003). "Bioavailability of iron to *Trichodesmium* colonies in the western subtropical Atlantic Ocean." *Limnology And Oceanography* 48(6): 2250-2255.

Altabet, M. A. (1988). "Natural $^{15}\text{N}/^{14}\text{N}$ Ratios as a Tool for Studying the Nitrogen- Cycle of the Upper Ocean." *Abstracts of Papers of the American Chemical Society* 195: 86-GEOC.

Altabet, M. A. (1988). "Variations in Nitrogen Isotopic Composition between Sinking and Suspended Particles - Implications for Nitrogen Cycling and Particle Transformation in the Open Ocean." *Deep-Sea Research Part a-Oceanographic Research Papers* 35(4): 535-554.

Altabet, M. A., R. Francois, D. W. Murray and W. L. Prell (1995). "Climate-Related Variations in Denitrification in the Arabian Sea from Sediment $^{15}\text{N}/^{14}\text{N}$ Ratios." *Nature* 373(6514): 506-509.

Altabet, M. A., M. J. Higginson and D. W. Murray (2002). "The effect of millennial-scale changes in Arabian Sea denitrification on atmospheric CO₂." *Nature* 415(6868): 159-162.

Altabet, M. A., C. Pilskaln, R. Thunell, C. Pride, D. Sigman, F. Chavez and R. Francois (1999). "The nitrogen isotope biogeochemistry of sinking particles from the margin of the Eastern North Pacific." *Deep-Sea Research Part I-Oceanographic Research Papers* 46(4): 655-679.

Aluwihare, L. I., D. J. Repeta and R. F. Chen (1997). "A major biopolymeric component to dissolved organic carbon in surface sea water." *Nature* 387(6629): 166-169.

Alvarez-Salgado, X. A. and A. E. J. Miller (1998). "Simultaneous determination of dissolved organic carbon and total dissolved nitrogen in seawater by high temperature catalytic oxidation: conditions for precise shipboard measurements." *Marine Chemistry* 62(3-4): 325-333.

Alvarez, M., H. L. Bryden, F. F. Perez, A. F. Rios and G. Roson (2002). "Physical and biogeochemical fluxes and net budgets in the subpolar and temperate North Atlantic." *Journal of Marine Research* 60(2): 191-226.

Amon, R. M. W. and R. Benner (1994). "Rapid-Cycling of High-Molecular-Weight Dissolved Organic-Matter in the Ocean." *Nature* 369(6481): 549-552.

Anderson, L. A. and J. L. Sarmiento (1994). "Redfield Ratios Of Remineralization Determined By Nutrient Data-Analysis." *Global Biogeochemical Cycles* 8(1): 65-80.

Anderson, T. R. (1992). "Modeling the Influence of Food C/N Ratio, and Respiration on Growth and Nitrogen-Excretion in Marine Zooplankton and Bacteria." *Journal of Plankton Research* 14(12): 1645-1671.

Anderson, T. R. and P. Pondaven (2003). "Non-redfield carbon and nitrogen cycling in the Sargasso Sea: pelagic imbalances and export flux." *Deep-Sea Research Part I-Oceanographic Research Papers* 50(5): 573-591.

Antia, N. J., P. J. Harrison and L. Oliveira (1991). "The Role of Dissolved Organic Nitrogen in Phytoplankton Nutrition, Cell Biology and Ecology." *Phycologia* 30(1): 1-89.

Armstrong, F. A. J. and P. M. S. Williams, J.D.H. (1966). "Photooxidation of organic matter in sea water by ultraviolet radiation, analytical and other applications." *nature* 211: 481-483.

Arrigo, K. R. (2005). "Marine Microorganisms and global nutrient cycles." *Nature* 437: doi:10.1038/nature04158.

Azam, F., T. Fenchel, J. G. Field, J. S. Gray, L. A. Meyerreil and F. Thingstad (1983). "The Ecological Role of Water-Column Microbes in the Sea." *Marine Ecology-Progress Series* 10(3): 257-263.

Baker, A. R., S. D. Kelly, K. F. Biswas, M. Witt and T. D. Jickells (2003). "Atmospheric deposition of nutrients to the Atlantic Ocean." *Geophysical Research Letters* 30(24,2296, doi:10.1029/2003GL018518).

Baker, A. R. and K. L. Linge (2005). *The solubility of aerosol iron and phosphorus across the tropical Atlantic*. ASLO meeting, Santiago de Compostela, Spain.

Bange, H. W., T. Rixen, A. M. Johansen, R. L. Siefert, R. Ramesh, V. Ittekkot, M. R. Hoffmann and M. O. Andreae (2000). "A revised nitrogen budget for the Arabian Sea." *Global Biogeochemical Cycles* 14(4): 1283-1297.

Bange, H. W., S. Wajih, A. Naqvi and L. A. Codispoti (2005). "The nitrogen cycle in the Arabian Sea." *Progress In Oceanography* 65(2-4): 145-158.

Barbeau, K., E. L. rue, K. W. Bruland and A. Butler (2001). "Photochemical cycling of iron in the surface ocean mediated by microbial iron(III)-binding ligands." *Nature* 413: 409-413.

Barlow, R. G., J. Aiken, G. F. Moore, P. M. Holligan and S. Lavender (2004). "Pigment adaptations in surface phytoplankton along the eastern boundary of the Atlantic Ocean." *Marine Ecology-Progress Series* 281: 13-26.

Barlow, R. G., D. G. Cummings and S. W. Gibb (1997). "Improved resolution of mono- and divinyl chlorophylls a and b and zeaxanthin and lutein in phytoplankton extracts using reverse phase C-8 HPLC." *Marine Ecology-Progress Series* 161: 303-307.

Bates, N. R. (2001). "Interannual variability of oceanic CO₂ and biogeochemical properties in the Western North Atlantic subtropical gyre." *Deep-Sea Research Part II-Topical Studies in Oceanography* 48(8-9): 1507-1528.

Bates, N. R. and D. A. Hansell (2004). "Temporal variability of excess nitrate in the subtropical mode water of the North Atlantic Ocean." *Marine Chemistry* 84(3-4): 225-241.

Bates, N. R., A. F. Michaels and A. H. Knap (1996). "Seasonal and interannual variability of oceanic carbon dioxide species at the US JGOFS Bermuda Atlantic time-series study (BATS) site (vol 43, pg 347, 1996)." *Deep-Sea Research Part II-Topical Studies In Oceanography* 43(4-6): 1435-1435.

Bauer, J. E., C. E. Reimers, E. R. M. Druffel and P. M. Williams (1995). "Isotopic Constraints on Carbon Exchange between Deep-Ocean Sediments and Sea-Water." *Nature* 373(6516): 686-689.

Benitez-Nelson, C. R. (2000). "The biogeochemical cycling of phosphorus in marine systems." *Earth-Science Reviews* 51(1-4): 109-135.

Benner, R. and B. Biddanda (1998). "Photochemical transformations of surface and deep marine dissolved organic matter: Effects on bacterial growth." *Limnology and Oceanography* 43(6): 1373-1378.

Benner, R., B. Biddanda, B. Black and M. McCarthy (1997). "Abundance, size distribution, and stable carbon and nitrogen isotopic compositions of marine organic matter isolated by tangential-flow ultrafiltration." *Marine Chemistry* 57(3-4): 243-263.

Benner, R. and J. D. Pakulski (1994). "Abundance and Distribution of Carbohydrates in the Ocean." *Abstracts of Papers of the American Chemical Society* 207: 99-GEOC.

Benner, R., J. D. Pakulski, M. McCarthy, J. I. Hedges and P. G. Hatcher (1992). "Bulk Chemical Characteristics of Dissolved Organic-Matter in the Ocean." *Science* 255(5051): 1561-1564.

Bergman, B. (2001). "Nitrogen-fixing cyanobacteria in tropical oceans, with emphasis on the Western Indian Ocean." *South African Journal Of Botany* 67(3): 426-432.

Berman-Frank, I., J. T. Cullen, Y. Shaked, R. M. Sherrell and P. G. Falkowski (2001). "Iron availability, cellular iron quotas, and nitrogen fixation in *Trichodesmium*." *Limnology And Oceanography* 46(6): 1249-1260.

Biersmith, A. and R. Benner (1998). "Carbohydrates in phytoplankton and freshly produced dissolved organic matter." *Marine Chemistry* 63(1-2): 131-144.

Bjornsen, P. K. (1988). "Phytoplankton Exudation of Organic-Matter - Why Do Healthy Cells Do It." *Limnology and Oceanography* 33(1): 151-154.

Brandes, J. A. and A. H. Devol (2002). "A global marine-fixed nitrogen isotopic budget: Implications for Holocene nitrogen cycling." *Global Biogeochemical Cycles* 16(4): art. no.-1120.

Brandes, J. A., A. H. Devol, T. Yoshinari, D. A. Jayakumar and S. W. A. Naqvi (1998). "Isotopic composition of nitrate in the central Arabian Sea and eastern tropical North Pacific: A tracer for mixing and nitrogen cycles." *Limnology And Oceanography* 43(7): 1680-1689.

Broecker, S. W. and T.-H. Peng (1982). "Tracers in the sea." *Columbia University, Palasades*. N.Y.

Bronk, D. A. and P. M. Glibert (1993). "Application of a N-15 Tracer Method to the Study of Dissolved Organic Nitrogen Uptake During Spring and Summer in Chesapeake Bay." *Marine Biology* 115(3): 501-508.

Bronk, D. A., P. M. Glibert, T. C. Malone, S. Banahan and E. Sahlsten (1998). "Inorganic and organic nitrogen cycling in Chesapeake Bay: autotrophic versus heterotrophic processes and relationships to carbon flux." *Aquatic Microbial Ecology* 15(2): 177-189.

Bronk, D. A., P. M. Glibert and B. B. Ward (1994). "Nitrogen Uptake, Dissolved Organic Nitrogen Release, and New Production." *Science* 265(5180): 1843-1846.

Bronk, D. A., M. W. Lomas, P. M. Glibert, K. J. Schukert and M. P. Sanderson (2000). "Total dissolved nitrogen analysis: comparisons between the persulfate, UV and high temperature oxidation methods." *Marine Chemistry* 69(1-2): 163-178.

Bryden, H. L., M. J. Griffiths, A. M. Lavin, R. C. Millard, G. Parrilla and W. M. Smethie (1996). "Decadal changes in water mass characteristics at 24 degrees N in the subtropical North Atlantic ocean." *Journal Of Climate* 9(12): 3162-3186.

Butler, E. I., S. Knox and M. I. Liddicoat (1979). "The relationship between inorganic and organic nutrients in seawater." *Jurnal of The Marine Biological Association, UK* 59: 239-250.

Capone, D. G., J. A. Burns, J. P. Montoya, A. Subramaniam, C. Mahaffey, T. Gunderson, A. F. Michaels and E. J. Carpenter (2005). "Nitrogen fixation by *Trichodesmium* spp.: An important source of new nitrogen to the tropical and subtropical North Atlantic Ocean." *Global Biogeochemical Cycles* 19(2): art. no.-GB2024.

Capone, D. G. and E. J. Carpenter (1982). "Nitrogen-Fixation In The Marine-Environment." *Science* 217(4565): 1140-1142.

Capone, D. G., M. D. Ferrier and E. J. Carpenter (1994). "Amino-Acid Cycling in Colonies of the Planktonic Marine Cyanobacterium *Trichodesmium-Thiebautii*." *Applied and Environmental Microbiology* 60(11): 3989-3995.

Capone, D. G., J. P. Zehr, H. W. Paerl, B. Bergman and E. J. Carpenter (1997). "Trichodesmium, a globally significant marine cyanobacterium." *Science* 276(5316): 1221-1229.

Carlson, C. A. and H. W. Ducklow (1995). "Dissolved Organic-Carbon in the Upper Ocean of the Central Equatorial Pacific-Ocean, 1992 - Daily and Finescale Vertical Variations." *Deep-Sea Research Part II-Topical Studies in Oceanography* 42(2-3): 639-656.

Carlson, C. A., H. W. Ducklow and A. F. Michaels (1994). "Annual Flux of Dissolved Organic-Carbon from the Euphotic Zone in the Northwestern Sargasso Sea." *Nature* 371(6496): 405-408.

Carlsson, C. A., Hansell D.A., Peltzer E.T., Smith Jr W.O. (2000). "Stock and dynamics of dissolved and particulate organic matter in the Southern Ross Sea, Antarctica." *Deep-Sea Research Part b*- 42: 3201-3225.

Carpenter, E. J. (1983). "Physiology And Ecology Of Marine Planktonic Oscillatoria (Trichodesmium)." *Marine Biology Letters* 4(2): 69-85.

Carpenter, E. J., H. R. Harvey, B. Fry and D. G. Capone (1997). "Biogeochemical tracers of the marine cyanobacterium Trichodesmium." *Deep-Sea Research Part I-Oceanographic Research Papers* 44(1): 27-38.

Carpenter, E. J., A. Subramaniam and D. G. Capone (2004). "Biomass and primary productivity of the cyanobacterium Trichodesmium spp. in the tropical N Atlantic ocean." *Deep-Sea Research Part I-Oceanographic Research Papers* 51(2): 173-203.

Cavender-Bares, K. K., D. M. Karl and S. W. Chisholm (2001). "Nutrient gradients in the western North Atlantic Ocean: Relationship to microbial community structure and comparison to patterns in the Pacific Ocean." *Deep-Sea Research Part I-Oceanographic Research Papers* 48(11): 2373-2395.

Checkley, D. M. and C. A. Miller (1989). "Nitrogen Isotope Fractionation By Oceanic Zooplankton." *Deep-Sea Research Part A-Oceanographic Research Papers* 36(10): 1449-1456.

Cho, B. C. and F. Azam (1988). "Major Role of Bacteria in Biogeochemical Fluxes in the Oceans Interior." *Nature* 332(6163): 441-443.

Christensen, J. P., J. W. Murray, A. H. Devol and L. A. Codispoti (1987). "Denitrification in continental shelf sediments has a major impact on the oceanic nitrogen budget." *Global Biogeochemical Cycles* 1: 97-116.

Church, M. J., H. W. Ducklow and D. M. Karl (2002). "Multiyear increases in dissolved organic matter inventories at station ALOHA in the North Pacific Subtropical Gyre." *Limnology and Oceanography* 47(1): 1-10.

Clark, L. L., E. D. Ingall and R. Benner (1998). "Marine phosphorus is selectively remineralized." *Nature* 393(6684): 426-426.

Codispoti, L. A. (1989). *Phosphorus vs. nitrogen limitation of new and export production*. New York, John Wiley & Sons.

Codispoti, L. A. (1995). "Biogeochemical Cycles - Is the Ocean Losing Nitrate." *Nature* 376(6543): 724-724.

Codispoti, L. A., J. A. Brandes, J. P. Christensen, A. H. Devol, S. W. A. Naqvi, H. W. Paerl and T. Yoshinari (2001). "The oceanic fixed nitrogen and nitrous oxide budgets: Moving targets as we enter the anthropocene?" *Scientia Marina* 65: 85-105.

Codispoti, L. A. and T. T. Packard (1980). "Denitrification Rates In The Eastern Tropical South-Pacific." *Journal Of Marine Research* 38(3): 453-477.

Codispoti, L. A. and F. A. Richards (1976). "Analysis Of Horizontal Regime Of Denitrification In Eastern Tropical North Pacific." *Limnology And Oceanography* 21(3): 379-388.

Collier, J. L., Brahamsha B., Palenik B. (1999). "the marine cyanobacterium Synechococcus sp. WH7805 requires urease to utilise urea as a N source: molecular-genetic and biochemical analysis of the enzyme." *Microbiology* 145: 447-459.

Cornell, S., A. Rendell and T. Jikells (1995). "Atmospheric inputs of dissolved organic nitrogen to the oceans." *Nature* 376: 234-246.

Croot, P. L., P. Streu and A. R. Baker (2004). "Short residence time for iron in surface seawater impacted by atmospheric dry deposition from Saharan dust events." *Geophysical Research Letters* 31(23): art. no.-L23S08.

Cunha, L. C. D., C. L. Quere' and B. Buitenhuis (2005). *Riverine influence in the tropical Atlantic ocean biogeochemistry*. ASLO Meeting, Santiago de Compostela, Spain.

D'Elia, C. F., P. A. Steudler and N. Corwin (1977). "Determination of total nitrogen in aqueous samples using persulfate digestion." *Limnology and Oceanography* 2(4): 760-764.

Delaney, M. L. (1998). "Phosphorus accumulation in marine sediments and the oceanic phosphorus cycle." *Global Biogeochemical Cycles* 12(4): 563-572.

Deutsch, C., N. Gruber, R. M. Key, J. L. Sarmiento and A. Ganachaud (2001). "Denitrification and N₂ fixation in the Pacific Ocean." *Global Biogeochemical Cycles* 15(2): 483-506.

Devol, A. H. (1991). "Direct Measurement of Nitrogen Gas Fluxes from Continental-Shelf Sediments." *Nature* 349(6307): 319-321.

Devol, A. H. (2002). "Global change - Getting cool with nitrogen." *Nature* 415(6868): 131-132.

Druffel, E. R. M., P. M. Williams, J. E. Bauer and J. R. Ertel (1992). "Cycling of Dissolved and Particulate Organic-Matter in the Open Ocean." *Journal of Geophysical Research-Oceans* 97(C10): 15639-15659.

Ducklow, H. W. (1999). "The bacterial component of the oceanic euphotic zone." *Fems Microbiology Ecology* 30(1): 1-10.

Dyhrman, S. T., E. A. Webb, D. M. Anderson, J. W. Moffett and J. B. Waterbury (2002). "Cell-specific detection of phosphorus stress in *Trichodesmium* from the western north Atlantic." *Limnology And Oceanography* 47(6): 1832-1836.

Emerson, S., S. Mecking and J. Abell (2001). "The biological pump in the subtropical North Pacific Ocean: Nutrient sources, Redfield ratios, and recent changes." *Global Biogeochemical Cycles* 15(3): 535-554.

Emerson, S., P. Quay, D. Karl, C. Winn, L. Tupas and M. Landry (1997). "Experimental determination of the organic carbon flux from open-ocean surface waters." *Nature* 389(6654): 951-954.

Eppley, R. and B. J. Peterson (1979). "Particulate organic matter flux and planktonic new production in the deep ocean." *Nature* 282: 677-680.

Falkowski, P. G. (1997). "Evolution of the nitrogen cycle and its influence on the biological sequestration of CO₂ in the ocean." *Nature* 387(6630): 272-275.

Falkowski, P. G. (2000). "Rationalizing elemental ratios in unicellular algae." *J. Phycol* 36: 3-6.

Fieux, M., R. Molcard, R. Morrow, A. Kartavtseff and A. G. Ilahude (2005). "Variability of the throughflow at its exit in the Indian Ocean." *Geophysical Research Letters* 32: L14616.

Galloway, J. N., F. J. Dentener, D. G. Capone, E. W. Boyer, R. W. Howarth, S. P. Seitzinger, G. P. Asner, C. C. Cleveland, P. A. Green, E. A. Holland, D. M. Karl, A. F. Michaels, J. H. Porter, A. R. Townsend and C. J. Vorosmarty (2004). "Nitrogen cycles: past, present, and future." *Biogeochemistry* 70(2): 153-226.

Ganachaud, A. and C. Wunsch (2002). "Oceanic nutrient and oxygen transports and bounds on export production during the World Ocean Circulation Experiment." *Global Biogeochemical Cycles* 16(4): art. no.-1057.

Ganeshram, R. S., T. F. Pedersen, S. E. Calvert and J. W. Murray (1995). "Large Changes In Oceanic Nutrient Inventories From Glacial To Interglacial Periods." *Nature* 376(6543): 755-758.

Gao, Y., Y. J. Kaufman, D. Tanre, D. Kolber and P. G. Falkowski (2001). "Seasonal distributions of aeolian iron fluxes to the global ocean." *Geophysical Research Letters* 28(1): 29-32.

Glibert, P. M., Kana T.M., Olson R.J., Kirchman D.L., Alberte R.S. (1986). "Clonal comparison of growth and photosynthetic responses to nitrogen availability in marine *Synechococcus* sp." *Journal of Experimental Marine Biology and Ecology* 101: 199-208.

Glibert, P. M. and D. A. Bronk (1994). "Release of Dissolved Organic Nitrogen by Marine Diazotrophic Cyanobacteria, *Trichodesmium* Spp." *Applied and Environmental Microbiology* 60(11): 3996-4000.

Gordon, A. L. (1986). "Inter ocean exchange of thermocline water." *J. Geophys. Res.* 91: 5037-5047.

Goudie, A. S. (1983). "Dust Storms In Space And Time." *Progress In Physical Geography* 7(4): 502-530.

Green, P. A., C. J. Vorosmarty, M. Meybeck, J. N. Galloway, B. J. Peterson and E. W. Boyer (2004). "Pre-industrial and contemporary fluxes of nitrogen through rivers: a global assessment based on typology." *Biogeochemistry* 68(1): 71-105.

Gruber, N. (2004). The dynamics of the marine nitrogen cycle and its influence on atmospheric CO₂. *The ocean carbon cycle and climate*. M. F. a. T. Oguz. Dordrecht, NATO ASI Series, Kluwer Academic: 97-148.

Gruber, N. and J. L. Sarmiento (1997). "Global patterns of marine nitrogen fixation and denitrification." *Global Biogeochemical Cycles* 11(2): 235-266.

Hansell, D. A., N. R. Bates and D. B. Olson (2004). "Excess nitrate and nitrogen fixation in the North Atlantic Ocean." *Marine Chemistry* 84(3-4): 243-265.

Hansell, D. A. and C. Carlson (2002). *Biogeochemistry of marine dissolved organic matter*, Academic Press.

Hansell, D. A. and C. A. Carlson (1998). "Net community production of dissolved organic carbon." *Global Biogeochemical Cycles* 12(3): 443-453.

Hansell, D. A. and C. A. Carlson (2001). "Biogeochemistry of total organic carbon and nitrogen in the Sargasso Sea: control by convective overturn." *Deep-Sea Research Part II-Topical Studies in Oceanography* 48(8-9): 1649-1667.

Hansell, D. A. and R. A. Feely (2000). "Atmospheric intertropical convergence impacts surface ocean carbon and nitrogen biogeochemistry in the western tropical Pacific." *Geophysical Research Letters* 27(7): 1013-1016.

Hansell, D. A. and T. Y. Waterhouse (1997). "Controls on the distributions of organic carbon and nitrogen in the eastern Pacific Ocean." *Deep-Sea Research Part I-Oceanographic Research Papers* 44(5): 843-857.

Hansell, D. A., P. M. Williams and B. B. Ward (1993). "Measurements of DOC and DON in the Southern California Bight Using Oxidation by High-Temperature Combustion." *Deep-Sea Research Part I-Oceanographic Research Papers* 40(2): 219-234.

Hasegawa, T., I. Koike and H. Mukai (2000). "Dissolved organic nitrogen dynamics in coastal waters and the effect of copepods." *Journal of Experimental Marine Biology and Ecology* 244(2): 219-238.

Hattori, A. (1983). Denitrification and dissimilatory nitrogen reduction. *Nitrogen in the marine environment*. E. J. in Carpenter, and Capone, D. G., editors. New York, Academic Press: 191-232.

Hedges, J. I. and R. G. Keil (1995). "Sedimentary Organic-Matter Preservation - An Assessment And Speculative Synthesis." *Marine Chemistry* 49(2-3): 81-115.

Hellerman, S. and M. Rosenstein (1983). "Normal monthly wind stress over the world ocean with error estimates." *Journal Of Physical Oceanography* 13: 1093-1104.

Hood, R. R., N. R. Bates, D. G. Capone and D. B. Olson (2001). "Modeling the effect of nitrogen fixation on carbon and nitrogen fluxes at BATS." *Deep-Sea Research Part II-Topical Studies in Oceanography* 48(8-9): 1609-1648.

Hood, R. R., V. J. Coles and D. G. Capone (2004). "Modeling the distribution of Trichodesmium and nitrogen fixation in the Atlantic Ocean." *Journal of Geophysical Research-Oceans* 109(C6): art. no.-C06006.

Hoppe, H. G. (2003). "Phosphatase activity in the sea." *Hydrobiologia* 493(1-3): 187-200.

Howarth, R. W., R. Marino, J. Lane and J. J. Cole (1988). "Nitrogen fixation in freshwater, estuarine, and marine ecosystems. 2. Biogeochemical controls." *Limnol. Oceanogr* 33: 688-701.

Howell, E. A., S.C. Doney, R.A. Fine, D.B. Olson. (1997). "Geochemical estimates of denitrification in the Arabian Sea and the Bay of Bengal during WOCE." *Geophysical Research Letters* 24: 2549-2552.

Hubberton, U., Lara R.J., Kattner G. (1995). "Refractory organic compounds in polar waters: relationship between humic substances and amino acids in the Arctic and Antarctic." *Journal of Marine Research* 53(137-149).

Ittekkot, V. and R. Arain (1986). "Nature Of Particulate Organic-Matter In The River Indus, Pakistan." *Geochimica Et Cosmochimica Acta* 50(8): 1643-1653.

Jackson, G. A. and P. M. Williams (1985). "Importance of Dissolved Organic Nitrogen and Phosphorus to Biological Nutrient Cycling." *Deep-Sea Research Part a-Oceanographic Research Papers* 32(2): 223-235.

Jahnke, R. A. and D. B. Jahnke (2000). "Rates of C, N, P and Si recycling and denitrification at the US Mid-Atlantic continental slope depocenter." *Deep-Sea Research Part I-Oceanographic Research Papers* 47(8): 1405-1428.

Jenkins, W. J. (1988). "Nitrate Flux into the Euphotic Zone near Bermuda." *Nature* 331(6156): 521-523.

Jenkins, W. J. (1991). "Determination Of Isopycnic Diffusivity In The Sargasso Sea." *Journal Of Physical Oceanography* 21(7): 1058-1061.

Jenkins, W. J. (1998). "Studying subtropical thermocline ventilation and circulation using tritium and He-3." *Journal of Geophysical Research-Oceans* 103(C8): 15817-15831.

Jenkins, W. J. and S. C. Doney (2003). "The subtropical nutrient spiral." *Global Biogeochemical Cycles* 17(4): art. no.-1110.

Jenkins, W. J. and J. C. Goldman (1985). "Seasonal Oxygen Cycling and Primary Production in the Sargasso Sea." *Journal of Marine Research* 43(2): 465-491.

Jenkins, W. J. and D. W. R. Wallace (1992). Tracer-based inferences of new primary production in the sea. *Primary Productivity and Biogeochemical cycles in the Sea*. P. G. a. W. A. D. Falkowski: pp299-316.

Jickells, T. D., Z. S. An, K. K. Andersen, A. R. Baker, G. Bergametti, N. Brooks, J. J. Cao, P. W. Boyd, R. A. Duce, K. A. Hunter, H. Kawahata, N. Kubilay, J. laRoche, P. S. Liss, N. Mahowald, J. M. Prospero, A. J. Ridgwell, I. Tegen and R. Torres (2005). "Global iron connections between desert dust, ocean biogeochemistry, and climate." *Science* 308(5718): 67-71.

Kahler, P., P. K. Bjornsen, K. Lochte and A. Antia (1997). "Dissolved organic matter and its utilization by bacteria during spring in the Southern Ocean." *Deep-Sea Research Part II-Topical Studies in Oceanography* 44(1-2): 341-353.

Karl, D., R. Letelier, L. Tupas, J. Dore, J. Christian and D. Hebel (1997). "The role of nitrogen fixation in biogeochemical cycling in the subtropical North Pacific Ocean." *Nature* 388(6642): 533-538.

Karl, D., A. Michaels, B. Bergman, D. Capone, E. Carpenter, R. Letelier, F. Lipschultz, H. Paerl, D. Sigman and L. Stal (2002). "Dinitrogen fixation in the world's oceans." *Biogeochemistry* 57(1): 47-+.

Karl, D. M., Bidigare, R.R., Letelier RM. (2001). "Long-term changes in plankton community structure and productivity in the Northen Subtropical Pacific Gyre: the domain shift hypothesis." *Deep-Sea Research Part b* 48: 1449-1470.

Karl, D. M., K. M. Bjorkman, J. E. Dore, L. Fujiki, D. V. Hebel, T. Houlihan, R. M. Letelier and L. M. Tupas (2001). "Ecological nitrogen-to-phosphorus stoichiometry at station ALOHA." *Deep-Sea Research Part II-Topical Studies in Oceanography* 48(8-9): 1529-1566.

Karl, D. M. and K. Yanagi (1997). "Partial characterization of the dissolved organic phosphorus pool in the oligotrophic North Pacific Ocean." *Limnology and Oceanography* 42(6): 1398-1405.

Keil, R. G. and D. L. Kirchman (1999). "Utilization of dissolved protein and amino acids in the northern Sargasso Sea." *Aquatic Microbial Ecology* 18(3): 293-300.

Kerouel, R. and A. Aminot (1996). "Model compounds for the determination of organic and total phosphorus dissolved in natural waters." *Analytica Chimica Acta* 318(3): 385-390.

Kirkwood, D. S., A. Aminot and S. R. Carlberg (1996). "The 1994 QUASIMEME laboratory performance study: Nutrients in seawater and standard solutions." *Marine Pollution Bulletin* 32(8-9): 640-645.

Knapp, A. N., D. M. Sigman and F. Lipschultz (2005). "N isotopic composition of dissolved organic nitrogen and nitrate at the Bermuda Atlantic time-series study site." *Global Biogeochemical Cycles* 19(1): art. no.-GB1018.

Koroleff, F. (1983). "Determination of total phosphorus in natural waters by persulphate oxidation." *ICES, interlab. rep. Ref L.* 3: 19.

Kristensen, E., A. H. Devol and H. E. Hartnett (1999). "Organic matter diagenesis in sediments on the continental shelf and slope of the Eastern Tropical and temperate North Pacific." *Continental Shelf Research* 19(10): 1331-1351.

Kumar, M. D., M. D. George and R. Sen Gupta (1992). Inputs from Indian rivers to the ocean: a synthesis. *Oceanography of the Indian Ocean*. B.N.Desai. New Delhi, Oxford & IBH Publishing: 347-358.

LaRoche, J. and E. Breitbarth (2005). "Importance of the diazotrophs as a source of new nitrogen in the ocean." *Journal Of Sea Research* 53(1-2): 67-91.

Lavin, A. M., H. L. Bryden and G. Parrilla (2003). "Mechanisms of heat, freshwater, oxygen and nutrient transports and budgets at 24.5(\circ N) in the subtropical North Atlantic." *Deep-Sea Research Part I-Oceanographic Research Papers* 50(9): 1099-1128.

Ledwell, J. R., A. J. Watson and C. S. Law (1993). "Evidence For Slow Mixing Across The Pycnocline From An Open- Ocean Tracer-Release Experiment." *Nature* 364(6439): 701-703.

Libby, P. S. and P. A. Wheeler (1997). "Particulate and dissolved organic nitrogen in the central and eastern equatorial Pacific." *Deep-Sea Research Part I-Oceanographic Research Papers* 44(2): 345-361.

Lipschultz, F. (2001). "A time-series assessment of the nitrogen cycle at BATS." *Deep-Sea Research Part II-Topical Studies In Oceanography* 48(8-9): 1897-1924.

Lipschultz, F., N. R. Bates, C. A. Carlson and D. A. Hansell (2002). "New production in the Sargasso Sea: History and current status." *Global Biogeochemical Cycles* 16(1): art. no.-1001.

Liu, K. K., M. J. Su, C. R. Hsueh and G. C. Gong (1996). "The nitrogen isotopic composition of nitrate in the Kuroshio Water northeast of Taiwan: Evidence for nitrogen fixation as a source of isotopically light nitrate." *Marine Chemistry* 54(3-4): 273-292.

Loh, A. N. and J. E. Bauer (2000). "Distribution, partitioning and fluxes of dissolved and particulate organic C, N and P in the eastern North Pacific and Southern Oceans." *Deep-Sea Research Part I-Oceanographic Research Papers* 47(12): 2287-2316.

Mackenzie, F. T. (1998). *Our Changing Planet: An Introduction to Earth System Science and Global Environmental Change*, Prentice-Hall, Upper Saddle River, NJ.

Mahaffey, C., R. G. Williams, G. A. Wolff and W. T. Anderson (2004). "Physical supply of nitrogen to phytoplankton in the Atlantic Ocean." *Global Biogeochemical Cycles* 18(1): art. no.-GB1034.

Mahaffey, C., R. G. Williams, G. A. Wolff, N. Mahowald, W. Anderson and M. Woodward (2003). "Biogeochemical signatures of nitrogen fixation in the eastern North Atlantic." *Geophysical Research Letters* 30(6): art. no.-1300.

Mantoura, R. F. C., C.S. Law, N.J.P Owens, P.H. Burkill, E.M.S. Woodward, R.J.M. Howland and C.A.Llewellyn. (1993). "Nitrogen biogeochemical cycling in the northwestern Indian Ocean." *Deep-Sea Research II* 40: 651-671.

Maranon, E., P. M. Holligan, M. Varela, B. Mourino and A. J. Bale (2000). "Basin-scale variability of phytoplankton biomass, production and growth in the Atlantic Ocean." *Deep-Sea Research Part I-Oceanographic Research Papers* 47(5): 825-857.

Mariotti, A., J. C. Geromon, P. Huebert and P. Keiser (1981). "Experimental determination of nitrogen kinetic isotope fractionation: some principles; illustration for the denitrification and nitrification processes." *Plant Soil* 62: 413-430.

Martin, A. P. and P. Pondaven (2003). "On estimates for the vertical nitrate flux due to eddy pumping." *Journal of Geophysical Research-Oceans* 108(C11): art. no.-3359.

Martinez, J. and F. Azam (1993). "Aminopeptidase activity in marine chroococcoid cyanobacteria." *Applied and Environmental Microbiology* 59(11): 3701-3707.

McDonagh, E. L., H. L. Bryden and B. A. King (2005). "Using shipboard measurements and lowered ADCP data to inform geostrophic calculations." *Deep-Sea Research I* submitted.

McGillicuddy, D. J. and A. R. Robinson (1997). "Eddy-induced nutrient supply and new production in the Sargasso Sea." *Deep-Sea Research Part I-Oceanographic Research Papers* 44(8): 1427-1450.

McGillicuddy, D. J., A. R. Robinson, D. A. Siegel, H. W. Jannasch, R. Johnson, T. Dickey, J. McNeil, A. F. Michaels and A. H. Knap (1998). "Influence of mesoscale eddies on new production in the Sargasso Sea." *Nature* 394(6690): 263-266.

Menzel, D. W. and J. H. Ryther (1960). "The annual cycle of primary production in the Sargasso Sea off Bermuda." *Deep-Sea Research* 6: 351-367.

Michaels, A., Karl D. and Capone D. (2001.). "Element stoichiometry, new production and nitrogen fixation." *Oceanography* 14: 68-77.

Michaels, A. F., D. Olson, J. L. Sarmiento, J. W. Ammerman, K. Fanning, R. Jahnke, A. H. Knap, F. Lipschultz and J. M. Prospero (1996). "Inputs, losses and transformations of nitrogen and phosphorus in the pelagic North Atlantic Ocean." *Biogeochemistry* 35(1): 181-226.

Mills, M. M., C. Ridame, M. Davey, J. La Roche and R. J. Geider (2004). "Iron and phosphorus co-limit nitrogen fixation in the eastern tropical North Atlantic." *Nature* 429(6989): 292-294.

Mino, Y., T. Saino, K. Suzuki and E. Maranon (2002). "Isotopic composition of suspended particulate nitrogen (delta N-15(sus)) in surface waters of the Atlantic Ocean from 50 degrees N to 50 degrees S." *Global Biogeochemical Cycles* 16(4): art. no.-1059.

Mline, A., E. Achtenberg and A. T. e. al. (2005). *Dissolution of iron dust form dusts in the North Atlantic surface waters*. ASLO meeting, Santiago de Compostela, Spain.

Montesinos, M. L., Herrero A., Flores E. (1997). "Amino acid transport in taxonomically diverse cyanobacteria and identification of two genes encoding elements of a neutral amino acid permease putatively involved in recapture of leaked hydrophobic amino acids." *Journal of Bacteriology* 179(3): 853-862.

Montoya, J. P., E. J. Carpenter and D. G. Capone (2002). "Nitrogen fixation and nitrogen isotope abundances in zooplankton of the oligotrophic North Atlantic." *Limnology and Oceanography* 47(6): 1617-1628.

Moore, L. R., Post A.F., Rocap G., Chisholm S.W. (2002). "Utilization of different nitrogen sources by the marine cyanobacteria Prochlorococcus and Synechococcus." *Limnology and Oceanography* 47(4): 989-996.

Mopper, K., X. L. Zhou, R. J. Kieber, D. J. Kieber, R. J. Sikorski and R. D. Jones (1991). "Photochemical Degradation of Dissolved Organic-Carbon and Its Impact on the Oceanic Carbon-Cycle." *Nature* 353(6339): 60-62.

Mulholland, M. R., D. A. Bronk and D. G. Capone (2004). "Dinitrogen fixation and release of ammonium and dissolved organic nitrogen by *Trichodesmium IMS101*." *Aquatic Microbial Ecology* 37(1): 85-94.

Mulholland, M. R., S. Floge, E. J. Carpenter and D. G. Capone (2002). "Phosphorus dynamics in cultures and natural populations of *Trichodesmium* spp." *Marine Ecology-Progress Series* 239: 45-55.

Naqvi, A. (1994). Denitrification processes in the Arabian Sea. *The Biogeochemistry of the Arabian Sea*. D. Lal. Bangalore, Indian Acad. of Sci.: 181-202.

Naqvi, S. W. A. (1987). "Some Aspects Of The Oxygen-Deficient Conditions And Denitrification In The Arabian Sea." *Journal Of Marine Research* 45(4): 1049-1072.

Naqvi, S. W. A. and M. S. Shailaja (1993). "Activity Of The Respiratory Electron-Transport System And Respiration Rates Within The Oxygen Minimum Layer Of The Arabian Sea." *Deep-Sea Research Part II-Topical Studies In Oceanography* 40(3): 687-695.

Nevison, C., R. Weiss and D. Erikson (1995). "Global oceanic emissions of nitrous oxide." *J. Geophys. Res.* 100: 15809-15820.

Obernosterer, I., R. Sempere and G. J. Herndl (2001). "Ultraviolet radiation induces reversal of the bioavailability of DOM to marine bacterioplankton." *Aquatic Microbial Ecology* 24(1): 61-68.

Ogawa, H., Y. Amagai, I. Koike, K. Kaiser and R. Benner (2001). "Production of refractory dissolved organic matter by bacteria." *Science* 292(5518): 917-920.

Ono, S., Najjar, R., Ennyu, A., and Bates, N.R. (2001). "Shallow remineralization in the Sargasso Sea estimated from seasonal variations in oxygen, dissolved inorganic carbon and nitrate." *Deep-Sea Research II* 48: 1567-1582.

Orcutt, K. M., F. Lipschultz, K. Gundersen, R. Arimoto, A. F. Michaels, A. H. Knap and J. R. Gallon (2001). "A seasonal study of the significance of N-2 fixation by *Trichodesmium* spp. at the Bermuda Atlantic Time-series Study (BATS) site." *Deep-Sea Research Part II-Topical Studies In Oceanography* 48(8-9): 1583-1608.

Oschlies, A. (2002). "Nutrient supply to the surface waters of the North Atlantic: A model study." *Journal of Geophysical Research-Oceans* 107(C5): art. no.-3046.

Oschlies, A. and V. Garcon (1998). "Eddy-induced enhancement of primary production in a model of the north Atlantic Ocean." *Nature* 394(6690): 266-269.

Oschlies, A. and V. Garcon (1999). "An eddy-permitting coupled physical-biological model of the North Atlantic - 1. Sensitivity to advection numerics and mixed layer physics." *Global Biogeochemical Cycles* 13(1): 135-160.

Palenik, B., et al. (2003). "The genome of a motile marine *synechococcus*." *Nature* 424(9652): 1037-1042.

Palenik, B. and S. E. Henson (1997). "The use of amides and other organic nitrogen sources by the phytoplankton *Emiliania huxleyi*." *Limnology and Oceanography* 42(7): 1544-1551.

Palenik, B. and F. M. M. Morel (1990). "Amino-Acid Utilization by Marine-Phytoplankton - a Novel Mechanism." *Limnology and Oceanography* 35(2): 260-269.

Partensky, F., W. R. Hess and D. Vaulot (1999). "Prochlorococcus, a marine photosynthetic prokaryote of global significance." *Microbiology and Molecular Biology Reviews* 63(1): 106-+.

Pearl, H. W. (1991). "Ecophysiological and trophic implications of light stimulated amino acid utilization in marine picoplankton." *Applied and Environmental Microbiology* 57: 473-479.

Prospero, J. M., K. Barrett, T. Church, F. Dentener, R. A. Duce, J. N. Galloway, H. Levy, J. Moody and P. Quinn (1996). "Atmospheric deposition of nutrients to the North Atlantic Basin." *Biogeochemistry* 35(1): 27-73.

Raimbault, P., W. Pouvesle, F. Diaz, N. Garcia and R. Sempere (1999). "Wet-oxidation and automated colorimetry for simultaneous determination of organic carbon, nitrogen and phosphorus dissolved in seawater." *Marine Chemistry* 66(3-4): 161-169.

Redfield, A. C., Ketchum B.H., Richards F.A. (1963). *The Influence of Organisms on the Composition of Sea Water*.

Ridal, J. J. and R. M. Moore (1990). "A Reexamination of the Measurement of Dissolved Organic Phosphorus in Seawater." *Marine Chemistry* 29(1): 19-31.

Rintoul, S. R. and C. Wunch (1991). "Mass, heat oxygen and nutrient fluxes and budgets in the North Atlantic Ocean." *Deep-Sea Research Part a-Oceanographic Research Papers* 38(1): s-355-s377.

Rippka, R., Coursin T., Hess W., Lichlē C., Scanlan D.J., Palinska K.A., Iteman I., Partensky F., Houmard J., Herdman M. (2000). "Prochlorococcus marinus Chisholm et al. 1992 subsp. *pastoris* subsp.nov. strain PCC9511, the first axenic chlorophyll a₂/b₂-containing cyanobacterium (Oxyphotobacteria)." *International Journal of Systematic and Evolutionary Microbiology* 50(1833-1847).

Robbins, P. E. and J. M. Toole (1997). "The dissolved silica budget as a constraint on the meridional overturning circulation of the Indian Ocean." *Deep-Sea Research I* 44(5): 879-906.

Saino, T. and A. Hattori (1987). "Geographical Variation Of The Water Column Distribution Of Suspended Particulate Organic Nitrogen And Its N-15 Natural Abundance In The Pacific And Its Marginal Seas." *Deep-Sea Research Part A-Oceanographic Research Papers* 34(5-6): 807-827.

Sala, M. M., M. Karner, L. Arin and C. Marrase (2001). "Measurement of ectoenzyme activities as an indication of inorganic nutrient imbalance in microbial communities." *Aquatic Microbial Ecology* 23(3): 301-311.

Sanders, R. and T. Jickells (2000). "Total organic nutrients in Drake Passage." *Deep-Sea Research Part I-Oceanographic Research Papers* 47(6): 997-1014.

Sanders, R., E. McDonagh, H. Bryden, C. Powell, S. Cunningham, A. Landolfi and W. J. Jenkins (2005). "Recent increases in oceanic dissolved oxygen levels, the mechanisms driving these increases and their implications for the marine and terrestrial carbon sinks in the 2000's." *Geophysical Research Letters*, submitted.

Sanudo-Wilhelmy, S. A., A. B. Kustka, C. J. Gobler, D. A. Hutchins, M. Yang, K. Lwiza, J. Burns, D. G. Capone, J. A. Raven and E. J. Carpenter (2001). "Phosphorus limitation of nitrogen fixation by *Trichodesmium* in the central Atlantic Ocean." *Nature* 411(6833): 66-69.

Schott, F. A., M. Dengler and R. Schoenfeldt (2002). "The Shallow overturning Circulation of the Indian Ocean." *Progress In Oceanography* 53: 57-103.

Seitzinger, S. P. and A. E. Giblin (1996). "Estimating denitrification in North Atlantic continental shelf sediments." *Biogeochemistry* 35: 235-260.

Seitzinger, S. P. and C. Kroeze (1998). "Global distribution of nitrous oxide production and N inputs in freshwater and coastal marine ecosystems." *Global Biogeochem. Cycles* 12: 93-113.

Sharp, J. H. (1997). "Marine dissolved organic carbon: Are the older values correct?" *Marine Chemistry* 56(3-4): 265-277.

Sharp, J. H., R. Benner, L. Bennett, C. A. Carlson, S. E. Fitzwater, E. T. Peltzer and L. M. Tupas (1995). "Analyses of Dissolved Organic-Carbon in Seawater - the Jgofs Eqpac Methods Comparison." *Marine Chemistry* 48(2): 91-108.

Sigman, D. M., M. A. Altabet, D. C. McCorkle, R. Francois and G. Fischer (1999). "The delta N-15 of nitrate in the Southern Ocean: Consumption of nitrate in surface waters." *Global Biogeochemical Cycles* 13(4): 1149-1166.

Sirocko, F. M., M. Sarnthein, H. Lange and H. Erlenkauser (1991). "Atmospheric summer circulation and coastal upwelling in the Arabian Sea during the Holocene and the last glaciation." *Quat. Res.* 36: 72-93.

Skoog, A., B. Biddanda and R. Benner (1999). "Bacterial utilization of dissolved glucose in the upper water column of the Gulf of Mexico." *Limnology and Oceanography* 44(7): 1625-1633.

Smith, S. V., W. J. Kimmerer and T. W. Walsh (1986). "Vertical Flux and Biogeochemical Turnover Regulate Nutrient Limitation of Net Organic Production in the North Pacific Gyre." *Limnology and Oceanography* 31(1): 161-167.

Subramaniam, V. (1979). "Chemical and suspended sediment characteristics of river waters of India." *Journal Of Hydrology* 41: 37-55.

Takahashi, T., W. S. Broecker and S. Langer (1985). "Redfield ratio based on chemical data from isopycnal surfaces." *J. Geophys. Res.* 90: 6907-6924.

Tanoue, E. (1996). "Characterization of the particulate protein in Pacific surface waters." *Journal of Marine Research* 54(5): 967-990.

Tanoue, E., M. Ishii and T. Midorikawa (1996). "Discrete dissolved and particulate proteins in oceanic waters." *Limnology and Oceanography* 41(6): 1334-1343.

Thingstad, T. F., A. Hagstrom and F. Rassoulzadegan (1997). "Accumulation of degradable DOC in surface waters: Is it caused by a malfunctioning microbial loop?" *Limnology and Oceanography* 42(2): 398-404.

Thingstad, T. F. and F. Rassoulzadegan (1999). "Conceptual models for the biogeochemical role of the photic zone microbial food web, with particular reference to the Mediterranean Sea." *Progress in Oceanography* 44(1-3): 271-286.

Thingstad, T. F. and E. Sakshaug (1990). "Control of Phytoplankton Growth in Nutrient Recycling Ecosystems - Theory and Terminology." *Marine Ecology-Progress Series* 63(2-3): 261-272.

Trick, C. G. and S. W. Wilhelm (1995). "Physiological changes to the coastal marine cyanobacterium *Synechococcus* sp. PCC7002 exposed to low ferric iron levels." *Marine Chemistry* 50: 207-217.

Tyrrell, T. (1999). "The relative influences of nitrogen and phosphorus on oceanic primary production." *Nature* 400(6744): 525-531.

Valderrama, J. C. (1981). "The Simultaneous Analysis of Total Nitrogen and Total Phosphorus in Natural-Waters." *Marine Chemistry* 10(2): 109-122.

Venter, J. C., Remington, Karin, Heidelberg, John F., Halpern, Aaron L., Rusch, Doug, Eisen, Jonathan A., Wu, Dongying, Paulsen, Ian, Nelson, Karen E., Nelson, William, Fouts, Derrick E., Levy, Samuel, Knap, Anthony H., Lomas, Michael W., Nealson, Ken, White, Owen, Peterson, Jeremy, Hoffman, Jeff, Parsons, Rachel, Baden-Tillson, Holly, Pfannkoch, Cynthia, Rogers, Yu-Hui, Smith, Hamilton O. (2004). "Environmental Genome Shotgun Sequencing of the Sargasso Sea." *Science* 304: 66-74.

Vidal, M., C. M. Duarte and S. Agusti (1999). "Dissolved organic nitrogen and phosphorus pools and fluxes in the central Atlantic Ocean." *Limnology and Oceanography* 44(1): 106-115.

Vidal, M., C. M. Duarte, S. Agusti, J. M. Gasol and D. Vaque (2003). "Alkaline phosphatase activities in the central Atlantic Ocean indicate large areas with phosphorus deficiency." *Marine Ecology-Progress Series* 262: 43-53.

Voss, M., P. Croot, K. Lochte, M. Mills and I. Peeken (2004). "Patterns of nitrogen fixation along 10N in the tropical Atlantic." *Geophysical Research Letters* 31(23): art. no.-L23S09.

Wada, E. and A. Hattori (1976). "Natural Abundance Of N-15 In Particulate Organic-Matter In North Pacific Ocean." *Geochimica Et Cosmochimica Acta* 40(2): 249-251.

Wada, E. H., A. (1991). "Nitrogen in the sea: forms, abundances, and rate processes." *CRC Press*.

Wada, E. M. H., Minagawa M (1991). "The use of stable isotopes for food web analysis." *Crit Rev Food Sci Nutr* 30: 361-371.

Waser, N. A., W. G. Harrison, E. J. H. Head, B. Nielson, V. A. Lutz and S. E. Calvert (2000). "Geographic variations in the nitrogen isotope composition of surface particulate nitrogen and new production across the North Atlantic Ocean." *Deep-Sea Research Part I-Oceanographic Research Papers* 47(7): 1207-1226.

Welschmeyer, N. A. (1994). "Fluorometric analysis of Chlorophyll a in the presence of Chlorophyll b and Phepigments." *Limnology and Oceanography* 39(8): 1985-1992.

Wilhelm, S. W. and C. Trick (1994). "Iron limited cyanobacteria: multiple siderophore production is a common response." *Limnology And Oceanography*(39): 1979-1984.

Williams, P. l. (1990). "The importance of losses during microbial growth: commentary on the physiology, measurement and ecology of the release of dissolved organic material." *Marine Microbiology Food Web* 4: 175-206.

Williams, R. G. and M. J. Follows (1998). "The Ekman transfer of nutrients and maintenance of new production over the North Atlantic." *Deep-Sea Research Part I-Oceanographic Research Papers* 45(2-3): 461-489.

Williams, R. G. and M. J. Follows (2005). *Nutrient streams: How are they formed and what is their effect in the north Atlantic?* ALSO meeting, Santiago de Compostela, Spain.

Witt, M. (2003). Studies of Trace Metals in the Atmosphere. School of Environmental Sciences. Norwich, University of East Anglia.

Wu, J., Chung SW, Wen LS, Liu KK, Lee Chen YL, Chen HY, Karl D. (2003). "Dissolved inorganic phosphorus, dissolved iron, and trichodesmium in the oligotrophic South China Sea." *Global Biogeochemical Cycles* 17(1): 1008, doi:10.1029/2002GB001924.

Wu, J., Sunda W., Boyle E.A., Karl D.M. (2000). "Phosphate depletion in the western North Atlantic ocean." *Science* 289: 759-762.

Wu, J. P., S. E. Calvert and C. S. Wong (1997). "Nitrogen isotope variations in the subarctic northeast Pacific: Relationships to nitrate utilization and trophic structure." *Deep-Sea Research Part I-Oceanographic Research Papers* 44(2): 287-314.

Zehr, J. P., J. B. Waterbury, P. J. Turner, J. P. Montoya, E. Omoregie, G. F. Steward, A. Hansen and D. M. Karl (2001). "Unicellular cyanobacteria fix N-2 in the subtropical North Pacific Ocean." *Nature* 412(6847): 635-638.

Zubkov, M. V., Fuchs B.M., Tarran G.A., Burkhill P.H., Amann R. (2003). "High rate of uptake of organic nitrogen compounds by Prochlorococcus Cyanobacteria as a key to their dominance in oligotrophic oceanic waters." *Applied and Environmental Microbiology* 69(2): 1299-1304.